Histopathological aspects of idiopathic chronic hepatitis and antibody-mediated injury to the liver allograft

Neves Souza, Lara

Awarding institution:
King's College London

HISTOPATHOLOGICAL ASPECTS OF IDIOPATHIC CHRONIC HEPATITIS AND ANTIBODY-MEDIATED INJURY TO THE LIVER ALLOGRAFT

Lara Neves Souza

Institute of Liver Studies

Division of Transplantation, Immunology and Microbial Biology

School of Life Sciences and Medicine

King's College London

This thesis is submitted for the degree of Doctor of Philosophy

October 2018

ACKNOWLEDGEMENTS

The completion of this thesis was possible with the contribution of several individuals. Firstly, I would like to thank my supervisors, Dr Alberto Quaglia and Prof Alberto Sanchez-Fueyo. Alberto Quaglia helped me in the development of every stage of my PhD. He motivated me to think and supported me since I first expressed my intention to do a PhD in liver transplantation pathology at King's. His expertise as a liver pathologist was extremely valuable, as was his encouragement, especially when research results did not go as expected. Alberto Sanchez-Fueyo introduced me to the world of molecular analysis, challenged me to see my research findings from a different perspective and helped me at key stages of my research with his knowledge, focus and pragmatism.

I am very grateful to the *Coordenação de Aperfeiçoamento de Pessoal de Nível Superior* (CAPES) from the Brazilian Ministry of Education, and the program *Ciência sem Fronteiras* (Science without Borders) for entirely funding my PhD. This research would not have been possible without sponsorship.

Besides my supervisors, there were several other contributors to the development of this thesis. Dr Oltin Pop offered invaluable theoretical and practical assistance with staining, including conventional and fluorescence immunostaining and multiplexing. The staff of the histology department within King's Institute of Liver Studies (ILS) where my research was conducted welcomed me and taught me important practical skills such as cutting FFPE

biopsies, performing staining and automated immunohistochemistry. Dr Rodrigo de Martino helped me to conduct the failed grafts' analysis, going through endless biopsy archive files and writing with me a paper for publication. Marc Martinez-Llordella taught me how to extract RNA from biopsies and helped me develop practical skills for working in laboratory. Dr Olivia Shaw was in charge of the donor-specific antibodies testing at Guy's Hospital. Dr Jake Demetris, Andrew Lesniak and Kumiko Isse from the department of Pathology of the University of Pittsburgh Medical Center welcomed and helped me during my internship in their laboratory where I learned to perform quantum dots, multiplex staining and image analysis. They also offered to digitalize my research slides when needed. The staff from the Hepatic and Digestive Diseases (CIBEREHD) of the Instituto de Salud Carlos III in Spain and Juan José Lozano performed the RNA sequencing and gene expression analysis, respectively. I would like to thank Dr Corina Cotoi, Alex Pacheco and Dr Eliano Riani for their support and friendship throughout the years.

Living in London during the PhD was a great challenge. The absence of family and friends, the need to communicate in a different language, the lonely nature of my PhD research, and the frequently unappealing weather were only bearable with the support of my family and friends. My husband Vitor believed in me and motivated me to pursuit a PhD when I did not think I was capable. During all the years of my research, he has been extremely supportive and helped me to keep my focus and sense through the most difficult times. He also shared the care of our son Bernardo, born in the middle of my research, and later of our second son Vinicius, born a few days after my

PhD viva. Becoming a mother during a PhD and being pregnant again while writing the thesis were particularly challenging and at moments it seemed impossible to successfully accomplish both missions. I would like to thank my parents, Angela and Péricles, and mother-in-law, Eleonora, who offered their help with the children in several occasions. My parents have always supported my decisions and encouraged me to pursue my dreams, and taught me the importance of dedication and perseverance. I am grateful to my siblings, Mila and Vítor, who have supported me in the best and worst times and have always been enthusiastic of my accomplishments. My Brazilian friends Ana, Michel, Rayane, Diloá and little Flora have been a pleasant company, and an actual family away from home.

I would also like to thank Prof Norma Jucá, from Recife, Brazil, who was the first pathologist to appreciate and encourage my interest in liver and liver transplantation pathology. The biopsy slides she shared with me and case discussions we had motivated me to deep my knowledge and decide to pursuit a PhD in liver transplantation. I am also grateful to my training preceptors, Prof Roberto Vieira de Melo, Prof Mariana Lira, Dr Daniela Takano, Dr Ana Lucia Antonino, Dr Edna Sales and Prof Daisy Lima who inspired me with their dedication and expertise as pathologists.

ABSTRACT

BACKGROUND AND AIM: Histological abnormalities in protocol biopsies of liver allografts are common, particularly idiopathic post-transplant chronic hepatitis (IPTH) and fibrosis. Recently, emerging evidence suggests that antibody-mediated rejection (AMR) might play a role in acute and chronic liver allograft injury, but this is not well defined as in other allograft organs. This research consisted of a histopathological study of liver allografts, with emphasis on IPTH and AMR. The aim was to investigate IPTH as a cause of allograft loss, and to correlate histological findings of post-transplant biopsies, including IPTH, fibrosis and specific cell phenotypes, with signs of AMR and with gene expression profile. **METHODOLOGY**: Three cohorts corresponding to three distinct post-transplantation settings were analysed: failed allografts removed at retransplantation, long-term protocol biopsies of clinically asymptomatic liver recipients, and for cause biopsies with a diagnosis of cellular/T-cell mediated rejection (TCMR). Several parameters of allograft injury were scored by two pathologists on HE and reticulin stained slides. Fibrosis was digitally measured in Sirius Red slides (collagen proportionate area). Multiplex immunostaining with quantum dots and fluorescent dyes was performed and digital image analysis was conducted to quantify B cells, plasma cells and T cells and their subtypes. RNA was extracted from biopsies and analysed with RNA sequencing, and the results compared to gene signatures of known liver pathologies. **RESULTS**: A steady increase in IPTH leading to allograft loss was observed, and this was the main reason for retransplantation conducted >10 years after primary transplantation in children

in the most recent era. The protocol biopsies of 73% of children were abnormal, and IPTH associated with fibrosis was the most common finding. Donor-specific antibodies (DSA) were present in 69% of recipients, mainly class II DSA, and were associated with lobular inflammation. Portal microvascular C4d positivity (C4d+) was linked to a humoral inflammatory cell profile (B cells and plasma cells), central perivenulitis, lobular inflammation, and each sinusoidal and centrilobular fibrosis. The combination of DSA+C4d+ was also associated with central perivenulitis and sinusoidal fibrosis, and additionally, to interface activity. B cells and plasma cells were linked to fibrosis in all compartments. In biopsies with rejection, portal microvascular C4d+ was a specific and sensitive indicator of DSA II. Bile duct loss in this group was strongly linked to DSA, and portal fibrosis to DSA+C4d+. Considering current Banff criteria for AMR, 12% of patients in the protocol biopsy group, and a fourth of patients in the rejection cohort had a diagnosis of chronic and acute AMR established, respectively. Gene expression profiles were not significantly different between patients with and without DSA.

CONCLUSION: IPTH can slowly evolve to allograft failure. The associations found in both biopsy cohorts (protocol and rejection) between fibrosis and DSA+C4d+ (and a humoral inflammatory profile in protocol biopsies) suggest that unexplained fibrosis in both settings is likely connected to AMR. In long-term post-transplant biopsies of asymptomatic children, unexplained inflammation, especially interface activity, central perivenulitis and lobular inflammation (even mild), also seem to represent chronic ongoing AMR. When diagnosis of TCMR is established, the possibility of concurrent AMR should be carefully considered, and the finding of bile duct loss should be regarded

as a potential sign of AMR. Gene signatures of AMR could not be found. This highlights the importance of histological assessment in monitoring allograft health, even when patients are clinically asymptomatic with normal liver function tests.

TABLE OF CONTENTS

1 INTRODUCTION 11
1.1 Background 11
1.1.1 Long-term allograft histology 11
1.1.2 Donor-specific antibodies and antibody-mediated rejection in the liver graft 15
1.1.3 B cells, plasma cells and a possible local role 22
1.1.4 New technologies 24
1.2 Research gap 30
1.3 Research Hypothesis 31
1.4 Research aims 31
1.5 Studies on three liver transplant patient cohorts 32
1.6 Ethical approval 32
2 FAILED LIVER ALLOGRAFTS 34
2.1 RATIONALE FOR STUDYING EXPLANTED ALLOGRAFTS 34
2.2 MATERIAL AND METHODS 34
2.2.1 Patients and Data 34
2.2.2 Histology 36
2.2.3 Statistical analysis 38
2.3 RESULTS 38
2.4 DISCUSSION 49
3 PAEDIATRIC PROTOCOL BIOPSIES 54
3.1 RATIONALE FOR STUDYING PROTOCOL BIOPSIES 54
3.2 MATERIAL AND METHODS 55
3.2.1 Patients and Data 55
3.2.2 DSA testing 56
3.2.3 Histology 56
3.2.3.1 HE and reticulin 56
3.2.3.2 Sirius Red 60
3.2.3.3 C4d immunohistochemistry 61
3.2.3.4 Quantum dots and T cell immunostaining 64
3.2.3.5 Conventional immunofluorescence and B cell staining 83
3.2.4 Image Analysis 96
3.2.4.1 Collagen proportionate area 96
3.2.4.2 Qdots cell counts 97
3.2.4.3 Conventional immunofluorescence 100
3.2.5 Statistical analysis 107
3.3 RESULTS 109
3.3.1 Clinical data 109
3.3.2 Initial histological assessment (HE and reticulin staining) 112
3.3.3 Comparison of fibrosis assessment: conventional and digital 123
3.3.4 Fibrosis, inflammation and clinical parameters 126
3.3.5 DSA: general results 129
3.3.6 DSA and clinical parameters 130
3.3.7 DSA, inflammation and fibrosis 133

3.3.8 C4d immunohistochemistry 138
3.3.9 DSA and C4d immunohistochemistry 141
3.3.10 C4d and Inflammation 142
3.3.11 C4d and fibrosis 145
3.3.12 C4d in combination with DSA and Inflammation 148
3.3.13 C4d in combination with DSA and fibrosis 151
3.3.14 Inflammatory cells: general results 154
3.3.15 Inflammatory cells and Fibrosis 155
3.3.16 Inflammatory cells and DSA 157
3.3.17 Inflammatory cells and C4d 157
3.3.18 Inflammatory cells and DSA combined with C4d 160
3.3.19 Expression of granzyme B by B cells 163
3.4 DISCUSSION 167
3.4.1 Overview 167
3.4.2 Value of collagen proportionate area 173
3.4.3 DSA 174
3.4.4 C4d 176
3.4.5 AMR and DSA in combination with C4d 179
3.4.6 Central perivenulitis and centrilobular fibrosis 182
3.4.7 Quantification of inflammatory cells 184
3.4.8 Local role of B cells 185
3.4.9 Summary 187
4 FOR CAUSE BIOPSIES WITH REJECTION 189
4.1 RATIONALE FOR STUDYING FOR CAUSE BIOPSIES WITH REJECTION 189
4.2 MATERIAL AND METHODS 189
4.2.1 Patients and Data 189
4.2.2 Histology 190
4.2.3 DSA testing 191
4.2.4 RNA extraction 191
4.2.5 RNA sequencing and analysis of gene expression data 192
4.2.6 Statistical analysis 192
4.3 RESULTS 193
4.3.1 Demographic Data 193
4.3.2 DSA: overall results 197
4.3.3 DSA and clinical parameters 200
4.3.4 Histology 203
4.3.4.1 HE and reticulin assessment 203
4.3.4.2 C4d immunohistochemistry 206
4.3.5 DSA and Histology (HE and reticulin) 208
4.3.6 DSA and C4d immunohistochemistry 213
4.3.7 C4d and inflammation 215
4.3.8 C4d and fibrosis 218
4.3.9 C4d and other histological parameters 221
4.3.10 C4d with DSA and inflammation 221
4.3.11 C4d with DSA and fibrosis 225
4.3.12 Criteria for acute AMR 228

4.3.13 Gene expression 239
4.4 DISCUSSION 240
4.4.1 Overview 240
4.4.2 DSA 245
4.4.3 C4d and DSA combined with C4d 250
4.4.4 Summary 253
5 CONCLUSION 256
6 REFERENCES 265
7 PERSONAL BIBLIOGRAPHY 281

1 INTRODUCTION

1.1 Background

1.1.1 Long-term allograft histology

Since first performed by Starzl and colleagues in 1963[1], human liver transplantation (LT) has advanced dramatically and is now well established as the treatment of choice in patients with severe chronic and acute liver diseases of several aetiologies[2-6]. In the United Kingdom, over a thousand LTs were conducted in the year April 2017 to March 2018[7].

Over the last decades, advances in organ preservation, surgical techniques, selection of candidates and donors, critical care, and immunosuppression have immensely improved the outcome for transplant patients[8-10]. This improvement has essentially been related to a reduction of complications in the first 12 months post-transplantation[8,10-11]. In addition, the new generation of antivirals should decrease considerably the incidence of viral hepatitis C recurrence following LT[12].

In this context, the physical integrity of the allograft in the long-term, as well as conditions that interfere with it outside the spectrum of recurrent viral hepatitis, have increasingly gained relevance[12-13]. Histopathological assessment of liver allograft biopsies plays an important role in patient management after LT, particularly in the context of subclinical allograft injury, as it provides relevant information not available through peripheral blood tests or molecular analysis[14-16].

In the last decade, long-term follow-up studies have shown that liver allograft biopsy specimens obtained years after transplantation frequently display inflammatory changes of chronic hepatitis that cannot be ascribed to a particular cause, termed ‘unexplained chronic hepatitis’ or ‘idiopathic post-transplant chronic hepatitis’ (IPTH)[17-22]. Its prevalence increases with time after LT, with an incidence of about 60% at 10 years post-transplantation[20,23].

The histological picture of IPTH includes a predominantly portal-based mononuclear inflammatory infiltrate, interface hepatitis, and lobular inflammation, in the absence of bile duct damage, ductopenia or obvious endotheliitis[2,23-25]. Some authors believe that IPTH could represent a form of rejection[20,23-24,26]. Late episodes of acute T-cell-mediated rejection (TCMR), occurring several months post-transplant, frequently present particular histological changes distinct from those of early acute rejection. These changes include milder, mostly lymphocytic inflammatory infiltrate and lack the classical features of TCMR such as obvious bile duct injury and endotheliitis. These histological features overlap with those of IPTH, chronic viral hepatitis and autoimmune/*de novo* autoimmune hepatitis[21,23-24,26-27].

Importantly, IPTH is associated with progressive fibrosis, leading to advanced stage fibrosis/cirrhosis[23]. Seyam and colleagues[26] found that nearly 40% of adults who developed cirrhosis after liver transplantation had no obvious aetiology for the fibrosis, and previous biopsies of all of them showed IPTH. Fibrosis is also a very common finding of late post-transplant biopsies, especially in children[14,23,28-31].

Liver fibrosis is the liver wound healing response to recurrent or continuing injury and results from disproportionate accumulation of

extracellular matrix proteins, particularly collagen[32]. It typically happens in chronic liver disease, in an attempt of the liver to heal from repeated injury[32,33]. When acute liver damage occurs, liver cells usually regenerate, inflammatory cells effectively remove cellular debris, and some remodelling of the extracellular matrix happens. If injury persists chronically, however, the regenerative process might not be able to replace lost tissue. In that case, excessive collagen is deposited in portal tracts, lobule and/or surrounding central veins, creating fibrous septa and changing the liver architecture[33]. Thus, the development of fibrosis is a natural but harmful process that happens in the progression of chronic liver disease[34-35].

Scoring methods exist to quantify liver fibrosis. The suitability of traditional scoring systems such as METAVIR[36] and Ishak[37] for quantifying fibrosis in liver allografts has been questioned, since these systems were designed to evaluate fibrosis in native livers with chronic viral hepatitis[36-39]. The scores were created to stage livers in which the fibrogenic process is primarily portal-based and only affects the lobule and perivenular region in advanced stages. In liver allografts, however, the process of collagen deposition can target both portal and central/perivenular areas or even be mostly directed against the latter, especially in the paediatric population[40-41].

In the transplantation setting, Venturi and colleagues[42] proposed a new scoring system specifically designed to quantify fibrosis of liver allografts of children. It includes the staging of fibrosis in three compartments: portal tracts, central veins (zone 3), and sinusoids (zone 1 and 2). The detailed system is depicted in

Table 1.

Although the LAFSc[42] system proposed by Venturi and colleagues has the advantage of assessing fibrosis in three compartments, it does not rank portal fibrosis in a detailed manner as does the Ishak system. For instance, early bridging fibrosis and end-stage cirrhosis are classified equally at the same "level" of portal fibrosis (stage 3) by the LAFSc, whilst in the Ishak system, they are assigned to considerably different categories (stage 3 and stage 6, respectively).

Table 1. **Liver graft fibrosis semiquantitative scoring system (LAFSc)**[42]

Region/ Structure	0	1	2	3
Portal	No fibrosis	Portal fibrosis in <50% of portal tracts	Portal fibrosis in >50% of portal tracts or periportal fibrous septa	Bridging fibrosis (portal-portal and/or portal-central) with or without nodules
Centrilobular vein (zone 3)	No fibrosis	Circular perivenular fibrosis in <50% of central veins	Circular perivenular fibrosis in >50% of central veins or fibrous septa into perivenular parenchyma	Marked perivenular fibrosis with bridging (central-central and/or central-portal)
Sinusoids (zone 1,2)	No fibrosis	Thin collagen deposits in <50% of sinusoids	Thin collagen deposits in >50% or thicker fibrosis in <50% of sinusoids	Thick, diffuse sinusoidal fibrosis

An additional possibility for staging fibrosis in the liver allograft is to digitally quantify the ratio of fibrosis in relation to the whole biopsy area, termed

collagen proportionate area (CPA), by image analysis of the biopsy slides. For this digital quantitative assessment, it is necessary to apply a staining for collagen with good contrast between positivity and background, such as Sirius Red (Picrosirius red).

Some authors suggest this is a more robust method to assess liver fibrosis than conventional scores, with less inter-observer variability and better correlation with clinical outcome[43-47]. Of note, most of the studies that have employed CPA to quantify fibrosis were performed in native liver samples, and a few in liver allografts with recurrent viral hepatitis[43,47-49]. Therefore, digital quantification of fibrosis through CPA is still not well-established in the assessment of fibrosis post-transplantation for a vast range of allograft conditions.

In the last decade, several studies from different centres have reported high prevalence of fibrosis in late post-transplant biopsies, especially of paediatric liver recipients, including patients with normal liver biochemistry[23,28,41,50-51]. Some authors have suggested that fibrosis in these patients might be a result of late rejection, which can have a humoral component[52-53], but this hypothesis needs further confirmation.

1.1.2 Donor-specific antibodies and antibody-mediated rejection in the liver graft

Donor-specific antibodies (DSA) are antibodies developed by the transplant recipient which can react against molecules present in the donor organ, causing tissue damage. The deleterious effects of DSA, particularly those produced against donor HLA molecules, for the allograft and their

negative impact on transplant outcome have been consistently recognized in most solid organ transplantation settings[60-66].

DSA can be present prior to transplantation (preformed or pre-existent DSA) or can be produced after the donor organ is implanted (*de* novo DSA). In the former, they are produced in response to previous sensitisation of the recipient with foreign antigens during blood transfusion, pregnancy or former transplantation[76-77]. Preformed DSA that continue to be detected after transplantation are called persistent. Anti-HLA DSA can be directed towards class I or class II HLA molecules.

In contrast to what has been described in kidney, pancreas, and heart transplantation, until recently the liver allograft was considered resistant to injury caused by DSA[21,54-57]. Several factors contribute to this immunological peculiarity, including:

1) large hepatic sinusoidal surface which dilutes pre-formed antibodies;

2) secretion of soluble class I HLA (human leukocyte antigen) antigens by the allograft, that bind to recipient alloantibodies forming immune complexes that are then phagocytised by Kupffer cells;

3) the ability of Kupffer cells to clear not only immune complexes, but also platelet aggregates, activated complement and antibodies;

4) restricted expression of HLA class II molecules in the liver microvasculature;

5) the marked ability of the hepatocyte to regenerate after injury;

6) continuous contact with intestinal microbial products leading to a tolerogenic setting with low HLA II expression[12,57-59]. Some of these mechanisms are depicted in Figure 1 (extracted from Taner et al, 2014[57]).

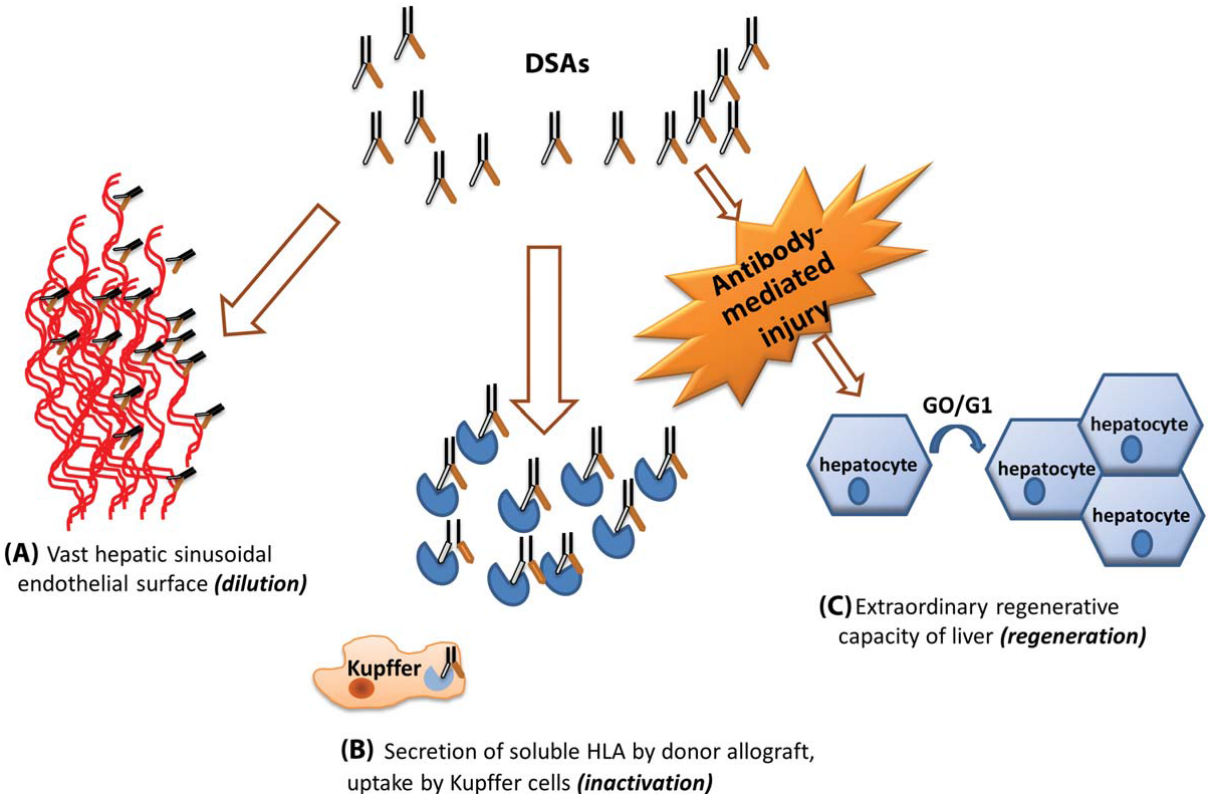

Figure 1. **Mechanisms behind the liver graft resistance to injury mediated by donor-specific antibodies (Taner et al, 2014)[57]**

More recently, a number of reports have described associations between circulating DSA, particularly *de novo* DSA, and liver tissue injury, including acute and chronic rejection, fibrosis, chronic inflammation, overall allograft outcome, biliary complications and the failure to develop operational tolerance[21,28,55,57,67-75]. Despite these associations, a pathogenic role for DSA in acute and chronic allograft damage has not been unambiguously established in liver transplantation.

Whereas preformed DSA seem to have significant effect on the outcome of other transplanted organs, such as kidney and heart, in the context of liver transplantation, most pre-existent DSA, especially against class I HLA antigens, disappear soon after transplantation with no obvious allograft

damage[58]. Pre-existent DSA of high MFI, especially class II, are more likely to persist and are associated with higher risk of TCMR, and possibly, combined TCMR and antibody-mediated rejection (AMR)[58,80-81].

The low frequency of anti-class I HLA DSA post-liver transplantation could be linked to the vast physiological expression of HLA I in all liver cell types (it is only weaker in hepatocytes)[58,82-83]. As mentioned above, soluble class I HLA is secreted by the liver graft and inactivated by Kupffer cells[57]. On the other hand, the expression of HLA II in normal livers is restricted to dendritic cells in portal, perivenular and subcapsular regions[84]. The lower expression and secretion of class II HLA could lead to less efficient clearing of these antibodies in the liver graft[12].

De novo DSA develop in 8-15% of patients who undergo liver transplantation, most commonly towards the class II HLA-DQ isotype[85-86]. Since DQ is the HLA molecule with the lowest expression in the liver, the higher frequency of anti-HLA-DQ DSA might result from the liver incapability to absorb and remove it from the circulation[86]. Another factor that may contribute to the higher prevalence of HLA-DQ antibodies is the fact that the genes that encode both the α and β chains of HLA-DQ are polymorphic, in contrast to what happens with other HLA class II proteins such as HLA-DR, which are polymorphic only in the β chain[87].

Since the development of the original assays capable of detecting circulating anti-HLA antibodies, which were based on complement-dependent cytotoxicity (CDC), the detection of these antibodies has greatly improved. The assays have evolved from the use of donor cell-based methods to current solid-phase immunoassays, such as the Luminex platform, that enables

specific and semiquantitative detection of HLA antibodies[57,78]. In this method, the strength of the binding between an anti-HLA antibody and its antigen is measured through the mean fluorescence intensity, or MFI[79].

Despite associations between circulating DSA and graft injury, at present the diagnosis of AMR in the liver is not as well established as it is for kidney, heart and lung allografts[88]. In fact, until recently, there were no consensus histological criteria for the diagnosis of acute AMR in the liver[59]. Recently, the Banff study group on allograft pathology proposed diagnostic criteria for acute AMR in the liver, comprising circulating DSA, tissue C4d staining, compatible histology and the exclusion of other causes that may produce similar injury[89].

It is possible that some histological features previously attributed to TCMR, such as mixed inflammatory infiltrate including eosinophils, may correspond to a combination of TCMR and AMR[59]. Combined TCMR and AMR is common in rejection episodes across a variety of solid organ allografts, and the same overlap has been described in the liver setting[59,90]. In fact, the lack of adequate criteria to accurately differentiate TCMR and AMR makes it difficult to diagnose liver AMR outside of the early post-transplant period, making it challenging to establish or refute a role for humoral rejection in patients with late acute or chronic graft injury[57,59,91].

Inflammatory insults such as TCMR or recurrent hepatitis C induce/upregulate the expression of HLA molecules in the liver allograft (particularly class II expression in endothelial cells, biliary cells and hepatocytes)[92-93], leading to or increasing DSA production and consequently antibody-mediated injury[12,58,94]. This mechanism explains why acute AMR

can improve with treatment not specifically directed at antibodies, since the decrease in inflammation downregulates the expression of class II HLA in the liver[12,58].

Chronic AMR normally manifests as an indolent injury, with low-grade lymphoplasmacytic inflammation in portal and perivenular sites, subclinical progressive fibrosis in patients with normal/mildly abnormal liver biochemistry, and with variable C4d positivity on immunohistochemistry[58,95-96]. Chronic AMR in the liver allograft is likely to be more prevalent than previously thought[28,95].

In 2016, the Banff group first proposed diagnostic criteria for chronic AMR in liver allografts. Similar to acute AMR, diagnosis was based on DSA, C4d, histology and exclusion of other injuries[53]. However, in comparison with the diagnostic criteria for acute AMR, the histological parameters of chronic AMR are less specific and less well validated, making this diagnostic challenging[88]. The range of pathological manifestations and consequences of potential AMR in patients with chronic liver injury is in need of additional study[28,97].

C4d is a complement split product whose presence marks activation of the classical/lecithin pathway of the complement cascade. It is an established marker of AMR in kidney and heart transplantation[99]. The fact that C4d binds to tissue near the spot of activation, by a covalent bond that does not normally break, make this marker suitable for recognition through immunohistochemistry in transplantation[99]. However, the sensitivity of C4d immunohistochemistry in formalin-fixed, paraffin embedded (FFPE) biopsy

specimens as a marker of antibody-mediated damage is lower outside of the early acute AMR setting[58,98-99].

The inclusion of C4d immunostaining in the transplantation setting allowed direct visualization of the link between DSA and tissue injury at places where antibodies bind in grafts. This produced growing interest in antibody-mediated mechanisms and their involvement in rejection[100]. C4d might also work as a biomarker to help identify patients at risk of antibody-mediated injury/disease in other contexts, such as autoimmune diseases and pregnancy[100].

Tissue immunostaining for C4d is currently required for the diagnosis of AMR in all solid organ allografts. Nevertheless, its functional significance and diagnostic utility in the liver transplantation have never been as well established as in cardiac and renal allografts[21,101]. Some studies have questioned the reliability of C4d in fixed tissue sections and suggested that immunofluorescence (IF) on frozen tissue should be the gold standard[102]. However, in most centres, only FFPE tissue sections are available for immunostaining. Other authors have described different patterns of C4d positivity to be associated with AMR[55,97,103].

A recent multicentre study on C4d staining of FFPE liver graft biopsies found that strong, diffuse C4d staining in portal veins and portal capillaries was recognisable in typical cases of acute AMR[98]. Nonetheless, this study only included gold standard cases: typical acute AMR leading to graft failure within the first month post-transplantation. The performance of C4d staining in cases of AMR outside of the classical early acute context has not been properly approached[88,98,104].

The process of AMR involves activation of B cells and plasma cells, which produce antibodies that bind to HLA (and less frequently non-HLA) molecules present in the graft[56,88,105]. Acutely, these antibodies lead to complement fixation, causing tissue damage and coagulation, and activation of complement also stimulates macrophages and neutrophils which further injure the endothelium[55,61]. Moreover, antibodies and complement seem to induce gene expression in endothelial cells, causing arteries and basement membrane remodelling that results in permanent anatomical damage and compromise graft function irreversibly[61].

1.1.3 B cells, plasma cells and a possible local role

At present, little is comprehended about the role of B cells in native and grafted liver, probably due to the small number of resident B cells in healthy liver and the consequent difficulty of experimentally isolating and analysing them[106]. B cells mature in the bone marrow, and their activation, differentiation and proliferation happen inside lymphoid follicles in secondary lymphoid organs, including lymph node, tonsil, spleen, and mucosal lymphoid tissue[107-108].

The classical role attributed to B cells is participation in humoral immunity. The process starts when B cells inside lymphoid follicles are activated by antigens, receive T-cell help, form germinal centres and differentiate into plasma cells that secrete antibodies, or into memory B-cells[108]. More recent studies have suggested antibody-independent roles for B cells, including secretion of inflammatory cytokines, antigen presentation and regulation of T cells and dendritic cells[109].

The research of Novobrantseva *et al.*[110] on liver regeneration following acute injury found that B cells were required for the development of fibrosis, and B cell–deficient mice had markedly reduced collagen deposition compared to controls. Interestingly, the effects of B cells on liver fibrosis were antibody-independent, as mice with normal B cells but no immunoglobulin had similar collagen deposition as controls. T cells did not have a role in that particular model of liver fibrosis, as T cell-deficient mice showed similar fibrosis as the control group[110]. Thus, the role of B cells in liver fibrosis seems to be mediated by local mechanisms.

A link between B cell activation and fibrosis has also been verified in humans with systemic sclerosis. Characteristic B lymphocyte gene signatures were found in skin biopsies of patients with this disease[112]. Abnormally enhanced B cell proliferation was also demonstrated in lung tissue affected by systemic sclerosis[113]. Additionally, a study demonstrated that human B cells can express granzyme B (GrzB) after stimulation (vaccination) with viral antigens[114].

The GrzB molecule consists of a cytolytic granule protein with proapoptotic effects, classically associated with effector cells such as CD8+ T cells and natural killer (NK) cells, and it had not previously been observed in B lymphocytes. It was postulated that expression of GrzB by B cells corresponded to a mechanism for an early immune response to certain viral infections, capable of inducing viral cell death, while T cells are still being recruited[114]. GrzB-secreting B cells were also found to induce tumour cell apoptosis by delivering GrzB to neoplastic cells. Additionally, roles alternative to apoptotic have been attributed to granzymes, such as matrix degradation

or remodelling[114-116]. These extracellular functions could explain the relationship between B cells and fibrosis.

A recent study found that the majority of plasma cells in human tonsils express GrzB[117-118]. Through immunofluorescence, the authors verified both immunoglobulin and GrzB expression in different cellular compartments within the same plasma cell. This finding could potentially reflect a local role for plasma cells, challenging the traditional idea that these cells only act by secreting antibodies that act remotely.

Plasma cells have classically been considered essentially as a short-lived end-stage product of the B cell differentiation line[108]. This idea is changing, as plasma cells have now been shown to live for long periods of time in appropriate survival niches such as inflamed tissue, lymphoid organs and bone marrow, and they play a role in immunological memory. This means that plasma cells present in damaged liver grafts are capable of surviving for long periods and could possibly have local roles besides producing antibodies[108]. Although it has been hypothesized that the presence of B cells and particularly of plasma cells may be implicated in the development of fibrosis associated with IPTH in liver grafts[18], this relationship has not been investigated.

1.1.4 New technologies

Currently, biopsy assessment represents the gold standard method for evaluation of liver allograft health. It is particularly important to detect subclinical injuries such as inflammation and fibrosis, and to direct the management of immunosuppressive therapies[13,119-121]. Several technologies

are emerging as important complementary tools in the study of hepatic pathology, such as multiplex staining with Quantum dots, microarray high throughput gene expression profiling and more recently, next generation RNA-sequencing.

These new methods have the potential to greatly improve the information that can be obtained from histology[122]. Furthermore, they can help understand the immunological mechanisms of tissue injury and of allograft acceptance and will eventually be incorporated into the routine histology workflow and very likely exert a transformative impact in the field [122].

In the last decade, quantum dots (Qdots) have increasingly been used in histology. Qdots are non-organic fluorophores that consist of semiconductor nanocrystals with singular optical properties in comparison to organic fluorophores(Tholouli, 2008 #72). They have exceedingly high fluorescence efficiency, wide excitation range of wavelengths and narrow, symmetric emission spectra due to their defined crystalline structure[123]. Because most atoms in each Qdot crystal are excited simultaneously, the result is a strong emission signal.

The advantages of quantum dots over conventional fluorophores used in routine immunofluorescence include brighter emission signals, minimal photobleaching, and the ability to permanently mount and store the slides conventionally without significant signal loss[16,123-124]. These distinctive optical properties make them near-perfect fluorescent markers, and there has been rapid development of their use for bioimaging[16,124]. Furthermore, the ability of Qdots to be conjugated to a variety of biological targets, such as antibodies

conventionally used for immunostaining, is of particular relevance to histology research[124].

All these features have attracted increasing interest over recent years in the use of Qdots. In particular, their narrow emission wavelength enables the combination of various distinctive Qdots to different antibodies, thus allowing multiplex immunostaining for quantification and co-localization of up to 5 antigens simultaneously in a single tissue section[16,123]. This is a key advantage of Qdots when compared to conventional immunohistochemistry, which usually allows quantification of one or two antigens per tissue section. It is particularly useful for classifying and quantifying different cell populations in a biopsy.

A recent study observed that, in addition to superior brightness and photostability when compared to organic fluorophores, Qdots show less autofluorescence due to the lower wavelength excitation needed to obtain a signal[125]. These fluorophores are both sensitive and specific, even for tissues usually viewed as problematic due to high autofluorescence, such as liver and kidney[125]. The research concludes that Qdots, with an appropriate light source and detection system, may be the best choice for multiplex immunostaining and quantification of molecular signals on FFPE tissue sections[125].

Genetics and molecular biology have also undergone a massive revolution in the past few decades. Progress in chemistry and engineering have enabled faster and more accurate study of large sets of genes and their products through techniques such as genomics, transcriptomics, metabolomics and proteomics[126]. The development of high-throughput

technologies and matching computational analyses have led to important changes in gene expression studies, which have expanded from the measurement of few transcripts at a time to the analysis of whole genome transcriptomes[127].

In the last decade, microarray technology has been used to study transplantation, research T-cell mediated acute rejection and chronic rejection, and identify the gene signatures of operational tolerance[128]. The aim of microarray studies is to compare gene expression between two different groups with a single difference (rejection versus no-rejection), and results may be used to predict which patients might have a particular outcome/condition (i.e, rejection, tolerance) based on their gene expression profile[128-129].

Microarray experiments provide expression levels for thousands of genes, generating vast amounts of data. The complexity of the resulting data is due both to the high number of genes evaluated per sample and to the disparity between the number of genes and relatively small number of samples usually analysed in most experiments[126,128]. These complex datasets cannot be properly analysed using traditional comparative statistics and require appropriate bioinformatics/biostatistics knowledge, team work, and familiarity with relevant software to ensure good criteria for quality control, classification, normalization, clustering and pathway analysis[128]. The conventional p value for reliability is replaced by q-value (called false discovery rate, FDR), another adjustment necessary for the analysis of high-dimensional datasets that takes into account the problems posed by multiple hypothesis testing[126].

Microarray has produced significant data in transplantation research and has been the main method for profiling large-scale gene expression until

a few years ago. Nevertheless, this technology has limitations, including the requirement for previous knowledge about genome sequences, high levels of background noise due to cross-hybridization and the limited dynamic scope of gene detection (it is easier to detect signals from highly expressed genes) because of signal background and saturation. Additionally, the comparison of levels of gene expression between different experiments is challenging with the data requiring complicated normalization[129].

The more recent emergence of next-generation sequencing (NGS) technologies, particularly RNA sequencing (RNA-Seq) for mapping and quantifying transcriptomes (complete sets of transcripts in a cell), has clear advantages over microarrays and is likely to further revolutionize transcriptomic analysis[127,129-130].

In RNA sequencing, small RNA fragments are isolated and purified and then converted to a library of cDNA fragments with adaptors attached to the end or both ends of each fragment[127,129]. The cDNA molecules in the library are identified by high-throughput sequencing and overlapping short sequences are obtained. These resulting reads are aligned with a reference genome or transcriptome to produce a base-resolution profile of expression for each gene. They can also be assembled *de novo* in order to create a genome-scale transcription map containing the structure and expression level of each gene[127,129]. The sequencing process involves millions of parallel reactions, and RNA-Seq allows fast sequencing of large sections of RNA or DNA covering entire genomes[131].

The advantages of RNA-Seq over microarray include higher reliability, higher specificity, more effective detection of rare or low abundant transcripts,

larger dynamic range (it can quantify small sequencing reads), unbiased recognition of new transcripts (since there is no need for transcript-specific probes), and elimination of the risk of probe design errors, which are reasonably common in microarray[128-129]. In fact, RNA-Seq represents the first sequencing-based technology which enables examination of the entire transcriptome in a highly automated and quantitative way[129].

The technical advances in the last years have also enabled complex molecular analysis of suboptimal biological material, such as formalin-fixed, paraffin-embedded biopsy specimens. Currently, next-generation technologies, including RNA-Seq, can be effectively applied to archival diagnostic FFPE tissue. Two recent studies have analysed human FFPE biopsy specimens of prostate cancer using two different gene expression platforms (Ion AmpliSeq Transcriptome Human Gene Expression Kit and Affymetrix Human Exon 1.0 ST GeneChip). They demonstrated that very small quantities of RNA (a few nanograms) obtained from FFPE diagnostic biopsy specimens can generate high-quality data enabling successful gene expression profiling[132-133]. Other recent studies have also successfully analysed gene expression in human tissue obtained from FFPE sections using Ion AmpliSeq gene expression platform[134-137].

Londoño *et al.* recently studied protocol biopsies of adult liver recipient grafts that were more than 10 years old, and were able to correlate histology with molecular analysis[138]. The gene expression profiling was assessed using RNA-Seq (Ion AmpliSeq platform) on RNA obtained from recipient FFPE liver biopsies. The authors found that inflammatory subclinical injury, which was present in 67% of patients, was associated with gene expression profiles

indicating TCMR. More specifically, portal inflammation, interface hepatitis and portal fibrosis were correlated with up-regulation of genes previously known to be associated with TCMR molecular pathways. Interestingly, the patients who had the highest levels of rejection-related genes developed progressive graft fibrosis during follow-up. However, fibrosis during follow-up was measured indirectly through transient elastography, not on biopsy.

1.2 Research gap

A review of the literature indicated a need for further research on long-term histological changes in liver allografts, particularly idiopathic post-transplant hepatitis and fibrosis. Study is needed to clarify correlation of these conditions with circulating DSA, tissue C4d staining and gene expression patterns. Moreover, while it is documented that IPTH is associated with fibrosis and potentially leads to allograft failure, there are few if any studies investigating patterns of injury in failed liver grafts removed at retransplantation that gauge the impact of IPTH. There is also a shortage of research analysing specific inflammatory cell types in long-term liver allograft biopsies (such as T cell subsets, B cells and plasma cells) and correlating those with histological parameters and signs of humoral injury. While a potential local role for B cells and plasma cells is indicated, expression of granzyme B by these cells has not yet been investigated in human liver. Finally, there has been growing interest in DSA in liver transplantation, but the effector role of these antibodies in mediating acute and chronic graft damage remains contentious in the liver allograft. Despite advances in the use of RNA

sequencing in transplantation, there are no studies using next-generation sequencing to investigate gene expression patterns in liver recipients with and without DSA.

1.3 Research Hypothesis

DSAs have a pathogenic role in acute and chronic liver graft injury; AMR is involved in the development of idiopathic post-transplant hepatitis and graft fibrosis leading to graft failure, and possibly in some cases of T-cell mediated rejection. B cells and plasma cells may have a local role linked to the development of graft fibrosis. Gene expression analysis could deliver greater understanding of long term liver graft injury.

1.4 Research aims

An opportunity to study liver transplantation histology in patient cohorts at King's College Hospital prompted research based on the above discussion. The following research aims were defined:

- Investigate whether idiopathic post-transplant hepatitis can progress to liver allograft failure
- Characterise long-term protocol biopsies histologically, including the inflammatory cell population, and correlate histological parameters with DSA and C4d
- Verify whether the associations present in protocol biopsies are also present in for-cause biopsies with rejection
- Investigate expression of granzyme B by B cells and plasma cells

- Analyse whether the presence of DSA, or association with tissue C4d staining, is linked with specific histological findings and molecular profiling in the context of T-cell-mediated rejection and of long-term subclinical graft damage.

1.5 Studies on three liver transplant patient cohorts

The current chapter introduced the research hypothesis and aims of this study, based on a review of the literature. The subsequent research involved three distinct patient cohorts, approached using different methods and showing distinct results, therefore a specific chapter is dedicated to each cohort, with respective methods, results and discussion (Chapters 3-5).

Chapter 2 consists of a study on the causes of allograft failure based on liver recipients who underwent retransplantation at King's College Hospital over a period of 27 years. Chapter 3 contains a detailed study of long-term liver protocol biopsies of children, emphasizing AMR and the link between inflammation, fibrosis, DSA and C4d. Chapter 4 is a study of for cause biopsies with rejection and compares histology, DSA and gene expression.

In Chapter 5, the connections between the three study cohorts are discussed and final considerations and conclusions made. The final sections are: Bibliographic References and Personal Bibliography.

1.6 Ethical approval

Ethical approval was obtained to use archival FFPE liver biopsies from King's College Hospital patients from the National Research Ethics Service Committee London: King's College Research Ethics Committee REC 05/Q0703/239. For DSA testing, liver recipients' serum samples from the Institute of Liver Studies paediatric biobank were used. Biobank samples are obtained with appropriate consent in place for clinical and research use.

2 FAILED LIVER ALLOGRAFTS

2.1 RATIONALE FOR STUDYING EXPLANTED ALLOGRAFTS

The first stage of the current research consisted of investigating the causes of graft failure leading to retransplantation from the histological perspective, and to examine possible changes in histology with the evolution of clinical care and immunosuppression throughout the years. An analysis of failed allografts was made, because they represent the endpoint of several pathogenic processes affecting the transplanted liver and because the amount of tissue available allowed a more detailed and accurate histological assessment in comparison to needle biopsies. A review was made of the histology of all liver allografts that were removed at retransplantation at King's College Hospital, in a period from the beginning of the transplantation programme in 1987 until 2014. This study has been published in *Clinical Transplantation* in 2017[139].

2.2 MATERIAL AND METHODS

2.2.1 Patients and Data

The first study was drawn from all patients submitted to liver retransplantation at least once at King's College Hospital from January 1987 to April 2014. The initial selection was made using the Institute of Liver Studies[139] histology electronic database, which allows searching of histological reports by specimen type. Because the electronic records were

introduced from 2000, the histology paper archive was also searched for histological reports of grafts removed from 1987 to 1999. To ensure all failed allografts were included, another researcher examined the paper files independently. In order to ensure accuracy of the data retrieved, the information from the histology reports was compared with the Liver Transplant Coordinator's list of liver recipients. Additional information was retrieved as necessary using the Electronic Patients Records (EPR) and the Institute of Liver Studies Clinical Electronic Database (Liverware). Histological slides were reviewed by two pathologists (L.N.S. and A.Q.) in those cases without a well-defined diagnosis or with conflicting histology and clinical information.

The following clinical data on each patient/graft was included: recipient's gender and age, reason for primary transplantation and retransplantation, time spent between the primary and subsequent transplant(s) and the date of regraft. All liver recipients who were at least 17 years old at the time of the primary transplant were considered adults, and those who were younger, children. In order to examine possible changes in the histology of failed grafts over the years, the study was divided into three eras: era A, from 1987 to 1994; era B, from 1995 to 2001 and era C, from 2002 to 2014. The division into eras was intended to reflect progress in immunosuppression as well as the centre's increasing expertise in LT.

In the first era, the initial standard immunosuppressive regime in adults and children was cyclosporine, azathioprine and steroid. The latter was withdrawn 3 months following transplantation in adults in all eras, except in those patients with primary autoimmune liver disease. In the second era, adult recipients received cyclosporine or tacrolimus, according to aetiology of liver

disease or involvement in a randomised controlled trial, and steroid for 3 months (or indefinitely for patients with autoimmune disease). In both eras B and C, paediatric patients were given tacrolimus and steroid, and the dose of steroid in children was reduced to 0.01mg/kg after 3 weeks of transplantation. In era C, adult recipients received tacrolimus, and 3 months of steroids (Table 2). Specific antibodies were used electively in eras B and C in approximately 20% of patients. The following drugs were used on individual cases: mycophenolate, sirolimus, basiliximab, anti-thymocyte globulin (ATG), and a bolus of high-dose corticosteroid followed by mono/polyclonal antibodies.

Table 2. **Standard immunosuppression in each era in adults and children**

Era	Adults	Children
A (87-94)	CsA + AZA (+ 3 months of steroid)*	CsA + AZA + steroid
B (95-01)	CsA + AZA **or** TAC (+ 3 months of steroid)*	TAC + steroid
C (02-14)	TAC (+ 3 months of steroid)*	TAC + steroid

CsA, cyclosporine; AZA, azathioprine; TAC, tacrolimus

** Steroid was continued indefinitely in adult recipients who underwent transplantation for autoimmune liver disease*

2.2.2 Histology

For each failed allograft removed at retransplantation, the complete histological report was reviewed. The report included the pathologist's macroscopic and microscopic description of the specimen, diagnosis and comments. The latter usually consisted of the link that the pathologist had

made between histological findings and clinical setting, questions and requests for further information and/or suggestions for other conditions to investigate.

Failed grafts were classified into one of the following categories: **Hepatic artery thrombosis**: clinical diagnosis of hepatic artery thrombosis, documented by imaging, and compatible histology; **Chronic rejection**: histology showing chronic ductopenic rejection fitting the Banff criteria[165]; **Acute rejection[166]**: acute TCMR on histology meeting the Banff criteria[167]; **Recurrent**: clinically recurrent primary liver disease and corresponding histology; **Primary non-function (PNF)**: early graft failure and acute liver injury histologically with no recognizable technical or immunological aetiology; **Biliary**: clinical diagnosis of cholangiopathy documented by imaging and confirmed histologically without concomitant hepatic artery thrombosis (ischaemic cholangiopathy secondary to HAT was considered into the HAT category); **Miscellaneous**: graft loss for a well-defined condition that did not fit into one of the previous categories, such as venous thrombosis, haemorrhage leading to ischaemia, post-transplant lymphoproliferative disorder and liver abscesses with biliary sepsis combined to hepatitis B recurrence; **Unknown**: idiopathic graft failure despite review of histological and clinical data; **IPTH**: cases clinically labelled as chronic graft dysfunction, with histology showing unspecific, mostly lymphocytic inflammation and concomitant fibrosis (at least bridging/Ishak stage 3), with no obvious aetiology for the graft injury despite review of clinical records and biopsy slides. These cases were not classified into the unknown category because they shared a particular pattern of damage, distinct from the other grafts in that category.

The histology of these grafts was further examined by reviewing both the explanted grafts and previous biopsies from those patients.

2.2.3 Statistical analysis

Data were analysed statistically using SPSS version 23.0 (IBM Corp, 2015). Continuous variables were presented as median and range whilst categorical variables were presented as number and percentage. The Fisher's exact test was used to compare categorical variables.

2.3 RESULTS

The number of primary liver transplants performed in King's College Hospital between January 1987 and April 2014 was 4236, of which 3298 were in adult and 938 in paediatric recipients. The number of primary transplantations in each era was 741 (era A), 1198 (era B) and 2297 (era C). In total, 8.4% of adults (276) and 12.6% of children (118) experienced successive liver transplantation at least once, receiving 460 allografts. The overall rate of retransplantation remained constant through the eras (10.8%), with 80, 130 and 250 regrafts in eras A, B and C respectively. The average adult recipient age at retransplant was 44.7 years, and average paediatric age 6.8 years. Recipients were half male, half female with a few extra male at 55.5% and 50.7% of adults and children, respectively.

Overall, hepatic artery thrombosis was the main indication for retransplantation in adults (28.8%) followed by liver disease recurrence (21.8%) then chronic rejection (16.5%, Table 3). In paediatric recipients, the

leading reasons for subsequent transplantation were, again, hepatic artery thrombosis (28.8%), but then chronic rejection (18.7%) followed by biliary complications (12.9%) (Table 4). The proportion of retransplantation for other indications in adults and children are detailed in Table 3 and Table 4, respectively.

Table 3. **Indications for retransplantation in adults**

INDICATION	Era A, n (%)	Era B, n (%)	Era C, n (%)	Total, n (%)
HAT	9 (15.3)	24 (26.7)	62 (36.1)	95 (29.6)
Recurrent	11 (18.6)	26 (28.9)	33 (19.2)	70 (21.8)
CR	21 (33.9)	12 (13.3)	20 (11.6)	53 (16.5)
PNF	2 (3.4)	10 (11.1)	15 (8.7)	27 (8.4)
Miscellaneous	5 (8.4)	8 (8.9)	14 (8.1)	27 (8.4)
Unknown	9 (15.2)	3 (3.3)	9 (5.2)	21 (6.5)
IPTH	0 (0)	3 (3.3)	11 (6.4)	14 (4.4)
Biliary	1 (1.7)	4 (4.4)	5 (2.9)	10 (3.1)
ACR	1 (1.7)	0 (0)	3 (1.7)	4 (1.2)
Total	59 (18.4)	90 (28.0)	172 (53.6)	321 (100)

HAT, hepatic artery thrombosis; CR, chronic rejection; PNF, primary non-function; IPTH, idiopathic posttransplant hepatitis; ACR, acute rejection; n, number of retransplantation; %, percentage of retransplantation.

Table 4 (below). **Indications for retransplantation in children**

INDICATION	Era A, n (%)	Era B, n (%)	Era C, n (%)	Total, n (%)
HAT	2 (9.5)	14 (35.0)	22 (28.2)	40 (28.8)
CR	5 (23.8)	11 (27.5)	10 (12.8)	26 (18.7)
Biliary	3 (14.3)	4 (10.0)	11 (14.1)	18 (12.9)
Unknown	4 (19.0)	3 (7.5)	7 (9.0)	14 (10.1)
Miscellaneous	2 (9.5)	4 (10.0)	8 (10.3)	14 (10.1)
IPTH	0 (0)	1 (2.5)	11 (14.1)	12 (8.6)
PNF	3 (14.3)	2 (5.0)	4 (5.1)	9 (6.5)
ACR	2 (9.5)	1 (2.5)	2 (2.6)	5 (3.5)
Recurrent	0 (0)	0 (0)	3 (3.8)	3 (2.2)
Total	21 (15.1)	40 (28.8)	78 (56.1)	139 (100)

HAT, hepatic artery thrombosis; CR, chronic rejection; IPTH, idiopathic posttransplant hepatitis; PNF, primary non-function; ACR, acute rejection; n, number of retransplantation; %, percentage of retransplantation.

Further examination was then made of the two diagnostic categories without an obvious reason for retransplantation: unknown and IPTH. In the unknown group, 94% of the cases (91% of the adults and all the children) presented clinically with acute graft dysfunction, usually in the first weeks post-transplant, frequently referred as non-thrombotic infarct. Histologically, all allografts displayed areas of infarction, usually confluent, in the absence of vascular thrombosis, except in two cases (one had thrombus in large portal vein and hepatic artery branches and the other showed thrombosis of small veins in the hilum).

Concomitant acute rejection was present in half (49%) of the patients with acute unknown graft failure. In 30% of allografts, the centrilobular region was reported as the main site of graft injury (centrilobular cell loss/coagulative necrosis). In a third of patients (36%), AMR was considered in the differential diagnosis but was not established. These cases in particular presented as an acute graft failure in the early post-transplant period and showed massive necrosis and/or obvious arteritis accompanied by moderate to severe cellular rejection.

The remaining minority of cases in the unknown category (5.7%) presented clinically with a chronic graft dysfunction whose cause was not clear after histological examination. Histological findings of their explants included perivenular and bridging cell loss and congestion without fibrosis, thick fibro-adipose adhesions at the liver surface, ischaemic changes, and in one case, vascular changes indicating chronic rejection without associated bile duct injury/loss.

With regards to the failed allografts in the IPTH category, all exhibited a mononuclear inflammatory cell infiltrate on histology, which affected portal tracts, interface and sometimes also centrilobular areas (Figure 8). Two-thirds (65%) of the allografts in this category already had advanced-stage fibrosis with features of cirrhosis[168], whilst a third (35%) had bridging fibrosis without advanced nodular transformation. These failed allografts showed different degrees of inflammatory activity, plasmacytosis, cholestasis and pericentral fibrosis (including centro-central bridging).

Injury to small or large intrahepatic ducts, portal or centrilobular venular endothelium and/or foamy cell arteriopathy were not present, and the overall histological picture was dominated by fibrosis, variable degrees of architectural distortion and chronic hepatitis. There were no specific histological or clinical features to allow diagnosis of specific aetiologies for the process of graft deterioration. Hepatitis E, however, was not tested in many cases and could not be tested retrospectively.

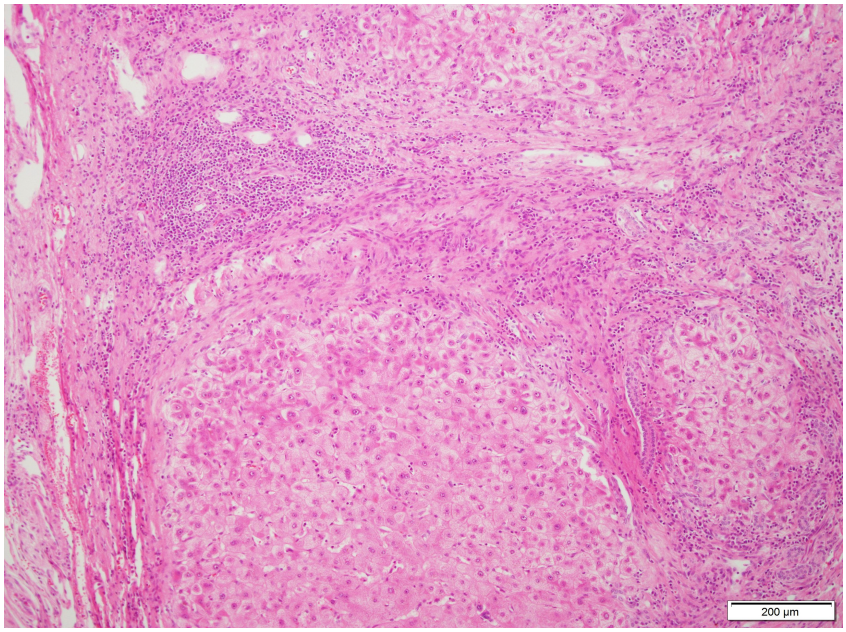

Figure 2. **Failed liver graft, removed 18 years posttransplant for biliary atresia.** *Bridging fibrosis with parenchymal nodular transformation and chronic porto-septal hepatitis (H&E, 100x).*

The analysis of previous biopsies of grafts with IPTH revealed that, besides portal inflammation, most paediatric recipients had former central perivenulitis (75%) and perivenular fibrosis (58%). In adults, the percentage of central perivenulitis was 33%, and perivenular fibrosis 25%. Nonetheless, 50% of adults' grafts already showed advanced stage fibrosis at the time of the first posttransplant biopsy. In these cases, the initial target of the fibrosing process could not be established. By the time of graft removal, 58% of children and 75% of adults in the IPTH hepatitis category showed advanced stage fibrosis.

Considering the eras: the contribution of chronic rejection as a reason for retransplantation decreased steadily in adults, from 34% to 13% and 12% in eras A, B and C, respectively (Figure 3). On the other hand, IPTH hepatitis, which was not an indication for regraft in adults in the first era, accounted for 6.4% of the graft failures

in the last era. Hepatic artery thrombosis also increased as a reason for subsequent transplantation, from 15.3% to 26.7% and 36% in eras A, B and C respectively. The difference in proportion of transplantation for these causes across the 3 eras were statistically significant ($p<0.001$, Fisher's exact test).

The percentage of paediatric retransplantation for chronic rejection increased from 24% in the first to 28% in the second era, and then dropped to 13% in the last era. Similar to the adult group, IPTH hepatitis also showed a consistent rise in children, from none in the first era to 2.5% and 14% of explanted grafts in eras B and C, respectively, becoming the second leading indication for retransplantation in era C, together with biliary complications (Figure 4). Hepatic artery thrombosis accounted for 9.5% of paediatric retransplantation in era A and 28% in era C, being the main reason for regraft in era C. The difference in proportion of transplantation for these causes across the 3 eras were statistically significant ($p<0.001$, Fisher's exact test).

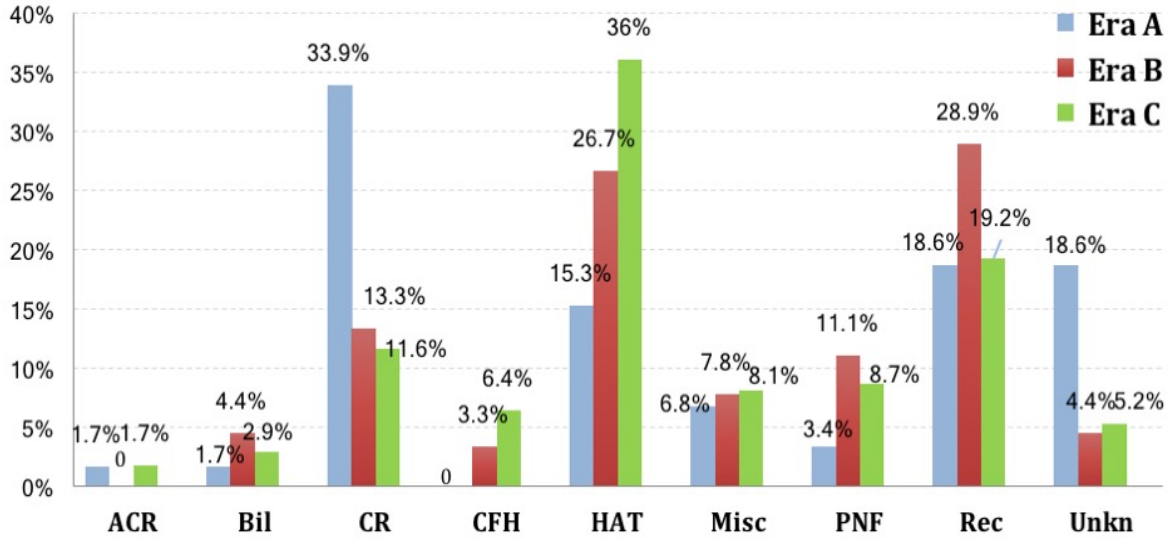

Figure 3. **Indications for retransplantation in adults.** *ACR, acute rejection; Bil, biliary; CR, chronic rejection; IPTH, idiopathic posttransplant hepatitis; HAT, hepatic artery thrombosis; Misc, miscellaneous; PNF, primary non-function; Rec, recurrent liver disease; Unkn, unknown.*

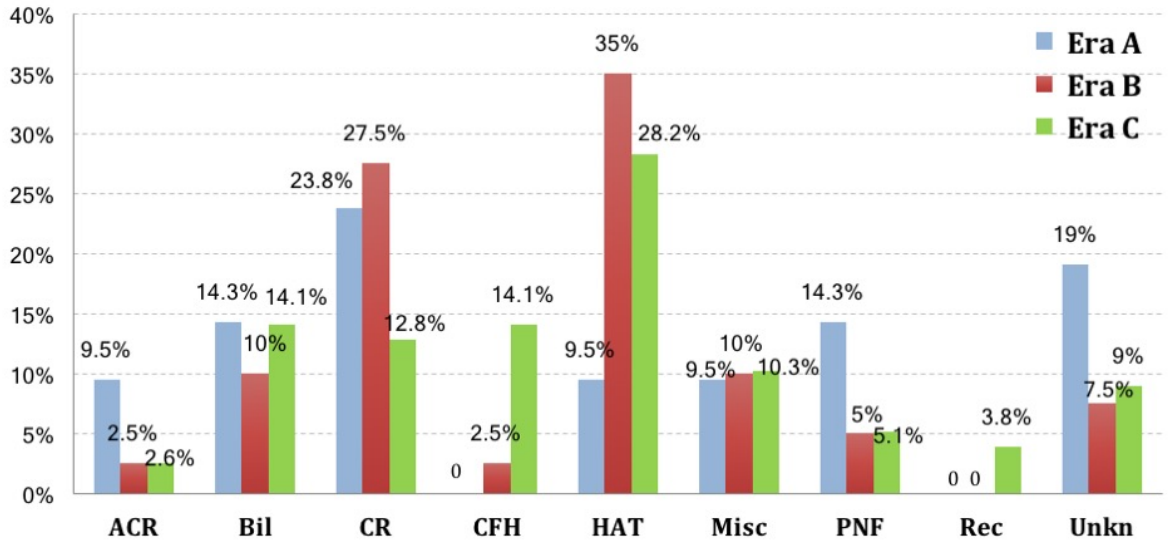

Figure 4. **Indications for retransplantation in children.** *ACR, acute rejection; Bil, biliary; CR, chronic rejection; IPTH, idiopathic posttransplant hepatitis; HAT, hepatic artery thrombosis; Misc, miscellaneous; PNF, primary non-function; Rec, recurrent liver disease; Unkn, unknown.*

The survival of liver recipients and allografts following transplantation has generally increased through the years (Chapter 1). This has resulted in growing interest in long-term graft pathology and histological damage, particularly in paediatric recipients, whose allografts should ideally last many decades after transplantation[14,19,21,23-24,39,170]. Considering the long-term outcome, and in order to reflect the current clinical and surgical practice, allografts removed 10 years or longer after the primary LT in the most recent era (era C) were examined (Table 5). In adult patients, recurrent liver disease accounted for just over half of late graft failures (54%). The following main indications were IPTH and hepatic artery thrombosis, each representing about one-fourth of retransplants.

In paediatric liver recipients, IPTH was the leading reason for late retransplantation in the last era, responsible for 40% of regrafts. Biliary complications accounted for 20% and chronic rejection for 15% of cases. Two children underwent retransplantation for recurrent liver disease. They were both initially transplanted for primary sclerosing cholangitis (PSC), had a clinical history and cholangiography compatible with recurrent PSC, and their graft histology was highly consistent with primary disease recurrence (both patients showed chronic cholangiopathy with cholangitis, ductopenia of small bile ducts, cholestasis, biliary-type bridging fibrosis).

Table 5. **Indications for retransplantation in era C >10 years post-LT**

INDICATION	**ADULTS, n (%)**	**CHILDREN, n (%)**
Recurrent	14 (54)	2 (10)
IPTH	5 (19)	8 (40)
HAT	4 (15)	2 (10)
Miscellaneous	2 (8)	1 (5)
Biliary	1 (4)	4 (20)

CR	0 (0)	3 (15)
Total	26 (100)	20 (100)

IPTH, idiopathic posttransplant hepatitis; HAT, hepatic artery thrombosis; CR, chronic rejection

Average time elapsed between primary and successive transplantation for each indication, in all eras, was analysed (Table 6). IPTH showed the longest time to retransplantation in children (10.8 years). In adults, recurrent autoimmune liver disease and IPTH presented virtually the same longest time to regraft (8.8 years). Figure 5 and Figure 6 depict the median and time range from transplantation to retransplantation for each indication in adults and children, respectively. In both figures, each asterisk signifies an extreme outlier (a value >3 times the interquartile range from a quartile), and each circle shows other (non-extreme) outliers, values between 1.5-3 interquartile range from the upper or lower edge of the box.

Table 6. **Time to retransplantation**

INDICATION	**TIME** (median and SD in years)	
	ADULTS	**CHILDREN**
PNF	0.01 (0.006)	0.01 (0.01)
Unknown	0.03 (0.03)	0.45 (5.45)
ACR	0.08 (1.38)	0.22 (0.95)
HAT	0.18 (3.60)	0.07 (3.29)
Miscellaneous	0.32 (5.00)	3.06 (6.39)
CR	1.02 (2.81)	0.97 (3.80)
Biliary	3.13 (3.48)	0.96 (4.78)
IPTH	8.76 (5.72)	10.82 (3.49)
Recurrent (all)	5.04 (5.08)	10.24 (4.27)

AILD	8.81 (5.12)	10.24 (4.27)
- Viral	3.73 (4.13)	
- Budd-Chiari	3.74 (5.81)	

SD, standard deviation; PNF, primary non-function; ACR, acute rejection; HAT, hepatic artery thrombosis; CR, chronic rejection; IPTH, idiopathic posttransplant hepatitis; AILD, autoimmune liver disease.

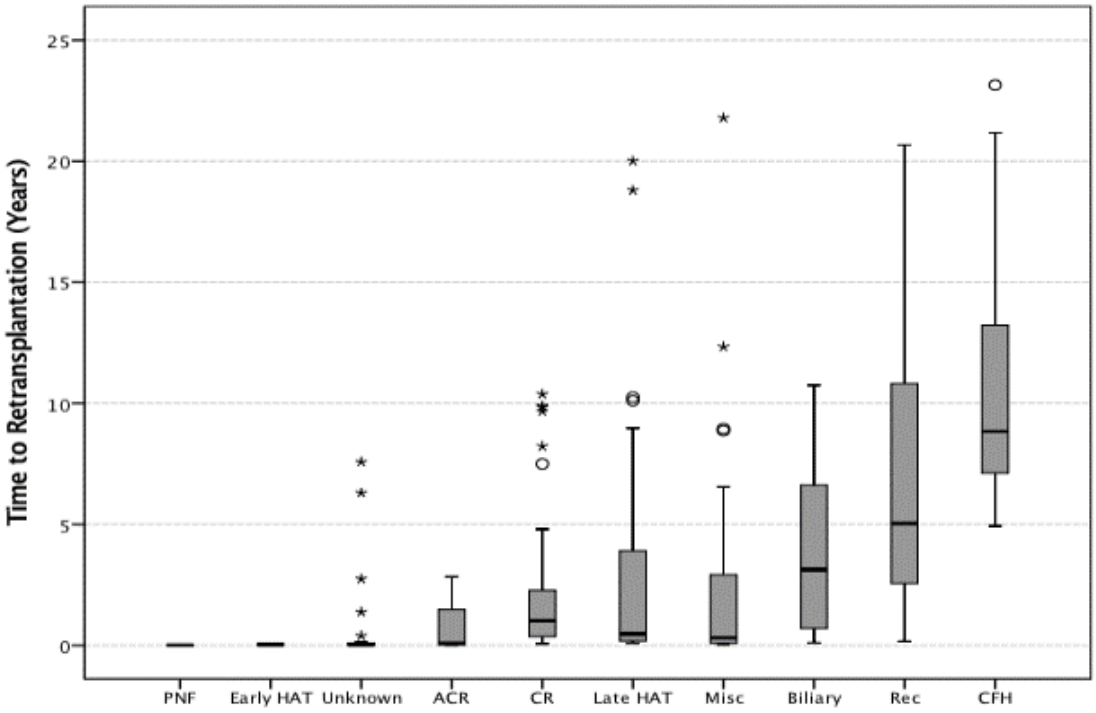

Figure 5. **Time to retransplantation per indication in adults**. *PNF, primary non-function; HAT, hepatic artery thrombosis; ACR, acute rejection; CR, chronic rejection; Misc, miscellaneous; Rec, recurrent disease; IPTH, idiopathic posttransplant hepatitis.*

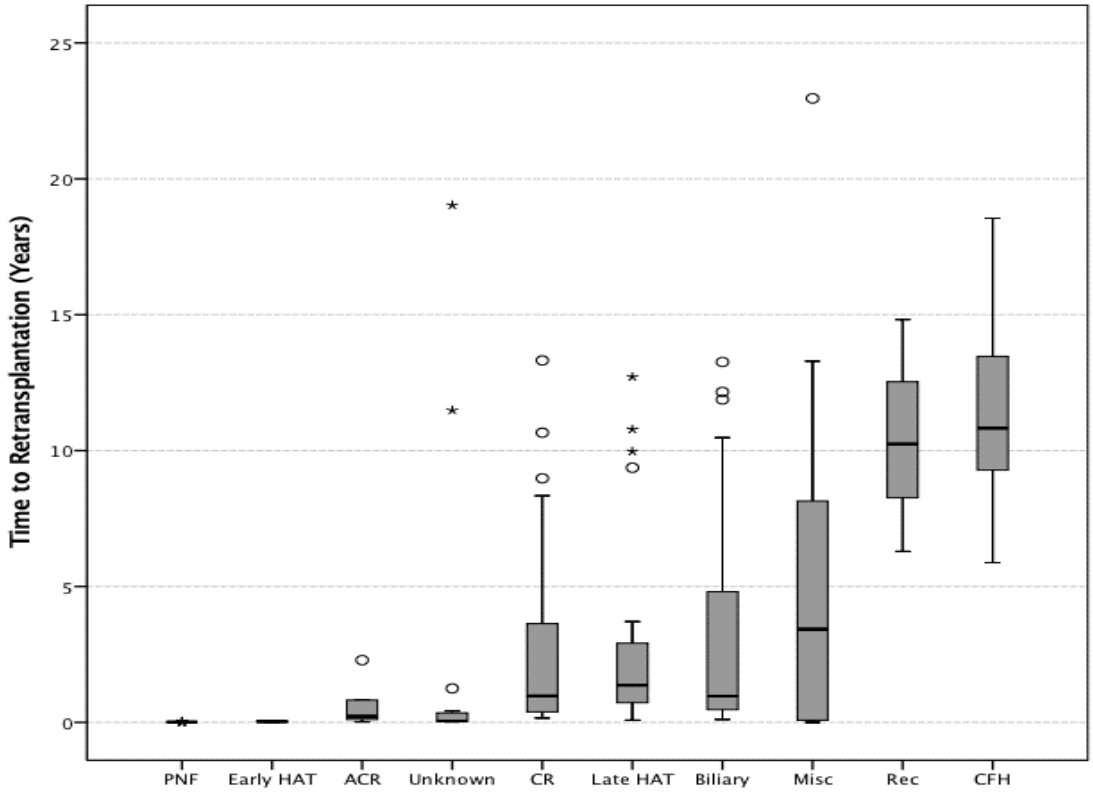

Figure 6. **Time to retransplantation per indication in children**. *PNF, primary non-function; HAT, hepatic artery thrombosis; ACR, acute rejection; CR, chronic rejection; Misc, miscellaneous; Rec, recurrent disease; IPTH, idiopathic posttransplant hepatitis.*

2.4 DISCUSSION

Causes for liver retransplantation were reviewed, focusing on the histology of failed allografts. The study benefitted from a large historical series, with biopsies available from the foundation of KCH's transplant program throughout its development over 27 years. Analysis showed a change in the histology of the explanted allografts during this period and in particular through the three eras defined essentially by changes in immunosuppression. The frequency of retransplantation was 8.5% in

adults and 13% in children. In general, the main cause of allograft loss was hepatic artery thrombosis, representing over a fourth of explants in both age groups. Comparable rates of HAT have been reported by other centres[171-172].

The total numbers and proportion of chronic rejection suffered significant decrease from the first to the last era in both adults and children, reflecting the change in immunosuppressive drugs, especially the introduction of tacrolimus[172-175]. The reason for the small increase in the proportion of retransplantation for chronic rejection in children from era A to era B (from 24% to 28%) is not clear. While this could be explained if many children who lost their allografts in era B had actually undergone primary LT in era A, as they would have received cyclosporine as the initial immunosuppression; in fact, 82% of children who underwent retransplantation in era B also had their primary transplant in that same era. Therefore, no explanation was found for this temporarily increase in the rate of chronic rejection in the paediatric population in era B. It is also possible that some of these children, despite transplanted in era B when tacrolimus was given, might have received cyclosporine, but the lack of data on immunosuppression for virtually all patients who underwent LT in eras A and B prevented further conclusions.

Idiopathic posttransplant hepatitis, on the other hand, has gained importance over the years, becoming the main cause of late retransplantation in children in the last era and accounting for 14% of all graft failures in this age group in era C. This histological pattern of injury was more frequent in paediatric recipients than in adults, an observation consistent with previous data reporting higher frequency of IPTH and fibrosis in children[23,121,170]. As mentioned in Chapter 1, IPTH is a common histological finding in long-term protocol biopsies of children, is linked to the development of advanced stage fibrosis, and is likely to represent a form of rejection[14,20,23,26,53].

Additionally, some cases of IPTH might be due to viruses[20]. Hepatitis E virus (HEV) in particular has been linked to chronic hepatitis and fibrosis in some liver transplant recipients[177-178]. Most patients in the present study cohort had not been tested for hepatitis E virus, which only became part of the viral screening in specific cases in the last era. At King's College Hospital, up to present, there have been only a few individual liver recipients who showed allograft dysfunction and had positive RNA testing for hepatitis E virus in the post-transplant setting, and all of these were children.

The present study on failed liver allografts showed that retransplantation for IPTH usually happened more than 8 years and 10 years after primary LT in children and adults, respectively. Most recipients had been asymptomatic, with stable liver function tests for many years. Biopsy was not performed until graft dysfunction became clinically evident. The biopsy then often revealed advanced fibrosis, in a background of non-specific chronic hepatitis of the graft.

Previous studies have reported low sensitivity of standard liver biochemistry tests to predict allograft damage, and significant histological injury is frequent in protocol biopsies of recipients with normal liver function tests[13,23,120]. The role of histopathology in monitoring post-transplant long-term outcome therefore remains fundamental, particularly when considering immunosuppression minimization or withdrawal[176-178].

In the current cohort, primary liver disease recurrence, particularly hepatitis C, represented the main reason for late retransplantation in adults. It is likely, however, that hepatitis C might decrease substantially due to the new generation of antiviral drugs that should become more widely available in the next years. Therefore, IPTH will possibly become the leading cause of late allograft failure in adults. Graft loss due

to hepatitis B recurrence has declined steadily since the start of antiviral therapy and immunoglobulin prophylaxis in the 1990's.

Increasing evidence indicates that AMR[182] is involved in the pathogenesis of liver graft damage and influences post-transplant outcome[21,57,90]. As mentioned in Chapter 1, acute AMR in the liver is frequently associated with acute TCMR[59,90]. In severe cases of acute AMR, the allograft presents early failure and a histological picture similar to marked preservation/reperfusion damage, infarction or haemorrhagic necrosis[55].

In the current series, 94.3% of the patients in the unknown category (whose allografts failed for unidentified reason) developed clinically an acute/subacute liver failure and showed histologically extensive areas of infarct or haemorrhagic necrosis. Acute TCMR was evident in almost half of these biopsies, and AMR was actually ventured by the pathologist in over a third of them. It is possible that AMR could have contributed to a proportion of these acute idiopathic graft failures. Furthermore, humoral rejection could have also triggered the original endothelial injury that initiated the immunological cascade resulting in hepatic artery thrombosis in some patients who underwent retransplantation for this reason.

Unfortunately, DSA test is not routinely performed at KCH but is requested on a clinico-histological basis when AMR is suspected. To perform the DSA test retrospectively stored serum samples of the patients in this series were sought, but most did not have serum available. This lack of systematic DSA data and the retrospective nature of the analysis did not allow further comment on the role of AMR in the allograft losses in this study cohort. Because of the absence of DSA information, C4d immunohistochemistry in the histological specimens was also not performed, as C4d should always be interpreted in combination with DSA. The contribution of AMR

in cases of acute idiopathic graft loss and hepatic artery thrombosis could be better addressed by prospective studies correlating DSA and histology in these settings.

Humoral mechanisms have also been linked to late idiopathic graft fibrosis, particularly in perivenular area in children[28,41,72]. In the present cohort, the review of biopsies preceding retransplantation showed perivenular fibrosis in 58% of children who had graft failure for IPTH. The diagnosis of chronic AMR in the liver graft is still under consideration, and the presence of DSA is a mandatory criterion[53,183]. Therefore, diagnosis of chronic AMR could not be confirmed or refuted in grafts that failed for chronic fibrosing idiopathic hepatitis. It is likely that graft failure in this group (CFH) was secondary to a slowly evolving form of rejection, possibly with a humoral component, which progressed throughout several years and eventually led to graft dysfunction and loss.

In summary, by analysing the failed liver grafts explanted during almost three decades of KCH's liver transplantation programme, a change was observed in the histological patterns of injury. Idiopathic posttransplant hepatitis, probably representing a slowly-progressing phenotype of rejection, represented the main cause for late retransplantation in children in the most recent era and was the second most likely cause in adults. This highlights the role of protocol biopsy in monitoring liver grafts in the long-term. AMR might contribute to the pathogenesis of unexplained inflammation and fibrosis, and this needs to be further clarified by studies correlating circulating antibodies, detailed histology including C4d immunostaining, and clinical parameters. Systematic testing for hepatitis E virus in instances of unexplained chronic hepatitis of the graft is recommended.

3 PAEDIATRIC PROTOCOL BIOPSIES

3.1 RATIONALE FOR STUDYING PROTOCOL BIOPSIES

In the previous chapter (Chapter 2), the causes of allograft failure were investigated and the increasing relevance of IPTH and progressive fibrosis leading to allograft loss became evident, especially in the paediatric population. Many children had showed normalgraft function and so were not biopsied for many years after LT. Only when they presented with abnormal liver biochemistry did they undergo graft biopsy, which showed advanced liver fibrosis, and eventually they developed allograft failure.

This prompted a study of protocol biopsies of asymptomatic liver recipients to look for histological abnormalities, specially IPTH and fibrosis, which could be predictors of progressive graft injury. Histological features were compared with circulating DSA and C4d immunohistochemistry. This could improve understanding of the histological changes and of the pathogenic role of antibodies in long-term allograft injury, which could not be confirmed in the failed allograft group.

Possible associations between lymphocyte subsets and other histological signs of graft injury and antibody-mediated rejection were also investigated as well as expression of granzyme B by B cells and/or plasma cells.

3.2 MATERIAL AND METHODS

3.2.1 Patients and Data

Protocol biopsies of liver transplant recipients were located using the histology electronic database. Because liver protocol biopsies have not been routinely performed at KCH, there were no adult patients who had undergone liver allograft protocol biopsies. In contrast, among the paediatric group, fifty-eight liver recipients had had one protocol biopsy several years post-transplant (from 8.6-15.6 years), as part of a historical clinical follow-up study. All children undergoing protocol biopsy were asymptomatic, and biopsy was performed to ensure that the normal clinical picture had a normal histological counterpart. No additional studies had been conducted in these specimens other than routine diagnostic assessment by a liver histopathologist.

Clinical data retrieved for the paediatric patients consisted of: indication for liver transplantation; patient date of birth; age at transplantation and at biopsy; type of donation - donation after cardiac death (DCD), donation after brain death (DBD) or living-donor liver transplantation (LDLT); type of allograft received (whole, split, reduced); initial immunosuppressive regime and regime in use at time of biopsy; liver biochemistry; previous biopsy-proven episodes of rejection, clinical outcome and circulating autoantibodies at the time of biopsy. Liver biochemistry function tests included: aspartate aminotransferase (AST) and alanine aminotransferase (ALT); bilirubin; gamma-glutamyl transferase (GGT) and alkaline phosphatase (AP); platelet counts.

In addition to histology and clinical data, the donor HLA information was found. Then recipient blood serum samples were retrieved to test for DSA; most children who underwent protocol biopsy had serum collected at the time of biopsy and stored in the

biobank for future research, although some samples had already been used and were no longer available.

3.2.2 DSA testing

DSA testing was performed in the laboratory where routine diagnostic samples are analysed for antibodies, at Guy's and St Thomas's NHS Foundation Trust. Samples were retrieved, prepared and sent for analysis by the present author, who maintained personal contact with the pathologist responsible for the analysis. OneLambda mixed and single antigen bead kits (LABScreen, One Lambda, Canoga Park, CA) were used. Initially, a mixed test was performed to screen for the presence of antibodies. Then, the single-antigen test was carried out on cases that were positive in prescreening, in order to identify specific DSA types and MFI values, as specified in the manufacturer's protocol. Antibodies to HLA A, B, C, DR, DQ and DP were measured. Samples with DSA measured at over 1000 MFI were considered positive.

3.2.3 Histology

3.2.3.1 HE and reticulin

Two pathologists (A.Q. and L.N.S.) reviewed the original hematoxylin and eosin (HE)- and reticulin-stained biopsy slides together, made an overall assessment and scored a series of histological parameters. The scoring system (Table 7) was adapted from that designed for the assessment of long-term biopsies of liver transplant recipients participating in the multicentre *Liver Immunosuppression Free Trial* (LIFT), an immunosuppression withdrawal trial led by KCH.

Table 7. **Histological score for grading and staging of HE and reticulin stained biopsies**

	Number of complete portal tracts
	Number of central veins
Lobular inflammation:	0, none 1, mild (sinusoidal cells and/or mild focal necrosis), 2, moderate (multiple necro-inflammatory foci), 3, marked (confluent or bridging necrosis);
CP:	0, none 1, mild (patchy, focal perivenular inflammation) 2, moderate (affecting most central veins), 3, marked (confluent/bridging necrosis);
Portal inflammation:	0, none 1, mild (small groups of inflammatory cells in some/all portal tracts) 2, moderate (expansive inflammatory infiltrate in some portal tracts) 3, marked (severe inflammation expanding most or all portal tracts)
Interface hepatitis:	0, none 1, mild (focal, in few portal tracts) 2, moderate (focal in most or continuous in a minority of portal tracts) 3, severe (continuous around most portal tracts)
Bile duct lesion:	0, none 1, minimal (intraepithelial inflammatory cells or abnormal cholangiocytes) 2, moderate (epithelial lesions in most portal tracts without destruction) 3, marked (destructive lesions of bile ducts)
Portal vein endotheliitis:	0, absent 1, mild (mild inflammation in a minority of portal tracts) 2, moderate (mild inflammation in most portal tracts or moderate inflammation in a minority of portal tracts) 3, marked (moderate to severe inflammation, in most/all portal tracts)
Ductular reaction:	0, absent 1, present

Hepatocanalicular cholestasis:	0, absent 1, focal at higher magnification (400x) 2, centrilobular, obvious at 100x magnification 3, midzonal with/without periportal
Cholangiolar cholestasis:	0, absent 1, present
Steatosis:	0, < 5% of hepatocytes 1, 5-33% of hepatocytes 2, 33-66% of hepatocytes 3, > 66% of hepatocytes
Portal fibrosis (Ishak)[37]:	0, none 1, fibrous expansion of a minority of portal tracts, 2, fibrous expansion of most/all portal tracts without bridging 3, fibrous expansion of most/all portal tracts with occasional portal-portal bridging (fibrous septa) 4, marked bridging fibrosis (portal-portal and/or portal-central) 5, marked bridging fibrosis with occasional nodules 6, cirrhosis
Portal fibrosis (Venturi et al)[42]:	0, none 1, non-expanding fibrosis in <50% of portal tracts 2, fibrosis in >50% of portal tracts and/or short periportal septa 3, portal-portal or portal-central bridging fibrosis, with or without nodules
Sinusoidal fibrosis (Venturi et al)[42]:	0, none 1, thin focal collagen deposits in <50% of sinusoids 2, thin diffuse collagen deposits in >50% or thick fibrosis in <50% of sinusoids 3, thick and diffuse fibrosis in >50% of sinusoids
Centrilobular fibrosis (Venturi et al) [42]:	0, none 1, circular perivenular fibrosis in <50% of central veins without invasion into perivenular parenchyma 2, circular perivenular fibrosis in >50% of central veins or expansion into short fibrous septa in perivenular parenchyma 3, marked centrilobular fibrosis with bridging to other central and/or portal areas
Nodular regenerative hyperplasia:	0, absent 1, focal 2, diffuse

According to the overall assessment, the biopsies were categorized as "normal/minimal changes", "chronic hepatitis of the graft" or "rejection". Biopsies

classified as chronic hepatitis of the graft showed at least moderate (grade 2) portal inflammation, or mild (grade 1) portal inflammation associated with interface activity, central perivenulitis and/or with lobular inflammation ≥2. Cases with isolated central perivenulitis were also considered as chronic hepatitis of the graft. Biopsies with only mild (grade 1) portal inflammation were considered normal/minimal changes. The diagnosis of rejection was established based on Banff criteria [143].

Although both Ishak and Venturi *et al.* staging systems were used to score portal fibrosis, in the Results and Discussion sessions of this and the next Chapter (chapters 3 and 4), when referring to portal fibrosis, only the Ishak system will be considered (unless otherwise specified). Ishak was chosen for scoring portal fibrosis because this system provides more detailed information and considers a wider range of degrees of fibrosis.

The threshold considered for portal fibrosis was Ishak ≥2 (fibrous expansion of most portal tracts). Ishak stage 2 was selected instead of stage 1 because the latter corresponds to mild fibrosis affecting a minority of portal tracts. The differentiation between stage 1 and stage 0 (no fibrosis) can be very subtle, and the expansion of only a minority of portal tracts often corresponds to a patchy process, which might have no pathological significance and is more prone to sampling variability.

In stage 2, on the other hand, the fibrous expansion is a more widespread process, involving >50% of portal tracts, and differentiation from stage 0 is clearer. Stage 2 was selected for cut-off instead of stage 3 also to facilitate the comparison of results with previous studies of paediatric protocol biopsies. Most of these studies used less detailed fibrosis scoring systems in which the first degree of portal fibrosis considered was portal fibrous expansion without bridging/fibrous septa[23,29]. Having an experienced liver pathologist performing the histological assessment, familiar with

the Ishak score, was essential to ensure consistency of the results. At some points in the current research, statistical associations were observed between higher degrees of fibrosis and other clinical or histological parameters. In such cases, the threshold of fibrosis is specifically stated.

For sinusoidal and centrilobular fibrosis, Venturi stage ≥2 was chosen as the threshold for similar reasons. In the sinusoidal fibrosis scoring, stage 1 corresponds to thin focal fibrosis in <50% of sinusoids. As with portal fibrosis, this often corresponds to a patchy process, more susceptible to sample variability, and of questionable significance. Stage 2 sinusoidal fibrosis represents a more widespread/significant process (diffuse thin fibrosis in most sinusoids or thick patchy fibrosis). For centrilobular fibrosis, stage 1 also refers to patchy fibrosis (in <50% of central areas), whereas stage 2 corresponds to a more diffuse/significant process with perivenular fibrosis in >50% of central veins and/or expansion into fibrous septa to adjacent parenchyma.

Additional biopsy sections were obtained to perform Sirius Red staining, immunohistochemistry for C4d and combined immunostaining for quantifying inflammatory cells.

3.2.3.2 Sirius Red

Sirius Red staining was performed by this thesis' author (L.N.S.) following the method routinely used for diagnostic specimens in the Liver Histopathology Laboratory of King's College Hospital. The protocol consisted of eight steps, detailed in Table 8.

Table 8. **Protocol for Sirius Red staining**

1. Deparaffinize with xylene for 10 minutes
2. Rehydrate with 100% ethanol, then lower concentrations (70%, 30%), then distilled water
3. Treat with Weigert's iron haematoxylin* for 10 min to stain nuclei
4. Wash in running distilled water for 10 min
5. Treat with Sirius Red solution** for 1 hour
6. Wash in acidified water*** 3 times
7. Allow slides to dry, dip in xylene and mount with DPX

**Weigert's iron haematoxylin was prepared by mixing equal parts of Weigert's A and Weigert's B solution. Weigert's A was composed of 0.4g of ferric chloride, 100mL of distilled water and 0.75mL of hydrochloric acid and Weigert's B comprised 1g of haematoxylin and 100mL of 95% ethanol. **Picro-Sirius Red was made by adding 0.5g of Sirius red F3B to 500ml of saturated aqueous solution of Picric acid. ***Acidified water consisted of 2.5ml of glacial acetic acid to 500ml of distilled water.*

Once staining was complete, the biopsies were digitalized using a brightfield slide scanner that produced high-resolution digital images (NanoZoomer-XR Digital slide scanner C12000-01, Hamamatsu Photonics, Hamamatsu, Japan).

3.2.3.3 C4d immunohistochemistry

The wide range of protocols for C4d immunohistochemistry in FFPE liver tissue is probably responsible for the variability and inconsistency of this staining when comparing samples prepared at different times, in different laboratories or with different reagents (antibodies). The threshold employed to consider a staining as

positive and the scoring system also vary between publications[91,97-98,100,103,140-142]. As the antibody initially used in the present research was not producing reliable results, a few different primary C4d antibodies were optimized to provide consistent staining. Some primary antibodies that showed consistent results in other centres were not available for purchase in the UK.

In a multicentre study[98] including the Liver Histopathology Laboratory of the Institute of Liver Studies of King's College Hospital, liver, kidney and heart allograft tissue samples were combined on a single paraffin block using tissue microarray (TMA), and the sections were stained for C4d and assessed by pathologists of each centre. Correlation between histology and a series of clinical parameters, including DSA and outcome, were used to identify the best C4d protocols. The most robust automated method identified in the multicentre study was selected for the present research.

The automated immunostainer available to the Liver Histopathology Laboratory was a Leica Bond-Max (Leica Biosystems, UK). All reagents (except primary antibodies), were part of the recommended Leica Bond-max kit. The staining protocol is detailed below, in Table 9. The washing steps were done with TRIS buffered saline (Leica Bond wash, Leica Biosystems, UK), and Bond Polymer Refine Detection kit was used for detection (Leica Biosystems, UK). A biopsy section of a liver allograft in which AMR was diagnosed was included in each batch as a positive control. As all the histological procedures in this research, the C4d staining was conducted by L.N.S.

Table 9. **Protocol for C4d immunohistochemistry on FFPE liver tissue**

1.	Deparaffinization with xylene for 10 minutes

2.	Heat-induced epitope retrieval (HIER) for 30 minutes with ER2 solution (high pH)
3.	Wash
4.	Protein block for 5 minutes (standard time)
5.	Wash
6.	Incubation with a cocktail of two primary C4d antibodies for 30 minutes: a rabbit monoclonal (clone SP91, Cell Marque/Merck KGaA, Darmstadt, Germany), and a rabbit polyclonal (Cell Marque/Merck KGaA, Darmstadt, Germany), both diluted at 1:50 in Leica primary antibody diluent solution
7.	Wash
8.	Incubation with secondary antibody with HRP (horseradish peroxidase)
9.	Wash
10.	Incubation with DAB (3,3' Diaminobenzidine) chromogen
11.	Wash
12.	Hematoxylin counterstaining for nuclei visualization (Leica Bond-Max kit)
13.	Mount

Fifty out of the 52 study biopsies were stained for C4d (2 biopsies had too little tissue for analysis). The scoring system employed to evaluate the C4d staining was the same as that of the multicentre C4d study[98], which considered the distribution and intensity of C4d staining independently in each of the following compartments: portal vein; portal capillaries; hepatic artery; portal stroma; central vein and sinusoids. Because the Banff diagnostic criteria for AMR in the liver requires C4d+ in portal microvascular endothelium, which includes portal veins and portal capillaries, the category “portal microvascular endothelium” was included to the results. Positive staining in “any compartment” was added as a further category for C4d results. The system used for grading the distribution and intensity of C4d deposition in each compartment is specified in Table 10 below.

Table 10. **C4d scoring system**

Grade	**Distribution**	**Intensity**
0	None	None
1	Minimal (<10%)	Weak
2	Focal (10-50%)	Moderate
3	Diffuse (>50%)	Strong

Outside the context of acute AMR, the sensitivity of C4d staining is lower, and diffuse C4d deposition is very rare. For this reason, all biopsies with at least focal C4d staining in a given compartment were considered as C4d+ (in that compartment).

3.2.3.4 Quantum dots and T cell immunostaining

One of the objectives of this research was to study the inflammatory cell population, quantifying specific cell types. These data were to be correlated with other histological parameters, including C4d, DSA and clinical data. In particular, a possible link between B cells and/or plasma cells and fibrosis was investigated. Multiplex staining was used in order to quantify different cell phenotypes in the same tissue section.

Quantum dots (Qdots) have advantages over conventional fluorophores/fluorescent dyes, with a narrow emission range allowing the combined use of multiple Qdots of different wavelengths for multiplex staining without signal overlap (Chapter 1). After studying the use of Qdots in histology, two different methods of immunostaining with Qdots were tested:

1. applying a conventional primary antibody followed by a Qdots-conjugated secondary antibody
2. labelling the conventional primary antibody with Qdots.

The main advantage of the first option was the commercial availability of secondary antibodies conjugated with Qdots, and robust results using this method had been published[16]. The main disadvantages included the longer time required to perform sequential primary-secondary antibody staining (for multiple antigens) and the possibility of cross-reaction between antibodies. For instance, a secondary antibody could potentially bind to a non-target primary antibody from the same host species as its target primary antibody. Although in theory this cross-reaction could be eliminated by selecting primary antibodies from different host species and highly adsorbed secondary antibodies, when considering a panel of more than 3 antibodies, it becomes difficult to find primary antibodies from distinct host species. This is because most primary antibodies validated for use in FFPE sections are produced in rabbit or mouse. An antibody from a third species can sometimes be found, however, combinations with more than three antibodies are virtually impossible to find.

The principal advantages of labelling primary antibodies with Qdots (option 2) were: elimination of the need for secondary antibodies and consequently, less cross-reaction, and decreased total staining time. The detailed protocol for both methods of Qdots staining will be described in the next paragraphs.

For both Qdots immunostaining protocols, 4μm thick FFPE tissue sections were cut from training biopsy specimens of normal and cirrhotic liver obtained from the histology archive. For staining with Qdots-conjugated secondary antibody, a primary monoclonal mouse anti-human cytokeratin-7 antibody was chosen (clone OV-TL

12/30, Dako, Glostrup, Denmark) for its consistent results and a staining pattern easy to recognise.

In both staining protocols, all washing steps consisted of 3 washes of 5 minutes in PBS (phosphate-based saline) unless stated otherwise. The complete protocol for immunostaining with Qdot-conjugated secondary antibody is presented in Table 11 below. The staining was assessed using a Leica DMR microscope, with a Leica DFC7000 T camera and a standard DAPI/blue, TRITC/red and FITC/green fluorescence filter set.

Table 11. **Protocol for immunostaining with Qdot-conjugated secondary antibody**

1.	Deparaffinization with xylene for 10 minutes
2.	Rehydration with ethanol 100% for 15 min, followed by distilled water for 10 min
3.	HIER with sodium citrate buffer (pH6.0) at 99°C for 20 min (in water bath)
4.	After buffer/slides reach room temperature, wash
5.	Protein block with 6% bovine serum albumin (BSA) in PBS for 1h at room temperature
6.	Incubation overnight at 4°C with primary CK7 antibody (1:100 concentration)
7.	Wash
8.	Incubation with donkey anti-mouse Qdot655-conjugated secondary antibody (Invitrogen, Paisley, UK) for 1-hour at room temperature
9.	Wash
10.	Dehydration with ethanol
11.	Dip slides in xylene and mount with Qmount™ Qdot Mounting Media (Invitrogen, Paisley, UK)

For immunostaining with Qdots-labelled primary antibody, the steps preceding the incubation with primary antibody were similar to the previous protocol (deparaffinization, rehydration, HIER, protein block). In this case, however, the CK7 primary antibody was labelled with Qdot655 using the SiteClick™ Antibody Labelling Kit (Life Technologies, Carlsbad, CA, USA), following the steps recommended by the manufacturer. The process involved modifying the antibody's carbohydrate domain by removing terminal galactose residues in its Fc region, then attaching an azide-containing sugar to the modified carbohydrate domain, and conjugating the antibody with Qdots nanocrystals. The reaction relies on 6 steps, the first five of which are depicted in Figure 7. The first step consists of antibody concentration and buffer

exchange, and is required if the chosen antibody has a concentration of less than 2 mg/mL or contains azide or PBS. The primary antibody used fulfilled both criteria.

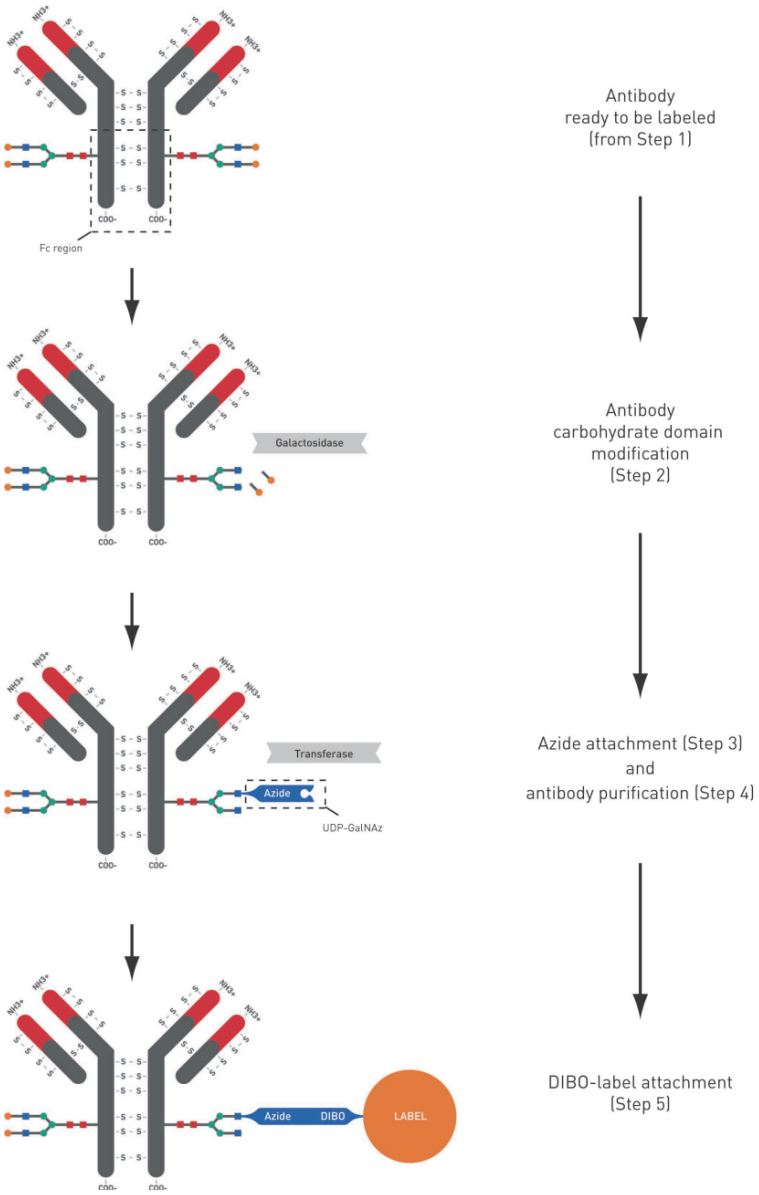

Figure 7. **Workflow for primary antibody labelling with quantum dots**

The next steps were: modification of the antibody carbohydrate domain; azide attachment; purification and concentration of azide-modified antibody; conjugation with DIBO-modified Qdots label; and purification and concentration of antibody conjugate. Figure 7 was extracted from SiteClick™ Antibody Labeling Kits datasheet, available for download at

https://www.thermofisher.com/order/catalog/product/S10453. The protocol for immunostaining with Qdot-labelled primary antibody is detailed in Table 12. The staining results were assessed using the same fluorescence microscope previously mentioned (Leica DMR).

Table 12. **Protocol for immunostaining with Qdot-labelled primary antibody**

1. Deparaffinization with xylene for 10 minutes
2. Rehydration with ethanol 100% for 15 min, followed by distilled water for 10 min
3. HIER with sodium citrate buffer (pH6.0) at 99°C for 20 min (in water bath)
4. After buffer/slides reach room temperature, wash
5. Protein block with 6% bovine serum albumin (BSA) in PBS for 1h at room temperature
6. Incubation overnight at 4°C with primary CK7 antibody labelled with Qdots* (1:5, 1:10, 1:50 and 1:100 concentration)
7. Wash
8. Dehydration with ethanol
9. Dip slides in xylene and mount with Qmount™ Qdot Mounting Media (Invitrogen, Paisley, UK)

* *The method used for labelling the primary CK7 antibody with Qdots is shown in Figure 7.*

The first immunostaining method, using a primary standard (CK7) antibody and a secondary Qdots-conjugated antibody produced a strong fluorescent signal with minimal background in both normal and cirrhotic liver tissue (Figure 8 and Figure 9, respectively).

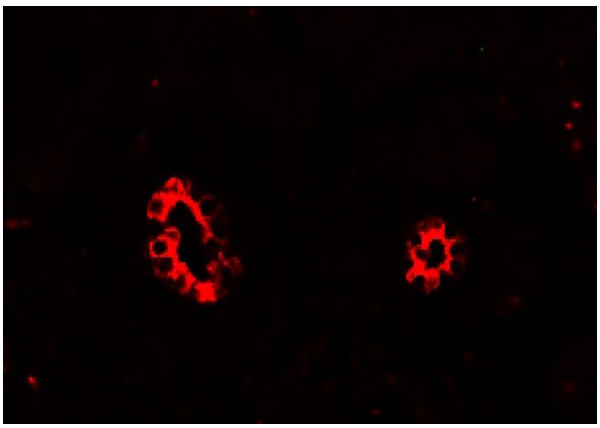

Figure 8. **Normal liver stained with CK7 primary antibody + donkey anti-mouse Qdot655 secondary antibody**. *Bile ducts in red*.

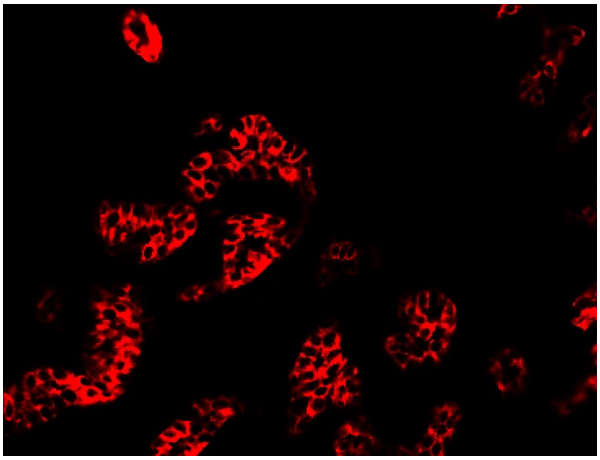

Figure 9. **Cirrhotic liver stained with CK7 primary antibody + donkey anti-mouse Qdot655 secondary antibody**. *Bile ducts and ductular reaction in red*.

Despite the positive initial result of the first method (secondary Qdots-conjugated antibody), after a week, the Qdots signal disappeared completely and no residual staining remained. The second protocol, with Qdot-labelled CK7 antibody was unsuccessful, and there was no staining of bile ducts, even at the highest concentration of antibody (1:5).

It appeared that the setup of Qdot immunofluorescence was challenging and the results inconsistent in more than one laboratory (which I discovered after contacting pathologists from other centres). Further work with Qdots was developed

in the Division of Liver and Transplantation Pathology in the University of Pittsburgh Medical Centre (UPMC), where I was accepted by Dr A. J. Demetris as Visiting Research Fellow in Transplant Pathology.

A robust method for multiplex Qdots staining, digital imaging and image analysis were developed in transplant pathology specimens. The mounting media provided and recommended by the manufacturer for Qdots staining was in fact responsible for the vanishing of the Qdots signal in my initial samples. Additionally, the use of biotin-conjugated secondary antibodies followed by streptavidin-conjugated Qdots, standard at UPMC, increased the final brightness.

The equipment required to image slides with Qdots staining needs to have specialised excitation and emission filters. Normal fluorescence excitation filters are not suitable to analyse Qdots, as all Qdots will be excited and appear simultaneously. That is because although different Qdots have different emission wavelengths, most Qdots share an extremely similar spectrum of excitation, which is considerably larger than that of conventional fluorophores and, most importantly, corresponds to the excitation range of most standard fluorescence filters. Thus, if one assesses a triple staining containing Qdots 605, 655 and 705, for instance, with a conventional fluorescence filter, all three Qdots will be excited and emit signal simultaneously in any filter. As the emission colours do not have marked contrast with each other (orange, red and far red), then without appropriate Qdots filters it is not possible to distinguish and quantify the individual antigens.

Figure 10 shows the specific excitation (dash lines) and emission (solid lines) wavelength for nuclear marker 4',6-diamidino-2-phenylindole (DAPI) and for 3 of the most widely used Qdots: 605, 655 and 705 (whose emission peaks match their names). It is noticeable that the excitation range of Qdots overlaps with that of DAPI.

Figure 11 shows the range for the standard DAPI/blue, FITC/green and TRITC/red excitation filters, represented by the grey, blue and green areas, in addition to the Qdots and DAPI excitation and emission spectra. It can be observed that all filter ranges are within the excitation spectra of Qdots. Therefore, using a fluorescence microscope with a conventional filter set, the signal from all Qdots become visible simultaneously. Both Figure 10 and Figure 11 were created using the Fluorescence SpectraViewer tool[153].

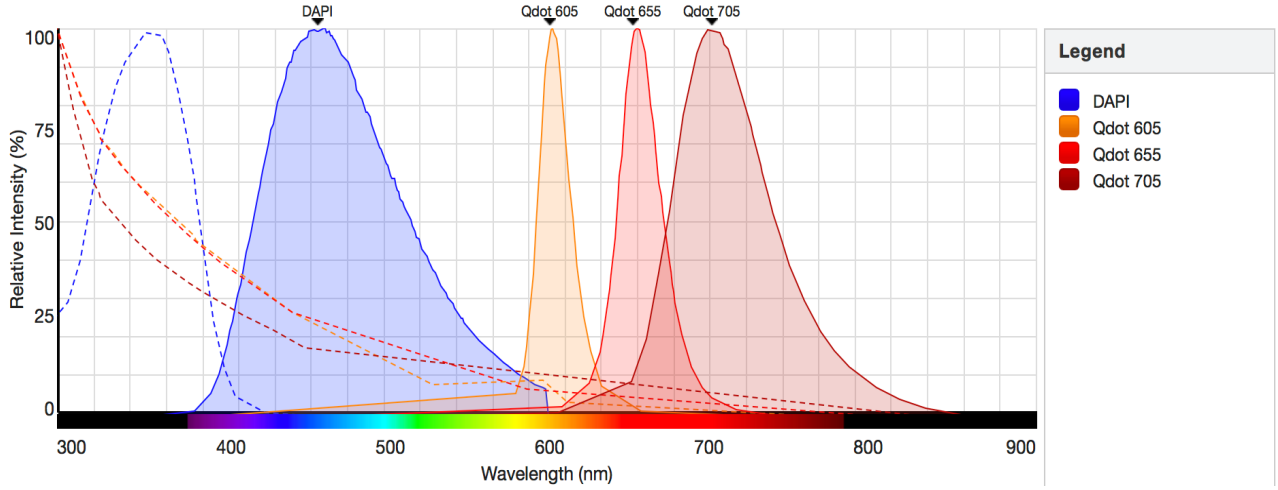

Figure 10. **DAPI and Qdots excitation and emission spectrum**

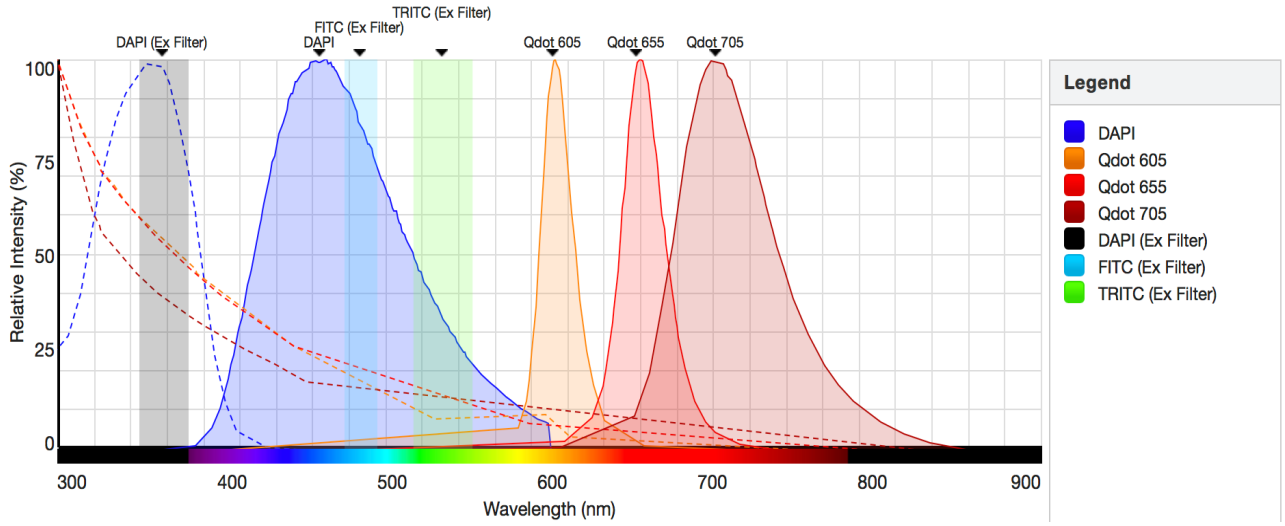

Figure 11. **Excitation filters, DAPI and Qdots excitation and emission spectrum**

In Pittsburgh, it was possible to use the image analysis software developed there: IAE-NearCYTE (http://nearcyte.org). This tissue cytometry software defines cells, enabling the delimitation of areas with different cell types depending on a user-defined classification. The software also quantifies cells/antigen expression. The area to be analysed can be selected regions or the whole biopsy area obtained from the whole, automatically scanned image. Whole biopsy images were used with the software tools to quantify cells. Tools used included: nuclei segmentation; channels overlay; compartments delimitation and cut-offs (of size, intensity of signal, etc.) for positive objects.

Back in London, and based on the experience at Pittsburgh, new Qdots immunostaining protocols were designed for quantification of T cells and their subtypes (helper, cytotoxic and regulatory T cells) and for quantification of B cells, plasma cells and granzyme B (GrzB). Primary antibodies were used from different species in order to eliminate cross-reaction between secondary antibodies and non-target primary antibodies. Due to the limited range of host species of primary antibodies available for immunostaining in fixed tissue (essentially mouse and rabbit,

rarely rat), a three-antigen combination protocol was selected and multiplex staining of 4 or 5 antigens in one section was not possible. Biotinylated secondary antibodies were followed by streptavidin-conjugated Qdots, as this method generated stronger signal.

The aim of the T cell staining was to quantify the following subtypes: helper, cytotoxic and regulatory T cells. For this, the following combination of primary antibodies were selected: CD4, CD8 and FoxP3. The B cell staining should allow quantification of B cells, plasma cells and expression of GrzB by these cells, thus CD20, CD138 and GrzB primary antibodies were chosen. The protocol was optimised for the following primary antibodies: CD4 (clone 4B12, Dako, Glostrup, Denmark), CD8 (clone C8/144B, Dako, Glostrup, Denmark), FoxP3 (clone PCH 101, eBioscience, San Diego, CA, USA), CD20 (clone L26, Dako, Glostrup, Denmark), CD138 (polyclonal, Atlas antibodies, Stockholm, Sweden) and GrzB (clone 496B, eBioscience, San Diego, CA, USA).

First, Qdot immunostaining was optimised for each primary antibody individually by testing different antibody concentrations, incubation times and temperatures, antigen retrieval buffers (pH6, pH8, pH9) and antigen retrieval times. Then, the three antibodies and Qdots were combined in sequential staining. It was especially challenging and time consuming to optimize both triple staining, in particular to guarantee that all antibodies worked consistently with the same antigen retrieval.

Because the CD4 antibody showed inconsistent results, other CD4 antibodies from different manufacturers were tested, and still yielded variable, non-reliable results. Other researchers also reported variable results with CD4 antibodies in FFPE liver tissue, because of variability in tissue fixation time and on paraffin block storage time. Since some of the selected research paraffin blocks had been in the archive for

many years, it was likely that fixation time was different among them (as these were real diagnostic biopsies). This could be the reason for the inconsistent results.

Therefore, instead of CD4, a CD3 primary antibody was used in the triple panel. With CD3-CD8-FoxP3 combined staining, the total T cell population could be quantified, and the cytotoxic and regulatory subtypes separately labelled and quantified specifically. The selection of a Qdot with different wavelength to each antigen was made considering the following general rule of immunofluorescence/Qdot sstaining: the brightest Qdots, with strongest signal (for instance, Qdot 655, in the red emission spectra) were chosen to bind to the less expressed antigens.

Because FoxP3 expression is nuclear, a Qdot to match this antigen had to have a specific wavelength to avoid overlap with the DAPI emission spectrum. Therefore, FoxP3 was assigned Qdot 705, which has a far-red emission signal that is distant from the DAPI blue emission wavelength (Figure 10). With this, the possibility of bleeding through from DAPI (which has the brightest signal of all) into the Qdot 705 acquisition filter was eliminated, so the signal captured by this filter would only reflect FoxP3 expression.

A nuclear marker is vital in most types of tissue staining, and is essential for identifying and quantifying most nucleated cells. DAPI is a fluorescent DNA stain in the blue spectrum widely used as nuclear counterstaining for fluorescence microscopy. It has high photostability (especially if stored with antifade mounting media) and its spectral characteristics allow its combination with other fluorophores for multiplexing[154-157].

During optimization of staining, positive and negative controls were used in each batch of slides, to evaluate the results. Tonsil and lymph node tissue were used as positive controls and results compared to the expected staining pattern depicted in

both the Human Protein Tissue Atlas[158-159] and the specification datasheet for the primary antibodies (when this information was available). Negative controls consisted of the same tissue as each of the positive controls (lymph node or tonsil) and test sample (liver) which were submitted to exactly the same staining steps except for addition of the primary antibody. It took several months to optimize individual and combined staining, and the protocol for the combination of primary antibodies and Qdots is specified in Table 13 and Table 14 below:

Table 13. **T cell CD3-CD8-FoxP3 immunostaining with Qdots**

Primary antibody (clone)	Primary antibody species	Primary antibody dilution	Primary antibody incubation	Company (catalogue number)	Qdot
Foxp3 (PCH101)	Rat	1:75	Overnight 4°C	eBioscience (14-4776-80)	705
CD8 (C8/144B)	Mouse	1:100	1h room temperature	Dako (M7103)	655
CD3 (polyclonal)	Rabbit	1:150	1h room temperature	Dako (A0452)	605

Table 14 (below). **B cell CD20-CD138-GrB immunostaining with Qdots**

Primary antibody (clone)	Primary antibody species	Primary antibody dilution	Primary antibody incubation	Company (catalogue number)	Qdot
GrB (496B)	Rat	1:50	Overnight 4°C	eBioscience (14-8889-82)	705
CD138 (polyclonal)	Rabbit	1:50	1h room temperature	Atlas (HPA006185)	655
CD20 (L26)	Mouse	1:200	1h room temperature	Dako (M0755)	605

In each of the three-antigen combined immunostaining, the first primary antibodies applied were the least frequently expressed: FoxP3 for the T cell, and GrzB for the B cell staining. In the T cell staining, diluting the Foxp3 antibody in 1.5% bovine serum albumin (BSA) in PBS instead of just PBS resulted in less background.

In regard to the Qdots, some technical aspects need to be considered when designing a staining protocol. Conventional hydrophobic/pap pens were avoided as they decreased the Qdot signal. A substitute histologic pen compatible with Qdots was used: Immedge (Vector laboratories, Burlingame, CA, USA). Protein block was not done with casein, as it might cause quenching of Qdots conjugates. A serum-free protein block (Dako, Glostrup, Denmark), routinely used in Dr A.J. Demetris' laboratory for Qdots staining, was chosen. Qdots were diluted in BSA in PBS. Different concentrations of BSA up to 6% were tested, and best results were achieved with 1.5% BSA. Qmount™ Qdot Mounting Media (Invitrogen, Paisley, UK) was avoided, and a substitute mounting medium compatible with Qdots was found: EcoMount

(Biocare Medical, Pacheco, CA, USA). Serum from the host species was added to each secondary antibody and each Qdot to avoid nonspecific binding. Finally, biotinylated secondary antibodies and streptavidin conjugated Qdots were used. Avidin and biotin blocking was with an avidin/biotin blocking kit (Vector laboratories, Burlingame, CA, USA) used before adding each primary antibody to avoid nonspecific binding of streptavidin-conjugated Qdots to liver tissue, producing background staining. The complete protocol for the T cells immunostaining and B cells immunostaining are detailed below in Table 15 and Table 16, respectively. All washing steps consisted of 3 washes in PBS, each lasting 5 minutes.

Table 15. **Protocol for T cell triple immunostaining with Qdots**

1.	Deparaffinization in xylene for 10 minutes (min)
2.	When tissue is dry, tissue delimitation with Immedge pen
3.	Rehydration with ethanol 100% for 10 min, followed by distilled water for 10 min
4.	HIER with TRIS EDTA buffer (pH 9) for 25 min at 99^{o}C in water bath
5.	Wait until slides reach room temperature, then wash
6.	Avidin block for 10 min
7.	Wash
8.	Biotin block for 10 min
9.	Wash
10.	Protein block for 15 min (Dako serum free protein block)
11.	1st **primary** antibody: FoxP3 (1:75) in 1.5% BSA, overnight at 4°C
12.	Wash
13.	1st **secondary** antibody: biotinylated goat anti-rat 1:3:200 (Ab : goat serum : PBS) for 30 min
14.	Wash
15.	1st Qdot: **Qdot 705** 1:1:50 (Qdot : goat serum : BSA in PBS) for 30 min
16.	Wash
17.	Avidin block for 10 min
18.	Wash
19.	Biotin block for 10 min
20.	Wash
21.	Protein block for 15 min
22.	2nd and 3rd **primary** antibodies: CD3 (1:150) and CD8 (1:100) in PBS for 1h
23.	Wash
24.	2nd **secondary** antibody (to bind to CD8): biotinylated horse anti-mouse 1:3:200 (Ab : horse serum : PBS) for 30 min
25.	Wash
26.	2nd Qdot: **Qdot 655** 1:1:50 (Qdot : horse serum : BSA in PBS) for 30 min
27.	Wash
28.	Avidin block for 10 min
29.	Wash
30.	Biotin block for 10 min
31.	Wash
32.	3rd **secondary** antibody (to bind to CD3): biotinylated goat anti-rabbit 1 : 3 : 200 (Ab : goat serum : PBS) for 30 min
33.	Wash
34.	3rd Qdot: **Qdot 605** 1 : 1 : 50 (Qdot : goat serum : BSA in PBS) for 30 min
35.	Wash
36.	DAPI nuclear staining (3 uL DAPI in 100 ml PBS) for 10 min
37.	Wash
38.	Dehydration with 100% ethanol (3x 5 min each)
39.	Dip in xylene and mount (EcoMount)

Table 16. **Protocol for B cell triple immunostaining with Qdots**

1.	Deparaffinization in xylene for 10 minutes (min)
2.	When tissue is dry, tissue delimitation with Immedge pen
3.	Rehydration with ethanol 100% for 10 min, followed by distilled water for 10 min
4.	HIER with TRIS EDTA buffer (pH 9) for 25 min at 99°C in water bath
5.	Wait until slides reach room temperature, then wash
6.	Avidin block for 10 min
7.	Wash
8.	Biotin block for 10 min
9.	Wash
10.	Protein block for 15 min (Dako serum free protein block)
11.	1st **primary** antibody: GrB (1:50) in PBS, overnight at 4°C
12.	Wash
13.	1st **secondary** antibody: biotinylated goat anti-rat 1:3:200 (Ab : goat serum : PBS) for 30 min
14.	Wash
15.	1st Qdot: **Qdot 705** 1:1:50 (Qdot : goat serum : BSA in PBS) for 30 min
16.	Wash
17.	Avidin block for 10 min
18.	Wash
19.	Biotin block for 10 min
20.	Wash
21.	Protein block for 15 min
22.	2nd and 3rd **primary** antibodies: CD138 (1:50) and CD20 (1:200) in PBS for 1h
23.	Wash
24.	2nd **secondary** antibody (to bind to CD138): biotinylated goat anti-rabbit 1:3:200 (Ab : goat serum : PBS) for 30 min
25.	Wash
26.	2nd Qdot: **Qdot 655** 1:1:50 (Qdot : horse serum : BSA in PBS) for 30 min
27.	Wash
28.	Avidin block for 10 min
29.	Wash
30.	Biotin block for 10 min
31.	Wash
32.	3rd **secondary** antibody (to bind to CD20): biotinylated horse anti-mouse 1 : 3 : 200 (Ab : horse serum : PBS) for 30 min
33.	Wash
34.	3rd Qdot: **Qdot 605** 1 : 1 : 50 (Qdot : goat serum : BSA in PBS) for 30 min
35.	Wash
36.	DAPI nuclear staining (3 uL DAPI in 100 ml PBS) for 10 min
37.	Wash
38.	Dehydration with 100% ethanol (3x 5 min each)
39.	Dip in xylene and mount (EcoMount)

Digital image analysis was necessary to quantify cell populations in whole tissue biopsies, and it requires digitalization of the slides. At the beginning of the current research, the liver histopathology laboratory at King's College Hospital was in the process of acquiring a high-resolution histology slide scanner, which would have specific Qdots filters installed. However, the acquisition of the scanner could not be completed, thus an alternative needed to be found to analyse the research slides.

As previously mentioned, Qdots are normally excited by any standard (excitation) filter on conventional fluorescence microscopes. Since a fluorescence microscope with standard blue/DAPI, green/FITC and red/TRITC filters was available, the results of single Qdot staining were evaluated using this equipment. Qdot 605 (orange) or Qdot 655 (red) were selected for their brightness when staining for individual antigens.

For combined three-antigen staining, besides not being able to differentiate the signal of the different antigens/Qdots, the microscope could not detect the third Qdot (Qdot 705) with an emission wavelength in the far-red spectrum. Therefore, when assessing the three-antigen staining in a conventional fluorescence microscope, I could only recognise two Qdots: Qdot 655 and Qdot 605, in red and orange, respectively. However, because these signals appeared concurrently, their colours were not very distinct from each other and the microscope did not have specific equipment to differentiate their wavelengths, the cells could not be quantified using this equipment. Furthermore, pictures could only be taken of individual fields of the slide, as the microscope did not acquire whole-slide images.

In summary, the available equipment was sufficient to identify the signal of two of the three Qdots present in the staining. While this generally confirmed that the

respective antigen staining worked, no detailed evaluation/quantification could be performed. Suitable equipment to evaluate the results required a slide scanner or fluorescence microscope with Qdot filters. Dr A. J. Demetris in Pittsburgh, USA, kindly agreed to digitalize the slides.

The Mirax MIDI WSI scanner, equipped with a Plan-Apochromat 40×/.95N.A. objective lens, AxioCam MRm digital CCD camera (Carl Zeiss, Jena, Germany) and specifically selected excitation/emission Qdot filters (Omega Optical, Battleboro, VT) was used. Test slides with each of the three-antigen Qdot immunostaining were digitalised and showed that both T cell and B cell staining had worked: the signal was strong, background was minimal, and the resulting images were suitable for digital analysis. Therefore, T cell staining was performed in all biopsies in the research cohort and the slides sent once more for imaging.

When performing the Qdots protocol, each stained slide was checked using the fluorescence microscope to confirm that CD3-Qdot605 and CD8-Qdot655 signals were present and strong before being sent to Pittsburgh. Although it was not possible to assess the FoxP3-Qdot705 signal in the three-antigen combined staining, since it had worked on test samples submitted to the same protocol, it was assumed that this antigen staining also had worked.

Nevertheless, after a few months, on receipt of the whole slide digitalized images, it was evident that the FoxP3 staining had not worked. This might have resulted from a problem with the batch of Foxp3 antibody. Consequently, instead of three-antigen immunostaining, a two-antigen CD3-CD8 staining was obtained. As turnaround time for further staining optimization was likely in the order of months, the experiments were not repeated for this thesis.

Furthermore, because the digital images had a particular extension format for Carl Zeiss equipment (.czi) instead of standard .tiff or .jpeg format, they could not be opened with a conventional image analysis software, such as Fiji/ImageJ. They could only be analysed with the bespoke software used in Pittsburgh: IAE-NearCYTE. Unfortunately, the software presented several recurring problems when used in London, which required several remote meetings with the software developer. Because of the problems with the software, the quantification of the CD3 and CD8 cells was finally performed by the software developer.

An additional limitation of the image analysis programme was that it could not separate anatomical areas in an automated fashion, such as portal tracts or centrilobular veins. It only showed the overall number of cells against the total surface area of the biopsy sample. Breakdown of the cell count according to the location of the cells in different areas would require constant manual input by a pathologist, which was not feasible.

Considering the lack of proper equipment at the current centre for Qdots slide imaging, the time spent to have the slides with the T cell staining digitalized and the problems with the image analysis software, Qdots were not used for the B cell staining. Despite investing a large amount of time in developing protocols using a new, potentially better technology, apparently, London's hospitals and Universities could not provide adequate facilities to continue with this state-of-the-art research.

3.2.3.5 Conventional immunofluorescence and B cell staining

As all staining performed during this research, the B cell staining using immunofluorescence was conducted by the research author (L.N.S.). The aim of

performing the B cell immunostaining was to quantify B cells and plasma cells in different regions of the tissue and also to verify whether either of these cell types expressed GrzB. This expression could indicate a possible local role for B cells and/or plasma cells (Chapter 1). Although not as good as Qdots staining, conventional fluorescence is a good option for three-antigen staining, even in FFPE tissue, as long as appropriate fluorophores with compatible spectral characteristics are used. Immunofluorescence in FFPE tissue is not routinely performed and has classically been considered as not doable, essentially for problems with innate autofluorescence and tissue quality[143-144].

In the last decade, however, several groups have developed protocols and reported robust results using single, double and multiplex immunofluorescence of fixed human tissue, frequently using archival samples[143-148]. According to Robertson *et al*.[143], after staining and imaging, slides can be kept at -20°C for large periods of time, beyond 250 days, with negligible loss of quality. In fact, the optimization of multiplex immunofluorescence in FFPE tissue and the possibility of long-term storage of slides could enable numerous studies in archival diagnostic samples.

Several aspects need to be considered to perform good quality, multiple antigen immunofluorescence staining with consistent results:

1. Choice of fluorophores needs to be compatible with the filters of the microscope where samples are to be analysed. In the present research, with the available microscope with standard blue-green-red filter set, only two antigens could be analysed (with the green and red filters), besides the nuclear DAPI stain (blue).
2. Fluorophores should have narrow emission wavelengths in order to avoid bleed-through (crossover) of a given fluorescent dye to the detection channel

of another (for instance, of a green fluorophore into the red channel). Fluorophores chosen should be spectrally different to (compatible with) the chosen nuclear counterstain.

3. Secondary antibodies (labelled with fluorescent dyes) should ideally originate from a single host species. This, combined with the use of serum of this (host) species for the protein block, avoids nonspecific binding and reduces background staining. All secondary antibodies used were raised in goat, and goat serum was used for the protein block.
4. Ideally, the secondary antibodies selected should have been pre-adsorbed/cross-adsorbed against both the host species of the primary antibodies, and the species of the tissue sample. This prevents species cross-reactivity of secondary antibodies and non-target primary antibodies and also minimizes background. Pre-adsorption is an additional step of purification performed to increase the specificity of a secondary antibody. The process consists of passing the solution of the secondary antibody through a column with serum proteins from possibly cross-reactive species. The non-specific antibodies are then retained in the column, while highly specific secondary antibodies pass through. Figure 12[149], shows a solution of secondary antibodies against rabbit IgG passing through a column with serum proteins of potentially cross-reactive species (sheep and bovine IgGs). Secondary antibodies with high specificity to the target (rabbit IgG) pass through the column, whereas those that show species cross-reaction (with either sheep or bovine IgG) stay bound to these proteins. This results in secondary antibody with high specificity for its target species. In the current protocol, I selected only

secondary antibodies which were cross-absorbed against the host species of non-target primary antibodies and the species of the liver samples[150].

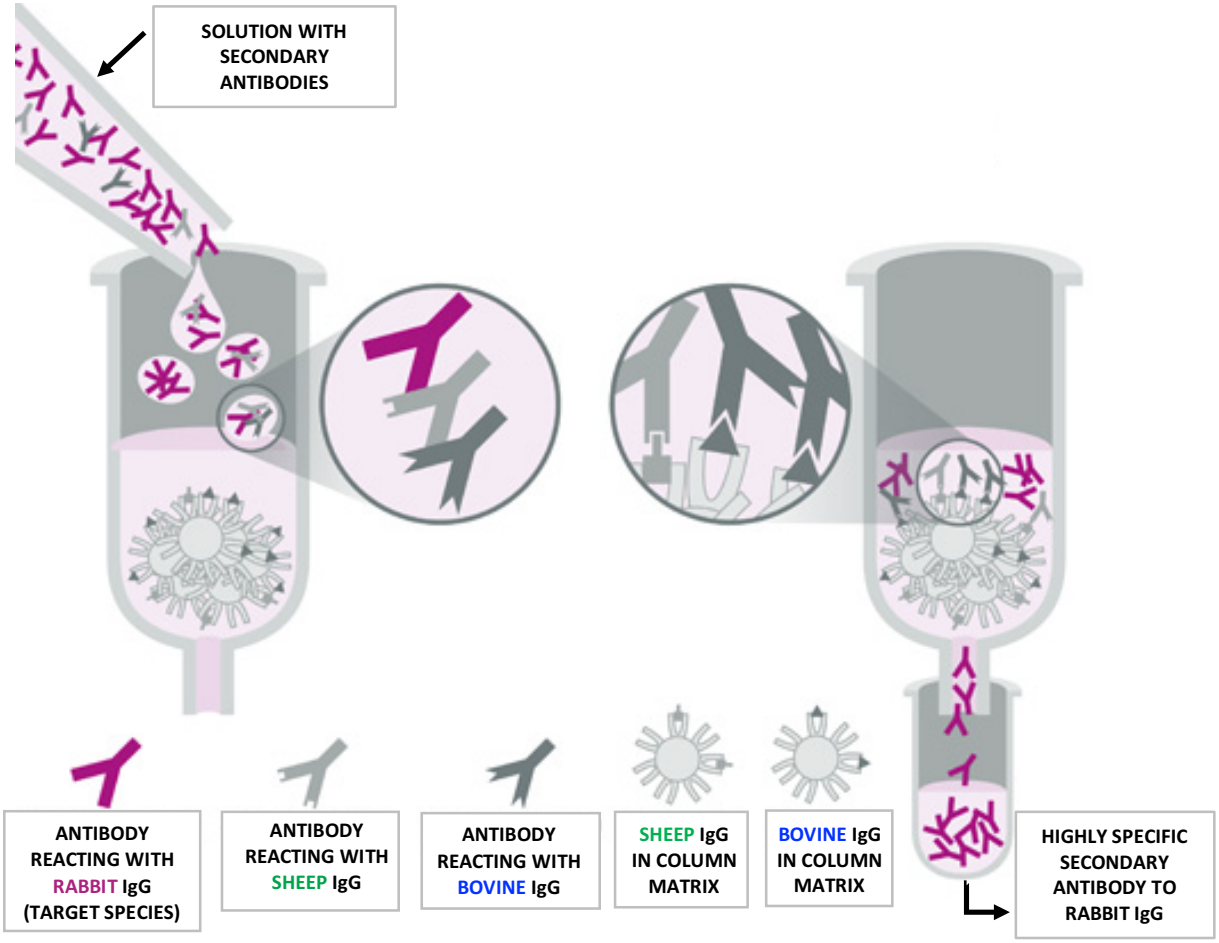

Figure 12. **Pre-adsorption of secondary antibodies**

Alexa Fluor (AF) fluorescent dyes (Invitrogen, Thermo Fisher Scientific, Carlsbad, California, USA) were chosen for their intense brightness, good stability in fluorescent mounting medium, and because they are the most used fluorophores in FFPE samples staining[144-148,151-152]. Slides stained with AF still had bright signal and

low bleaching after an initial assessment in the microscope (including pictures), and this signal was maintained after a month of storage at -20^{o}C (protected from light). Although not as stable in the long-term as Qdots, these dyes were a suitable alternative to Qdots for staining fixed tissue. DAPI was used for nuclear staining for the reasons previously explained.

My aim in performing the B cell immunostaining was to quantify B cells and plasma cells and also to verify whether either of these cells expressed granzyme B (GrzB). This expression could indicate a possible local role for B cells and/or plasma cells (Chapter 1). The protocol previously designed for B cell and plasma cell staining with Qdots included 3 primary antibodies: CD20, CD138 and GrzB. However, because of the microscope filters available, only two antibodies could be chosen (besides the DAPI for the nuclei).

Therefore, CD20, that marks B cells only, was substituted with CD79α (clone JCB117, Dako, Glostrup, Denmark), which recognizes both B cells and plasma cells. Therefore, if GrzB was expressed by only one of these cell types (plasma cells or B cells), double positive cells (CD79α+GrB+) would be seen amongst the CD79α+ cells. However, in case such CD79α+GrB+ cells were found, it would not be possible to differentiate between B cells and plasma cells with only two antibodies. So the CD138 antibody was included in a three-antibody staining protocol, with a secondary antibody conjugated with a far-red Alexa fluorophore. If CD79α+GrB+ cells were found in an initial assessment, a fluorescence microscope equipped with a far-red excitation filter and acquisition camera would be located for further analysis of CD138 staining.

I chose a fluorescent dye in the far-red spectrum for the additional antibody (CD138) for two reasons: 1) the far-red channel is a common filter in modern

fluorescence microscopes, and 2) it is compatible (shows low wavelength overlap) with the other selected fluorophores, in the blue, green and red spectra. I used the Fluorescence SpectraViewer tool[153] to select three Alexa Fluor dyes that could be combined in multiple antigen staining and were compatible with DAPI. The fluorophores and their respective excitation (dashed line) and emission (continuous line) wavelengths are depicted in Figure 13. The overlap between fluorophores is represented by the value of "Relative Intensity (%)" where the lines of different fluorophores meet.

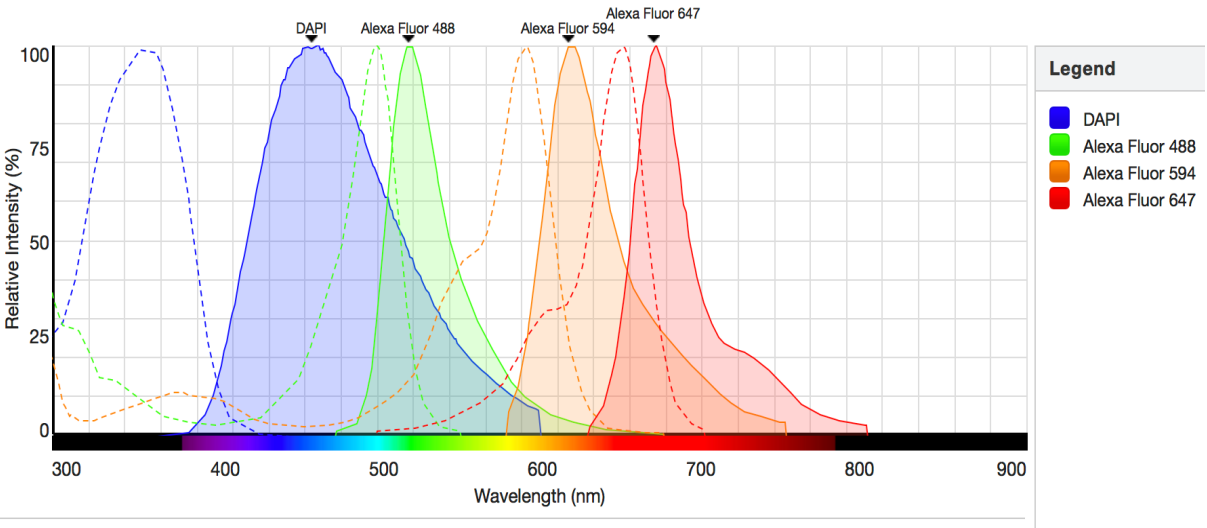

Figure 13. **Excitation and emission wavelenghts of chosen fluorophores**

The compatibility of different AF dyes to be used in combination is shown in Figure 14[160]. Green, blue and red rectangles mean high, medium and low compatibility, respectively. High compatibility between a pair of fluorophores indicates no bleed-through between them; medium compatibility implies low bleed-through, and low compatibility means significant bleed-though, thus the combination should be avoided.

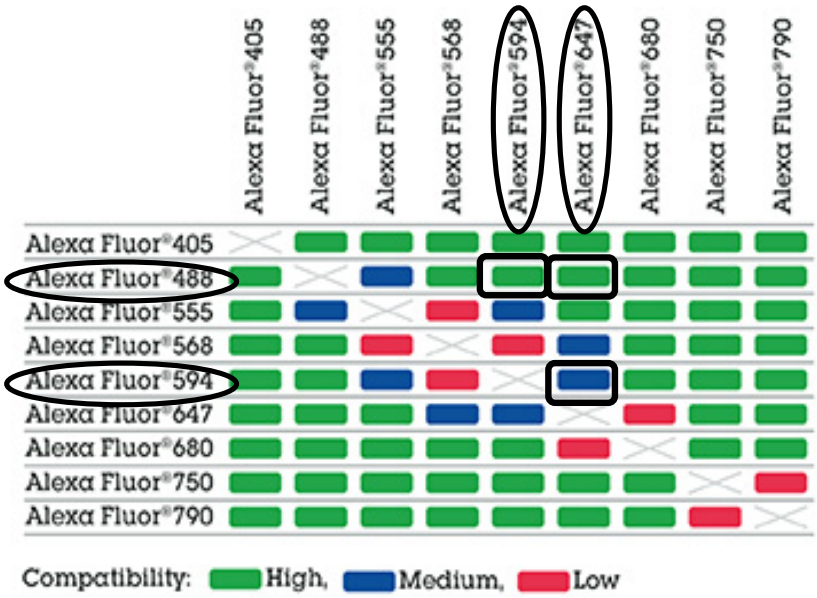

Figure 14. **Compatibility between different Alexa Fluor dyes for multiple antigen immunostaining**

Although the emission spectrum of DAPI and AF 488 overlap (Figure 13), their excitation range is distinct, with virtually no overlap, so they can be used in combination. Moreover, the fact that DAPI is a nuclear marker whereas GrzB is located in the cytoplasm helped evaluate possible bleed-through (which was not seen). The combination of AF 488 (used for GrzB) and each of the other fluorophores: AF594 (for CD79α) and AF 647 (for CD138) is highly compatible (Figure 14), with minimal spectral overlap (Figure 13).

Thus, the combination of primary antibodies and fluorophores chosen for the B-cell multiplex staining protocol was: GrzB-AF 488 (green), CD79α-AF 594 (red) and CD138-AF 647 (Table 17). There was some overlap between the excitation and emission spectrum of AF 594 (for CD79α) and AF 647 (for CD138), as seen in Figure 13, which meant there could potentially be some bleed-through between their

respective channels (red and far-red). Despite that, there were other features that helped me to evaluate bleed-through between the respective fluorescent channels, the main being the distinct staining patterns of CD79α and CD138 antibodies. Besides plasma cells, CD138 stained the hepatocyte membranes across the biopsies, whereas CD79α only highlighted individual cells. The number of CD138+ cells was also considerably lower than that of CD79α+ cells, and CD138+ cells (plasma cells) had more cytoplasm than the other CD79a+ cells (namely, B cells). Comparison between the single immunostaining of each of these antigens was done to validate multiplex staining.

Table 17. **Combination of antibodies for CD79α-CD138-GrzB immunofluorescence protocol**

Antibody (Clone)	Host species	Primary Antibody Dilution	Primary Antibody Incubation	Company (Catalogue Number)	AF-conjugated secondary antibody /Catalogue Number
CD79α (JCB117)	Mouse	1:25	1h, room temperature	Dako (M7050)	Goat anti-mouse AF594 (red) / A-11032
GrB (496B)	Rat	1:50	1h, room temperature	eBioscience (14-8889-82)	Goat anti-rat AF488 (green) / A-11006
CD138 (polyclonal)	Rabbit	1:75	1h, room temperature	Atlas (HPA006185)	Goat anti-rabbit AF 647 (far red) / A-21245

Some considerations must be made regarding optimization of the staining protocol. Different methods for protein block were attempted: skimmed milk (casein); BSA and serum-free protein block (Dako). The lowest background staining was achieved using a combination of 5% BSA and 2% serum from the host species of the

secondary antibody (goat). As to the order of antibodies, different methods were tested: 1) adding a primary antibody, then its corresponding secondary antibody, followed by another primary and secondary, in a sequence; 2) applying the primary antibodies simultaneously, followed by the secondary antibodies sequentially and 3) adding the primary antibodies simultaneously, then the secondary antibodies also concomitantly. The last method was less time consuming and produced similar results as the sequential approach, so was chosen.

Although only two antibodies could be assessed simultaneously, not three (due to the lack of far-red filter/channel), using the available fluorescence microscope, I performed three double staining (all possible combinations of two primary antibodies: CD138-CD79α, CD138-GrzB, CD79α-GrzB) using secondary antibodies conjugated with green (488) and red (594) AF. By performing double antigen stains with CD138-CD79α and CD138-GrzB (plus DAPI), no cross-reaction was observed between CD138 and each of the other antigens/primary antibodies. The distinct pattern of CD138 staining was particularly useful for this evaluation. When performing the final three-antigen staining, both GrzB and CD79α could be assessed in the green and red channel, respectively. The hepatocyte membrane did not appear in the green or the red fluorescence channel (in which GrzB+ cells and CD79α+ cells were observed, respectively). Therefore, the absence of cross-reaction and bleed-through were confirmed.

The fact that the primary antibodies chosen were from different species and the secondary antibodies were highly cross-adsorbed against the other primary antibody species (and the biopsy tissue species) allowed the simultaneous application of primary and secondary antibodies without cross-reaction. Details on the species

against which each secondary antibody had been cross-adsorbed are shown in Table 18. Extensive washing was performed after incubation with primary antibodies, to ensure that any antibody not bound to the tissue was removed (decreasing background staining).

Table 18. **Cross-adsorption of selected secondary Alexa Fluor-conjugated antibodies**

AF-conjugated secondary antibody (catalogue number)	Cross-adsorption classification	Cross-adsorption against
Goat anti-mouse AF594 (A-11032)	Highly cross-adsorbed	bovine IgG, goat IgG, **rabbit** IgG, **rat** IgG, **human** IgG and human serum
Goat anti-rat AF488 (A-11006)	Cross-adsorbed	**mouse** IgG, mouse serum and **human** serum
Goat anti-rabbit AF 647 (A-21245)	Highly cross-adsorbed	bovine IgG, goat IgG, **mouse** IgG, **rat** IgG and **human** IgG

Significant autofluorescence was evident in the red channel, from both hepatocytes (mainly due to the presence of lipofuscin) and in some biopsies, red blood cells. Because the autofluorescence could interfere with the interpretation of the CD79α staining, slides were dipped in Sudan black at the end of the staining to decrease autofluorescent emission. This considerably decreased tissue autofluorescence without significant reduction of the fluorophore signal. Sudan Black has been used for this purpose by other researchers[161-163].

The final, detailed protocol after optimization is below (Table 19). Washing steps consisted of 3 washes in PBS each lasting 5 minutes, unless stated otherwise.

Table 19. **Protocol for CD79α-CD138-GrzB immunofluorescence staining**

1.	Deparaffinization in xylene for 10 min
2.	When tissue is dry, delimitation with Immedge pen
3.	Rehydration with ethanol 100% for 10 min, followed by distilled water for 10 min
4.	HIER with EDTA buffer (pH 9) for 25 min at 99°C in water bath
5.	When slides/buffer reach room temperature, wash in distilled water (3x 5 min each)
6.	Wash (PBS)
7.	Protein block with 5% BSA (in PBS) + 2% goat serum for 1h
8.	Wash
9.	Primary antibodies: CD79α (1:25) + GrzB (1:50) + CD138 (1:75) in 1.5%BSA overnight at 4°C
10.	Wash extensively in PBS (6x 5 min each)
11.	Secondary antibodies: Goat anti-mouse AF 594 (to CD79α) + Goat anti-rat AF 488 (to GrB) + Goat anti-rabbit AF 647 (to CD138) at 1:400 in 1.5%BSA **+** 1% Goat serum for 1h
12.	Wash
13.	DAPI for nuclear staining (3 uL DAPI in 100 ml PBS) for 10 min
14.	Wash
15.	Wash in distilled water (3x 5min each)
16.	Dip slides in Sudan black for 5 seconds
17.	Wash in tap water
18.	Wash in distilled water (3x 5min each)
19.	Mount (Dako fluorescence mounting medium)

During the preparation of the slides, a fluorescence microscope capable of assessing all three fluorophores and DAPI (with far-red filter) was located at the Nikon Imaging Centre at Guy's campus of King's College London. This facility provides access to advanced imaging equipment and training in microscopy techniques. Confocal microscopy is commonly used for assessing multiplex fluorescence staining and was the original method of choice to analyse co-localization of GrzB on B cells and plasma cells.

However, some modern microscopes are able to scan whole slide sections with exceedingly high precision by identifying several different focal planes through the tissue thickness, with results as accurate as confocal microscopy. This type of equipment has the advantage of imaging large areas of tissue instead of individual fields, which is essential for quantifying cells in whole biopsies. Slides were therefore digitalized using a motorised microscope for multi-dimensional imaging: the Eclipse Ti-2 inverted microscope (Nikon, Tokyo, Japan). This microscope can be used for both live cell imaging and fixed tissue biopsies. It captures an image from each microscope field, at the desired magnification, in each fluorescent channel. Those images are combined into a final image file of the whole biopsy for each fluorescent channel: blue, green, red and far-red.

Moreover, this microscope had a Perfect Focus System, which is a focal drift compensation mechanism that enables the equipment to stay on the correct focal plane despite the movement of the camera during the imaging of the whole slide. To generate the final in-focus image, the microscope captured several images at several focal planes/depths ("Z stacks") throughout the sample. In each image, distinct areas of the tissue would be in focus. The microscope software automatically removed the out-of-focus signal captured in individual images, and blended the in-focus areas together, generating the final in-focus digital image of the whole biopsy specimen. Figure 15, adapted from Planz *et al*.[164], illustrates the concept of the Z-stack.

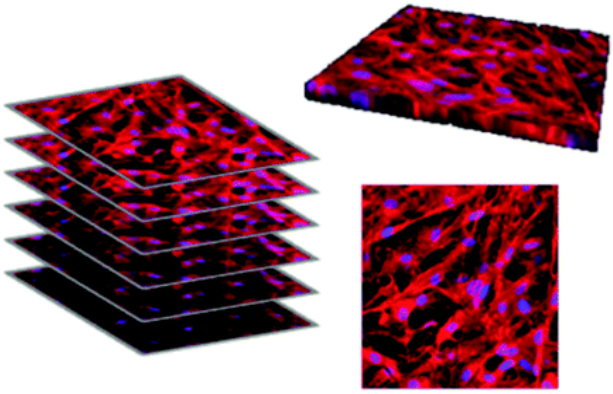

Figure 15. **Z-stack analysis of human skin cells with fluorescence-staining of the cell membrane (red) and cell nuclei (blue)**

The one problem when using this microscope for whole slide imaging was the excessive amount of time required to create high quality whole biopsy digital images using 4 fluorescence channels, in some cases taking over an hour to scan a single biopsy specimen. Furthermore, the equipment was not capable of detecting the tissue/biopsy area automatically, as some slide scanners are, and the final image needed to be in a square or rectangle shape, so for biopsies with an irregular shape, the microscope spent a long time digitalising areas with no tissue.

Additionally, each slide had to be manually positioned, and the equipment only accepted one slide at a time. The middle point of the biopsy was manually measured with a ruler for length and width, to place the exact centre of the tissue in the microscope field at the start of each digitalization. The microscope had to be set to the best focus for all fluorescent channels, so the equipment could maintain that exact focus through the Perfect Focus system. This process had to be repeated for each biopsy specimen. In summary, although very modern and able to digitalize three-antigen fluorescence staining, the equipment was not practical for scanning large slide

sets of whole biopsy samples, as it required several manual steps and constant supervision.

The 200x objective magnification was chosen for slide digitalization. This was accurate enough to allow quantification of cells and any higher magnification would demand an impracticable amount of time per scan. In addition, the Qdot T-cell stained slides had been digitalized using the same magnification, and this was recommended by the image analysis software developer in Pittsburgh.

3.2.4 Image Analysis

3.2.4.1 Collagen proportionate area

The digital quantification of fibrosis in Sirius Red stained biopsies was performed using NIH ImageJ software (available at http://rsb.info.nih.gov/ij/). The CPA (CPA) was calculated in percentage by dividing the area of fibrosis by the whole biopsy area. The steps for defining the CPA in ImageJ are specified in Table 20 below.

Table 20. **Steps for measuring CPA using ImageJ**

1.	Menu, select 'Analyse' → 'Set Measurement' → choose 'Area' and 'Limit to threshold' and unselect the other parameters → 'ok'
2.	Menu, select 'File' → 'Open' → choose image file to be analysed
3.	Menu, choose 'Image' → 'Type' → '32-bit'
4.	Menu, select 'Image' → 'Adjust threshold' → adjust the bottom pin until the whole tissue is selected (do not move the top pin) → 'Apply' → when the message about NaN appears, untick the box
5.	Menu, choose 'Analyse' → 'Measure' → 'ok'. The resulting number is the measurement of the whole tissue area in pixels.
6.	Close the image without saving
7.	Re-open the image (see step 2)
8.	Menu, choose 'Image' → 'Adjust" → "Color threshold". Three parameters appear: Hue, Saturation and Brightness. The first (top) pin of Saturation and Brightness should be adjusted until all the area stained with Sirius red is selected → 'Select'
9.	Menu, choose 'Analyse' → then 'Measure' → 'ok'. The resulting number is the measurement of the area of collagen
10.	Calculate the CPA (percentage) by dividing the collagen area by the whole biopsy area and multiplying by 100.

3.2.4.2 Qdots cell counts

Digital images of Qdots slides were analysed in Pittsburgh. The IAE-NearCYTE software automatically calculated the biopsy area in mm^2. The quantification of T cells was performed by software identification of all cells with a nucleus (positive DAPI) and CD3 cytoplasmic staining surrounding it. The threshold of staining/signal intensity for considering a cell positive for each antigen is determined by user input. Cells with nuclear staining that were double positive for CD3 and CD8 were considered cytotoxic T cells. Once the software showed positive cells for each antigen combination, further individualization, deletion or addition of cells could be done manually. For Qdots slides,

an automated quantification of cells that expressed each antigen was achieved by defining thresholds for brightness and contrast for each fluorescent channel, so the software would select positive cells and ignore background/autofluorescence. This worked for the Qdots stained slides because having a narrower emission spectra than conventional fluorescent dyes meant that the Qdots did not overlap significantly with liver autofluorescence. This was not the case of the biopsies stained with conventional fluorescence for B cells, though.

Figure 16 and Figure 17 show the process of cell identification and quantification in one study biopsy specimen (small portal tract). Figure 16 is a biopsy field stained with DAPI (blue), CD3 (red) and CD8 (green). CD3+CD8+ (double positive) cells appear yellow. Figure 17 shows the same biopsy area with individualized cells/objects, classified using the IAE-NearCYTE image analysis software. DAPI+ objects are outlined in black, DAPI+CD3+CD8- are outlined in red; DAPI+CD3+CD8+ appear in yellow and DAPI+CD3-CD8+ in green. The CD3-CD8+ (green) cells correspond to natural killer and dendritic cells that express CD8 but not CD3. These cells were not the focus of the present study.

Therefore, the total population of T cells included red (CD3+CD8-) and yellow (CD3+CD8+) cells. To enable comparison of the number of cells in biopsies of different sizes, the total number of cells was divided by the biopsy area, thus resulting in number of cells per mm^2. As previously mentioned, FoxP3 staining with Qdots did not work (Materials and Methods).

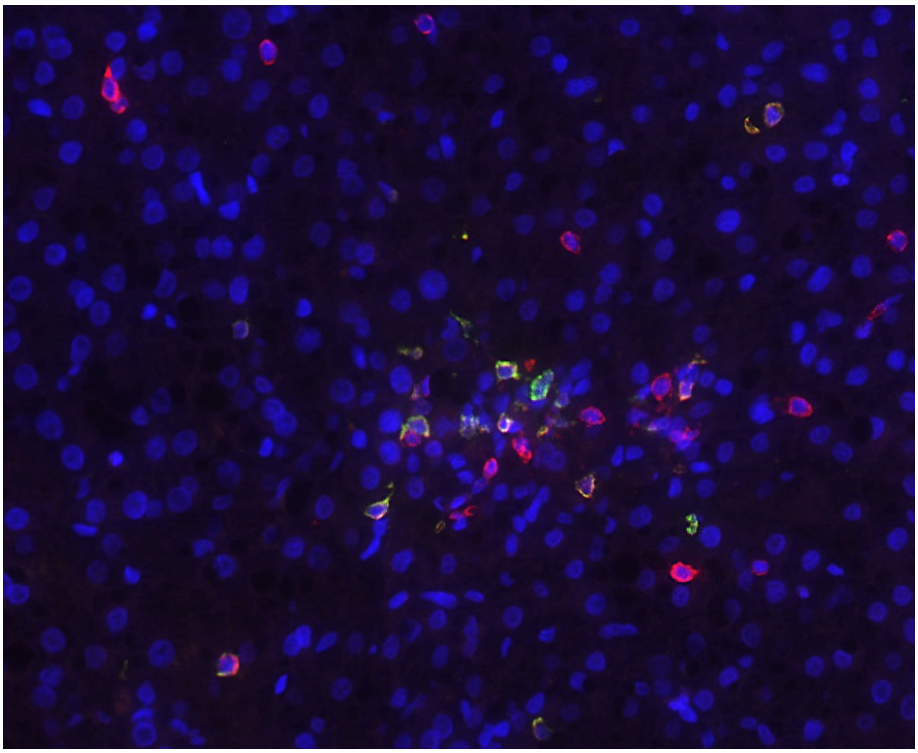

Figure 16. **DAPI + CD3 + CD8 Qdots immunostaining**

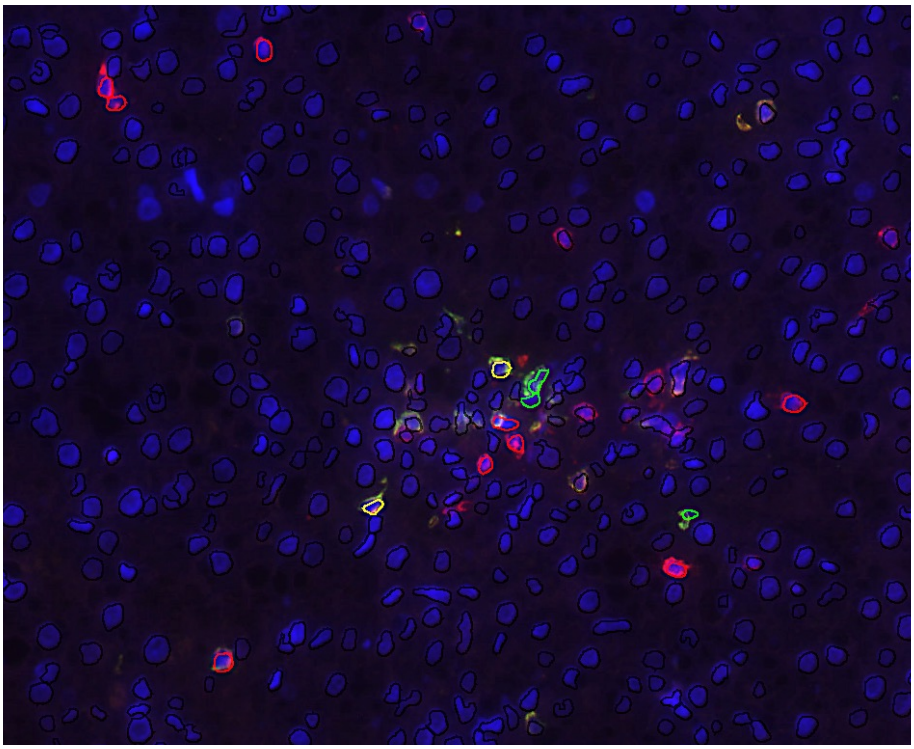

Figure 17. **DAPI + CD3 + CD8 Qdots immunostaining - Cell identification and classification.** *Same biopsy field as Figure 16 showing the process of cell recognition for different antigens by the software IAE-NearCYTE*

3.2.4.3 Conventional immunofluorescence

Slides stained with DAPI + CD79α + CD138 + GrzB with immunofluorescence were analysed with Fiji/ImageJ software. The initial idea was to conduct automated quantification of cells by defining (brightness and contrast) thresholds for each fluorescent channel, similar to what was done for Qdots stained slides. Nonetheless, unlike Qdots staining, the sections stained with conventional fluorescent dyes still displayed autofluorescence even after treatment with Sudan Black. For this reason, despite numerous attempts, including the use of an alternate image analysis software (NIS-Elements - Nikon, Tokyo, Japan), the automated quantification was not possible,

particularly in the red (CD79α) channel. Figure 18 depicts one biopsy in the red fluorescence channel (CD79α staining). The autofluorescence is noticeably strong in red blood cells and also present in hepatocytes.

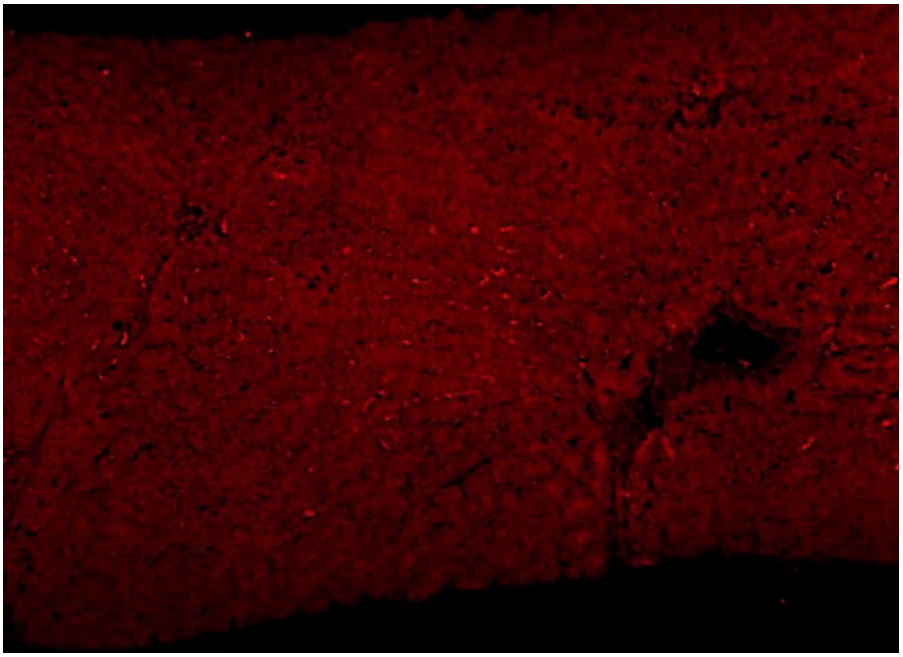

Figure 18. **CD79α staining in red channel displaying autofluorescence in red blood cells and hepatocytes**

When higher thresholds were imposed, to eliminate all background, real positive cells were overlooked (false negative), and when the threshold was lowered to incorporate all positive cells, it selected red blood cells (and sometimes hepatocytes) because of their autofluorescence (false positive). The possible option to quantify cells was then to manually select positive cells in Fiji/ImageJ. Despite the autofluorescence that prevented automated recognition and quantification of cells, CD79α+ cells could be easily recognised by human eye and differentiated from background. A tool in Fiji/ImageJ allowed the user to select each positive object, and

the software kept a record of labelled objects and displayed them, numbering them sequentially (Figure 19).

The quantification of CD79α+ was conducted through assessing both the red (CD79α) and the combined blue + red (DAPI+CD79α) channel images simultaneously in the screen (Figure 19). Whilst positive cells were more easily spotted in the red channel, overlaying with the blue channel ensured that every cell included in the quantification was a nucleated cell. This partially manual process allowed the cell quantification in whole biopsies, despite exceptionally time consuming due to the size of samples analysed (whole biopsy specimens), resulting files (up to 4 gigabytes per sample) and number of positive cells (as much as one thousand per biopsy).

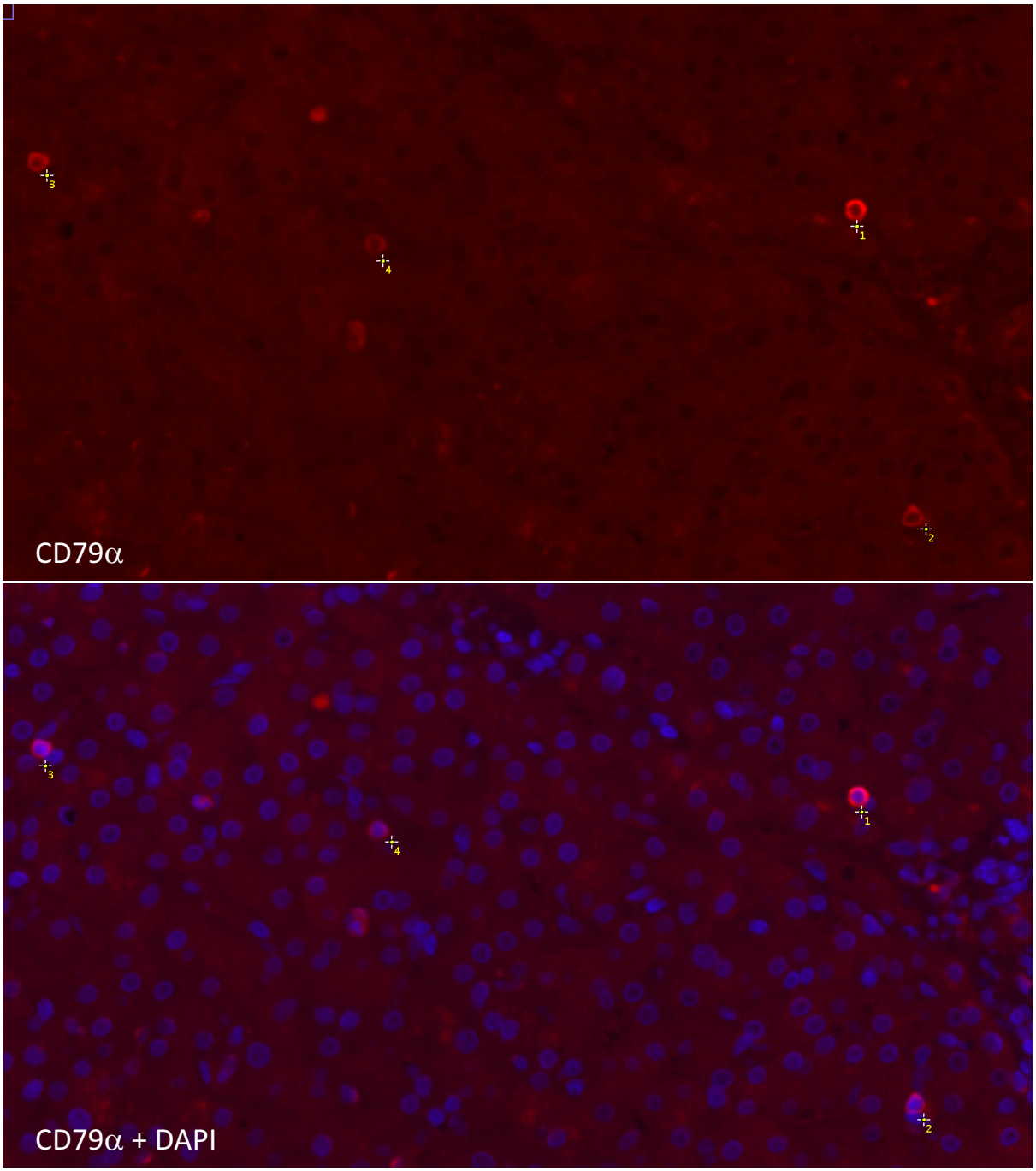

Figure 19. **Manual selection of objects/cells on Fiji/Image.** *CD79α staining with (lower image) and without (upper image) nuclear staining. Each number represents a CD79α+ cell identified by the user's manual selection in the software.*

Although no autofluorescence was observed in the far-red channel (CD138 staining), the quantification of plasma cells could not be automated due to staining of

hepatocytes' membranes and bile duct epithelial cells by CD138 antibody (Figure 20). Although this staining pattern prevented automated quantification of plasma cells, it was helpful to identify the architecture of the liver. In many biopsies, the exact location of plasma cells could be determined (portal, central, lobular). In others, however, this was not possible because of liver architectural distortion in consequence of extensive fibrosis. Thus, the location of plasma cells was not considered in the results, only the number of cells per biopsy area, similar to that done for B cells. The CD138+ cells were also easily recognized by human eye, despite the hepatocyte membranous staining, as shown in Figure 21 and Figure 22.

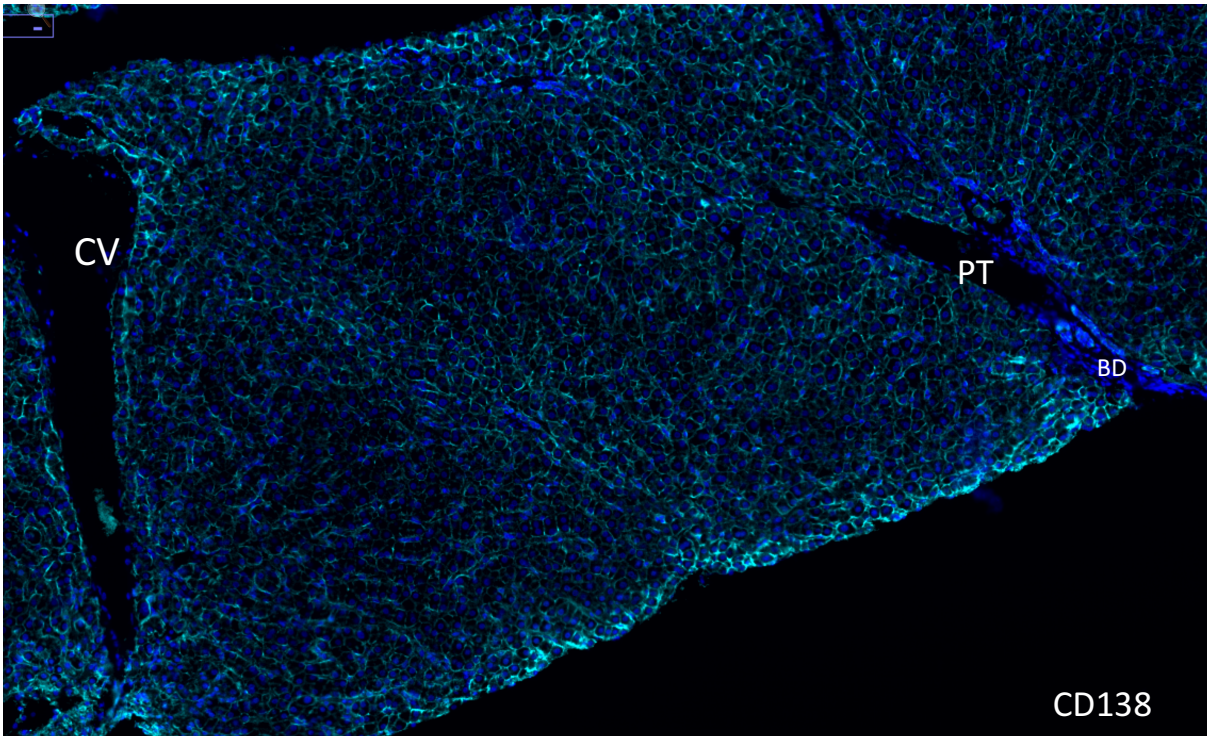

Figure 20. **CD138 staining highlighting the hepatocyte membranes.** *CV, central vein; PT, portal tract; BD, bile ducts*

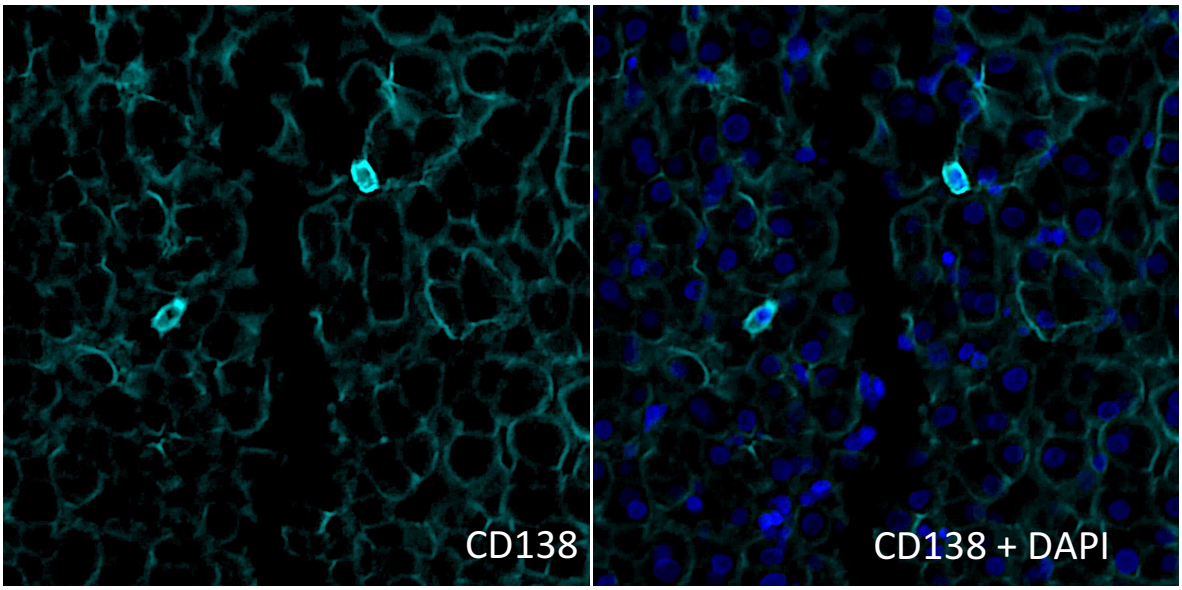

Figure 21. **Two plasma cells in the lobule (CD138+), clearly differentiated from the background hepatocyte staining due to cell shape and signal brightness**

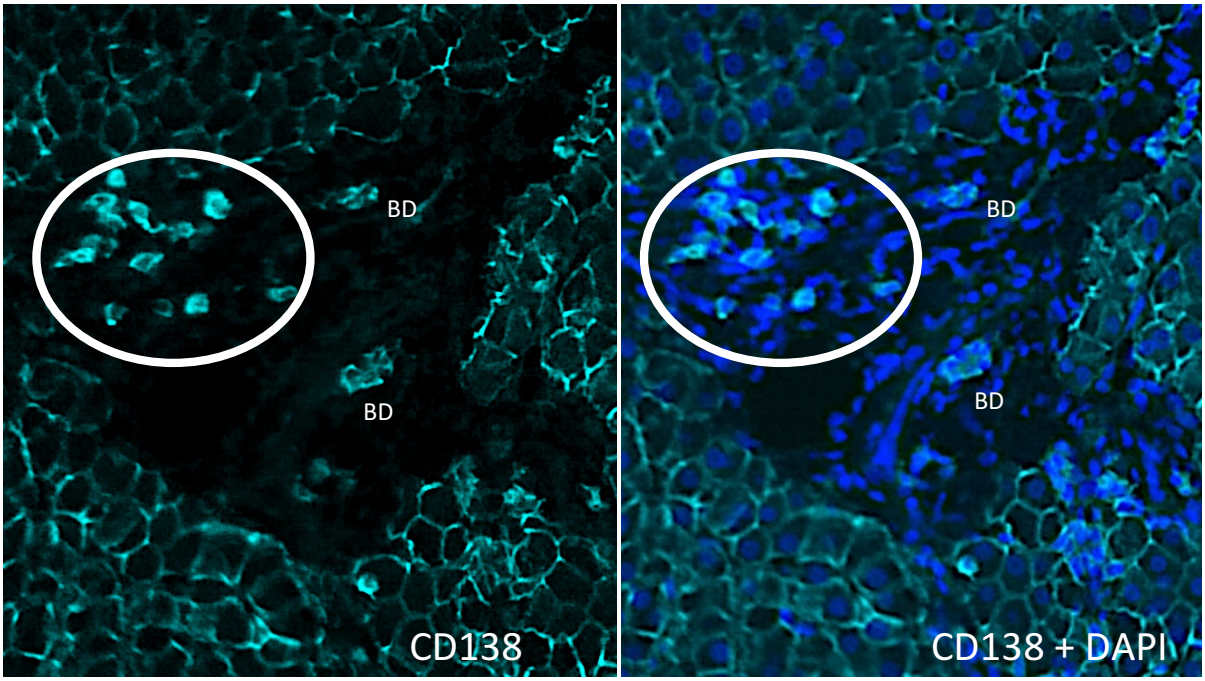

Figure 22. **A group of plasma cells in a portal tract (inside circle). They can be differentiated from bile duct epithelial cells by their bigger size, more abundant cytoplasm, shape and individual disposition.** *BD, bile duct.*

The analysis of double-positive CD79α+GrzB+ cells was conducted in two ways: by assessing the slides in the original fluorescence microscope (with blue-green-red filter set) and by examining the whole biopsy images acquired in the Nikon centre. In the microscope, each biopsy specimen was viewed individually at 200x magnification, switching filters to spot double positive cells. Then at 400x, pictures were acquired of all CD79α+GrB+ cells. Finally, the microscope images were compared with the whole biopsy images from each specimen to confirm that the double positive cells also appeared as double positive in the images acquired with the other equipment.

Because the whole biopsy images included an extra channel for the CD138 (far-red), the images from both equipment were compared to verify whether the CD79α+ cells expressing GrzB observed in the microscope were also positive for CD138 in the scanned image. In other words, assessing the specimens on the microscope was the best method to spot B cells/plasma cells that expressed GrzB (CD79α+GrB+), whereas the whole biopsy scanned image was the only method able to differentiate whether those cells were plasma cells (CD138+) or B cells (CD138-).

The image analysis of the biopsy slides required approximately two months. The total tissue area of each biopsy was calculated using similar method as that used to calculate the CPA in the Sirius red stained slides, above. The total number of CD79α+ cells and CD138+ cells in each biopsy was divided by the area of the biopsy, resulting in the number of cells per mm^2, as previously done for the quantification of T cells in Qdots stained slides. This adjustment allowed the comparison of number of cells among biopsies of different sizes. Table 21 shows the steps followed to perform the quantification of cells in each channel using Fiji/ImageJ.

Table 21. **Quantification of cells using Fiji/ImageJ**

1.	In menu, choose “File”, choose “Import” and select “Bio-Formats”
2.	When new window appears, in section stack viewing, choose hyperstack; in color mode, choose default; in memory management, select use virtual stack; in split into separate windows, select split channels.
3.	Once the 4 images are open (blue, green, red and far red fluorescence channel), in menu, choose “Image”, then “look up tables” and ascribe a different colour for each image.
4.	In menu, choose “Image”, then “adjust” and select “brightness/contrast”. Adjust the parameters (brightness and contrast) for each layer/channel as appropriate.
5.	In menu, choose “Image”, then “color” and select “merge channels”. For counting the cells in each channel (each antibody staining), choose the channel desired and the DAPI channel. Tick “create composite” and “keep source images” and click “ok”.
6.	Once the composite image is open, select the “multi-point tool” in menu and identify each positive cell by clicking/adding a label to it. The software keeps record of the number of cells (objects) selected.

3.2.5 Statistical analysis

Data were analysed statistically using SPSS version 23.0 (IBM Corp, 2015). Continuous variables were presented as median and range whilst categorical variables were presented as number and percentage. For most continuous variables, such as patient age at transplantation or number of inflammatory cells in a biopsy, the **median** was used to measure average tendency. The median is the middle number when the values of a given variable/parameter are put in order, and half of the samples will be below and half of the samples above that number. It is a superior measure

compared to the mean for variables with a wide range of values and with outliers (extreme values) or else for small samples, as it is not as influenced by extremes as the mean[165].

The **mean** (average) was used instead of the median when comparing degrees of inflammation or fibrosis between different groups. This choice was made because the scoring systems used to grade histologically inflammation or fibrosis incorporate a few discrete values with no extreme values/outliers. Most histological parameters scored had one of four possible values: 0, 1, 2 and 3 (corresponding to: absent, mild, moderate and severe intensity, respectively).

The Mann-Whitney (non-parametric) test was used to compare continuous variables between groups. The independent samples t test was not used because of the relatively small size of the sample.

The Fisher's exact test was used to compare categorical variables and validate differences in frequencies between different groups.

The Person's correlation test was used to correlate two continuous variables. For a significant p value, a correlation coefficient (r) from 0-0.3 was considered weak/no correlation; 0.3-0.5, moderate positive correlation (-0.3- -0.5, moderate negative correlation); and above 0.5, strong positive correlation (below -0.5, strong negative correlation).

For all tests, a p value of less than 0.05 was considered statistically significant. Throughout the tables in the Results sections, significant p values (<0.05) are presented in bold for quick visual recognition.

3.3 RESULTS

3.3.1 Clinical data

Five-hundred and thirty-nine children were transplanted between January 1989 and March 2003 at King's College Hospital. Fifty-eight of them were alive, under follow-up in the same centre, clinically asymptomatic, and consented to have a long-term post-transplant protocol biopsy as part of a clinical follow up study. The biopsies had been performed between 8.6-15.6 (average 11.9) years post-transplant. Thirty patients were male and 28 were female. The recipients' age at biopsy varied between 8.5 to 17.1 (average 13.2) years. Organ donation types were: 90% DBD; 8.6% living-relative liver transplant (LRLT) and one child (1.7%) DCD. Graft types were: 78% split graft, 19% whole, and 3.4% a reduced liver.

The indications for LT were: biliary atresia in 32 children; acute liver failure in 6; progressive familial intrahepatic cholestasis in 5; Alagille syndrome in 4; hepatoblastoma in 4; cryptogenic cirrhosis in 2; α1 anti-trypsin deficiency in 2; liver cystic fibrosis-related liver disease in 1; neonatal sclerosing cholangitis in 1 and cholestasis following total parenteral nutrition in 1 (Table 22). Average follow-up time after the protocol biopsy was 6.8 years (the range was 0-18.6 years). During this time, 4 patients (6.9%) required retransplantation and one died 3 days after surgery.

Table 22. **Indications for liver transplantation**

Indication for LT	Number (%)
Biliary atresia	32 (55.2%)

ALF	6 (10.3%)
PFIC	5 (8.6%)
Allagile syndrome	4 (6.9%)
Hepatoblastoma	4 (6.9%)
Cryptogenic cirrhosis	2 (3.5%)
α1ATD	2 (3.5%)
Cystic fibrosis	1 (1.7%)
Neonatal sclerosing cholangitis	1 (1.7%)
Cholestasis after TPN	1 (1.7%)
Total	58 (100%)

** TPN, total parenteral nutrition*

Data on the initial immunosuppression was available for 31 patients: 23 (74%) received cyclosporine and prednisone, 20 of them with azathioprine (AZA), 1 with mycophenolate mofetil (MMF) and 2 without a third agent. The remaining 8 patients received tacrolimus and prednisone. By the time of the protocol biopsy, 25 patients out of 58 (43%) used tacrolimus: 10 with prednisone + MMF, 12 with prednisone only, 2 with MMF and one as monotherapy. Cyclosporine was the chosen calcineurin inhibitor (CNI) in 23 patients (39.6%): 10 patients received it with prednisone and AZA, 4 with prednisone and MMF, 4 with MMF (no steroids), 2 with prednisone, 2 with AZA and one patient received cyclosporin as monotherapy. Additionally, 2 patients received prednisone with MMF (without CNI) and 2 patients were off immunosuppression at the time of biopsy (one for 8 months and one for 20 months). Details on these two patients without immunosuppression will be provided later in this chapter. Forty-five patients received steroids at the time of biopsy and 13 did not.

The average liver function tests (LFTs) at the time of protocol biopsy were: ALT 29.55 (from 4 to 92, reference value 5-55), AST 35.05 (from 14 to 109, reference value 10-50), bilirubin 15.00 (from 3 to 33, reference value 3-20), GGT 26.60 (from 5 to 134, reference value 1-55), AP 238.60 (from 75 to 516, reference value 30-130), platelets 224.07 (from 72 to 372, reference value 150-450) and international normalised value (INR) was 1.07 (from 0.86 to 1.36, reference value 0.9-1.20). Out of the 58, 52 recipients had AST within the normal range and only one had AST above 1.5 times the upper reference threshold at the time of protocol biopsy. Considering all LFTs, only 13 patients had completely normal liver biochemistry.

Regarding previous episodes of rejection, 62% of liver recipients had at least one biopsy showing rejection: 78% had early episode(s) of rejection, within 3 months post-transplant (most cases in the 1st month) and 22% had late rejection (which occurred between 4 months and 5 years after transplantation). A fifth (19%) of patients who had early rejection also developed late episode(s) of rejection.

Autoantibodies were present in 11 patients (19%) at the time of protocol biopsy: 8 (14%) had antinuclear antibodies (ANA), 2 (3.4%) had anti-smooth muscle antibodies (ASMA), and 1 child had anti-gastric parietal cell antibodies (GPC). Considering the ANA titres, two patients had 1/20, one had 1/40, one had 1/80, two had 1/160 and two had 1/640, all in nucleolar pattern except one who had speckled pattern (at 1/20). The titres of ASMA were 1/20 and 1/160, and the patient with GPC had weak positivity (exact titre not specified).

Anti-liver-kidney microsomal antibody (LKM) and mitochondrial antibodies were negative in all recipients. No patient with antibodies fulfilled the other criteria for *de novo* autoimmune hepatitis (AIH): raised immunoglobulins and raised AST.

3.3.2 Initial histological assessment (HE and reticulin staining)

Three biopsy specimens had too little tissue for an appropriate assessment and therefore were excluded from the study. From the 55 HE biopsy specimens analysed, 73% (40 biopsies) showed histological abnormalities. 40% (22) had unexplained chronic hepatitis of the graft (IPTH), in most cases (86%) associated with significant portal fibrosis (≥2) and/or pericentral or sinusoidal fibrosis (≥2); 20% (11) had significant portal fibrosis but no inflammation (7 were Ishak stage 3 or higher) and 7.3% (4) had centrilobular fibrosis and/or sinusoidal fibrosis (≥2) without inflammation or portal fibrosis; 1 patient had rejection (with active bile duct injury); 1 had a chronic cholangiopathy; and another, recurrent Hepatitis C virus (HCV). The two following figures show a protocol biopsy with chronic inflammation and advanced-stage fibrosis.

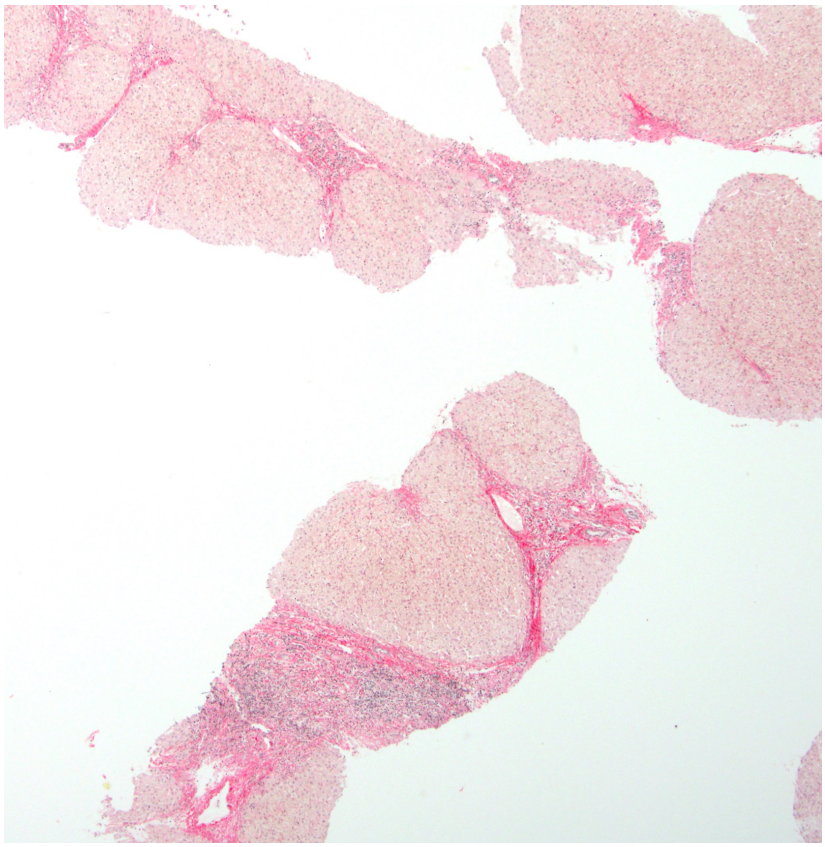

Figure 23. **Protocol biopsy 10 years post-transplant for biliary atresia.**

Fragmented biopsy showing bridging fibrosis with nodularity (Sirius Red, 40x)

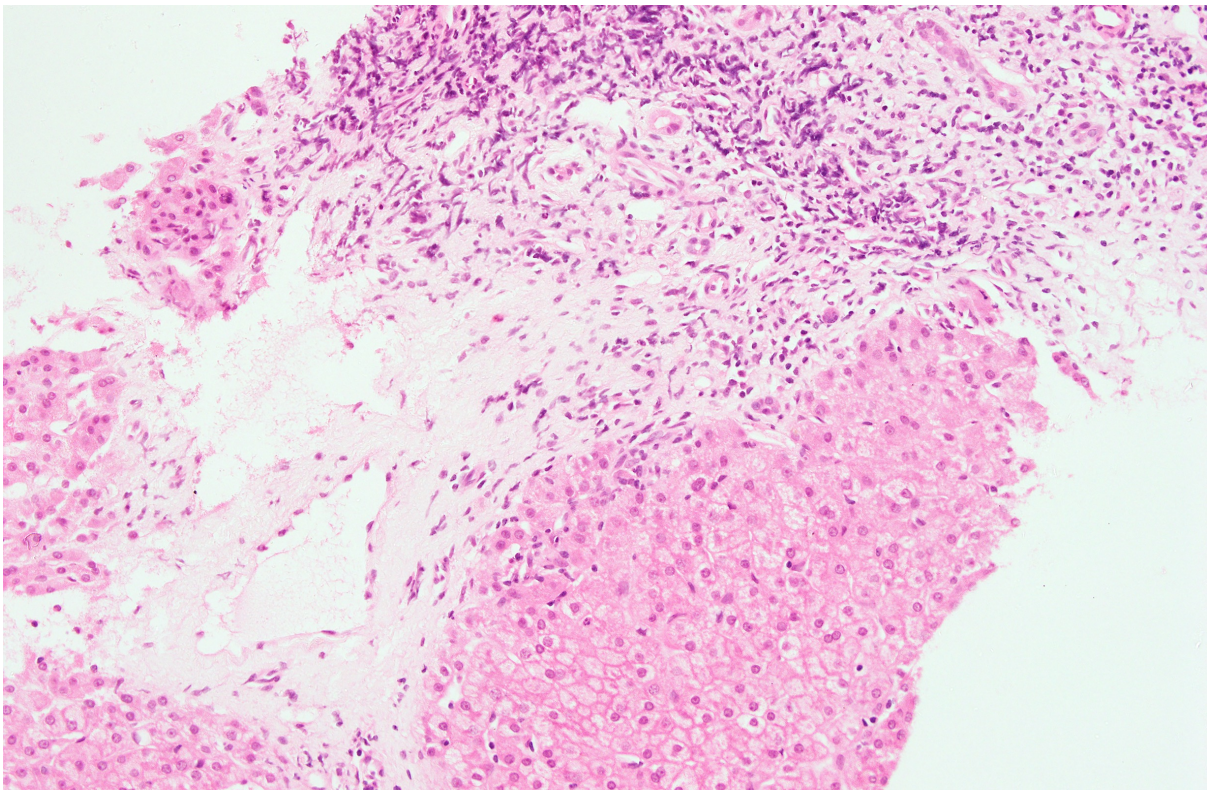

Figure 24. HE staining depicting chronic inflammation associated with fibrosis (200x, same biopsy of Figure 23)

Overall, 65.5% (36) of all protocol biopsies featured significant portal (≥2), centrilobular (≥2) or sinusoidal fibrosis (≥2). Portal fibrosis (≥2) was present in 56.4% (31), and bridging fibrosis or cirrhosis (≥3), in 40% (22). Only 27.3% of the biopsies analysed displayed a normal/near normal histology. The general overview of the initial histological assessment is depicted in Table 23.

Three patients were excluded from further histological assessment. One had histological signs of rejection, including bile duct damage and endotheliitis, so the diagnosis of late rejection was made. Another patient had cholangiopathy and a third had clinically recurrent HCV. Fifty-two biopsy specimens that showed no typical signs of rejection (no conspicuous bile duct damage/endotheliitis) or of other specific

aetiology for the histological findings were included in the study and submitted to additional staining and analysis.

Table 23. **Summary of main histological findings of protocol biopsies**

Histological findings	Number (%) of biopsies
IPTH + fibrosis	19 (34.5%)
Ishak 0/1 (CLF≥2 + Sin≥2)	1
Ishak 2 (+CLF ≥2 in two patients, +Sin ≥2 in one of them)	4
Ishak 3 (+CLF ≥2 in two patients, no Sin)	7
Ishak 4 (+CLF ≥2 in four patients, +Sin ≥2 in three of them)	5
Ishak 5 (+CLF ≥2 + Sin ≥2 in all)	2
Fibrosis only (Ishak ≥2, CLF ≥2 or Sin ≥2)	15 (27.3%)
Ishak 0/1 (+CLF ≥2 in all, +Sin ≥2 in one patient)	4
Ishak 2 (+CLF ≥2 in two patients, no Sin)	4
Ishak 3 (+CLF ≥2 in two patients, no Sin)	6
Ishak 4 (+CLF ≥2, no Sin)	1
Ishak 5	0
Normal/near normal	15 (27.3%)
IPTH (without fibrosis)	3 (5.5%)
Rejection	1 (1.8%)
Cholangiopathy	1 (1.8%)
Recurrent HCV	1 (1.8%)

Total	55 (100%)

CLF, centrilobular fibrosis; Sin, sinusoidal fibrosis; HCV, hepatitis C virus

The number of complete portal tracts in each biopsy varied from 3-16 (average 7.3) and the number of central veins, from 3-14 (average 5.9). The biopsy area varied from 3-20mm^2 (average 8.6). As to the grade of inflammation in each compartment, portal inflammation was present in 53.8% of biopsies: mild (grade 1) in most (42.3%), moderate (grade 2) in 11.5%. Interface activity was evident in 17% of biopsies, and was mild in all except one. Some degree of lobular inflammation was present in 44% of biopsies: mild/grade 1 in 37% and moderate in 7.7%. Central perivenulitis was present in 27% of patients and was typically mild (19%), although moderate in some cases (7.7%). A summary of the degree of inflammation in each compartment and other histological features assessed is presented in Table 24.

Only 11.5% of patients had bile duct injury on histology, which was mild in all cases. Bile duct loss and portal vein endotheliitis were not present in any biopsy specimen. Steatosis was conspicuous in 5.8% of biopsies, mild in all cases (affecting 5-30% of hepatocytes).

Table 24. **Inflammation Grading in each site**

Histological parameters	Number (%) of biopsies
Portal Inflammation	
Absent	24 (46.2%)
Mild (grade 1)	22 (42.3%)
Moderate (grade 2)	6 (11.5%)

Interface activity	
Absent	43 (82.7%)
Mild (grade 1)	8 (15.4%)
Moderate (grade 2)	1 (1.9%)
Lobular inflammation	
Absent	29 (55.8%)
Minimal (grade 1)	19 (36.5%)
Moderate (grade 2)	4 (7.7%)
CP	
Absent	38 (73.1%)
Mild (grade 1)	10 (19.2%)
Moderate (grade 2)	4 (7.7%)
Bile duct lesion	
Absent	46 (88.5%)
Minimal (grade 1)	6 (11.5%)
Moderate (grade 2)	0
Marked (grade 3)	0
Bile duct loss	
Absent	52 (100%)
Present	0
Portal vein endotheliitis	
Absent	52 (100%)
Mild (grade 1)	0
Moderate (grade 2)	0
Marked (grade 3)	0
Ductular reaction	
	0

Absent	10 (19.2%)
Focal	1 (1.9%)
Diffuse	
Hepatocanalicular cholestasis	
Absent	51 (98.1%)
Focal	1 (1.9%)
Diffuse centrilobular	0
Diffuse centrilobular and midzonal	0
Cholangiolar cholestasis	
Absent	52 (100%)
Present	0
Steatosis	
< 5% of hepatocytes	49 (94.2%)
5-33% of hepatocytes (grade 1)	3 (5.8%)
33-66% of hepatocytes (grade 2)	0
> 66% of hepatocytes (grade 3)	0

The proportion of biopsies showing different degrees of portal fibrosis according to Ishak and Venturi scores is depicted in Figure 25 and Figure 26, respectively. There were no biopsies classified as Ishak 6. Centrilobular fibrosis (CLF) was present in two-thirds of biopsies (67%): mild in 29%, moderate in 27% and severe in 12% (Figure 27). Sinusoidal fibrosis was evident in 60% of biopsies: 44% were mild (stage 1), 10%, moderate (stage 2) and 6% severe (stage 3), as shown in Figure 28. In terms of the digital analysis of fibrosis, the CPA varied from 0.3% to 9.4% of the biopsy area (mean 2.9%).

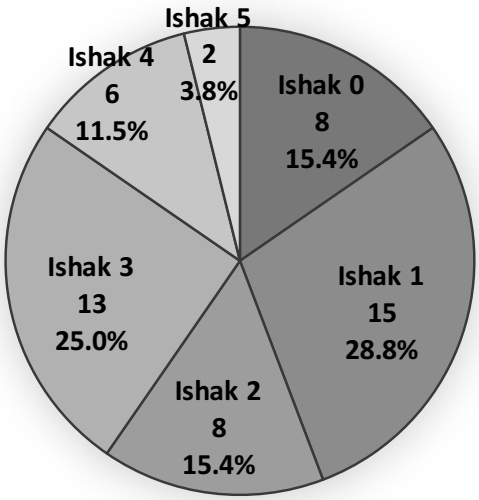

Figure 25 (above). **Portal Fibrosis (Ishak)**

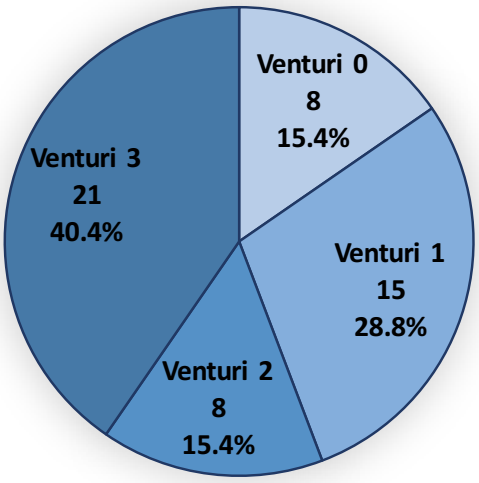

Figure 26 (above). **Portal Fibrosis (Venturi)**

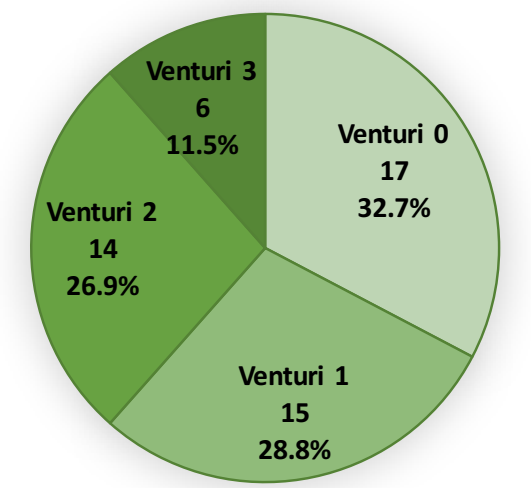

Figure 27 (above). **Centrilobular fibrosis**

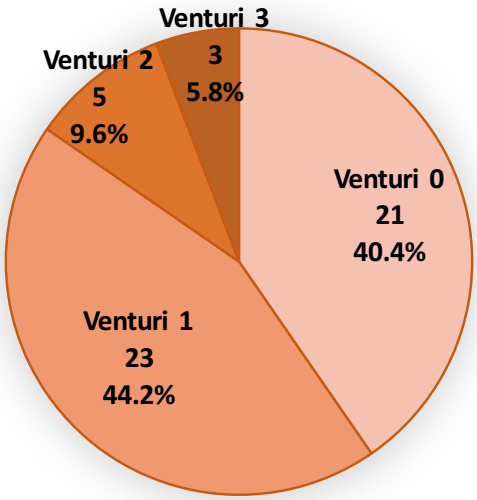

Figure 28. **Sinusoidal Fibrosis**

The presence of IPTH was strongly associated with portal and sinusoidal fibrosis ≥2, and also significantly associated with centrilobular fibrosis. Table 25 shows a comparison of the average and range degree of fibrosis per compartment between

patients with and without IPTH. The same table also compares the proportion of biopsies with fibrosis above specific thresholds between those with and without IPTH.

Throughout this Result section, mean/average scores are displayed in light grey cells and proportion/number of samples above specified thresholds in white cells.

Table 25. **IPTH and fibrosis**

Fibrosis per compartment	IPTH +	IPTH -	p value
Portal (mean and range)	2.8 (0-5)	1.4 (1-4)	**0.001**
Portal ≥2 (% and number)	81.8% (18/22)	36.7% (11/30)	**0.001**
Portal ≥3 (% and number)	63.6% (14/22)	23.3% (7/30)	**0.004**
Centrilobular (mean and range)	1.4 (0-3)	0.8 (0-3)	**0.023**
Centrilobular ≥1 (% and number)	86.4% (19/22)	53.3% (16/30)	**0.024**
Centrilobular ≥2 (% and number)	50% (11/22)	30% (9/30)	0.120
Sinusoidal (mean and range)	1.0 (0-3)	0.6 (0-3)	**0.039**
Sinusoidal ≥1 (% and number)	72.7% (16/22)	50% (15/30)	0.196
Sinusoidal ≥2 (% and number)	31.8% (7/22)	3.3% (1/30)	**0.007**
CPA (mean and range)	3.9% (0.7-9.1)	2.3% (0.33-9.7)	**0.039**

The two patients who no longer received immunosuppression by the time of protocol biopsy were both 16-years old, had undergone liver transplantation for biliary atresia, had normal LFTs and no circulating autoantibodies at biopsy. One of them was tested for DSA and had circulating class II DSA with high MFI (23606), anti-DQ and anti-DR subtypes. The other recipient did not have a sample for DSA testing.

These two children showed advanced stage fibrosis on biopsy, central perivenulitis (grade 1 in one and grade 2 in the other), marked centrilobular fibrosis and sinusoidal fibrosis (stage 3 in one, stage 1 in the other). The recipient who had DSA showed negative C4d staining (minimal weak staining in portal veins and stroma) and the second recipient showed focal moderate C4d deposition in portal capillaries and hepatic arteries. Clinical and histological details on these liver recipients, including histological findings, are shown in Table 26.

Table 26. **Clinical and histological characteristics of two patients off immunosuppression**

	Patient 1	Patient 2
Indication for LT	Biliary atresia	Biliary atresia
Gender	Male	Female
Age at LT	11 months	1 year
Time off immunosuppression	20 months	8 months
Age at protocol biopsy	16 years	16 years
AST at protocol biopsy (normal range 10-50)	38	26
Circulating DSA (at biopsy)	Class II (DR and DQ), total MFI 23,606	Not tested
Histological overview	Isolated CP with advanced stage fibrosis	Marked bridging and centrilobular fibrosis with mild CP and portal inflammation
Inflammation grading	CP 2; Lobular 2; Portal 0; Interface 0	CP 1; Lobular 1; Portal 1; Interface 0
Fibrosis staging	Ishak 5; CLF 3; Sinusoidal 3	Ishak 4; CLF 3; Sinusoidal 1
C4d immunohistochemistry	Negative (Minimal weak + in portal veins and portal stroma)	Positive in portal capillaries and hepatic arteries (focal moderate C4d+)
Outcome	Lost follow-up after protocol biopsy	Stable without immunosuppression 6 years after protocol biopsy

** CLF, centrilobular fibrosis; CP, central perivenulitis*

3.3.3 Comparison of fibrosis assessment: conventional and digital

Overal, mean CPA was significantly higher in biopsies with more advanced centrilobular and sinusoidal fibrosis. Mean CPAs for the following stages of

centrilobular fibrosis (CLF) were: 1.9% for stage 0/1; 4.4% for stage 2 and 7.3% for stage 3 ($p<0.001$, Figure 29). For sinusoidal fibrosis, median CPA was: 2.4% for stage 0/1; 5.8% for stage 2 and 8.8% for stage 3 ($p<0.001$, Figure 30). The CPA was not statistically associated with the degree of portal fibrosis.

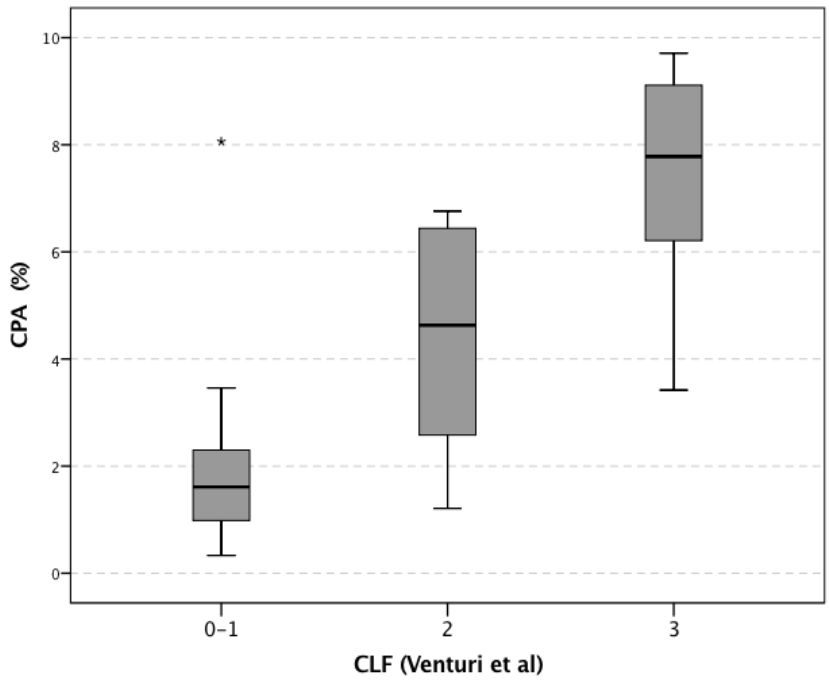

Figure 29 (above). **Median CPA and Centrilobular Fibrosis** (p<0.001)

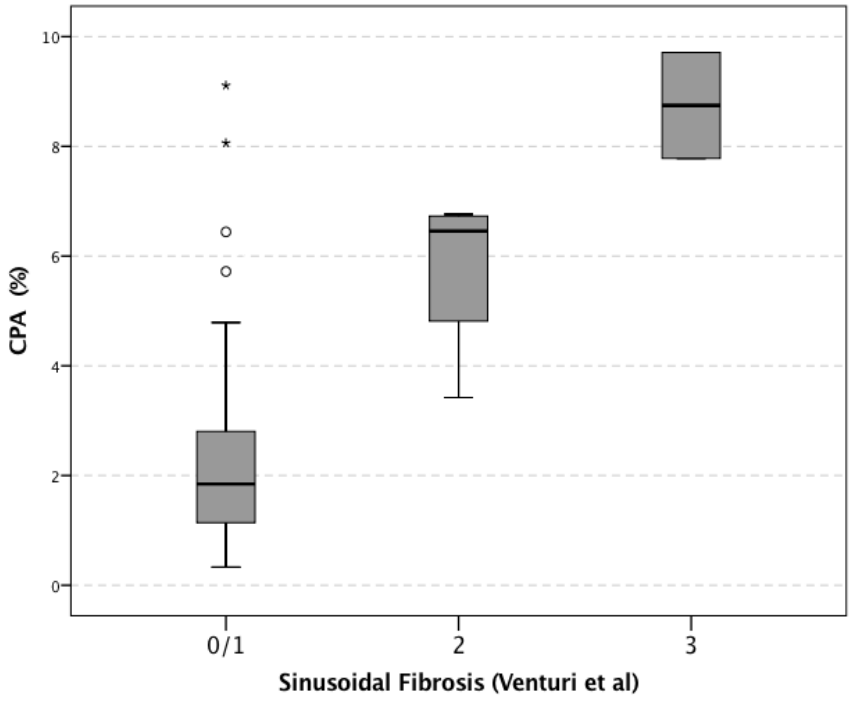

Figure 30. **Median CPA and Sinusoidal Fibrosis** (p<0.001)

3.3.4 Fibrosis, inflammation and clinical parameters

A strong statistical association was found between the presence of sinusoidal fibrosis and younger age at transplantation (p=0.009). The median age at LT of children who showed some degree of sinusoidal fibrosis (≥1) was 8.7 months versus 22.0 months of children without sinusoidal fibrosis (Figure 31). Considering the threshold ≥2 as significant sinusoidal fibrosis, the median age of patients with fibrosis was also smaller (7.7 versus 13.9 months), but the difference was not statistically significant (p=0.092).

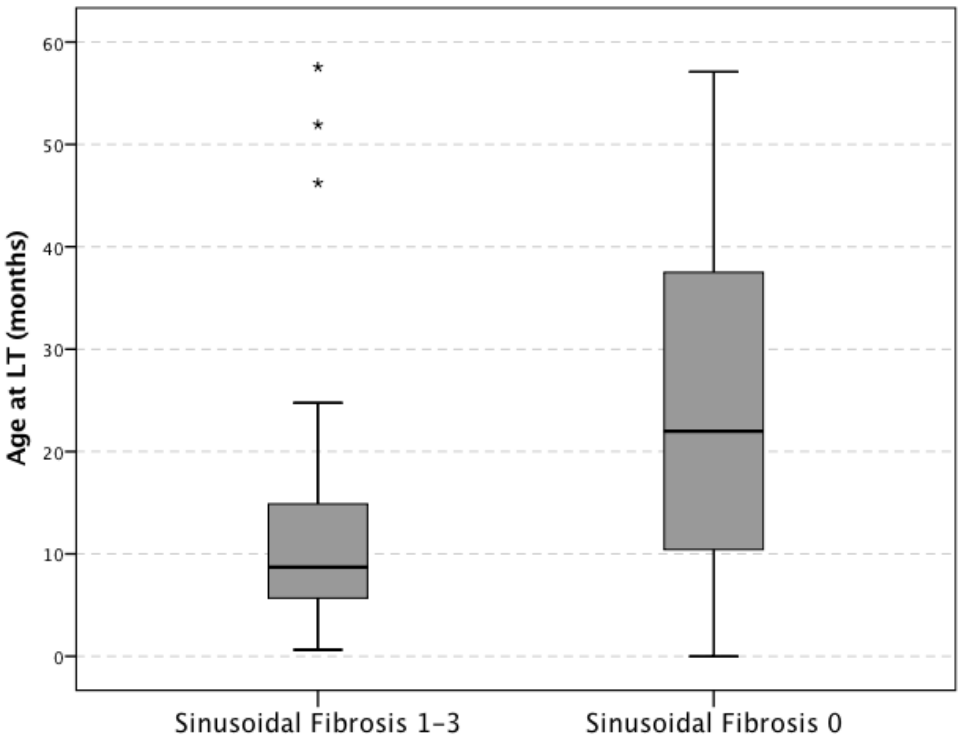

Figure 31 (above). **Age at LT and Sinusoidal fibrosis ≥1 (p=0.009)**

Portal fibrosis was significantly associated with steroid-free immunosuppression at the time of biopsy. The average degree of portal fibrosis was lower in patients receiving steroid (1 versus 3), as was the frequency of portal fibrosis stage ≥2 (48% versus 83% in patients not receiving steroid), as depicted in Table 27. Patients with steroid-free immunosuppression also had higher average scores of centrilobular fibrosis and CPA, but the differences were not statistically significant.

Table 27. **Steroid and fibrosis per compartment**

Fibrosis per compartment	Steroid +	Steroid -	p value
Portal (mean and range)	1.7 (0-5)	2.9 (0-5)	**0.023**
Portal ≥2 (% and number)	47.5% (19/40)	83.3% (10/12)	**0.046**
Portal ≥3 (% and number)	32.5% (13/40)	66.7% (8/12)	**0.048**
Centrilobular (mean and range)	0.9 (0-3)	1.5 (0-3)	0.221
Centrilobular ≥1 (% and number)	65% (26/40)	75% (9/12)	0.792
Centrilobular ≥2 (% and number)	35% (14/40)	50% (6/12)	0.500
Sinusoidal (mean and range)	0.7 (0-3)	0.7 (0-3)	0.688
Sinusoidal ≥1 (% and number)	62.5% (25/40)	50% (6/12)	0.617
Sinusoidal ≥2 (% and number)	15% (6/40)	16.7% (2/12)	1.000
CPA (mean and range)	2.8% (0.33-9.7)	3.8% (1.2-9.1)	0.221

Although all patients with poor outcome had portal fibrosis (≥2) as against 53% of those with good outcome, this difference was not statistically significant (p=0.245), likely due to the scarce number of patients with poor outcome during follow-up (only 3). Poor outcome was defined as allograft loss during follow up (until March 2018).

Outcome was not significantly associated with fibrosis in other compartments or with CPA.

The following clinical parameters did not show statistical association/correlation with fibrosis in any compartment or with the CPA: time from transplant to biopsy, type of calcineurin inhibitor used for immunosuppression (tacrolimus or cyclosporine), type of graft (whole or split), type of donation (DBD or DCD or LRLT), previous episodes of rejection, autoantibodies, and liver biochemistry (ALT, AST, bilirubin, GGT, AP, platelets, INR).

Patients receiving steroid-free immunosuppression showed almost double the rate of IPTH than those using steroid (67% versus 35%, respectively), and this difference was extremely close to statistical significance (p=0.051). Considering inflammation in each compartment, only moderate portal inflammation was significantly linked to steroid-free immunosuppression. Two-thirds of the patients with moderate portal inflammation did not receive steroid versus only 18% of those with no/mild portal inflammation (p=0.021). Although not significant, patients receiving steroids had lower average scores of inflammation in portal, interface and centrilobular compartments. Table 28 shows a comparison of the average score of inflammation per compartment and of the proportion of biopsies above certain thresholds of inflammation between patients receiving or not steroid.

Inflammation in each compartment was not associated with other clinical parameters: age at transplantation, time from transplant to protocol biopsy, type of calcineurin inhibitor used for immunosuppression, type of graft, type of donation, previous episodes of rejection, presence of autoantibodies and liver biochemistry.

Table 28. **Steroid and inflammation per compartment**

Inflammation per compartment	Steroid +	Steroid -	p value
Portal (mean and range)	0.6 (0-2)	1.0 (0-2)	0.104
Portal ≥1 (% and number)	50% (20/40)	75% (8/12)	0.510
Portal ≥2 (% and number)	5% (2/40)	33.3% (4/12)	**0.021**
Interface (mean and range)	0.1 (0-1)	0.4 (0-2)	0.082
Interface ≥1 (% and number)	12.5% (5/40)	33.3% (4/12)	0.185
Interface ≥2 (% and number)	0 (/40)	8.3% (1/12)	0.231
Lobular (mean and range)	0.5 (0-2)	0.5 (0-2)	0.825
Lobular ≥1 (% and number)	45% (18/40)	41.7% (5/12)	1.000
Lobular ≥2 (% and number)	92.5% (37/40)	91.7% (11/12)	1.000
CP (mean and range)	0.2 (0-2)	0.6 (0-2)	0.061
CP ≥1 (% and number)	20% (8/40)	50% (6/12)	0.063
CP ≥2 (% and number)	7.5% (3/40)	8.3% (1/12)	1.000
IPTH (% and number)	35% (14/40)	66.7% (8/12)	0.051

3.3.5 DSA: general results

DSA testing was performed in 34 (out of 52) liver recipients who had both donor HLA data and serum sample available for analysis. Twenty-four (71%) of them had circulating DSA at the time of protocol biopsy: 18 directed to class II, 2 to class I, and 4 to both class I and class II HLA antigens (Table 29). For class II subtypes, 50% of patients with class II DSA had anti-DQ antibodies only, 27% had both anti-DQ and anti-DR, and 23% had anti-DR only. No children had anti-DP HLA antibodies.

Table 29. **DSA test results**

DSA	Number (%)
Class II only	18 (52.9%)
Class I and II	4 (11.8%)
Class I only	2 (5.9%)
No DSA	10 (29.4%)

3.3.6 DSA and clinical parameters

There were no significant differences regarding clinical parameters between patients with and without DSA or DSA II. Nonetheless, the median age at transplantation of patients with DSA II was younger (9.7 versus 22 months) compared to those without these antibodies, and this difference was extremely close to statistical significance (p=0.052). Table 30 and Table 31 show clinical parameters in patients with and without circulating DSA and DSA II, respectively.

Table 30. **Clinical data and DSA**

Clinical parameters	DSA +	DSA -	p value
Male gender (% and number)	50% (12/24)	30% (3/10)	0.247
Age at LT (median and range in months)	11.6 (0.6-57.6)	19.7 (9.7-46.2)	0.088
Time from LT to biopsy (median and range)	11.7 (9.6-15.4)	11.2 (8.6-13.1)	0.756
Immunosuppression at biopsy, CNI (% and number): TAC CyA	 58.3% (14/24) 41.7% (10/24)	 50% (5/10) 50% (5/10)	 0.052
Immunosuppression at biopsy: Steroid (% and number)	79.2% (19/24)	60% (6/10)	0.160
Graft type (% and number): Whole Split Reduced	 20.8% (5/24) 79.2% (19/24) 0	 20% (2/10) 80% (8/10) 0	 0.401
Donation (% and number): DBD DCD LRLT	 91.7% (22/24) 0 8.3% (2/24)	 100%(10/10) 0 0	 0.269
AST (median and range)	30.5 (15-76)	28.5 (14-109)	0.849
Previous rejection (% and number)	62.5% (15/24)	70% (7/10)	0.346
Autoantibodies (% and number)	16.7% (4/24)	30% (3/10)	0.088
Poor outcome - death or graft loss (% and number)	8.3% (2/24)	10% (1/10)	0.115

LT, liver transplantation; CNI, calcineurin inhibitor; TAC, tacrolimus; CyA, cyclosporine; DBD, donation after brain death; DCD, donation after cardiac death; LRLT, living-related liver transplant.

Table 31. **Clinical data and DSA II**

Clinical parameters	DSA II +	DSA II -	p value
Male gender (% and number)	50% (11/22)	33.3% (4/12)	0.285
Age at LT, months (median and range in months)	10.2 (0.6-57.6)	22.0 (9.7-46.2)	0.052
Time from LT to biopsy (median and range)	11.0 (9.6-15.4)	12.0 (8.6-14.3)	0.791
Immunosuppression at biopsy, CNI (% and number): - TAC - CyA	 54.5% (12/22) 45.5% (10/22)	 58.3% (7/12) 41.7% (5/12)	0.063
Immunosuppression at biopsy: Steroid (% and number)	77.3% (17/22)	36.4% (8/12)	0.256
Graft type (% and number) - Whole - Split - Reduced	 18.2% (4/22) 81.8% (18/22) 0	 25% (3/12) 75% (9/12) 0	0.342
Donation (% and number) - DBD - DCD - LRLT	 90.9% (20/22) 0 9.1% (2/22)	 100%(12/12) 0 0	0.240
AST (median and range)	31.5 (15-76)	29.5 (14-109)	0.859
Previous rejection (% and number)	59.1% (13/22)	75% (9/12)	0.256
Autoantibodies (% and number)	18.2% (4/22)	25% (3/12)	0.124
Poor outcome - death or graft loss (% and number)	9.1% (2/22)	8.3% (1/12)	0.137

LT, liver transplantation; CNI, calcineurin inhibitor; TAC, tacrolimus; CyA, cyclosporine; DBD, donation after brain death; DCD, donation after cardiac death; LRLT, living-related liver transplant.

3.3.7 DSA, inflammation and fibrosis

Of the 24 liver recipients with circulating DSA, 20 (83.3%) had abnormal histology. Nine had IPTH associated with fibrosis; 9 had simply fibrosis; and 2 had IPTH only. All patients with IPTH and fibrosis had portal fibrosis (≥2), 6 also had significant centrilobular fibrosis (≥2) and 3 of them also had sinusoidal fibrosis ≥2 (besides portal and centrilobular fibrosis). As to the 9 patients with fibrosis only, 8 had portal fibrosis (≥2) and 1 had just centrilobular fibrosis (≥2).

Regarding the 10 recipients without DSA, 3 (30%) showed both IPTH and fibrosis, 3 (30%) had fibrosis only and 4 (40%) had normal histology. Forty percent of patients without DSA had normal histology versus only 16.7% of those with DSA, but this difference was not statistically significant. These results are depicted in Table 32.

Table 32. **Overal biopsy findings and DSA**

Histological findings	DSA +	DSA -	p value
IPTH + fibrosis	37.5% (9/24)	30% (3/10)	0.162
Fibrosis only (Ishak≥2, CLF≥2 or sinusoidal fibrosis≥2)	37.5% (9/24)	30% (3/10)	0.162
IPTH (without fibrosis)	8.3% (2/24)	0	0.317
Normal/near normal	16.7% (4/24)	40% (4/10)	0.151

As to the 22 recipients with DSA II, 18 (81.8%) had abnormal biopsy: 8 had IPTH associated with fibrosis; 8 had fibrosis only and 2 had IPTH only. Table 33 summarizes these findings.

Table 33. **Overal biopsy findings and DSA II**

Histological findings	DSA II +	DSA II -	p value
IPTH + fibrosis	36.4% (8/22)	33.3% (4/12)	0.438
Fibrosis only (Ishak ≥2, CLF ≥2 or Sin ≥2)	36.4% (8/22)	33.3% (4/12)	0.438
IPTH (without fibrosis)	9.1% (2/22)	0	0.212
Normal/near normal	18.2% (4/22)	33.3% (4/12)	0.259

The histological parameters in patients with and without DSA are shown in Table 34. The parameters are expressed in average and range or percentage and number of cases. Lobular inflammation was the only parameter significantly different between patients with and without DSA. On multivariate analysis, lobular inflammation was also the only parameter significantly associated with the presence of DSA (p=0.044). Figure 32 shows a biopsy with lobular inflammation and concomitant circulating DSA.

Table 34. **Detailed histological parameters and DSA**

Histological parameter	**DSA +**	**DSA -**	**p value**
Portal fibrosis Ishak (mean and range)	2.3 (0-5)	2.0 (1-4)	0.522
Portal fibrosis Ishak ≥2 (% and number)	70.8% (17/24)	50% (5/10)	0.221
Portal fibrosis Ishak ≥3 (% and number)	50% (12/24)	30% (3/10)	0.247
CLF (mean and range)	1.1 (0-3)	1.1 (0-3)	0.737
CLF present (% and number)	70.8% (17/24)	70% (7/10)	0.633
CLF ≥2 (% and number)	41.7% (10/24)	30% (3/10)	0.406
Sinusoidal fibrosis (mean and range)	0.8 (0-3)	0.5 (0-2)	0.205
Sinusoidal fibrosis present (% and number)	66.7% (16/24)	40% (4/10)	0.145
Sinusoidal fibrosis ≥2 (% and number)	12.5% (3/24)	10% (1/10)	0.666
CPA (mean and range)	2.3 (0.34-7.78)	3.1 (0.33-8.06)	0.331
Portal Inflammation (mean and range)	0.7 (0-2)	1.0 (0-2)	0.247
Portal inflammation moderate* (% and number)	8.3% (2/24)	30% (3/10)	0.138
Interface activity (mean and range)	0.2 (0-1)	0.2 (0-2)	0.549
Interface activity present (% and number)	20.8% (5/24)	10% (1/10)	0.416
Interface activity moderate* (% and number)	0 (/24)	10% (1/10)	0.294
Portal vein endotheliitis (mean and range)	0 (0)	0 (0)	1.000
CP (mean and range)	0.3 (0-2)	0.2 (0-1)	0.369
CP present (% and number)	33.3% (8/24)	20% (2/10)	0.367
CP moderate* (% and number)	12.5% (3/24)	0 (/10)	0.338
Lobular inflammation (mean and range)	0.6 (0-2)	0.1 (0-1)	**0.018**
Lobular inflammation present (% and number)	54.2% (13/24)	10% (1/9)	**0.019**
Lobular inflammation moderate* (% and number)	12.5% (3/24)	0 (/10)	0.338
Bile duct injury (mean and range)	0.2 (0-1)	0.2 (0-1)	0.819
Bile duct loss present (% and number)	0 (0)	0 (0)	1.000
Canalicular cholestasis (mean and range)	0 (0)	0 (0)	1.000
Ductular reaction present (% and number)	20.8% (5/24)	40% (4/10)	0.230

CLF, centrilobular fibrosis

** No patients had grade 3 inflammation in any of these compartments: portal, interface, lobular and central veins*

Table 35. **Detailed histological parameters and DSA II**

Histological parameter	DSA II +	DSA II -	p value
Portal fibrosis Ishak (mean and range)	2.4 (0-5)	2.0 (1-4)	0.470
Portal fibrosis Ishak ≥2 (% and number)	68.2% (15/22)	58.3% (7/12)	0.084
Portal fibrosis Ishak ≥3 (% and number)	54.5% (12/22)	25% (3/12)	0.098
CLF (mean and range)	1.1 (0-3)	1.1 (0-3)	0.970
CLF present (% and number)	68.2 (15/22)	75% (9/12)	0.244
CLF ≥2 (% and number)	40.9% (9/22)	33.3% (4/12)	0.427
Sinusoidal fibrosis (mean and range)	0.8 (0-3)	0.5 (0-2)	0.159
Sinusoidal fibrosis present (% and number)	68.2 (15/22)	41.7% (5/12)	0.154
Sinusoidal fibrosis ≥2 (% and number)	13.6% (3/22)	8.3% (1/12)	0.275
CPA (mean and range)	2.4% (0.34-7.78)	2.9% (0.33-8.06)	0.563
Portal Inflammation (mean and range)	0.7 (0-2)	1.0 (0-2)	0.397
Portal inflammation moderate* (% and number)	9.1% (2/22)	25% (3/12)	0.111
Interface activity (mean and range)	0.2 (0-1)	0.3 (0-2)	1.000
Interface activity present (% and number)	18.2% (4/22)	16.7% (2/12)	0.486
Interface activity moderate* (% and number)	0 (/22)	8.3% (1/12)	**0.041**
Portal vein endotheliitis (mean and range)	0 (0)	0 (0)	1.000
CP (mean and range)	0.3 (0-2)	0.3 (0-2)	0.752
CP present (% and number)	27.3% (6/22)	33.3% (4/12)	0.346
CP moderate* (% and number)	9.1% (2/22)	8.3% (1/12)	0.416
Lobular inflammation (mean and range)	0.6 (0-2)	0.2 (0-1)	0.122
Lobular inflammation present (% and number)	50% (11/22)	25% (3/12)	0.158
Lobular inflammation moderate* (% and number)	13.6% (3/22)	0 (/12)	0.193
Bile duct injury (mean and range)	0.2 (0-1)	0.2 (0-1)	0.913
Bile duct loss present (% and number)	0 (0)	0 (0)	1.000
Canalicular cholestasis (mean and range)	0 (0)	0 (0)	1.000
Ductular reaction present (% and number)	22.7% (5/22)	33.3% (4/12)	0.163

CLF, centrilobular fibrosis

** No patients had grade 3 inflammation in any of these compartments: portal, interface, lobular and central veins*

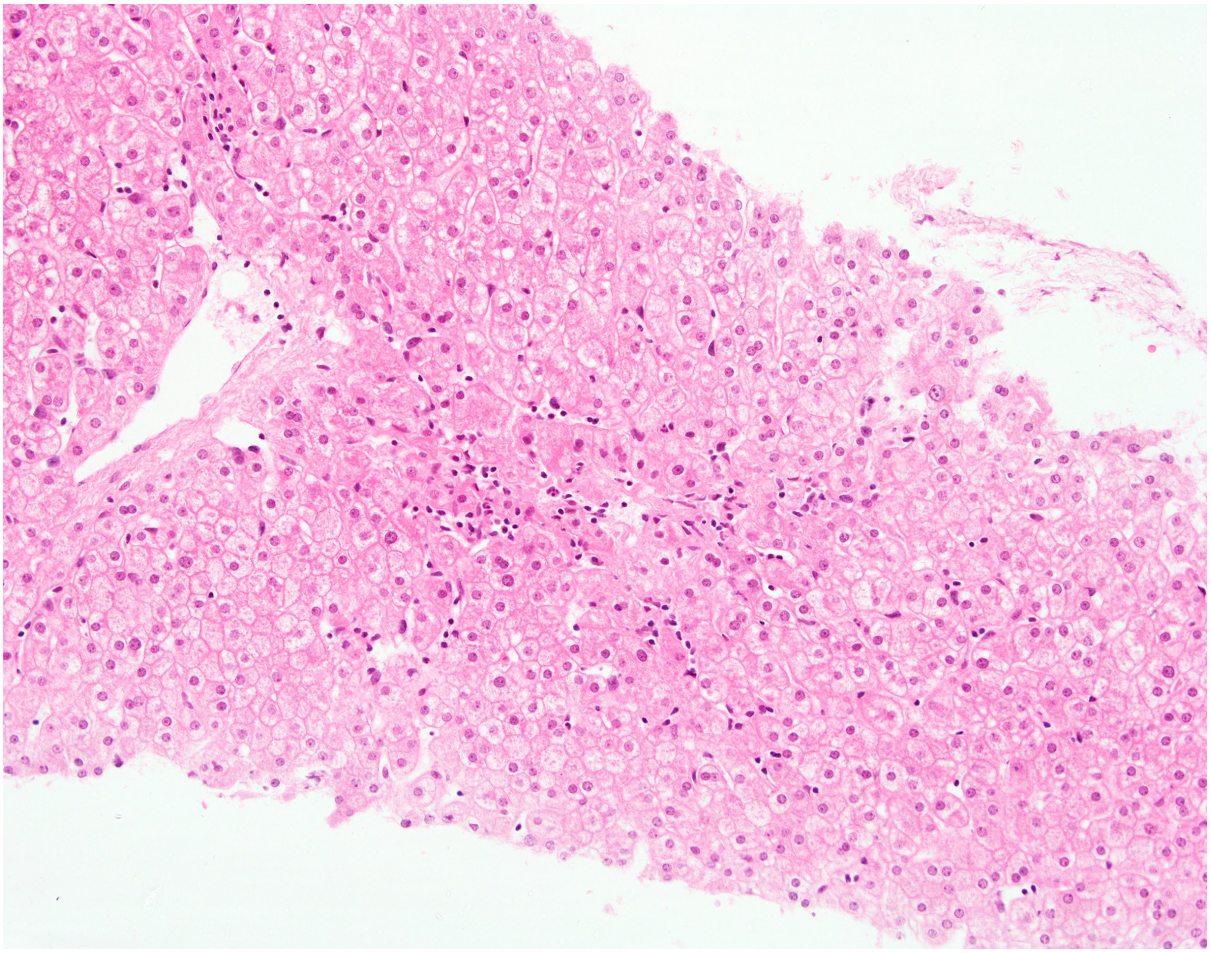

Figure 32. **Protocol biopsy 15 years post-transplantation for biliary atresia showing moderate (grade 2) lobular inflammation. The patient had circulating class I and II DSA, total MFI of 59,000 (HE, 200x).**

3.3.8 C4d immunohistochemistry

Fifty out of the 52 biopsy blocks had enough tissue for additional staining and C4d immunohistochemistry was performed. The overall quality of C4d staining was good with little background in most samples, which did not interfere with the assessment (Figure 33). Control samples stained appropriately. The association between C4d, DSA and other histological parameters are explored in the following sections of this chapter. Overall, 34% of biopsies had at least focal C4d deposition in one or more compartments and were considered C4d positive (C4d+).

One-fourth of biopsies showed portal endothelial microvascular C4d+ (in portal veins or portal capillaries). This was included as a separate category/compartment because it was the criteria used for C4d+ in the Banff chronic AMR score[53]. The specific proportion of biopsies with at least focal C4d deposition in each individual compartment was: in portal veins, 16%; portal capillaries, 16%; portal stroma, 10%; hepatic arteries, 18%; central veins, 4%; sinusoids, 2%. The results of the C4d assessment for each compartment are depicted in Table 36.

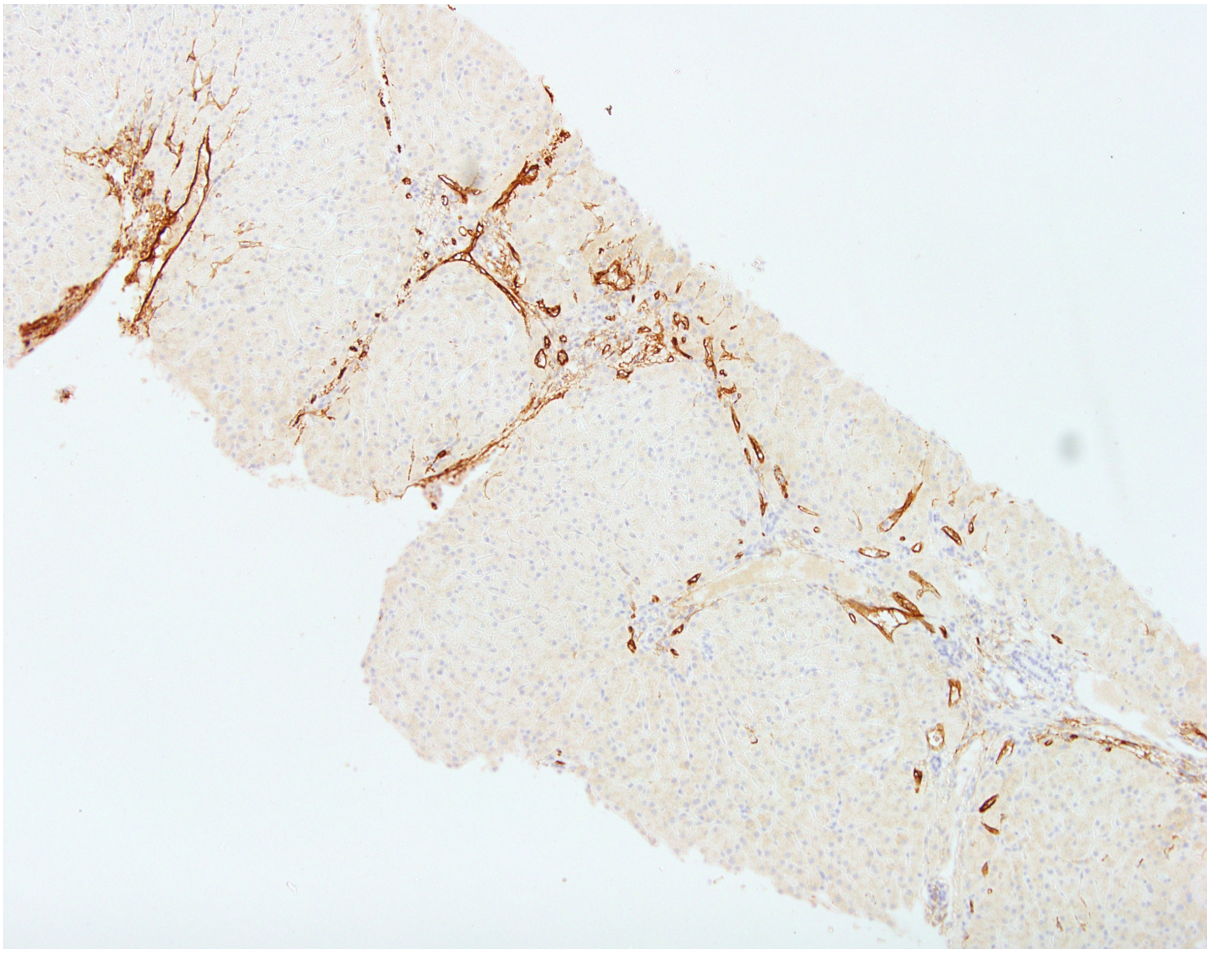

Figure 33. **Biopsy with strong diffuse C4d staining in vascular compartments and minimal background, which did not interefere with interpretation**

Table 36. **C4d deposition per compartment**

Location	Pattern of staining	Number (%)
Portal veins	Negative	31 (62%)
	Minimal	11 (22%)
	Focal and weak	4 (8%)
	Focal and moderate/strong	4 (8%)
	Diffuse	0
Portal capillaries	Negative	40 (80%)
	Minimal	2 (4%)
	Focal and weak	2 (4%)
	Focal and moderate/strong	3 (6%)
	Diffuse	3 (6%)
Hepatic artery	Negative	37 (74%)
	Minimal	4 (8%)
	Focal and weak	2 (4%)
	Focal and moderate/strong	2 (4%)
	Diffuse	5 (10%)
Portal stroma	Negative	36 (72%)
	Minimal	9 (18%)
	Focal and weak	2 (4%)
	Focal and moderate/strong	1 (2%)
	Diffuse	2 (4%)
Central veins	Negative	43 (86%)
	Minimal	5 (10%)
	Focal and weak	0
	Focal and moderate/strong	1 (2%)
	Diffuse	1 (2%)
Central stroma	Negative	46 (92%)
	Minimal	3 (6%)
	Focal and weak	0
	Focal and moderate/strong	1 (2%)
	Diffuse	0
Sinusoids	Negative	47 (94%)
	Minimal	2 (4%)
	Focal and weak	0
	Focal and moderate/strong	1 (2%)
	Diffuse	0

3.3.9 DSA and C4d immunohistochemistry

Thirty-four patients had both DSA and C4d data. Although overall patients with DSA had higher proportion of C4d+ in most compartments, particularly in portal veins, the differences were not statistically significant. Table 37 and Table 38 show the frequency of C4d+ per compartment in patients with and without circulating DSA and DSA II, respectively.

Table 37. **C4d deposition and circulating DSA**

C4d+ in	DSA +	DSA -	p value
Portal microvascular endothelium	16.7% (4/24)	10% (1/10)	0.535
Portal vein	16.7% (4/24)	0 (0/10)	0.296
Portal capillaries	12.5% (3/24)	10% (1/10)	1.000
Hepatic artery	20.8% (5/24)	10% (1/10)	0.644
Portal stroma	16.7% (4/24)	10% (1/10)	0.535
Central vein	4.2% (1/24)	0 (0/10)	1.000
Sinusoids	4.2% (1/24)	0 (0/10)	1.000
Any compartment	37.5% (9/24)	20% (2/10)	0.437

Table 38. **C4d deposition and circulating class II DSA**

C4d+ in	DSA II +	DSA II -	p value
Portal microvascular endothelium	13.6% (3/22)	8.3% (1/12)	1.000
Portal vein	13.6% (3/22)	8.3% (1/12)	1.000
Portal capillaries	9.1% (2/22)	16.7% (2/12)	0.602
Hepatic artery	18.2% (4/22)	16.7% (2/12)	1.000
Portal stroma	13.6% (3/22)	16.7% (2/12)	1.000

Central vein	4.5% (1/22)	0 (/12)	1.000
Sinusoids	4.5% (1/22)	0 (/12)	1.000
Any compartment	36.4% (8/22)	25% (3/12)	0.705

3.3.10 C4d and Inflammation

Central perivenulitis was significantly associated with C4d+ in portal vascular structures (portal microvascular endothelium and hepatic arteries). Lobular inflammation was also associated with C4d+ in hepatic arteries, as depicted in Table 39. Patients with portal inflammation and interface activity also had higher proportions of C4d+ in most compartments, particularly portal capillaries, but this was not significant.

Considering the average inflammation score, C4d+ (in portal microvascular endothelium, portal veins and hepatic arteries) was linked to significantly higher degree of lobular inflammation (Table 40). Positive C4d staining in all portal vascular compartments was also associated with higher average score of central perivenulitis.

Table 39. **Frequency of C4d+ in each compartment versus inflammation in portal tracts, interface, lobule and central veins**

C4d+ in	Portal inflammation			Interface			Lobular inflammation			CP		
	+	-	p value	+	-	p value	+	-	p value	+	-	p value
Portal microvascular endothelium	25.9% (7/27)	8.7% (2/23)	0.649	37.5% (3/8)	16.7% (7/42)	0.168	31.8% (7/22)	10.7% (3/28)	0.144	46.2% (6/13)	10.8% (4/37)	**0.013**
Portal vein	18.5% (5/27)	13.0% (3/23)	0.853	37.5% (3/8)	11.9% (5/42)	0.076	27.3% (6/22)	7.1% (2/28)	0.144	38.5% (5/13)	8.1% (3/37)	**0.022**
Portal capillaries	22.2% (6/27)	8.7% (2/23)	0.541	37.5% (3/8)	11.9% (5/42)	0.076	27.3% (6/22)	7.1% (2/28)	0.144	38.5% (5/13)	8.1% (3/37)	**0.022**
Hepatic artery	18.5% (5/27)	17.4% (4/23)	1.000	25% (2/8)	16.7% (7/42)	0.238	31.8% (7/22)	7.1% (2/28)	**0.047**	38.5% (5/13)	10.8% (4/37)	**0.034**
Portal stroma	14.8% (4/27)	4.3% (1/23)	0.674	25% (2/8)	7.1% (3/42)	0.102	13.6% (3/22)	7.1% (2/28)	0.820	15.4% (2/13)	8.1% (3/37)	0.468
Central vein	3.7% (1/27)	4.4% (1/23)	1.000	12.5% (1/8)	2.4% (1/42)	0.134	4.5% (1/22)	3.6% (1/28)	1.000	7.7% (1/13)	2.7% (1/37)	0.291
Sinusoids	3.7% (1/27)	0 (/23)	1.000	12.5% (1/8)	0 (/42)	0.074	4.5% (1/22)	0 (/28)	0.718	7.7% (1/13)	0 (/37)	0.173
Any compartment	3.7% (10/27)	3.0% (7/23)	0.882	37.5% (3/8)	33.3% (14/42)	0.484	45.5% (10/22)	25% (7/28)	0.253	53.8% (7/13)	27% (10/37)	0.133

Table 40. **Average degree of inflammation in each compartment versus C4d positivity or negativity in each site**

Inflammation grade per compartment (mean and range)	**Portal inflammation**			**Interface**			**Lobular inflammation**			**Central vein (CP)**		
C4d staining per compartment (+ or -)	**+**	**-**	p value	**+**	**-**	p value	**+**	**-**	p value	**+**	**-**	p value
Portal microvascular endothelium	0.9 (0-2)	0.6 (0-2)	0.183	0.3 (0-1)	0.1 (0-2)	0.202	0.8 (0-2)	0.4 (0-2)	**0.045**	0.7 (0-2)	0.2 (0-2)	**0.009**
Portal vein	0.9 (0-2)	0.6 (0-2)	0.323	0.4 (0-1)	0.1 (0-2)	0.084	0.9 (0-2)	0.4 (0-2)	**0.031**	0.7 (0-2)	0.2 (0-2)	**0.013**
Portal capillaries	1.0 (0-2)	0.6 (0-2)	0.103	0.4 (0-1)	0.1 (0-2)	0.084	0.9 (0-2)	0.4 (0-2)	0.067	0.8 (0-2)	0.2 (0-2)	**0.013**
Hepatic artery	0.8 (0-2)	0.7 (0-2)	0.579	0.2 (0-1)	0.2 (0-2)	0.607	0.9 (0-2)	0.4 (0-2)	**0.037**	0.7 (0-2)	0.2 (0-2)	**0.031**
Portal stroma	1.0 (0-2)	0.6 (0-2)	0.256	0.4 (0-1)	0.2 (0-2)	0.140	0.8 (0-2)	0.4 (0-2)	0.259	0.6 (0-2)	0.2 (0-2)	0.375
Central vein	1.0 (0-2)	0.7 (0-2)	0.663	0.5 (0-1)	0.2 (0-2)	0.199	0.5 (0-1)	0.5 (0-2)	0.955	1.0 (0-2)	0.2 (0-2)	0.272
Sinusoids	-	0.6 (0-2)	-	-	0.2 (0-2)	-	-	0.5 (0-2)	-	-	0.2 (0-2)	-
Any compartment	0.7 (0-2)	0.7 (0-2)	0.685	0.2 (0-1)	0.2 (0-2)	0.859	0.7 (0-2)	0.4 (0-2)	0.078	0.4 (0-2)	0.2 (0-2)	0.106

** Only one biopsy showed C4d+ in sinusoids. It was not possible to obtain mean inflammation scores and p value based on a single specimen*

3.3.11 C4d and fibrosis

Centrilobular and sinusoidal fibrosis (≥2) were individually associated with C4d+ in portal microvascular endothelium. Sinusoidal fibrosis was also strongly associated with C4d+ in portal veins, present in 57% of patients with and 9% of those without sinusoidal fibrosis (p=0.004). Patients with portal fibrosis had higher frequency of C4d+ than those without, particularly in portal capillaries (21.4% versus 9.1%), but this was not significant for any compartment. Table 41 shows the proportion of C4d+ in biopsies with and without significant fibrosis in each compartment. Considering the average score of fibrosis, patients with C4d+ in portal microvascular endothelium had higher degrees of sinusoidal and centrilobular fibrosis and of CPA, as depicted in Table 42.

Overall, considering both inflammation and fibrosis, C4d staining in portal microvascular endothelium was significantly associated with central perivenulitis, lobular inflammation, and with CPA, sinusoidal and centrilobular fibrosis.

Table 41. **Frequency of C4d+ in each compartment versus fibrosis in sinusoids, central veins and portal tracts**

C4d+ in	Sinusoidal fibrosis			Centrilobular fibrosis			Portal fibrosis		
	≥2	**0/1**	p value	**≥2**	**0/1**	p value	**≥2**	**0/1**	p value
Portal microvascular endothelium	57.1% (4/7)	14.0% (6/43)	**0.022**	36.8% (7/19)	9.7% (3/31)	**0.048**	25% (7/28)	13.6% (3/22)	0.738
Portal vein	57.1% (4/7)	9.3% (4/43)	**0.004**	26.3% (5/19)	9.7% (3/31)	0.345	17.9% (5/28)	13.6% (3/22)	1.000
Portal capillaries	28.6% (2/7)	14.0% (6/43)	0.178	26.3% (5/19)	9.7% (3/31)	0.345	21.4% (6/28)	9.1% (2/22)	0.629
Hepatic artery	28.6% (2/7)	16.3% (7/43)	0.198	26.3% (5/19)	12.9% (4/31)	0.445	17.9% (5/28)	18.2% (4/22)	1.000
Portal stroma	14.3% (1/7)	9.3% (4/43)	0.291	10.5% (2/19)	9.7% (3/31)	1.000	14.3% (4/28)	4.5% (1/22)	0.682
Central vein	14.3% (1/7)	2.3% (1/43)	0.107	10.5% (2/19)	0 (/31)	0.269	7.1% (2/28)	0 (/22)	0.747
Sinusoids	14.3% (1/7)	0 (/43)	0.058	5.3% (1/19)	0 (/31)	0.476	3.6% (1/28)	0 (/22)	1.000
Any compartment	57.1% (4/7)	30.2% (13/43)	0.105	52.6% (10/19)	22.6% (7/31)	**0.047**	39.3% (11/28)	27.3% (6/22)	0.773

Table 42. **Average degree of fibrosis in each compartment and CPA versus C4d positivity or negativity in each site**

Fibrosis score per compartment (mean and range)	**Sinusoidal (Venturi)**			**Centrilobular (Venturi)**			**Portal (Ishak)**			**CPA (%)**		
C4d staining per compartment (+ or -)	**+**	**-**	p value	**+**	**-**	p value	**+**	**-**	p value	**+**	**-**	p value
Portal microvascular endothelium	1.2 (0-3)	0.6 (0-3)	**0.025**	1.9 (0-3)	0.9 (0-3)	**0.010**	2.1 (0-5)	2.0 (0-5)	0.842	5.3 (1.0-9.7)	2.4 (0.3-8.1)	**0.005**
Portal vein	1.3 (0-3)	0.6 (0-3)	**0.042**	1.7 (0-3)	1.0 (0-3)	0.070	1.9 (0-5)	2.0 (0-5)	0.714	4.6 (0.9-9.7)	2.7 (0.3-9.1)	**0.049**
Portal capillaries	1.0 (0-3)	0.7 (0-3)	0.248	1.8 (0-3)	0.9 (0-3)	0.070	2.4 (0-5)	1.9 (0-5)	0.448	4.8 (1-9.1)	2.6 (0.3-9.7)	**0.019**
Hepatic artery	0.9 (0-2)	0.7 (0-3)	0.482	1.4 (0-3)	1.0 (0-3)	0.377	2.0 (0-5)	2.0 (0-5)	0.918	4.5 (0.8-9.1)	2.6 (0.3-9.7)	0.118
Portal stroma	0.8 (0-2)	0.7 (0-3)	0.846	1.4 (0-3)	1.0 (0-3)	0.566	3 (1-5)	1.9 (0-5)	0.119	2.4 (1-6.2)	3.1 (0.3-9.7)	0.584
Central vein	1.0 (0-2)	0.7 (0-3)	0.746	2.5 (2-3)	1 (0-3)	0.066	4 (3-5)	1.9 (0-5)	0.072	5.5 (4.8-6.2)	2.9 (0.3-9.7)	0.118
Sinusoids	-	0.7 (0-3)	-	-	1 (0-3)	-	-	1.9 (0-5)	-	-	2.9 (0.3-9.7)	-
Any compartment	0.9 (0-3)	0.6 (0-3)	0.123	1.5 (0-3)	0.8 (0-3)	0.055	2.1 (0-5)	1.9 (0-5)	0.644	4.1 (0.8-9.7)	2.4 (0.3-8.1)	**0.030**

** Only one biopsy showed C4d+ in sinusoids. It was not possible to obtain mean inflammation score and p value based on a single specimen*

3.3.12 C4d in combination with DSA and Inflammation

Since circulating DSA and tissue C4d deposition are considered the traditional markers of AMR[182] and are both required for the diagnosis of chronic AMR and interpreted in association, I investigated whether the presence of both DSA and C4d+ (DSA+C4d+) was significantly related to other histological parameters.

DSA+C4d+ (in portal microvascular endothelium, and specifically in portal veins and portal capillaries) was associated with the presence of interface activity and central perivenulitis. More in details, DSA+C4d+ in portal capillaries was present in 50% of patients with interface and in none of those without interface (p=0.003). Similarly, DSA+C4d+ in portal veins was present in 40% of patients with central perivenulitis and in none of those without (p=0.007). The proportion of C4d positivity in biopsies with and without inflammation in each compartment is shown in Table 43.

Considering specifically class II DSA, the only significant association was observed between interface and C4d+ in portal capillaries (combined with DSA II), although the difference in proportions was narrower than for DSA overall (33% versus 0 instead of 50% versus 0, respectively), as depicted in Table 44.

Table 43. **DSA + C4d+ and inflammation in portal tracts, interface, lobule and central veins**

DSA+C4d+ in	Portal Inflammation			Interface activity			Lobular Inflammation			CP		
	+	-	p value	+	-	p value	+	-	p value	+	-	p value
Portal microvascular endothelium	19.1% (4/21)	0 (/13)	0.100	50% (3/6)	3.6% (1/28)	**0.015**	21.4% (3/14)	5% (1/20)	0.287	40% (4/10)	0 (/24)	**0.007**
Portal vein	19.1% (4/21)	0 (/13)	0.121	50% (3/6)	3.6% (1/28)	**0.015**	21.4% (3/14)	5% (1/20)	0.287	40% (4/10)	0 (/24)	**0.007**
Portal capillaries	14.3% (3/21)	0 (/13)	0.113	50% (3/6)	0 (/28)	**0.003**	14.3% (2/14)	5% (1/20)	0.555	30% (3/10)	0 (/24)	**0.020**
Hepatic artery	14.3% (3/21)	15.4% (2/13)	0.301	33.3% (2/6)	10.7% (3/28)	0.346	28.6% (4/14)	5% (1/20)	0.140	30% (3/10)	8.3% (2/24)	0.236
Portal stroma	14.3% (3/21)	7.7% (1/13)	0.286	33.3% (2/6)	7.1% (2/28)	0.207	21.4% (3/14)	5% (1/20)	0.287	20% (2/10)	8.3% (2/24)	0.571
Central vein	4.8% (1/21)	0 (/13)	0.149	16.7% (1/6)	0 (/28)	0.216	7.1% (1/14)	0 (/20)	0.458	10% (1/10)	0 (/24)	0.274
Sinusoids	4.8% (1/21)	0 (/13)	0.149	16.7% (1/6)	0 (/28)	0.216	7.1% (1/14)	0 (/20)	0.458	10% (1/10)	0 (/24)	0.274
Any compartment	28.6% (6/21)	23.1% (3/13)	0.306	50% (3/6)	21.4% (6/28)	0.347	42.9% (6/14)	15% (3/20)	0.167	50% (5/10)	16.7% (4/24)	0.143

Table 44. **DSA II + C4d+ and inflammation in portal tracts, interface, lobule and central veins**

DSA **II**+ C4d+ in	**Portal Inflammation**			**Interface activity**			**Lobular Inflammation**			**CP**		
	+	**-**	p value	**+**	**-**	p value	**+**	**-**	p value	**+**	**-**	p value
Portal microvascular endothelium	14.3% (3/21)	0 (/13)	0.113	33.3% (2/6)	3.6% (1/28)	0.077	14.3% (2/14)	5% (1/20)	0.586	30% (3/10)	0 (/24)	**0.033**
Portal vein	14.3% (3/21)	0 (/13)	0.113	33.3% (2/6)	3.6% (1/28)	0.077	14.3% (2/14)	5% (1/20)	0.586	30% (3/10)	0 (/24)	**0.033**
Portal capillaries	9.5% (2/21)	0 (/13)	0.513	33.3% (2/6)	0 (/28)	**0.027**	7.1% (1/14)	5% (1/20)	1.000	20% (2/10)	0 (/24)	0.080
Hepatic artery	9.5% (2/21)	15.4% (2/13)	0.260	16.7% (1/6)	10.7% (3/28)	0.868	21.4% (3/14)	5% (1/20)	0.287	20% (2/10)	8.3% (2/24)	0.571
Portal stroma	9.5% (2/21)	7.7% (1/13)	0.315	16.7% (1/6)	7.1% (2/28)	0.695	14.3% (2/14)	5% (1/20)	0.586	10% (1/10)	8.3% (2/24)	0.885
Central vein	4.8% (1/21)	0 (/13)	0.149	16.7% (1/6)	0 (/28)	0.216	7.1% (1/14)	0 (/20)	0.458	10% (1/10)	0 (/24)	0.274
Sinusoids	4.8% (1/21)	0 (/13)	0.149	16.7% (1/6)	0 (/28)	0.216	7.1% (1/14)	0 (/20)	0.458	10% (1/10)	0 (/24)	0.274
Any compartment	22.7% (5/21)	23.1% (3/13)	0.308	33.3% (2/6)	21.4% (6/28)	0.784	35.7% (5/14)	15% (3/20)	0.282	40% (4/10)	16.7% (4/24)	0.297

3.3.13 C4d in combination with DSA and fibrosis

The only significant associations were observed between sinusoidal fibrosis and DSA/DSA II+C4d+ in portal veins (and portal vascular endothelium), as shown in Table 45 and Table 46. Half of patients with sinusoidal fibrosis (≥2) showed DSA II+C4d+ in portal veins versus only 3.3% of those with no/mild sinusoidal fibrosis. Despite not significant, patients with fibrosis (≥2) in each compartment showed higher proportions of DSA+C4d+ in almost every site.

The three following figures show a protocol biopsy of a patient with circulating DSA, C4d+, sinusoidal fibrosis and central perivenulitis.

Table 45. **DSA + C4d+ and fibrosis in sinusoids, central veins and portal tracts**

DSA + C4d+ in	Sinusoidal fibrosis			Centrilobular fibrosis			Portal fibrosis		
	≥2	**0/1**	p value	**≥2**	**0/1**	p value	**≥2**	**0/1**	p value
Portal microvascular endothelium	50% (2/4)	6.7% (2/30)	**0.039**	23.1% (3/13)	4.8% (1/21)	0.344	18.2% (4/22)	0 (/12)	0.091
Portal vein	50% (2/4)	6.7% (2/30)	**0.039**	23.1% (3/13)	4.8% (1/21)	0.344	18.2% (4/22)	0 (/12)	0.091
Portal capillaries	25% (1/4)	6.7% (2/30)	0.322	15.4% (2/13)	4.8% (1/21)	0.544	13.6% (3/22)	0 (/12)	0.537
Hepatic artery	25% (1/4)	13.3% (4/30)	0.429	15.4% (2/13)	14.3% (3/21)	1.000	13.6% (3/22)	16.7%(2/12)	0.226
Portal stroma	25% (1/4)	10% (3/30)	0.379	15.4% (2/13)	9.5% (2/21)	0.913	18.2% (4/22)	0 (/12)	0.091
Central vein	25% (1/4)	0 (/30)	0.068	7.7% (1/13)	0 (/21)	0.611	4.5% (1/22)	0 (/12)	0.141
Sinusoids	25% (1/4)	0 (/30)	0.068	7.7% (1/13)	0 (/21)	0.611	4.5% (1/22)	0 (/12)	0.141
Any compartment	50% (2/4)	23.3% (7/30)	0.358	38.5% (5/13)	19.1% (4/21)	0.450	31.8% (7/22)	9.1% (2/12)	0.142

Table 46 (below). **DSA II + C4d+ and fibrosis in sinusoids, central veins and portal tracts**

DSA **II** + C4d+ in	**Sinusoidal fibrosis**			**Centrilobular fibrosis**			**Portal fibrosis**		
	≥2	**0/1**	p value	**≥2**	**0/1**	p value	**≥2**	**0/1**	p value
Portal microvascular endothelium	50% (2/4)	3.3% (1/30)	**0.016**	23.1% (3/13)	0 (/21)	0.087	13.6% (3/22)	0 (/12)	0.094
Portal vein	50% (2/4)	3.3% (1/30)	**0.016**	23.1% (3/13)	0 (/21)	0.087	13.6% (3/22)	0 (/12)	0.094
Portal capillaries	25% (1/4)	3.3% (1/30)	0.225	15.4% (2/13)	0 (/21)	0.139	9.1% (2/22)	0 (/12)	0.529
Hepatic artery	25% (1/4)	10% (3/30)	0.379	15.4% (2/13)	9.5% (2/21)	0.913	9.1% (2/22)	16.7%(2/12)	0.177
Portal stroma	25% (1/4)	6.7% (2/30)	0.269	15.4% (2/13)	4.8% (1/21)	0.714	13.6% (3/22)	0 (/12)	0.094
Central vein	25% (1/4)	0 (/30)	0.068	7.7% (1/13)	0 (/21)	0.611	4.5% (1/22)	0 (/12)	0.141
Sinusoids	25% (1/4)	0 (/30)	0.068	7.7% (1/13)	0 (/21)	0.611	4.5% (1/22)	0 (/12)	0.141
Any compartment	50% (2/4)	20% (6/30)	0.248	38.5% (5/13)	14.3% (3/21)	0.339	27.3% (6/22)	9.1% (2/22)	0.211

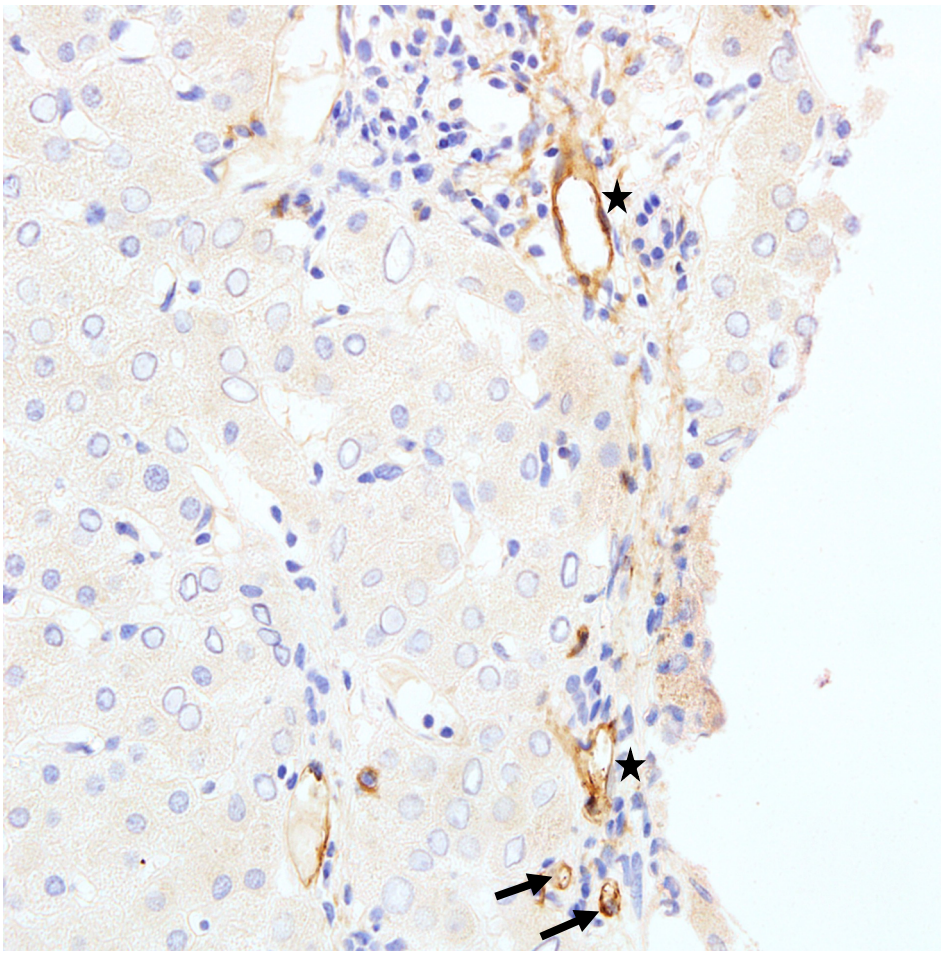

Figure 34. **C4d staining showing positivity in portal vein branches (stars) and portal capillaries (arrows)**

3.3.14 Inflammatory cells: general results

Although 52 biopsies were included in the study, in a number of biopsy specimens the inflammatory cells could not be analysed. Some specimens were excluded because the sections obtained for B cell and T cell staining were too small (less than $3mm^2$) or because the final digitalised image showed artefacts that interfered with the cell count: time limitations prevented repeat staining. Thus, 40

biopsies were stained and analysed for B cells and plasma cells, while 42 were analysed for T cells and CD8+ T cells.

For the specimens examined, the median biopsy area was 10.7 mm^2 (ranging from 3 to 20); the median number of B cells per mm^2 was 15.3 (range 4.5 - 45.4), and the median number of plasma cells per mm^2 was 1.67 (range 0 to 10). The total number of T cells per mm^2 varied extremely between biopsies, from 1.6 to 403.5 cells/mm^2 (median 91.2), and the number of cytotoxic T cells ranged from 1.4 to 193.2 cells/mm^2 (median 29.6). Table 47 shows the minimum, maximum and median number of inflammatory cells in the biopsy specimens.

Table 47. **Number of inflammatory cells in protocol biopsies**

Cell type	Minimum	Maximum	Median
B cells/mm^2	4.5	45.4	15.3
Plasma cells/mm^2	0	10.0	1.7
T cells/mm^2	1.6	403.5	91.2
CD8 T cells/mm^2	1.4	193.2	29.6

3.3.15 Inflammatory cells and Fibrosis

The number of plasma cells was strongly associated with sinusoidal fibrosis (p=0.008) and also significantly associated with centrilobular and portal fibrosis (p=0.043 and 0.041, respectively). Biopsies with portal fibrosis (≥2) also had significantly higher numbers of B cells (p=0.010). The association between sinusoidal fibrosis (≥2) and B cells was near significant (p=0.053).

Table 48. **Median number of inflammatory cells and fibrosis in sinusoids, central veins and portal tracts**

Cells/mm^2 (median)	**Sinusoidal fibrosis**			**Centrilobular fibrosis**			**Portal fibrosis**		
	≥2	**0/1**	p value	**≥2**	**0/1**	p value	**≥2**	**0/1**	p value
B cells	20.1	14.1	0.053	17.9	13.8	0.558	18.6	10.3	**0.010**
Plasma cells	4.2	1.4	**0.008**	4.0	1.1	**0.043**	2.1	1.2	**0.041**
T cells	220.8	64.9	0.353	105.2	64.9	0.808	95.7	47.0	0.513
CD8+ T cells	83.3	20.0	0.273	30.2	20.0	0.729	35.1	12.0	0.363

The measured CPA showed a significant moderate positive correlation with the number of B cells (p=0.037 and r=0.344). Although the Pearson's correlation coefficient (r) between CPA and plasma cells was 0.310 (indicating a moderate positive correlation), it did not quite reach statistical significance (p=0.062). However, considering the small size of the sample, and the limited importance of p value in the Pearson's correlation test, it is reasonable to assume that this result (**r**=0.310 and p=0.062) suggests a real, positive correlation between plasma cells and CPA.

There was no significant correlation between CPA and the number of T cells (r=0.068, p=0.681) or CD8+ T cells (r=0.191, p=0.243). A Pearson's correlation coefficient (r) from 0-0.3 was considered no/minimal correlation; 0.3-0.5, moderate correlation; and above 0.5, strong correlation (topic 3.2.5 of Materials and Methods, page 107).

3.3.16 Inflammatory cells and DSA

There were some differences in the numbers of B cells and T cells when biopsies were divided according to patients DSA (Table 49) and DSAII status (Table 50), but these were not statistically significant and will not be considered any further.

Table 49. **DSA and inflammatory cells**

	DSA +	DSA -	P value
B cells/mm^2	18.7	16.2	0.426
Plasma cells/mm^2	2.3	1.4	0.265
T cells/mm^2	106.7	162.2	0.760
CD8+ T cells/mm^2	29.6	48.2	0.760

Table 50 (below). **DSA II and inflammatory cells**

	DSA II +	DSA II -	P value
B cells/mm^2	18.7	16.2	0.482
Plasma cells/mm^2	2.3	1.7	0.340
T cells/mm^2	113.1	66.6	0.737
CD8+ T cells/mm^2	31.7	18.3	0.666

3.3.17 Inflammatory cells and C4d

Positive C4d staining in portal microvascular endothelium was significantly associated with higher number of B cells and of plasma cells, but not of T cells or CD8+ T cells (Table 51). The median number of plasma cells per mm^2 in biopsies with C4d+ in portal veins was more than double that of biopsies with negative C4d staining

in this compartment (3.9 versus 1.4, p=0.017). Interestingly, C4d+ in portal stroma was associated with significantly higher number of T cells (Table 51).

Table 51. **C4d+ and median number of B cells, plasma cells, T cells and CD8+ T cells**

	B cells (median/mm^2)			**Plasma cells (median/mm^2)**			**T cells (median/mm^2)**			**CD8+ T cells (median/mm^2)**		
C4d+ in	**Yes**	**No**	p value	**Yes**	**No**	p value	**Yes**	**No**	p value	**Yes**	**No**	p value
Portal microvascular endothelium	18.7	13.8	**0.037**	2.9	1.3	**0.035**	80.3	70.9	0.915	30.2	28.0	0.963
Portal vein	31.85	14.1	0.053	3.9	1.4	**0.017**	171.8	70.9	0.698	35.4	28.0	0.853
Portal capillaries	18.6	13.9	**0.037**	2.9	1.3	**0.035**	80.3	70.9	0.601	30.2	28.0	0.673
Hepatic artery	18.7	13.8	**0.037**	2.4	1.4	0.249	74.3	81.1	0.794	19.3	28.5	0.613
Portal stroma	20.6	14.8	0.529	3.3	1.5	0.475	265.7	56.5	**0.045**	79.0	19.1	0.107
Central vein*	-	14.8	-	-	1.7	-	-	72.6	-	-	24.4	-
Sinusoids*	-	14.8	-	-	1.7	-	-	72.6	-	-	24.4	-
Any compartment	18.6	13.8	0.107	2.2	1.3	0.186	105.2	56.5	0.534	33.1	19.1	0.517

** No biopsy specimens stained for B cell and T cell had C4d+ in central veins or/and sinusoids (the 2 biopsies with C4d+ in these sites were too small and thus were excluded from the analysis).*

3.3.18 Inflammatory cells and DSA combined with C4d

Although recipients with DSA/DSA II+C4d+ in almost all compartments had higher numbers of inflammatory cells of each subtype, these associations were not statistically significant (Table 52 and Table 53). This lack of significance may be due to the combination of a relatively small number of patients (34) for whom DSA data was obtained and the large variation in the numbers of inflammatory cells in the study biopsies.

Table 52. **DSA + C4d+ and median number of B cells, plasma cells, T cells and CD8+ T cells**

	B cells (median/mm^2)			**Plasma cells (median/mm^2)**			**T cells (median/mm^2)**			**CD8+ T cells (median/mm^2)**		
DSA + C4d+ in	**Yes**	**No**	p value	**Yes**	**No**	p value	**Yes**	**No**	p value	**Yes**	**No**	p value
Portal microvascular endothelium	32.4	17.9	0.165	3.6	1.7	0.190	269.2	105.2	0.343	51.5	29.0	0.511
Portal vein	32.4	17.9	0.165	3.6	1.7	0.190	269.2	105.2	0.393	51.5	29.0	0.511
Portal capillaries	32.4	17.9	0.165	3.6	1.7	0.190	269.2	105.2	0.393	51.5	29.0	0.511
Hepatic artery	26.4	17.7	0.065	3.0	1.8	0.453	103.4	106.7	0.741	26.2	29.6	0.741
Portal stroma	26.5	17.8	0.339	3.4	1.8	0.195	203.7	89.6	0.237	56.1	29.1	0.393
Central vein	-	17.7	-	-	2.1	-	-	105.2	-	-	33.1	-
Sinusoids	-	17.7	-	-	2.1	-	-	105.2	-	-	33.1	-
Any compartment	20.4	17.8	0.347	2.4	1.7	0.472	132.6	70.9	0.268	33.1	28.0	0.268

Table 53 (below). **DSA II + C4d+ and median number of B cells, plasma cells, T cells and CD8+ T cells**

	B cells (median/mm^2)			**Plasma cells (median/mm^2)**			**T cells (median/mm^2)**			**CD8+ T cells (median/mm^2)**		
DSA **II** + C4d+ in	**Yes**	**No**	p value	**Yes**	**No**	p value	**Yes**	**No**	p value	**Yes**	**No**	p value
Portal microvascular endothelium	30.1	18.2	0.405	3.9	1.8	0.308	285.7	89.7	0.220	67.4	28.5	0.281
Portal vein	30.1	18.2	0.405	3.9	1.8	0.308	285.7	89.7	0.220	67.4	28.5	0.281
Portal capillaries	30.1	18.2	0.405	3.9	1.8	0.308	285.7	89.7	0.220	67.4	28.5	0.281
Hepatic artery	20.4	17.8	0.165	2.4	2.0	0.700	132.6	105.2	0.555	33.1	29.0	0.511
Portal stroma	20.6	17.9	0.700	3.3	2.0	0.316	302.3	74.3	0.110	83.3	28.0	0.194
Central vein	-	17.9	-	-	2.0	-	-	105.2	-	-	29.0	-
Sinusoids	-	17.9	-	-	2.0	-	-	105.2	-	-	29.0	-
Any compartment	19.1	18.2	0.641	2.3	1.8	0.683	200.9	72.6	0.186	42.3	23.6	0.170

3.3.19 Expression of granzyme B by B cells

The analysis of the B cell immunofluorescence staining (CD79α, CD138, DAPI) revealed expression of GrzB by B lymphocytes (CD79α+CD138- cells) in 12 out of the 42 (28.6%) biopsies. In 11 biopsies, the double positive cells were observed in portal tracts and in one biopsy, in the lobular region. There were few GrzB+ B cells per biopsy, ranging from 1 to 4 cells (average 1.5). Because of the small number of biopsies with GrzB+ B cells, no statistical analysis was possible to correlate this with other parameters, such as degree of fibrosis and inflammation.

No double positive cells (CD79α+GrzB+CD138-) were present in the centrilobular/perivenular area and no plasma cells (CD79α+CD138+) were found to express GrzB. Examples of B cells expressing granzyme B (CD79α+GrzB+CD138-) in portal tracts and lobule are shown in the next three figures. The red images correspond to CD79α, the green images to GrzB, and cyan images to CD138 staining. The last image in each figure corresponds to the overlay of these three channels and DAPI (blue).

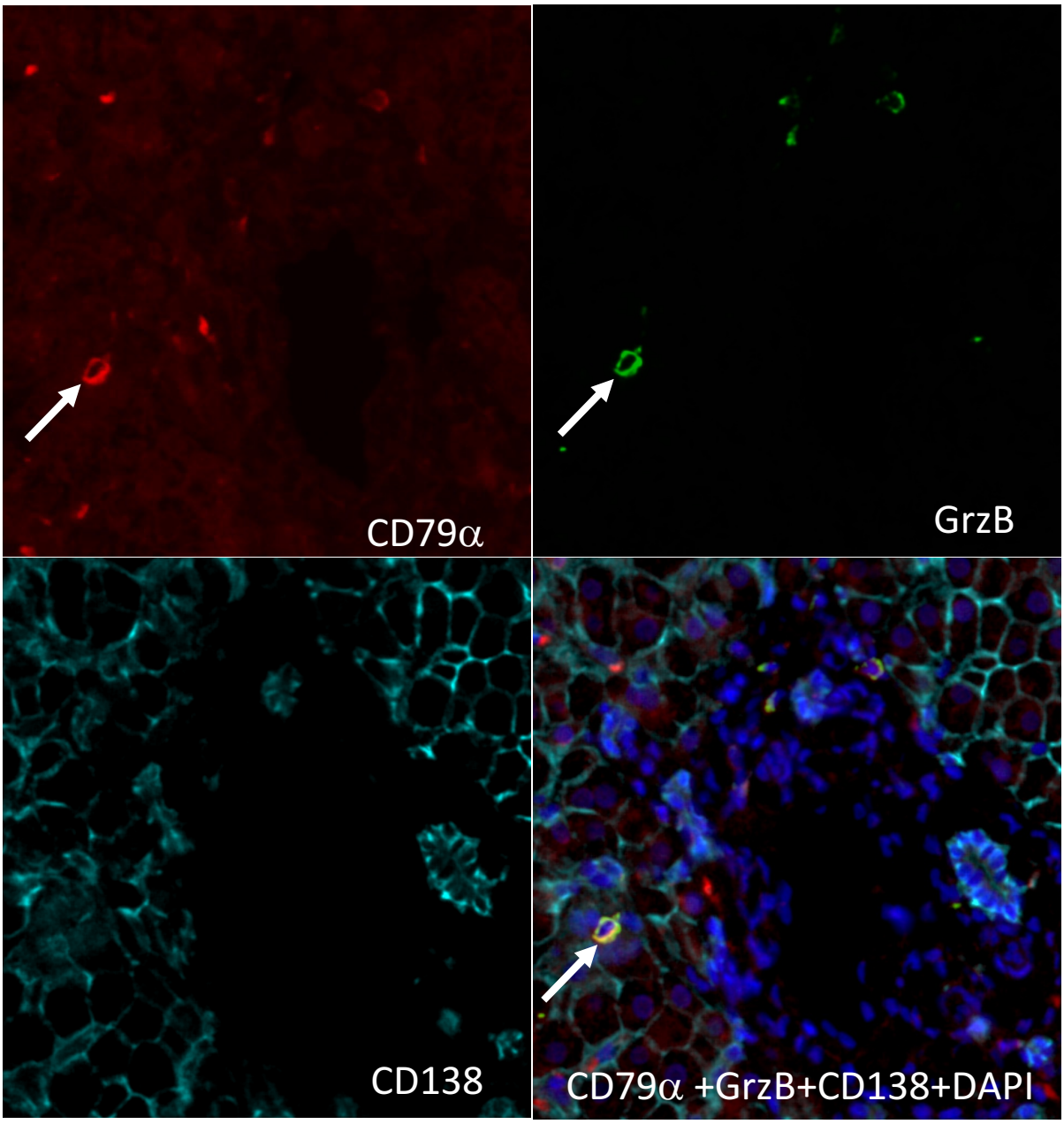

Figure 35. **Portal tract with a CD79α+ (red) CD138- (cyan) cell expressing granzyme B (green). The CD138 staining highlights portal bile ducts and hepatocyte membranes**

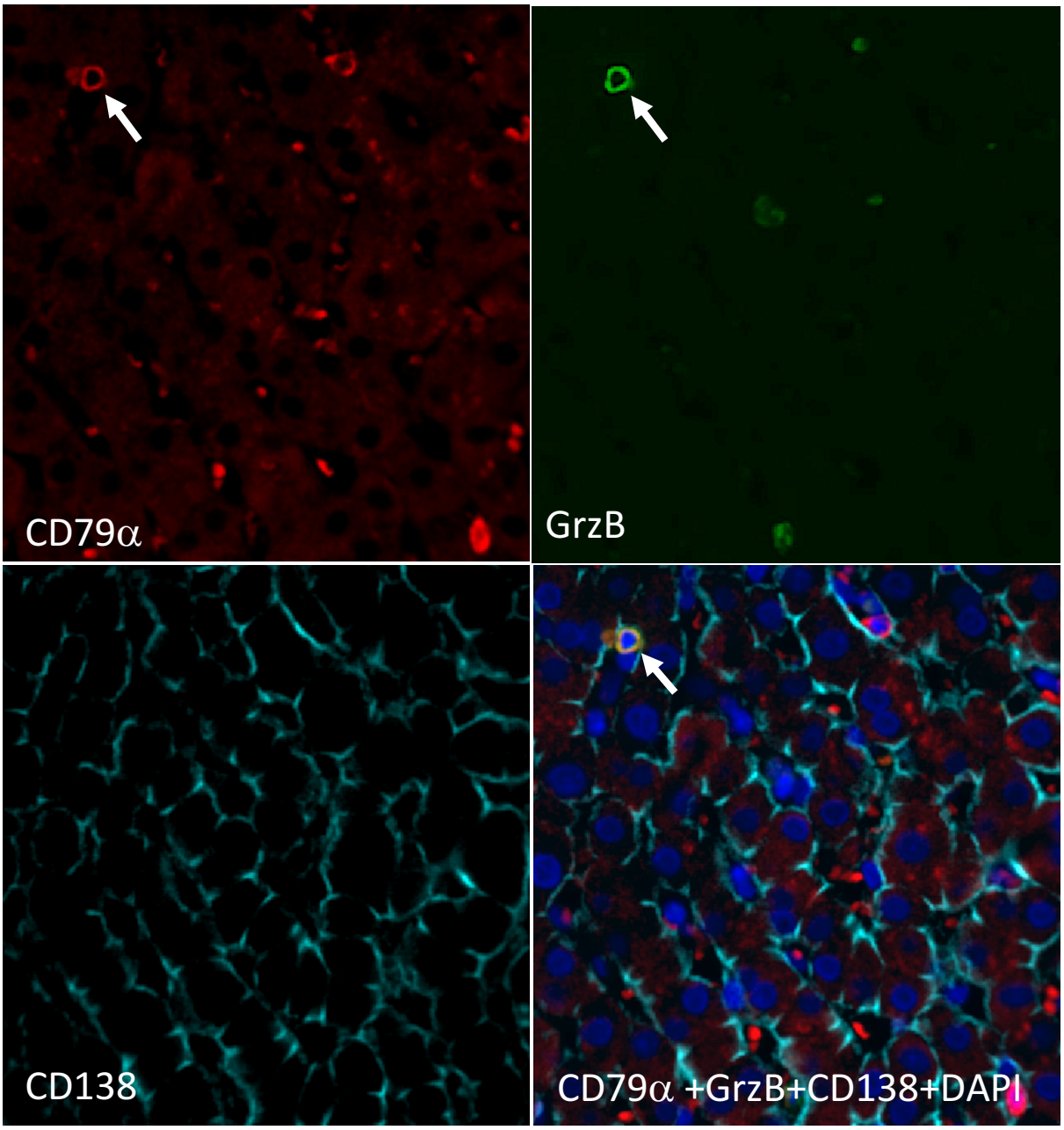

Figure 36. **Lobular area with a CD79α+ (red) CD138- (cyan) cell expressing granzyme B (green). Hepatocyte membranes are evident in the CD138 staining**

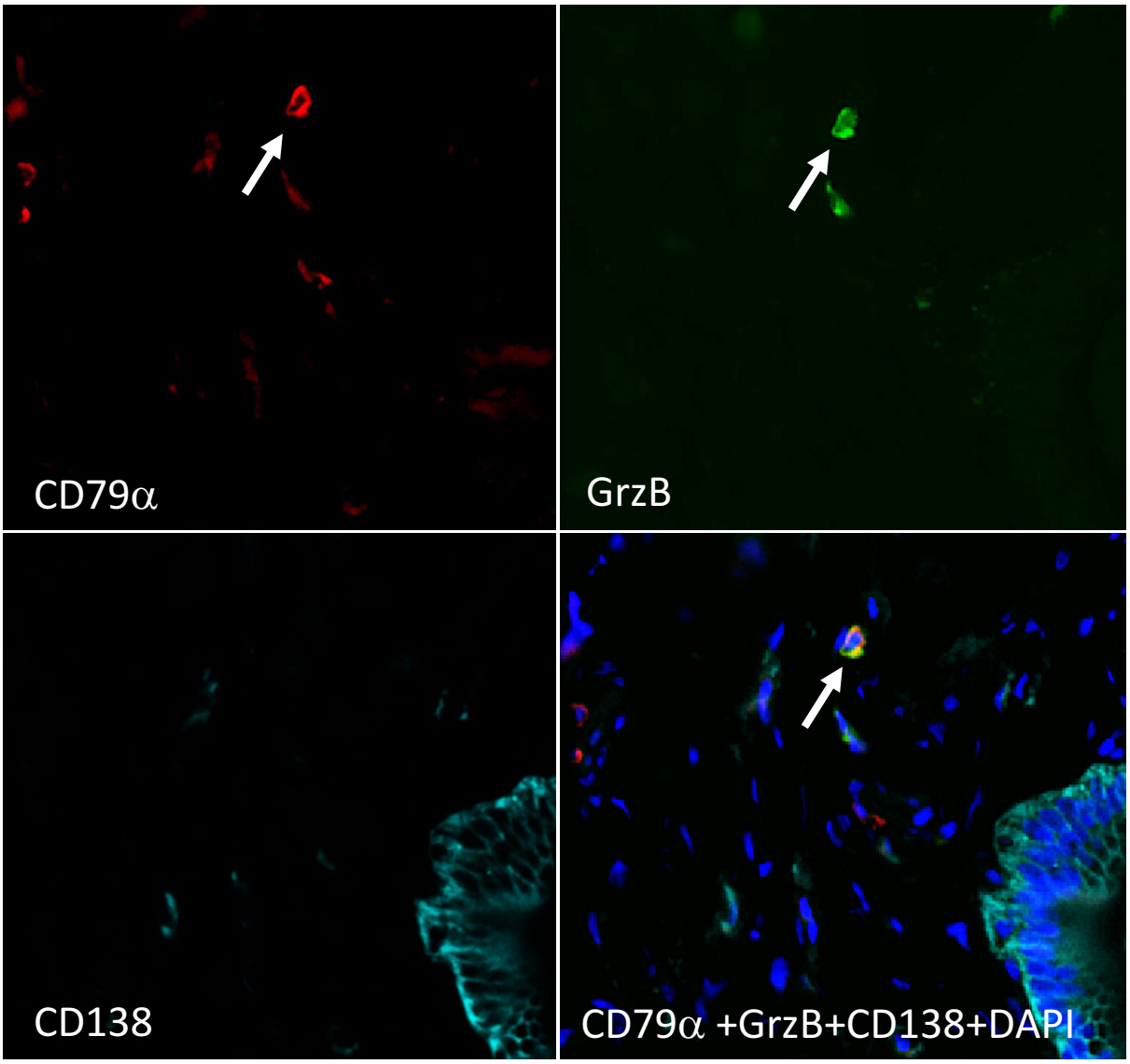

Figure 37. **Large portal tract with a CD79α+ (red) CD138- (cyan) cell expressing granzyme B (green). The CD138 staining highlights a large portal bile duct at the bottom right**

3.4 DISCUSSION

3.4.1 Overview

Analysis was conducted of 55 protocol biopsies obtained between 8.6-15.6 years post-transplant from children who were clinically asymptomatic. The average time from LT to protocol biopsy was 11.8 years and average age of patients at biopsy, 13.2 years. The most frequent indication for transplantation was biliary atresia. A high rate of abnormal histology was observed, consisting predominantly of chronic inflammation and fibrosis, in addition to a high prevalence of circulating DSA. Significant associations were found between clinical and histological parameters.

At the time of the protocol biopsy, 43% of patients received tacrolimus, 40% received cyclosporine and 78% of children also had steroids as part of their immunosuppression regime. Although no patient had clinical evidence of graft dysfunction and most had normal liver biochemistry, a few recipients had mildly abnormal liver enzymes at the time of protocol biopsy.

Two-thirds of children (66%) had at least one previous episode of acute rejection confirmed histologically, a frequency comparable to that found by Miyagawa-Hayashino *et al.* (67%)[28] and higher than that reported by other centres[40,184-185]. Autoantibodies were present in 19% of patients, a lower rate compared to that reported by Evans *et al*. in their paediatric protocol biopsy study, in which autoantibodies were detected in 57% of children at 10 years post-transplant[23].

Histological abnormalities were observed in the majority (73%) of biopsy specimens. Fibrosis was most common, affecting 60%, with 40% of biopsies already showing bridging fibrosis or cirrhosis. Unexplained chronic inflammation/IPTH was the second most frequent histological abnormality, present in 40% of transplant recipients

and typically accompanied by portal fibrosis (in 82% of cases). Fibrosis without inflammation was present in 27% of children.

Previous studies have reported high rates of abnormality in protocol biopsies of asymptomatic children, many of whom had normal liver biochemistry, and in some cases the biopsy findings led to a change in immunosuppression treatment[23,29,40,186]. This observation reinforces the relevance of protocol biopsies in monitoring allograft function and injury[13,19,96,120]. Currently, protocol biopsies are the only way of diagnosing hepatitis or fibrosis in paediatric liver recipients, since serum markers and non-invasive methods of fibrosis are still in need of further validation in children[187].

Scheenstra *et al.*[29] and Evans *et al.*[23] reported comparable rates of histological abnormality in 10-year protocol biopsies of children (69% and 79%, respectively). In the former study, fibrosis was the commonest histological finding, present in 69% of 10-year protocol biopsies, with 49% showing bridging fibrosis or cirrhosis, a slightly higher frequency than that of the current cohort (60% fibrosis and 40% bridging fibrosis or cirrhosis). Chronic inflammation, however, was a very unusual finding[29].

On the other hand, Evans *et al.* observed unexplained chronic hepatitis in almost two-thirds of protocol biopsies (64%)[23], a higher rate than found in the current study (40%). This difference might be due to an important distinction between the cohorts: whilst in the Evans series, the patients did not receive steroid as part of the immunosuppression, in the current study, most children (78%) did. Use of steroid might also explain the lower rate of autoantibodies found in the present study, compared to that reported previously (19% versus 57%)[23]. Low-dose steroids are usually incorporated in paediatric post-transplant long-term immunosuppression at King's College Hospital.

Despite being lower than that reported by Evans *et al.*[23], the prevalence of IPTH was substantial in the current study cohort (40%). This is even more true compared to Scheenstra *et al*'s analysis[29], in which patients also received steroids. Chronic inflammation was not relevant in Scheenstra's series, perhaps because the standard immunosuppressive regime consisted of triple therapy with cyclosporine, azathioprine and prednisolone, whereas in the current study cohort, most patients did not receive azathioprine, and 23% were under steroid-free immunosuppression by the time of biopsy.

In their study of late follow-up biopsies of paediatric recipients, Kosola *et al.*[188] found portal inflammation to be inversely associated with the use of steroid. Whilst only 14% of recipients receiving steroid had portal inflammation, almost half (47%) of those under steroid-free immunosuppression showed inflammatory activity in portal tracts (p=0.009)[188]. Another study of for cause post-transplant biopsies of paediatric patients also evidenced a link between the presence of fibrosis and steroid-free immunosuppression[50].

In the current analysis, steroid-free immunosuppression was individually associated with higher prevalence of IPTH (almost double), more severe portal inflammation and with portal fibrosis. Whereas only 5% of patients receiving steroid had moderate portal inflammation, one-third of those under steroid-free immunosuppression displayed this degree of inflammation (p=0.021, Table 28 on page 129). Other authors have reported an association between IPTH and steroid-free immunosuppression, autoantibodies and previous episodes of rejection[23,28,189]. In the present series, IPTH or inflammation in each compartment were not associated with the presence of autoantibodies. For portal fibrosis, the mean Ishak score of patients receiving steroid was 1.7 versus 2.9 for patients under steroid-free

immunosuppression (p=0.023). The proportion of portal fibrosis (Ishak ≥2) was 47% versus 83% (p=0.046) for patients receiving and not receiving steroid, respectively (Table 27 on page 127).

The rate of fibrosis was also slightly higher in Evans' series compared to the current study: bridging fibrosis or cirrhosis was present in 50% of 10-year protocol biopsies[23], in comparison to 40% in the current study. This is probably a consequence of the higher prevalence of chronic inflammation, since fibrosis is a result of repeated or ongoing liver injury[33].

Another study involving 10-year liver allograft biopsies of children transplanted for biliary atresia found abnormal histology in 73% of patients[40], a similar rate as the present study (73%). The main abnormalities in the published series, however, consisted of chronic rejection (41%) and mild centrilobular fibrosis (22%)[40]. The authors did not detail the histological features, including the criteria used to diagnose rejection. Thus, it is not possible to clarify whether biopsies with chronic inflammation, for instance, might have been classified as rejection[40].

Centrilobular/pericentral fibrosis was very common in the current series, being present in two-thirds (67%) of patients, moderate or severe (grade 2/3) in 38%. Previous publications have also reported considerable rates of centrilobular fibrosis in protocol biopsies, from 22.3% to 53.8%[40,-41]. Most studies on post-transplant protocol biopsies, however, used conventional fibrosis scoring systems, which did not take into consideration centrilobular fibrosis specifically. Scoring systems conventionally used to quantify liver graft fibrosis were intended to grade native liver biopsies with chronic viral liver diseases, in which the fibrogenic process targets primarily portal tracts[36-37,39] (Chapter 1). Centrilobular fibrosis is not specifically considered in these systems.

It is possible that in some paediatric protocol biopsies with advanced fibrosis, the fibrogenic process might have begun in the centrilobular area. In the current series, no association was observed between fibrosis, including centrilobular, and the presence of autoantibodies, like reported by Venturi *et al*.[190] and Evans *et al.*[23]. Sinusoidal fibrosis was also common in the current research cohort (present in 60% of biopsies), but was frequently mild/grade 1. Only 15% of patients had moderate-severe sinusoidal fibrosis.

In paediatric post-transplant long-term biopsies, the highest rate of fibrosis was reported by Ekong, at 97%[14]. Unlike the aforementioned studies, this involved clinically indicated biopsies as opposed to protocol, and the time interval post-transplantation was broader (from 3-11 years)[14]. In the current research, fibrosis without associated inflammation was present in 27% of biopsy specimens. In such instances, fibrosis might be consequent to previous inflammatory flares, such as subclinical episodes of rejection, cholangitis or viral hepatitis, that later resolved.

Although in the current study, a high frequency of previous episodes of rejection was observed (61.5%), no association was found between these (either early or late rejection) and fibrosis at protocol biopsy, unlike that previously reported[50]. Most biopsies showed inflammation in portal tracts (56%), frequently mild. Central perivenulitis was present in a quarter of biopsy specimens (27%), and interface activity in 15%. Other authors have reported comparable frequency of central perivenulitis in adult and paediatric liver allograft biopsies[111,191-192] (see below).

Considering the clinical parameters, patients who were younger at the time of transplantation showed a higher proportion of sinusoidal fibrosis (score $\geq$1) at the protocol biopsy (p=0.009, Figure 31 on page 119). Scheenstra *et al.*[29] also found an association between younger age at transplantation and fibrosis on protocol biopsy of

paediatric liver recipients, although the fibrosis assessment did not include centrilobular or sinusoidal compartments specifically.

Increasing evidence emerging from studies of protocol biopsies of children suggests that fibrosis in this context might be the result of an immune-mediated injury, such as rejection or even AMR (see below). Considering this, the link observed in the current study, between fibrosis and younger age, could be due to age-related particularities of the human immune system that might predispose younger individuals to rejection post-transplant, such as a higher production of immune cells in the thymus[193]. It could also result from a distinctive response of the immature immune system to the immunosuppressive therapy. Likely, the association between younger age and long-term fibrosis is complex, and a more complete understanding requires a comprehensive study of children's immune system development after transplantation, which is outside the scope of this research.

In the current cohort, fibrosis was not associated with other clinical parameters previously reported to be related, such as time since transplantation, the use of partial grafts, previous episodes of rejection or the presence of autoantibodies[28-29]. There was no difference in liver biochemistry between patients with and without fibrosis. The lack of correlation between fibrosis and liver function tests has been previously recognized[14,50,95,194-195].

Most cases of IPTH are thought to correspond to late rejection or chronic antibody-mediated rejection[19,21,53,170,187] (Chapter 2). Of note, the majority of patients in the current study were adolescents at the time of the protocol biopsy, and noncompliance is commonly observed in this age group, which shows a higher predisposition for developing late rejection[196].

In the current study, significant association was observed between IPTH and concomitant fibrosis in each compartment, and between IPTH and CPA (Table 25 on page 121), consistent with previous reports of a strong link between IPTH and progression of fibrosis[19,197].

3.4.2 Value of collagen proportionate area

In the present study, the digital quantitative measurement of fibrosis through CPA was significantly associated with sinusoidal and with centrilobular fibrosis. Interestingly, CPA was not statistically linked to portal fibrosis. During digital analysis of Sirius Red stained slides, the staining of the fibrous tissue in portal tracts frequently appeared lighter in colour compared to that of the perisinusoidal and pericentral fibrosis. Background staining of sinusoids with equivalent or stronger intensity compared to the portal tracts was frequently seen with Sirius Red staining.

Since the same threshold of colour and brightness had to be used for the analysis of the whole biopsy, usually some of the portal fibrous tissue was excluded from the selection in order to avoid false positive selection of other areas. These technical issues may explain the absence of statistical association between CPA and portal fibrosis in the current study.

CPA was significantly associated with IPTH (Table 25 on page 121) and strongly associated with C4d+ in portal microvascular endothelium (Table 42 on page 147). The link with IPTH was also significant for sinusoidal and for centrilobular fibrosis, and the association with C4d+ was also significant for fibrosis in each compartment assessed conventionally.

These results showed that, for paediatric protocol biopsies, CPA was a good indicator of the degree of sinusoidal and centrilobular fibrosis. Although the relevance

of the digital quantification of fibrosis has been well recognised in other settings, in the current study, CPA was not particularly useful when compared to the conventional semi-quantitative assessment of fibrosis in three compartments by a pathologist. Finally, despite being able to provide a continuous measurement of fibrosis, CPA does not provide information in terms of the location of fibrosis. This information is of particular relevance in the post-transplant setting, as fibrosis in different compartment(s) might result from distinct graft insults.

3.4.3 DSA

In the current study, circulating DSA were present in 71% of liver recipients at the time of protocol biopsy (Table 29 on page 130), in most cases directed to HLA class II only (75%), or to both HLA class I and II (17%). The prevalence of DSA in the current study was higher than that found by Miyagawa-Hayashino *et al.*[28] in long-term protocol biopsies of children (48%). Both studies involved the same method of DSA detection: OneLambda mixed and single antigen bead kits.

Nevertheless, immunosuppression regimes differed between the two cohorts: in the latter, tacrolimus was the initial CNI[28], whilst in the current series, most children (74%) received cyclosporine in the first years post-transplant. This distinction might account for the different proportion of DSA, as cyclosporine is associated with a higher risk of developing DSA[84]. Low levels of CNI were also observed to constitute a risk factor for development of DSA in the long-term post-transplant[84,198]. Unfortunately, in the current research, information on CNI at the time of protocol biopsy were not available for most patients.

Regarding the link between circulating DSA and other parameters: recipients with circulating class II DSA were younger at transplantation than those without these antibodies (median age 9.7 versus 22 months), and this difference was near significant (p=0.052, Table 31 on page 132). Association between younger recipient's age and DSA II has been previously reported[52,199-204]. As mentioned earlier about a similar association between younger age and fibrosis, this link is possibly related to immunological characteristics of young children. The physiological mechanism is not yet understood and has not been considered in these studies[52,199-104].

Although in the current cohort, patients with DSA/DSA II had higher proportions of fibrosis and higher average scores of fibrosis in portal tracts and sinusoids, the differences were not significant. Numerous studies have reported that liver recipients with circulating DSA, especially class II DSA, have higher degrees of fibrosis[28,50,198,205-207], which suggests that fibrosis in protocol biopsies might be related to antibody-mediated graft injury.

No significant association was found between DSA and previous episodes of rejection, autoantibodies, immunosuppression, graft type, donor type and LFTs, in contrast to previous reports[28,50,207]. Lack of significant association might be a consequence of the small number of patients in the current study for whom DSA data was obtained (34). Whereas Ruiz *et al.*[203] observed several liver recipients with DSA at high levels but with normal histology, in the current study, all except 2 patients with circulating DSA had abnormal histology (92%).

Ruiz *et al.*[203] also reported a higher incidence of inflammation in graft biopsies of children with circulating DSA compared to those without antibodies. In the current study, lobular inflammation was significantly associated with circulating DSA/DSA II. The frequency of lobular inflammation (scoring ≥1) was 54% versus 10% in liver

recipients with and without DSA, respectively (p=0.019, Table 34 on page 135). The average score for lobular inflammation was also significantly higher in patients with DSA (mean 0.6 versus 0.1, p=0.018, Table 34 on page 135).

Although a significant association was observed between moderate interface activity and the absence of DSA II (
Table 35 on page 136), there was actually only one biopsy with moderate interface (and this patient had class I DSA only). For this reason, this association was disregarded as being clinically significant and will not be further considered.

Interestingly, in a 5-year follow-up study of operationally tolerant paediatric liver recipients, Feng *et al.*[119] found a subset of patients with persistent DSA II who did not display an increase in inflammation or progressive fibrosis after discontinuing immunosuppression. Their research suggests that some liver allografts maintain stable histology despite the presence of DSA.

Therefore, although required for the development of chronic AMR and associated with graft inflammation and fibrosis, the presence of DSA might not necessarily lead to antibody-mediated allograft injury. This hypothesis is consistent with the current observation that recipients with DSA did not have significantly higher rates of fibrosis or inflammation in most compartments (except lobular), but those with both DSA and C4d+ had higher frequency of fibrosis and inflammation (further commented below).

3.4.4 C4d

Focal, positive C4d staining was present in a third of biopsy specimens in the current cohort. In contrast to the study by O'Leary *et al.*[183], significant associations

between C4d+ and the presence of DSA or DSA II were not observed (Table 37 and Table 38 on page 141). Despite the insignificance, C4d+ in portal veins was only observed in patients with circulating DSA. The limited number of patients with DSA information, particularly concerning patients with no circulating DSA (10) and the low frequency of C4d positive staining in the current study might have contributed to the lack of statistical association.

A single patient without DSA had C4d+ in portal capillaries, portal arteries and portal stroma. In this instance, C4d activation might have been triggered by other (non-HLA) antibodies reacting against donor antigens present in the allograft[57,208]. Although anti-HLA antibodies represent the majority of anti-donor antibodies and are classically associated with AMR, in some instances non-HLA antibodies, such as towards glutathione-S-transferase T1 (GSTT1) are expressed in the liver allograft and trigger antibody-mediated graft dysfunction[208].

Recently, Dao *et al.*[209] reported C4d+ in 58% of 10-year paediatric liver biopsies, a considerably higher prevalence than that of the current series. However, the authors included C4d staining in <10% of each given compartment/structure as positive, whereas in this thesis such degree of C4d deposition was considered negative/non-significant, similar to the threshold considered in the Banff criteria for chronic AMR[53].

Taner *et al.*[57] suggest that C4d is a better marker of chronic tissue injury than DSA. In this study, significant associations were found between C4d+ in portal microvascular endothelium and each central perivenulitis and lobular inflammation. Association was also found between C4d+ and fibrosis in sinusoids, centrilobular area and CPA (Table 39 to Table 42 on pages 143 to 147). Besides having a higher proportion of fibrosis and central perivenulitis, patients with C4d+ in portal vascular

structures also had significantly higher numbers of plasma cells and B cells in their biopsies, but not T cells (Table 51 on page 159). This finding further supports the idea of tissue C4d deposition as a marker of antibody-mediated graft injury. Although C4d+ in portal stroma was associated with higher number of T cells, staining in this compartment is regarded as less specific and not considered as a diagnostic criterion for AMR[53,183].

The current findings confirm that C4d deposition in portal microvascular endothelium in protocol biopsies is linked to chronic and active graft injury (manifested as fibrosis and inflammation) and to a humoral inflammatory cell profile. DSA was only associated with lobular inflammation. This supports the idea that C4d might be a better marker of chronic tissue injury than DSA[57]. Nevertheless, the lack of significant association between DSA and fibrosis or inflammation in other sites might be simply a reflection of the small number of recipients who had known DSA status.

In kidney transplantation, tissue C4d staining is a better predictor of graft failure than circulating DSA[210]. In liver transplantation, Fayek *et al.*[140] found that C4d deposition in portal veins was associated with a tendency to poorer outcome. In the current cohort, C4d+ was not significantly associated with poor outcome. However, the follow-up period of most recipients was short and only 3 patients had poor outcome during this time.

In the liver graft, the significance of C4d deposition in different compartments in fixed tissue is still in question. A recent global, multicentre study evaluated the quality of C4d immunostaining in FFPE liver grafts[98] and found that despite being a good marker for typical, florid cases of acute AMR, C4d might be negative or weak in less intense cases of acute AMR. In chronic AMR, the frequency of C4d positive staining is not established. In fact, the diagnosis of chronic AMR in the liver graft itself

is still under study, has gone through changes in recent years and is in need of histological criteria refinement[96,98,209].

The pathogenic role of DSA in chronic AMR is obscured by numerous confounding factors, including indolent evolution, immunosuppression and vast range of DSA MFI levels[53]. It is relevant to stress that liver function tests are often normal in recipients with chronic AMR, despite ongoing injury[53,95,104,202].

3.4.5 AMR and DSA in combination with C4d

In 2016, the Banff group on liver graft pathology made a list of criteria to diagnose probable chronic active AMR in liver allografts[53]: the presence of DSA, at least focal C4d deposition in portal microvascular endothelium, unexplained inflammation (portal or centrilobular with interface and/or perivenular necro-inflammatory activity) and fibrosis, and exclusion of other aetiologies. When the other criteria are met but C4d is negative or minimal, possible AMR is the diagnosis[53]. Considering these criteria, 4 out of the 34 patients in the current study who had known DSA status (12%) fulfilled the criteria of probable chronic active AMR, and other 5 patients (14.7%), of possible AMR.

Although most studies associate portal endothelial C4d staining with presumed chronic AMR lesions, the C4d deposition in the chronic setting is usually more focal in distribution and weaker in intensity compared to acute AMR lesions[53,97-98]. Furthermore, C4d deposition is more problematic in paraffin blocks that have been stored for several years[98]. In the current series, 8 biopsies that underwent immunostaining for C4d had been archived for more than 10 years. Seven of these were completely negative for C4d, and one biopsy had focal, moderate C4d+ staining in portal veins and portal capillaries. Because of such considerations, most authors

recommend that C4d staining should always be interpreted together with DSA[53,57-58]. In fact, the presence of DSA with C4d deposition is considered the traditional marker for humoral immunity[209] and both elements are required for diagnosis of AMR in the liver graft[53]. Nevertheless, because of this lower sensitivity of C4d staining, the mere lack of C4d+ does not exclude the possibility of chronic active AMR.

Considering the combination of DSA+C4d+ and DSA II+C4d+ in relation to other histological parameters, DSA+C4d+ in portal microvascular endothelium was statistically linked to a higher frequency of interface activity and central perivenulitis (Table 43 on page 149). In fact, the combination of DSA+C4d+ in portal capillaries was exclusive of patients with interface activity (p=0.003), and DSA+C4d+ in portal veins was only present in patients with central perivenulitis (p=0.007).

O'Leary[104,211] previously found that interface activity was associated with circulating post-transplant DSA and higher risk of liver graft loss, and included this feature in the proposed criteria for chronic AMR in the liver graft. In their recent study on chronic AMR, Dao *et al*.[209] found portal inflammation to be associated with both DSA and C4d+. Although in the current series DSA+C4d+ in portal veins or portal capillaries was only present in patients with portal inflammation, association was not significant.

Although lobular inflammation is not currently considered in the Banff criteria for the diagnosis of AMR[53], in the current cohort, this was the only histological parameter that was significantly associated with circulating DSA, and it was also associated with C4d+ in portal microvascular endothelium. Moreover, patients with lobular inflammation showed four times the proportion of DSA+C4d+ compared to those without inflammation in this compartment, although this difference was not statistically significant (Table 43 on page 149).

Interestingly, the finding of lobular inflammation in long-term post-transplant liver biopsies is often considered an indication of possible viral infection. The patients in the current cohort, however, had negative viral screening. Lobular inflammation has been associated with graft loss in O'Leary *et al*'s cohort and this parameter was included in the authors' proposed criteria for chronic AMR[183]. Hübscher *et al.*[212] suggest that diffuse lobular inflammation could represent a transitional phase between acute and chronic rejection.

In their study of 103 biopsies of 10 liver allografts that failed due to chronic ductopaenic rejection (CR), Quaglia *et al*.[213] discovered that lobular hepatitis preceded CR in 9 cases, and in the remaining patient, it became evident after diagnosis of CR. Since humoral mechanisms might be involved in the development of CR, it is tempting to hypothesize that lobular inflammatory activity could possibly be a phenotype of graft damage caused by circulating DSA. The relationship between lobular inflammation and AMR needs further study.

In regard to fibrosis, only sinusoidal fibrosis was significantly associated with DSA+C4d+ in portal veins in the current study (Table 45 on page 152). Association was stronger for class II DSA+C4d+ (Table 46 on page 153), and the rate of DSA II+C4d+ in portal veins in patients with and without sinusoidal fibrosis was 50% versus 3.3%, respectively (p=0.016). Previous research has suggested that fibrosis in paediatric protocol biopsies might be the result of chronic subclinical AMR[53,104,187,209]. Sinusoidal fibrosis has been associated with DSA and with allograft loss and therefore included in O Leary *et al*'s criteria for chronic AMR[183]. The Banff group suggested that atypical patterns of fibrosis might represent chronic AMR or mixed T-cell mediated and antibody mediated rejection[53]. In their recent review on humoral rejection in the

liver graft, Koo *et al*.[96] recommended that chronic AMR should always be included in differential diagnosis of unexplained graft fibrosis.

Dao *et al*.[209] recognised centrilobular fibrosis as a feature of chronic AMR in late protocol liver biopsies of children, linked to DSA+C4d+. In the current study, DSA+C4d+ in portal veins was more frequent in patients with centrilobular fibrosis (23% versus 0), but this contrast was not significant (Table 46 on page 153), possibly due to the small number of patients who had DSA information in the current cohort. This may account for the lack of significance between DSA+C4d+ and fibrosis in central and possibly portal areas.

3.4.6 Central perivenulitis and centrilobular fibrosis

Cumulative evidence considers that central perivenulitis is an indicator of late rejection[21,24,27]. Perivenular/centrilobular areas have effective (donor-derived) antigen-presenting cells, which make such regions susceptible to alloimmune response and subsequent graft injury[214]. In T-cell-mediated rejection (TCMR), the presence of central perivenulitis denotes higher severity of the rejection episode, which is less likely to respond to conventional immunosuppression than classical portal-based TCMR and has higher probability to evolve to chronic rejection[212].

Some authors believe that central perivenulitis represents an intermediate stage between acute and chronic rejection, normally preceding the irreversible loss of bile ducts[212,215-216]. In a study of 54 liver recipients, Nakazawa *et al.*[217] observed centrilobular injury in over two-thirds of patients who developed chronic rejection. Another study of protocol biopsies of 100 adult liver recipients verified that late central perivenulitis, which frequently appeared isolated (without concomitant portal features

of rejection), was linked to long-term graft injury[191]. The frequency of isolated central perivenulitis was shown to increase with time post-transplant[34]. The long-term outcome of recipients with isolated central perivenulitis and of those with central perivenulitis accompanying portal based TCMR was comparable, so it seems that the outcome is more dependent on the central injury than the portal[27,111].

In the current analysis, there was a strong association between central perivenulitis and DSA+C4d+ in portal microvascular endothelium (particularly in portal veins, Table 43 on page 149). Central perivenulitis and centrilobular fibrosis were also individually associated with C4d+ in portal microvascular endothelium (Table 39 and Table 41 on pages 143 and 146, respectively). This combination suggested that, besides a feature of late (T-cell-mediated) rejection, the presence of perivenular injury in protocol biopsies of children is likely to represent AMR.

Centrilobular injury as a possible phenotype of AMR could explain why CP is linked to more severe rejection episodes, poorer response to immunosuppression and a higher chance of progression to CR. The Banff group recently acknowledged that perivenular inflammation is one of the most frequent histological patterns of injury linked to chronic AMR, and it is currently incorporated to the histological criteria for the diagnosis of chronic active AMR[53]. In fact, each interface, portal and perivenular inflammation are currently included in the histological criteria for chronic AMR[53].

Yamada *et al.*[41] suggest that antibody-mediated immunity is involved in the development of centrilobular fibrosis. This pattern of fibrosis results from previous ongoing or repeated episodes of central perivenulitis. Interestingly, centrilobular fibrosis is not unusual in long-term biopsies of paediatric liver transplant recipients with circulating DSA, and might be reverted with increased immunosuppression[28,57].

An immunosuppression withdrawal study of 158 children 10 years post-transplant concluded that centrilobular fibrosis in long-term biopsies can be a marker of insufficient immunosuppression and might be related to antibody-mediated immunity[194]. Moreover, biopsies with centrilobular fibrosis have stronger C4d staining and higher numbers of B cells on immunohistochemistry, suggesting that humoral immunity is involved in the development of fibrosis in this site[41].

3.4.7 Quantification of inflammatory cells

The analysis of the inflammatory cells revealed that B cells and plasma cells were significantly associated with portal fibrosis and with C4d staining in portal microvascular endothelium (Table 48 and Table 51 on pages 156 and 159, respectively). Plasma cells in particular were associated with fibrosis in each compartment, the strongest link being with sinusoidal fibrosis. For instance, the median number of plasma cells in biopsies with centrilobular fibrosis ≥2 was almost four times higher than in biopsies with no/mild sinusoidal fibrosis (Table 48 on page 156).

T cells typically represent the majority of inflammatory cells in the liver, and are approximately 10 times more common than B cells[106]. In the current study, the median number of T cells in protocol biopsies was about six-times larger than that of B cells (Table 47 on page 155). Despite that, T cells (and CD8+ T cells) were not significantly associated with the presence of fibrosis in any given compartment, unlike B cells and plasma cells.

The association between fibrosis and a humoral inflammatory profile (B cells and plasma cells), in addition to the significant link found between fibrosis in most sites

and C4d+, and between sinusoidal fibrosis and DSA+C4d+, support the idea that unexplained fibrosis in protocol biopsies of children is likely a result of chronic subclinical AMR.

3.4.8 Local role of B cells

B cells are required for the development of liver fibrosis in mice, and this effect is antibody-independent and T cell-independent, therefore likely mediated by local roles of B cells[110] (Chapter 1). In humans, B cell activation has been associated with fibrosis in skin and lungs of patients with systemic sclerosis[112-113]. GrzB (granzyme B) is expressed by human B cells and plasma cells upon stimulation with viral antigens[114,118]. GrzB is a cytolytic granule protein with proapoptotic role, and is classically associated with cells with cytolytic function, such as NK cells and CD8 T cells, and had not been described in B lymphocytes before the study by Hagn *et al.*[114]. Granzyme molecules also seem to play alternative roles, besides the apoptotic, such as matrix degradation and remodelling[114-116].

In the present study of long-term post-transplant protocol biopsies, combined multiplex immunofluorescence was used to demonstrate that B cells express GrzB in human liver allografts, which has not yet been reported. Expression was seen in 28.6% of liver recipient's biopsies. Interestingly, the number of B cells that expressed GrzB in each biopsy was tiny (average 1.5 cells/biopsy) and these cells were typically located in portal tracts. No plasma cells were found to express GrzB. These GrzB-expressing B lymphocytes might be involved in matrix remodelling following inflammation, leading to allograft fibrosis. This expression of GrzB adds more complexity to the interpretation of B cell infiltrates in liver allograft biopsies. B cells are

usually considered part of the adaptive immune system, maturing into plasma cells that produce and secrete antibodies which act remotely. The expression of a molecule such as GrzB by B cells, however, endorses the theory that B cells also play a local role. This could change the way injuries/diseases in which these cells predominate are regarded, such as *de novo* autoimmune hepatitis/plasma cell hepatitis of the liver allograft.

Because the number of B cells showing GrzB expression in each individual biopsy was so small, it would be interesting to repeat the multiplex staining in serial sections of each biopsy specimen to identify other positive cells. It could also be valid to look for B cells and perhaps plasma cells expressing GrzB in larger histological specimens, such as failed liver allografts.

Interestingly, in the current analysis, T cells, despite representing the majority of the inflammatory population, were not associated with fibrosis in any compartment. Although T cells have a central role in cellular rejection in the transplantation setting, it seems that in protocol biopsies with chronic subclinical lesions, the pathologists should pay special attention to B cells and plasma cells, bearing in mind that they might have additional roles besides the production of antibodies. It is possible that specific subpopulations of T cells, particularly FoxP3, could be associated with histological findings and clinical parameters. Although the study of FoxP3 was planned, quantification of these cells was not possible in the current research due to technical problems.

3.4.9 Summary

In summary, the present study of long-term paediatric protocol biopsies confirmed a high prevalence of relevant histological abnormalities in biopsies of asymptomatic children, consistent with previous reports by other centres. A high frequency of circulating DSA was detected, mainly directed to class II HLA, and these antibodies were associated with active graft injury in the form of lobular inflammation. Children who were younger at transplantation were more likely to have sinusoidal fibrosis and class II DSA by the time of protocol biopsy. The reasons behind these links are not clear.

In the context of protocol biopsies, portal microvascular C4d staining appeared to be an indicator of antibody-mediated graft injury. It was significantly associated with a humoral inflammatory cell profile (B cells and plasma cells), with central perivenulitis and lobular inflammation, and with higher frequency of fibrosis in sinusoids and in central/pericentral regions. The combination of circulating DSA and tissue C4d+ in portal microvascular endothelium was also associated with central perivenulitis and sinusoidal fibrosis, and additionally, to interface activity. B cells and plasma cells were independently linked to fibrosis (in portal tracts and in all compartments, respectively).

These findings suggest that unexplained inflammation (particularly interface activity, central perivenulitis and lobular inflammation) and fibrosis (especially in sinusoids and centrilobular area) in protocol biopsies of children probably represent chronic AMR that might lead to allograft loss, consistent with what was observed in Chapter 2 (Failed Liver Allografts). Considering the Banff criteria for chronic AMR, over a fourth (26%) of paediatric protocol biopsies fulfilled criteria for either probable or possible AMR.

The current observations reinforce the crucial role of the histological assessment of liver allograft biopsies in the diagnosis of subclinical but potentially harmful pathological conditions, such as chronic AMR, and in management of immunosuppression. Chronic AMR, a recently acknowledged condition in liver transplantation, might cause progressive fibrosis in patients who are clinically well with normal liver function tests. Finally, the expression of GrzB by B cells in human liver allografts could mean a potential local role for B cells in the development of fibrosis, which needs to be further investigated.

In Chapter 2, the reasons for retransplantation over the years were explored, and a rising frequency of unexplained chronic hepatitis associated with fibrosis leading to allograft failure was found. In the current chapter, protocol biopsies and the association between histology, including subclinical inflammation and fibrosis, and circulating DSA, tissue C4d deposition, clinical parameters and inflammatory cell phenotype were analysed. Evidence for chronic AMR being involved in long-term graft damage, including inflammation and fibrosis in most compartments was found, and C4d revealed to be a useful marker of humoral injury in liver biopsies, although not sensitive.

Based on these findings, I decided to study liver allograft biopsies with diagnosis of TCMR to see whether in this distinct context, the presence of DSA and C4d+ were associated with specific or similar patterns of injury (Chapter 4).

4 FOR CAUSE BIOPSIES WITH REJECTION

4.1 RATIONALE FOR STUDYING FOR CAUSE BIOPSIES WITH REJECTION

In this study cohort, an analysis of for cause biopsies with a diagnosis of rejection was performed and the histology was correlated with circulating DSA and with gene expression. In the literature review, no previous research has compared all these parameters together. Therefore, a pathogenic role was sought for DSA by comparing the histological and transcriptional characteristics of liver biopsies with rejection.

4.2 MATERIAL AND METHODS

4.2.1 Patients and Data

All liver recipients who underwent a for cause allograft biopsy in which the diagnosis of (T-cell mediated) rejection had been made, and who were tested for DSA within two weeks of the biopsy were selected. Patients whose biopsy specimens were no longer in the hospital's archive and one patient with possibly recurrent hepatitis C were excluded from the study. When several biopsies had been performed for the same rejection episode, that selected was one obtained before starting treatment for rejection. In King's College Hospital, patients with suspected rejection normally undergo biopsy prior to treatment.

In total, 44 biopsy specimens corresponding to 44 liver recipients were included in the research. Patient demographic and clinical information was collected, including age, primary liver disease, baseline immunosuppression, time from transplant to

biopsy, liver biochemistry (AST, bilirubin, AP, GGT, INR) and clinical outcome. Patients were followed up until June 2018 or until allograft loss if this occurred before that date.

4.2.2 Histology

Two pathologists (A.Q. and L.N.S.), blinded to all clinical and serological data, assessed 44 biopsy slides originally stained for HE and reticulin, and graded a series of histological parameters using the same scoring system as Chapter 3 (Table 7 on page 57). Quality of staining was appropriate in all biopsy specimens.

The threshold for significant portal/periportal fibrosis was defined as Ishak stage ≥2 (fibrous expansion of most portal tracts), and for sinusoidal/subsinusoidal and centrilobular fibrosis, as Venturi stage ≥2, as previously done for protocol biopsies (Chapter 3, section 3.2.3.1, page 56). Because digital analysis of Sirius Red stained biopsies in the previous study cohort did not add value to the conventional scoring, it was not used here.

Immunohistochemistry for C4d was performed using precisely the same protocol as for the protocol biopsies (Chapter 3, section 3.2.3.3, page 61). Unfortunately, during this study, the C4d antibodies employed became unavailable to be ordered from the supplier. For this reason, only 21 out of the 44 study biopsy specimens were stained for C4d.

The assessment of C4d immunostaining was conducted using the same scoring system specified in Chapter 3 (section 3.2.3.3, page 61). The C4d positive threshold in a given compartment was defined as at least focal C4d staining in that

compartment (as used above for the protocol biopsy cohort). Minimal C4d deposition (<10%) was considered negative.

4.2.3 DSA testing

In this group of patients, DSA testing had previously been performed close to biopsy date (this was an inclusion criteria for the cohort selection). The diagnostic kits and protocol employed for DSA detection were as described in Chapter 3 (section 3.2.2, page 56).

4.2.4 RNA extraction

RNA was obtained from liver biopsies using RNeasy FFPE kit (Qiagen, UK). Firstly, excessive paraffin was removed from the biopsy blocks with a blade and eight 5μm sessions were cut from each block with a microtome and placed in 2 ml sterile plastic tubes. The tissue underwent the following steps according to the manufacturer's protocol: deparaffinization, incubation with lysis buffer, DNase treatment, ethanol addition and RNA elution through RNeasy MinElute spin column. Finally, sterile, RNAse-free distilled water was added to remove the RNA from the column membrane. Concentration and purity of resulting RNA were measured with Nanodrop (ThermoScientific). RNA samples were stored at -80°C until analysis.

4.2.5 RNA sequencing and analysis of gene expression data

The RNA extracted from the biopsies was sent for sequencing (RNASeq) at the Bioinformatic Platform of the Biomedical Research Center in Hepatic and Digestive Diseases (CIBEREHD), Instituto de Salud Carlos III, Spain. The sequencing protocol used was similar to that reported in a recent paper on molecular profiling of adult liver recipient biopsies, in which the current author participated[138]. A small amount of RNA (50ng) was used to generate sequencing libraries (with Ion AmpliSeq™ Transcriptome Human Gene Expression Kit, Thermo Fisher). Sequences were then compared to reference sequences that include over 20,000 genes in the AmpliSeq Human Gene Expression panel. The correlation patterns among genes were analysed with Weighted Gene Correlation Network Analysis (WGCNA) software.

Statistical significance for previously recognised groups of genes associated with biological pathways were computed with Quantitative Set Analysis for Gene Expression, and an FDR<0.10 was considered significant. Gene sets were incorporated from both the transplantation-related Pathogenesis-Based Transcript (PBT) from the Alberta Transplant Applied Genomics Centre (available at atagc.med.ualberta.ca/Research/GeneLists) and the Kyoto Encyclopedia of Genes and Genomes (KEGG) pathway databank.

4.2.6 Statistical analysis

The data were analysed using SPSS version 23.0 (IBM Corporation, 2015). Categorical variables are presented as number and percentage. Continuous variables are presented as median and range or mean/average and range. For most continuous variables, such as liver enzymes and patients age, the **median** was used to measure central tendency, as for the protocol biopsies (Chapter 3). For histological variables

with few possible discrete values, such as degree of fibrosis and inflammation, however, the **mean** (average) was used instead of the median (detailed explanation in section 3.2.5, page 107).

The Mann-Whitney (non-parametric) test was used to compare continuous variables between groups. Fischer's exact test was used to compare categorical variables and validate differences in frequencies between different groups. A p value of less than 0.05 was considered statistically significant.

4.3 RESULTS

4.3.1 Demographic Data

Between January 2012 and December 2015, 44 liver recipients had a clinically indicated graft biopsy with TCMR confirmed on histology, had undergone DSA testing within 2 weeks and had no evidence of recurrent disease. Although most patients had the biopsy performed before starting treatment for rejection, 7 patients underwent liver biopsy after the start of empirical treatment for rejection. The recipients' ages ranged from 9 months to 66.5 years (median 24.1 years), 68% (30) were adults and 32% (14) were children.

The biopsy was obtained between 6 days and 5.9 years after liver transplantation (median 164 days or 5.5 months). In most cases, the biopsy was performed later than the typical time when T-cell mediated rejection is diagnosed (usually the first month posttransplantation). This difference could be explained through the selection criteria, since only patients with rejection who were also tested for DSA were included, thus patients in which AMR was suspected. As patients with

typical TCMR that promptly resolves with conventional treatment are not usually tested for DSA, these were not included in the study. The indications for transplantation (LT) are specified in Table 54.

Table 54. **Indications for liver transplantation**

Indication for LT	Number (%)
Biliary atresia	9 (20.5%)
ALF	7 (15.9%)
AIH	5 (11.4%)
PBC	5 (11.4%)
PSC	4 (9.1%)
NASH	3 (6.8%)
HCV + HCC	3 (6.8%)
AIH/PSC	2 (4.5%)
Cryptogenic cirrhosis	2 (4.5%)
ALD	1 (2.3%)
HBV	1 (2.3%)
α1AT deficiency	1 (2.3%)
BSEP deficiency	1 (2.3%)

ALF, acute liver failure; AIH, autoimmune hepatitis; PBC, primary biliary cholangitis; PSC, primary sclerosing cholangitis; NASH, non-alcoholic steatohepatitis; HCV, hepatitis C virus; HCC, hepatocarcinoma; ALD, alcoholic liver disease; HBV, hepatitis B virus; α1AT, alpha-one anti-trypsin; BSEP, bile salt export pump

For baseline immunosuppression, 41 patients (93%) received tacrolimus: 18 combined with MMF, 17 on its own and 6 with sirolimus. Two patients received cyclosporine and MMF and 1 patient everolimus and MMF (Table 55). In addition, 33 recipients (75%) received steroid as part of the immunosuppression prior to the biopsy/rejection episode.

Table 55. **Baseline immunosuppression**

Baseline immunosuppression	Number (%) of patients
Tacrolimus	17 (38.6%)
Tacrolimus and MMF	18 (40.9%)
Tacrolimus and sirolimus	6 (13.6%)
Cyclosporine and MMF	2 (4.5%)
Everolimus and MMF	1 (2.3%)

The median and range of liver biochemistry tests at biopsy were: AST 201 IU/L (35 - 2642); bilirubin, 93 µmol/L (4 - 431); GGT 506 IU/L (34 - 2181); AP 422 IU/L (144 - 1796); INR 1.13 ratio (0.84 – 2.81, Table 56).

Table 56. **Liver biochemistry at biopsy**

Test	Patients Results (median and range)	Reference value (units)
AST	201 (35 - 2642)	10-50 IU/L
Bilirubin	93 (4 - 431)	3-20 µmol/L
GGT	506 (34 - 2181)	1-55 IU/L
AP	422 (144 - 1796)	30-130 IU/L
INR	1.13 (0.84 - 2.81)	0.9-1.2 ratio

In regard to clinical follow-up, median follow-up time after the biopsy was 3 years (from 7 days to 6.5 years). During this period, 25 patients (57%) were alive and had the same graft; 18 patients (41%) had poor outcome with graft loss and/or death, and 1 patient (2.3%) was lost to follow-up. From the 18 patients with poor outcome, 7 (16%) underwent retransplantation and survived, and 11 patients died (25%), 7 of

them as direct consequence of graft failure, 2 due to infection, 1 for acute respiratory distress syndrome after transplantation, and 1 in consequence of carotid haemorrhage following self-inflicted injuries in the context of steroid-induced psychosis during rejection treatment. Patient outcome is shown in Table 57.

Considering the 14 allograft losses (7 of which resulted in death), 10 allografts failed for chronic ductopaenic rejection (CR), 1 for recurrent PSC and rejection, 1 for acute TCMR with hepatic artery thrombosis, 1 for non-thrombotic infarction with rejection, and 1 for subacute liver failure which cause was not clear. The reasons for allograft loss are specified in Table 58. Therefore, in 13 out of 14 patients who lost their allografts (93%), rejection played a recognizable role in the organ failure. In the remaining patient with subacute liver allograft failure, it is not possible to confirm or exclude a role for rejection (including AMR) in the allograft loss.

Table 57. **Patient outcome**

Outcome	% and number
Alive with same graft	57% (25)
Graft failure and death	16% (7)
Graft failure, retransplantation and survived	16% (7)
Death (not directly linked to graft failure)	7% (4)
Lost to follow-up	2.3% (1)
Total	100% (44)

Table 58. **Reasons for graft failure**

Causes of graft loss	% and number
CR	71.4 % (10)
Recurrent PSC + TCMR	7.1 % (1)
TCMR + HAT	7.1 % (1)
Non-thrombotic infarction + rejection	7.1 % (1)
Subacute liver failure	7.1 % (1)
Total	100 % (14)

** CR, chronic rejection; PSC, primary sclerosing cholangitis;*

TCMR, T-cell mediated rejection; HAT, hepatic artery thrombosis

4.3.2 DSA: overall results

In this series, 29 patients (66%) had circulating DSA: 27 had class II (19 in isolation, 8 combined with class I) and 10 recipients had class I DSA (8 combined to class II, 2 in isolation, Table 59). For DSA subtypes: most patients with class II DSA had both anti-DQ and anti-DR antibodies (14 out of 27, 52%), and 13 recipients had anti-DQ antibodies only (48%, Table 60). Anti-DP antibodies were not detected in any liver recipient.

Table 59. **DSA test results**

DSA class	Number (%) of patients
II	19 (43.9%)
I and II	8 (18.2%)
I	2 (4.5%)
No DSA	15 (34.1%)

For class I DSA: 6 patients (60%) had anti-A and anti-B antibodies, and one of them also had anti-Cw antibodies. Two patients (20%) had anti-B antibodies only, 1 (10%) had Anti-A only and 1 (10%) had anti-Cw only (Table 61). The minimum, maximum and average MFI of DSA I, DSA II and total DSA are detailed in Table 62.

Table 60. **DSA II subtypes**

DSA II subtype	Number (%) of patients with DSA II
DQ and DR	14 (51.9%)
DQ only	13 (48.1%)
DR only	-
DP	-

Table 61 (below). **DSA I subtypes**

DSA I subtype	Number (%) of patients with DSA I
A and B	5 (50%)
A, B and Cw	1 (10%)
B	2 (20%)
A	1 (10%)
Cw	1 (10%)

Table 62 (below). **DSA total MFI**

DSA type	Sum of MFI (median and range)
Class I	8,163 (2,047-18,854)
Class II	17,655 (1,800-71,676)

Class I and II	16,951 (1,800-71,676)

4.3.3 DSA and clinical parameters

There was no significant association between clinical parameters and DSA, except for INR, which was lower in patients with these antibodies (1.04 versus 1.28). However, the median INR was inside the normal range in both groups of patients (DSA+ and DSA-). The median AP was higher in patients with DSA (518 versus 306, Table 63) and this difference was near statistical significance (p=0.057).

Table 63. **Clinical parameters and DSA**

Clinical parameter	DSA +	DSA -	p value
Age in years (mean and range)	21.6 (0.7-66.2)	33.9 (1.4-53.7)	0.325
Steroid use prior to rejection episode (% and number)	72.4% (21/29)	80% (12/15)	0.722
AST (median and range)	199 (44-762)	250 (35-2642)	0.068
Bilirubin	137 (3-514)	135 (6-397)	0.394
GGT	466.5 (34-2052)	533 (63-2181)	0.703
AP	518 (169-1796)	306 (144-963)	0.057
INR	1.04 (0.84-2.21)	1.28 (0.97-2.75)	**0.004**
Poor outcome - death or graft loss (% and number)	31% (9/29)	60% (9/15)	0.139

The presence of circulating DSA II at >10,000 mean fluorescence intensity (MFI) was strongly associated with younger recipient age (p=0.007). The median age of patients with DSA II above that threshold was 14.8 years versus 38.7 years of those with no/lower DSA II (Figure 38). Considering age groups: children accounted for 56%

of patients with DSA II >10,000 versus only 15% for those with no/lower DSA II (p=0.008, Table 64). Analysing both age and DSA II as continuous variables, there was significant negative moderate correlation between these parameters (Pearson's correlation coefficient, r=-0.339, p=0.024). In the scatter plot in Figure 39, it is possible to visualise that older liver recipients overall tended to have lower DSA II MFI than younger patients.

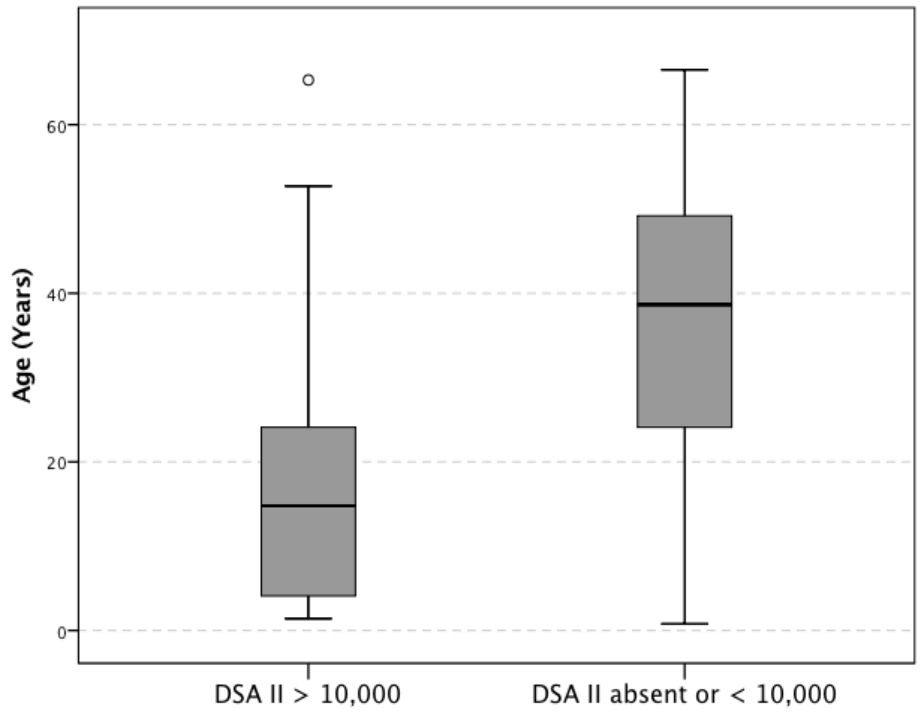

Figure 38 (above). **DSA II and patient age at biopsy** (p=0.007)

Table 64 (below). **Liver recipient age group and DSA II** (p=0.008)

Age group	DSA II >10,000	DSA II – or <10,000
Paediatric	56% (10/18)	15% (4/26)
Adult	44% (8/18)	85% (22/26)

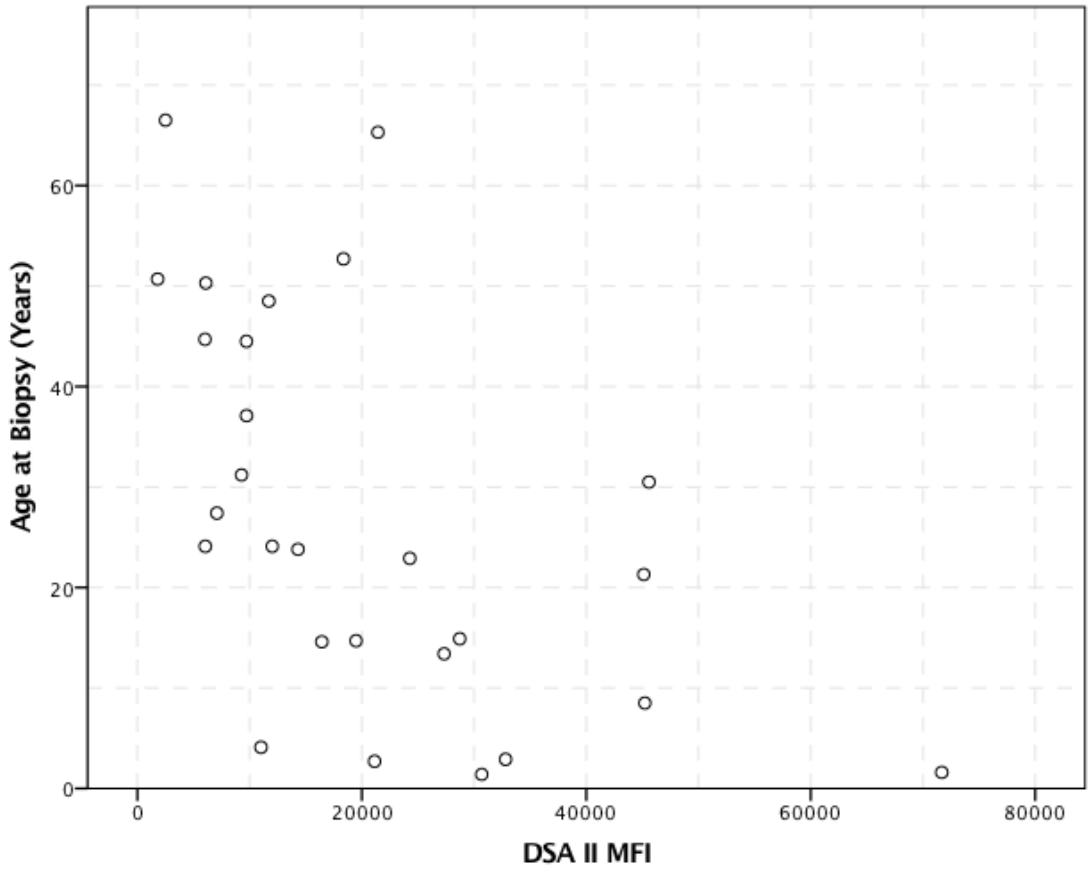

Figure 39. **Correlation between patients' age and DSA II MFI**

The presence of DSA II above 10,000 MFI was also statistically associated with lower proportion of poor outcome: 17% versus 60% for those with no/lower DSA II (p=0.005). At first glance, this association seems contradictory, since the presence of DSA II in high titres is classically linked to worse outcome. Nonetheless, because most patients with DSA II >10,000 were children (and those who were adults also tended to be younger), the association between good outcome and DSA II might simply reflect better health condition of younger patients.

Circulating DSA at the time of biopsy (regardless of type or MFI) were not associated with prior use of steroid, type of primary liver disease (autoimmune versus non-autoimmune, recurrent versus non-recurrent) or time from transplant to biopsy.

4.3.4 Histology

4.3.4.1 HE and reticulin assessment

Considering all biopsies: the median rejection activity index (RAI) was 6 (range 3 to 9). Bile duct lesion was conspicuous in all specimens, and of moderate or severe degree (grade 2/3) in 82%. A quarter of biopsies already displayed bile duct loss (27%), which was advanced (loss of >50% of bile ducts) in one patient only. Bile duct loss was only considered significant when >10% of portal tracts lacked bile duct and the remaining showed obvious bile duct injury. This confirmed that bile duct loss was the result of pathogenic damage, and not merely due to sample variability[218]. Portal vein endotheliitis was moderate or severe in 43% of patients. Central perivenulitis was observed in 80% of biopsies, and was moderate/severe in 59%. Most patients had moderate or severe portal (75%) and moderate or severe lobular (55%) inflammation.

Overall, 32% of biopsies displayed significant fibrosis, either portal (≥2), centrilobular (≥2) or sinusoidal (≥2). Portal fibrosis was present in a fourth of specimens, and 6.9% had at least bridging fibrosis (Ishak ≥3). Significant centrilobular and sinusoidal fibrosis were present in 16% and 6.8% of patients, respectively.

Table 65 displays the detailed histological assessment of HE and reticulin stained biopsies. Figure 40, Figure 41 and Figure 42 show the degree of fibrosis in portal, centrilobular and sinusoidal compartment, respectively.

Table 65. **Overall histological scoring (HE and reticulin staining)**

Portal Inflammation:	Absent	1 (2.3%)
	Mild	10 (23 %)
	Moderate	24 (55 %)
	Severe	9 (21 %)
Interface activity:	Absent	13 (30 %)

	Mild	17 (39 %)
	Moderate	10 (23 %)
	Severe	4 (9.1%)
Lobular inflammation:	Absent	0
	Mild	20 (46 %)
	Moderate	19 (43 %)
	Severe	5 (11 %)
Portal vein endotheliitis:	Absent	6 (14 %)
	Mild	19 (43 %)
	Moderate	17 (39 %)
	Severe	2 (4.5%)
CP:	Absent	9 (21 %)
	Mild	9 (21 %)
	Moderate	16 (36 %)
	Severe	10 (23 %)
Bile duct lesion:	Absent	0
	Mild	8 (18 %)
	Moderate	19 (43 %)
	Severe	17 (39 %)
Bile duct loss:	Absent	32 (73 %)
	Loss of <50%	11 (25 %)
	Loss of >50%	1 (2.3%)
Ductular reaction:	Absent	32 (73 %)
	Present	12 (27 %)
Canalicular cholestasis:	Absent	24 (55 %)
	Grade 1	13 (30 %)
	Grade 2	3 (6.8%)
	Grade 3	4 (9.1%)
Portal Fibrosis (Ishak):	Stage 0/1	33 (75 %)
	Stage 2	8 (18 %)
	Stage 3	1 (2.3%)
	Stage 4	1 (2.3%)
	Stage 5	1 (2.3%)
	Stage 6	0
Centrilobular fibrosis (Venturi):	Stage 0	30 (68 %)
	Stage 1	7 (16 %)
	Stage 2	4 (9.1 %)
	Stage 3	3 (6.8 %)
Sinusoidal fibrosis (Venturi):	Stage 0	35 (80 %)
	Stage 1	6 (14 %)
	Stage 2	1 (2.3%)
	Stage 3	2 (4.5%)

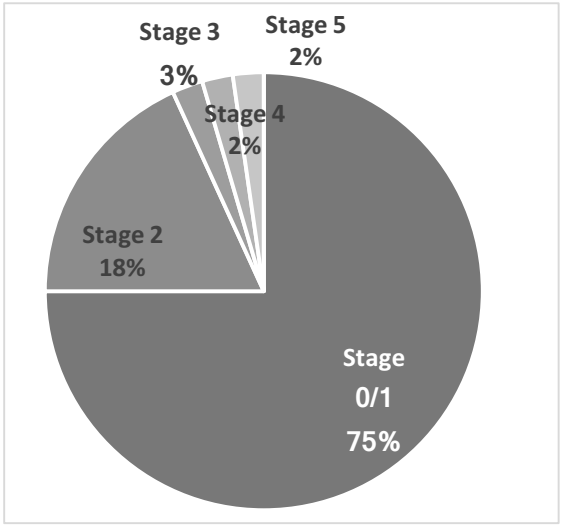

Figure 40 (above). **Portal Fibrosis staging**

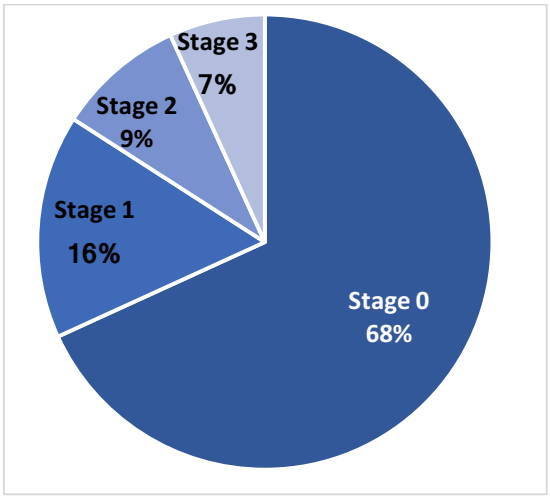

Figure 41 (above). **Centrilobular Fibrosis staging**

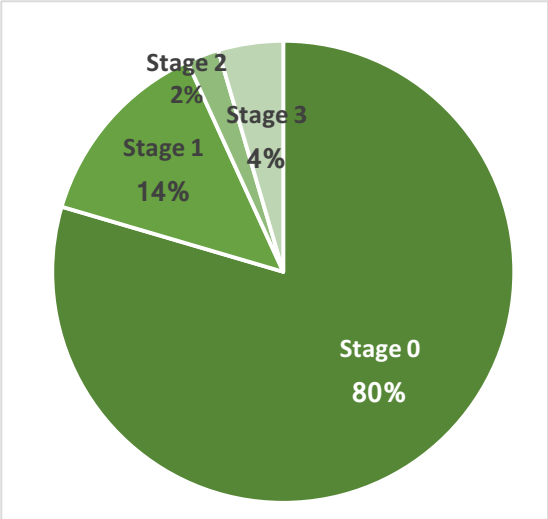

Figure 42. **Sinusoidal Fibrosis staging**

Significant portal fibrosis (Ishak ≥2) was associated with longer time from transplant to biopsy: 4.2 years versus 93 days for those without portal fibrosis (p=0.001). Sinusoidal and centrilobular fibrosis were not statistically associated with time from transplant to biopsy. Outcome was not significantly associated with any histological finding, including fibrosis or inflammation in each compartment or bile duct loss. The proportion of patients who had poor outcome was similar for recipients with and without bile duct loss: 46% versus 41%, respectively (p=0.333).

4.3.4.2 C4d immunohistochemistry

The quality of C4d immunostaining was good, as in the previous study group (protocol biopsies). C4d positivity (C4d+) in at least one compartment was observed in 86% (18/21) of biopsies stained for C4d. Positive C4d staining in portal microvascular endothelium (portal veins or portal capillaries) was present in 52% (11/21) of biopsies. The proportion of C4d+ in each compartment assessed was: portal

veins, 38.1%; portal capillaries, 14.3%; portal stroma, 52.4%; hepatic arteries, 28.6%; central veins, 9.5%; sinusoids,14.3% (Table 66).

Table 66. **C4d positivity per compartment**

Location	Grading (distribution and intensity)	Number (%)
Portal veins	Negative	7 (33.3%)
	Minimal	6 (28.6%)
	Focal and weak	1 (4.8%)
	Focal and moderate/strong	4 (19.1%)
	Diffuse	3 (14.3%)
Portal capillaries	Negative	16 (76.2%)
	Minimal	2 (9.5%)
	Focal and weak	0
	Focal and moderate/strong	3 (14.3%)
	Diffuse	0
Hepatic artery	Negative	13 (61.9%)
	Minimal	2 (9.5%)
	Focal and weak	0
	Focal and moderate/strong	5 (23.8%)
	Diffuse	1 (4.8%)
Portal stroma	Negative	6 (28.6%)
	Minimal	4 (19.1%)
	Focal and weak	2 (9.5%)
	Focal and moderate/strong	8 (38.1%)
	Diffuse	1 (4.8%)
Central veins	Negative	15 (71.4%)
	Minimal	4 (19.1%)
	Focal and weak	0
	Focal and moderate/strong	1 (4.8%)
	Diffuse	1 (4.8%)
Sinusoids	Negative	15 (71.4%)
	Minimal	3 (14.3%)
	Focal and weak	1 (4.8%)
	Focal and moderate/strong	1 (4.8%)
	Diffuse	1 (4.8%)

4.3.5 DSA and Histology (HE and reticulin)

Out of all the histological parameters assessed on HE and reticulin stained slides, only two parameters were significantly associated with the presence of

DSA/DSA II: bile duct loss and portal fibrosis. The presence of bile duct loss was strongly associated with DSA and with DSA II (p=0.003 and p=0.001,
Table 67 and Table 68, respectively). In fact, all 12 patients whose biopsies displayed bile duct loss had circulating class II DSA (all had anti-DQ isotype). One-quarter of them had concomitant class I DSA. Table 69 and Table 70 depict the DSA class and DSA subtype present in patients with bile duct loss.

Regarding fibrosis, the presence of portal fibrosis (≥2) was associated with circulating DSA II (p=0.031). The proportion of patients with and without DSA II who had portal fibrosis was 37% versus 6% respectively (Table 68). The remaining histological parameters assessed showed no significant association with DSA or DSA II. Figure 43 shows the proportion of patients with and without portal fibrosis who had circulating DSA II.

Table 67. **DSA and histological parameters (HE and reticulin)**

Parameter	DSA +	DSA -	p value
Portal fibrosis - Ishak (mean and range)	1.07 (0-4)	0.67 (0-5)	0.090
Portal fibrosis ≥2 (% and number)	34.5% (10/29)	6.7% (1/15)	0.067
CLF – Venturi (mean and range)	0.52 (0-3)	0.60 (0-3)	0.822
CLF present (% and number)	31% (9/29)	33.3% (5/15)	1.000
CLF ≥2 (% and number)	13.8% (4/29)	20% (3/15)	0.675
Sinusoidal fibrosis – Venturi (mean and range)	0.31 (0-3)	0.33 (0-3)	0.972
Sinusoidal fibrosis present (% and number)	20.7% (6/29)	20% (3/15)	1.000
Sinusoidal fibrosis ≥2 (% and number)	6.9% (2/29)	6.7% (1/15)	1.000
RAI (mean and range)	6.03 (3-9)	6.07 (3-9)	0.990
Portal Inflammation (mean and range)	1.9 (1-3)	2.0 (1-3)	0.722
Portal inflammation moderate-severe (% and number)	75.9% (22/29)	73.3% (11/15)	1.000

Portal inflammation severe (% and number)	17.2% (5/29)	26.7% (4/15)	0.464
Interface activity (mean and range)	1.0 (0-3)	1.33 (0-3)	0.369
Interface activity present (% and number)	69% (20/29)	73.3% (11/15)	1.000
Interface activity moderate-severe (% and number)	27.6% (8/29)	40% (6/15)	0.501
Portal vein endotheliitis (mean and range)	1.31 (1-3)	1.40 (1-3)	0.728
Portal vein endotheliitis present (% and number)	82.8% (24/29)	80% (12/15)	1.000
Portal vein endotheliitis moderate-severe (% and number)	41.4% (12/29)	46.7% (7/15)	0.759
CP (mean and range)	1.62 (0-3)	1.60 (0-3)	0.949
CP present (% and number)	79.3% (23/29)	80% (12/15)	1.000
CP moderate-severe (% and number)	58.6% (17/29)	53.3% (8/15)	0.759
Lobular inflammation (mean and range)	1.62 (1-3)	1.73 (1-3)	0.744
Lobular inflammation present (% and number)	100% (29/29)	100% (15/15)	-
Lobular inflammation moderate-severe (% and number)	51.7% (15/29)	53.3% (8/15)	1.000
Bile duct injury (mean and range)	2.24 (1-3)	2.13 (1-3)	0.630
Bile duct injury severe	41.4% (12/29)	33.3% (5/15)	0.748
Bile duct loss present (% and number)	41.4% (12/29)	0 (/15)	**0.003**
Canalicular cholestasis (mean and range)	0.72 (0-3)	0.67 (0-3)	0.978
Canalicular cholestasis present	44.8% (13/29)	46.7% (7/15)	1.000
Canalicular cholestasis ≥2	17.2% (5/29)	13.3% (2/15)	1.000
Ductular reaction present (% and number)	24.1% (7/29)	33.3% (5/15)	0.722

CLF, centrilobular fibrosis; RAI, rejection activity index

Table 68 (below). **DSA II and histological parameters (HE and reticulin)**

Parameter	DSA II +	DSA II -	p value
Portal fibrosis - Ishak (mean and range)	1.07 (0-4)	0.71 (0-5)	0.156

Portal fibrosis ≥2 (% and number)	37% (10/27)	5.9% (1/17)	**0.031**
CLF – Venturi (mean and range)	0.44 (0-3)	0.71 (0-3)	0.539
CLF present (% and number)	30% (8/27)	35% (6/17)	0.748
CLF ≥2 (% and number)	11.1% (3/27)	24% (4/17)	0.402
Sinusoidal fibrosis – Venturi (mean and range)	0.26 (0-3)	0.41 (0-3)	0.631
Sinusoidal fibrosis present (% and number)	19% (5/27)	24% (4/17)	0.716
Sinusoidal fibrosis ≥2 (% and number)	3.7% (1/27)	12% (2/17)	0.549
RAI (mean and range)	6 (3-9)	6.12 (3-9)	0.893
Portal Inflammation (mean and range)	1.9 (1-3)	2.0 (1-3)	0.689
Portal inflammation moderate-severe (% and number)	74% (20/27)	77% (13/17)	1.000
Portal inflammation severe (% and number)	19% (5/27)	24% (4/17)	0.726
Interface activity (mean and range)	1 (0-3)	1.29 (0-3)	0.396
Interface activity present (% and number)	67% (18/27)	76% (13/17)	0.735
Interface activity moderate-severe (% and number)	30% (8/27)	35% (6/17)	0.748
Portal vein endotheliitis (mean and range)	1.26 (0-3)	1.47 (0-3)	0.349
Portal vein endotheliitis present (% and number)	82% (22/27)	82% (14/17)	1.000
Portal vein endotheliitis moderate-severe (% and number)	3.7% (10/27)	53% (9/17)	0.359
CP (mean and range)	1.56 (0-3)	1.71 (0-3)	0.643
CP present (% and number)	78% (21/27)	82% (14/17)	1.000
CP moderate-severe (% and number)	59% (16/27)	52% (9/17)	0.760
Lobular inflammation (mean and range)	1.59 (1-3)	1.76 (1-3)	0.605
Lobular inflammation present (% and number)	100% (27/27)	100% (17/17)	-
Lobular inflammation moderate-severe (% and number)	52% (14/27)	53% (9/17)	1.000

Bile duct injury (mean and range)	2.26 (1-3)	2.12 (1-3)	0.482
Bile duct injury severe	44% (12/27)	29% (5/17)	0.360
Bile duct loss present (% and number)	44% (12/27)	0 (/17)	**0.001**
Canalicular cholestasis (mean and range)	0.74 (0-3)	0.65 (0-3)	0.947
Canalicular cholestasis present	44% (12/27)	47% (8/17)	1.000
Canalicular cholestasis ≥2	19% (5/27)	12% (2/17)	0.689
Ductular reaction present (% and number)	22% (6/27)	35% (6/17)	0.489

CLF, centrilobular fibrosis; RAI, rejection activity index

Table 69 (below). **DSA class in patients with bile duct loss**

DSA class	Number (%)
Class II only	9 (75%)
Class I and II	3 (25%)

Table 70 (below). **DSA subtype in patients with bile duct loss**

DSA subtype	Number (%)
DQ only	7 (58.3%)
DQ and DR	5 (41.7%)

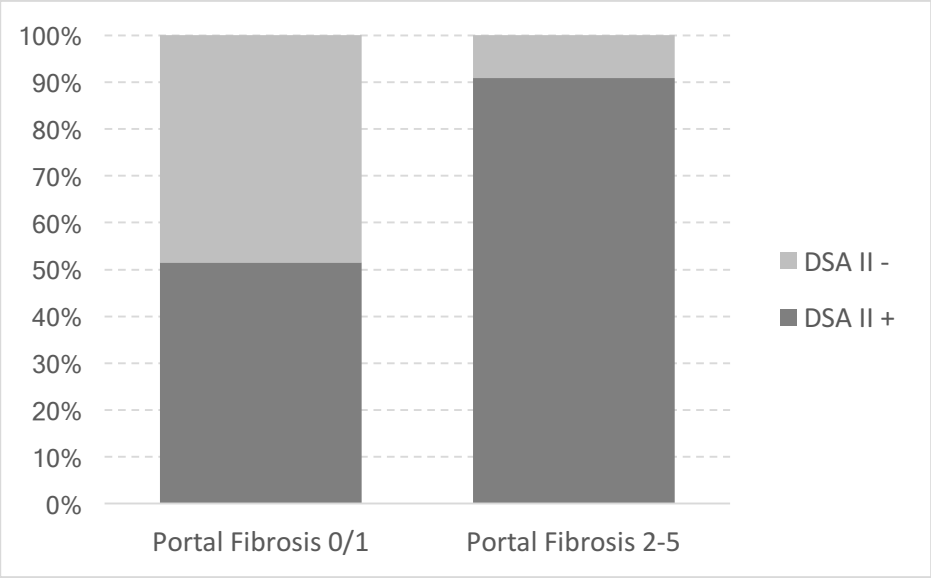

Figure 43 (above). **Portal fibrosis and DSA II** (p=0.031)

4.3.6 DSA and C4d immunohistochemistry

In this cohort, the presence of circulating DSA / DSA II was strongly associated with tissue C4d+ in portal microvascular endothelium and specifically in portal veins. The difference in proportions was even higher for DSA II than DSA overall (Table 71 and Table 72). Whereas 92% of patients with DSA II had C4d+ in portal microvascular endothelium, none of those without DSA II showed this positivity ($p<0.001$). Conversely, DSA II was present in all liver recipients with C4d deposition in portal endothelium versus just 10% without (Figure 44).

Although C4d positivity in other compartments was not significantly associated with DSA/DSA II, all patients with C4d positivity in any vascular compartment (including central vein and sinusoids) had circulating DSA (Table 71).

Table 71. **DSA and C4d positivity per compartment**

C4d+ in	DSA +	DSA -	P value
Portal microvascular endothelium	84.6% (11/13)	0 (/8)	**<0.001**
Portal vein	69.2% (9/13)	0 (/8)	**0.002**
Portal capillaries	27.1% (3/13)	0 (/8)	0.117
Hepatic artery	30.8% (4/13)	0 (/8)	0.096
Portal stroma	30.8% (4/13)	37.5% (3/8)	0.824
Central vein	15.4% (2/13)	0 (/8)	0.311
Sinusoids	15.4% (2/13)	0 (/8)	0.311
Any compartment	100% (13/13)	62.5% (5/8)	**0.031**

Table 72 (below). **DSA II and C4d positivity per compartment**

C4d+ in	DSA II +	DSA II -	P value
Portal microvascular endothelium	91.7% (11/12)	0 (/9)	**<0.001**
Portal vein	75% (9/12)	0 (/9)	**<0.001**
Portal capillaries	25% (3/12)	0 (/9)	0.133
Hepatic artery	33.3% (4/12)	0 (/9)	0.065
Portal stroma	33.3% (4/12)	33.3% (3/9)	0.860
Central vein	16.7% (2/12)	0 (/9)	0.260
Sinusoids	8.3% (1/12)	11.1% (1/9)	0.840
Any compartment	100% (12/12)	66.7% (6/9)	0.048

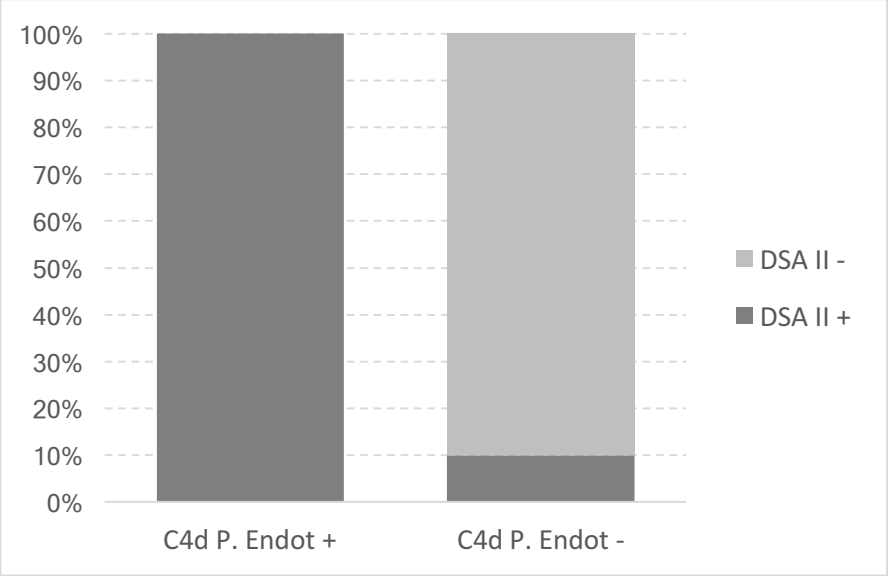

Figure 44 (above). **C4d+ in portal microvascular endothelium and DSA II** ($p<0.001$)

4.3.7 C4d and inflammation

Inflammation was present in all biopsies and inflammation scores were higher than in the protocol biopsy group (Chapter 3), as these patients had a diagnosis of rejection. For this reason, a threshold of 2 was deemed “significant” inflammation in each compartment (as opposed to 1 in Chapter 3).

Overall, inflammation in no individual compartment was statistically associated with C4d+. Despite being non-significant, patients with each interface or lobular inflammation (≥2) had higher proportions of C4d+ in most compartments, including portal vascular structures (Table 73). Biopsies with central perivenulitis also displayed a higher proportion of C4d+ in portal veins. Considering the degree of inflammation in each site as a continuous variable, patients with C4d+ in portal vascular structures also showed slightly higher scores of interface inflammation than those with negative C4d in these compartments (Table 74).

Table 73. **Frequency of C4d+ in each compartment versus inflammation in portal tracts, interface, lobule and central veins**

C4d+ in	Portal inflammation			Interface			Lobular inflammation			CP		
	≥2	0/1	p value	≥2	0/1	p value	≥2	0/1	p value	≥2	0/1	p value
Portal microvascular endothelium	53.8% (7/13)	50% (4/8)	1.000	63.6% (7/11)	40% (4/10)	0.395	61.5% (8/13)	37.5% (3/8)	0.387	57.1% (4/7)	50% (7/14)	1.000
Portal vein	46.2% (6/13)	37.5% (3/8)	1.000	54.5% (6/11)	30% (3/10)	0.387	53.9% (7/13)	25% (2/8)	0.367	57.1% (4/7)	35.7% (5/14)	0.397
Portal capillaries	15.4% (2/13)	12.5% (1/8)	1.000	18.2% (2/11)	10% (1/10)	1.000	15.4% (2/13)	12.5% (1/8)	1.000	14.3% (1/7)	14.3% (2/14)	1.000
Hepatic artery	23.1% (3/13)	12.5% (1/8)	1.000	27.3% (3/11)	10% (1/10)	0.586	23.1% (3/13)	12.5% (1/8)	1.000	14.3% (1/7)	21.4% (3/14)	1.000
Portal stroma	3.1% (4/13)	37.5% (3/8)	1.000	27.3% (3/11)	60% (6/10)	0.659	23.1% (3/13)	50% (4/8)	0.346	14.3% (1/7)	35.7% (5/14)	1.000
Central vein	15.4% (2/13)	0 (/8)	0.505	18.2% (2/11)	0 (/10)	0.476	15.4% (2/13)	0 (/8)	0.505	14.3% (1/7)	7.1% (1/14)	1.000
Sinusoids	15.4% (2/13)	0 (/8)	0.505	9.1% (1/11)	10% (1/10)	1.000	15.4% (2/13)	0 (/8)	0.505	14.3% (1/7)	7.1% (1/14)	1.000
Any compartment	84.6% (11/13)	87.5% (7/8)	1.000	81.8% (9/11)	90% (9/10)	1.000	84.6% (11/13)	87.5% (7/8)	1.000	85.7% (6/7)	85.7% (6/7)	1.000

Table 74. **Average degree of inflammation in each compartment versus C4d positivity or negativity in each site**

Inflammation grade per compartment (mean)	**Portal**			**Interface**			**Lobular**			**Central vein**		
C4d staining per compartment (+ or -)	**+**	**-**	p value	**+**	**-**	p value	**+**	**-**	p value	**+**	**-**	p value
Portal microvascular endothelium	1.9	1.9	0.912	1.4	1.1	0.650	1.8	1.9	0.940	1.0	1.3	0.481
Portal vein	2.0	1.8	0.737	1.4	1.1	0.516	1.9	1.8	0.762	1.1	1.2	0.765
Portal capillaries	2.0	1.9	0.673	1.3	1.2	0.914	1.7	1.9	0.707	1.0	1.2	0.711
Hepatic artery	2.5	1.8	0.158	1.5	1.2	0.665	1.8	1.9	0.848	1.0	1.2	0.777
Portal stroma	2.0	1.9	0.784	1.0	1.4	0.521	1.6	2.0	0.232	1.0	1.2	0.753
Central vein	2.5	1.5	0.345	2.0	1.16	0.367	2.0	1.8	0.701	1.5	1.1	0.753
Sinusoids	2.5	1.8	0.345	1.5	1.2	0.747	2.5	1.8	0.224	3.0	0.95	**0.032**
Any compartment	1.9	1.7	0.597	1.2	1.7	0.482	1.8	2.0	0.748	1.2	0.7	0.428

4.3.8 C4d and fibrosis

C4d+ in portal microvascular endothelium (p=0.024) and in portal veins (p=0.032) were significantly linked to portal fibrosis (≥2), as shown in Table 75. Whilst 88% of biopsies with portal fibrosis had C4d+ in portal microvascular endothelium, only 31% of those without fibrosis showed C4d deposition in this compartment. Centrilobular and sinusoidal fibrosis showed no significant association with C4d+ in any compartment.

Considering the degree of fibrosis in each compartment as a continuous variable, the mean/average degree of portal fibrosis was significantly higher in patients with C4d+ in portal microvascular endothelium (p=0.030, Table 76).

Table 75. **Frequency of C4d+ per compartment versus fibrosis in sinusoids, central veins and portal tracts**

C4d+ in	Sinusoidal fibrosis			Centrilobular fibrosis			Portal fibrosis		
	≥2	**0/1**	p value	**≥2**	**0/1**	p value	**≥2**	**0/1**	p value
Portal microvascular endothelium	33.3% (1/3)	55.6% (10/18)	0.586	20% (1/5)	62.5% (10/16)	0.149	87.5% (7/8)	30.8% (4/13)	**0.024**
Portal vein	33.3% (1/3)	44.4% (8/18)	1.000	20% (1/5)	50% (8/16)	0.338	75% (6/8)	23.1% (3/13)	**0.032**
Portal capillaries	0 (/3)	16.7% (3/18)	1.000	0 (/5)	18.8% (3/16)	0.549	12.5% (1/8)	15.4% (2/13)	1.000
Hepatic artery	0 (/3)	22.2% (4/18)	1.000	0 (/5)	25% (4/16)	0.532	37.5% (3/8)	7.7% (1/13)	0.253
Portal stroma	33.3% (1/3)	33.3% (6/18)	1.000	20% (1/5)	37.5% (6/16)	0.624	50% (4/8)	23.1% (3/13)	0.364
Central vein	0 (/3)	11.1% (2/18)	1.000	0 (/5)	12.5% (2/16)	1.000	0 (/8)	15.4% (2/13)	0.505
Sinusoids	33.3% (1/3)	5.6% (1/18)	0.271	20% (1/5)	6.3% (1/16)	0.429	0 (/8)	15.4% (2/13)	0.505
Any compartment	100% (3/3)	83.3% (15/18)	1.000	80% (4/5)	87.5% (14/16)	1.00	100% (8/8)	76.9%(10/13)	0.257

Table 76. **Average degree of fibrosis per compartment versus C4d positivity or negativity per site**

Fibrosis score per compartment (mean)	**Sinusoidal (Venturi)**			**Centrilobular (Venturi)**			**Portal (Ishak)**		
C4d staining per compartment (+ or -)	**+**	**-**	p value	**+**	**-**	p value	**+**	**-**	p value
Portal microvascular endothelium	0.5	0.6	0.825	0.6	1.1	0.489	1.8	1.0	**0.030**
Portal vein	0.6	0.5	0.755	0.7	1.0	0.587	1.8	1.2	0.088
Portal capillaries	0	0.6	0.256	0	1.0	0.100	1.0	1.5	0.637
Hepatic artery	0	0.7	0.177	0.3	1.0	0.241	1.8	1.4	0.350
Portal stroma	0.4	0.6	0.425	0.7	0.9	0.684	1.9	1.2	0.276
Central vein	0	0.6	0.366	0	1.0	0.191	0.5	1.5	0.235
Sinusoids	1.0	0.5	0.452	1.5	0.8	0.601	0.5	1.5	0.235
Any compartment	0.6	0.3	1.000	0.9	0.7	0.701	1.6	0.3	0.067

4.3.9 C4d and other histological parameters

The following parameters did not have a statistically significant association with C4d in any compartment scored: RAI, portal vein endotheliitis, bile duct lesion, bile duct loss, cholestasis and ductular reaction.

Despite not statistically significant, patients with bile duct loss had more than double the proportion of C4d+ in portal microvascular endothelium than those without bile duct loss: 83% versus 40% (p=0.149, Figure 45). The lack of statistical significance could be due to the tiny number of patients with bile duct loss who had C4d immunohistochemistry performed (only 6 patients).

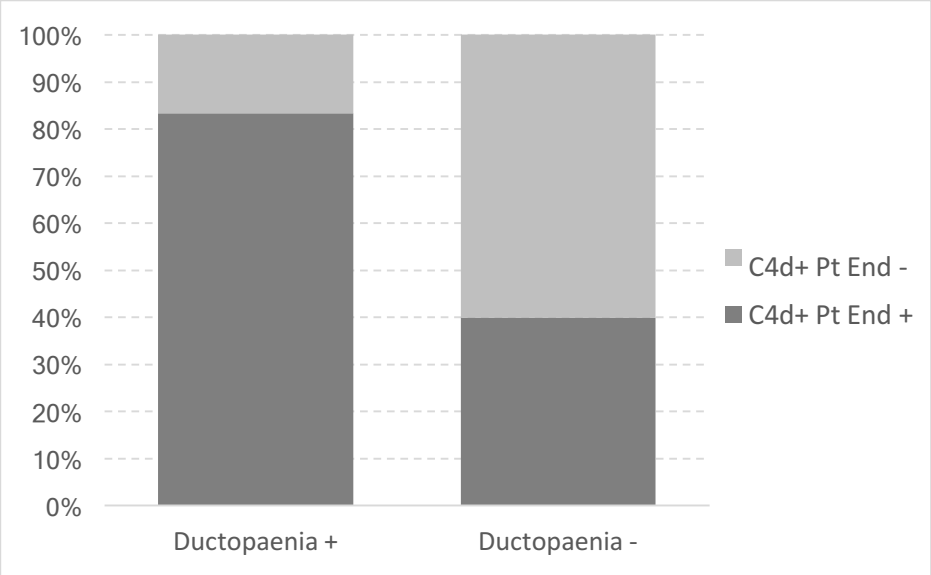

Figure 45. **Bile duct loss and C4d in portal microvascular endothelium** (p=0.149)

4.3.10 C4d with DSA and inflammation

There was no significant association between inflammation in any compartment and the combination of DSA+C4d+ or DSAII+C4d+, as shown in Table 77 and Table

78, respectively. Nonetheless, patients with interface and those with lobular inflammation had higher proportions of DSA/DSA II+C4d+ in portal vascular structures.

Table 77. **DSA + C4d+ and inflammation in portal tracts, interface, lobule and central veins**

DSA+C4d+ in	Portal Inflammation			Interface			Lobular Inflammation			Central perivenulitis		
	≥2	0/1	p value	≥2	0/1	p value	≥2	0/1	p value	≥2	0/1	p value
Portal microvascular endothelium	5.4% (7/13)	50% (4/8)	1.000	63.6% (7/11)	40% (4/10)	0.395	61.5% (8/13)	37.5% (3/8)	0.387	57.1% (4/7)	50% (7/14)	1.000
Portal vein	4.6% (6/13)	37.5% (3/8)	1.000	54.5% (6/11)	30% (3/10)	0.387	53.9% (7/13)	25% (2/8)	0.367	57.1% (4/7)	35.7% (5/14)	0.397
Portal capillaries	15.4% (2/13)	12.5% (1/8)	1.000	18.2% (2/11)	10% (1/10)	1.000	15.4% (2/13)	12.5% (1/8)	1.000	14.3% (1/7)	14.3% (2/14)	1.000
Hepatic artery	2.3% (3/13)	12.5% (1/8)	1.000	27.3% (3/11)	10% (1/10)	0.586	23.1% (3/13)	12.5% (1/8)	1.000	14.3% (1/7)	21.4% (3/14)	1.000
Portal stroma	15.4% (2/13)	25% (2/8)	0.618	18.2% (2/11)	20% (2/10)	1.000	15.4% (2/13)	25% (2/8)	0.618	14.3% (1/7)	21.4% (3/14)	1.000
Central vein	15.4% (2/13)	0 (/8)	0.505	18.2% (2/11)	0 (/10)	0.476	15.4% (2/13)	0 (/8)	0.505	14.3% (1/7)	7.1% (1/14)	1.000
Sinusoids	15.4% (2/13)	0 (/8)	0.505	9.1% (1/11)	10% (1/10)	1.000	15.4% (2/13)	0 (/8)	0.505	14.3% (1/7)	7.1% (1/14)	1.000
Any compartment	6.2% (8/13)	50% (4/8)	0.673	63.6% (7/11)	50% (5/10)	0.670	69.2% (9/13)	37.5% (3/8)	0.203	57.1% (4/7)	57.1% (8/14)	1.000

Table 78 (below). **DSA II + C4d+ and inflammation in portal tracts, interface, lobule and central veins**

DSA **II**+ C4d+ in	**Portal Inflammation**			**Interface**			**Lobular Inflammation**			**Central perivenulitis**		
	≥2	**0/1**	p value	**≥2**	**0/1**	p value	**≥2**	**0/1**	p value	**≥2**	**0/1**	p value
Portal microvascular endothelium	30.8% (4/13)	12.5% (1/8)	0.606	36.4% (4/11)	10% (1/10)	0.311	30.8% (4/13)	12.5% (1/8)	0.606	28.6% (2/7)	21.4% (3/14)	1.000
Portal vein	46.2% (6/13)	37.5% (3/8)	1.000	54.5% (6/11)	30% (3/10)	0.387	53.9% (7/13)	25% (2/8)	0.367	57.1% (4/7)	35.7% (5/14)	0.397
Portal capillaries	15.4% (2/13)	12.5% (1/8)	1.000	18.2% (2/11)	10% (1/10)	1.000	15.4% (2/13)	12.5% (1/8)	1.000	14.3% (1/7)	14.3% (2/14)	1.000
Hepatic artery	23.1% (3/13)	12.5% (1/8)	1.000	27.3% (3/11)	10% (1/10)	0.586	23.1% (3/13)	12.5% (1/8)	1.000	14.3% (1/7)	21.4% (3/14)	1.000
Portal stroma	15.4% (2/13)	25% (2/8)	0.618	18.2% (2/11)	20% (2/10)	1.000	15.4% (2/13)	25% (2/8)	0.618	14.3% (1/7)	21.4% (3/14)	1.000
Central vein	15.4% (2/13)	0 (/8)	0.505	18.2% (2/11)	0 (/10)	0.476	15.4% (2/13)	0 (/8)	0.505	14.3% (1/7)	7.1% (1/14)	1.000
Sinusoids	7.7% (1/13)	0 (/8)	1.000	9.1% (1/11)	0 (/10)	1.000	7.7% (1/13)	0 (/8)	1.000	14.3% (1/7)	0 (/14)	0.333
Any compartment	53.9% (7/13)	50% (4/8)	1.000	63.6% (7/11)	40% (4/10)	0.395	61.5% (8/13)	37.5% (3/8)	0.387	57.1% (4/7)	50% (7/14)	1.000

4.3.11 C4d with DSA and fibrosis

The combination of DSA/DSA II and C4d positivity in portal microvascular endothelium and specifically in portal veins was significantly associated with portal fibrosis. The frequency of DSA/DSA II+C4d+ in portal microvascular endothelium was 88% for patients with portal fibrosis versus 23% for those without fibrosis (p=0.024), as shown in Table 79 and Table 80. Fibrosis in other compartments was not linked to DSA/DSA II+C4d+.

Table 79. **DSA + C4d+ and fibrosis in sinusoids, central veins and portal tracts**

DSA + C4d+ in	Sinusoidal fibrosis			Centrilobular fibrosis			Portal fibrosis		
	≥2	**0/1**	p value	**≥2**	**0/1**	p value	**≥2**	**0/1**	p value
Portal microvascular endothelium	0 (/3)	27.8% (5/18)	0.549	0 (/5)	31.3% (5/16)	0.278	37.5% (3/8)	15.4% (2/13)	0.325
Portal vein	33.3% (1/3)	44.4% (8/18)	1.000	20% (1/5)	50% (8/16)	0.338	75% (6/8)	23.1% (3/13)	**0.032**
Portal capillaries	0 (/3)	16.7% (3/18)	1.000	0 (/5)	18.8% (3/16)	0.549	12.5% (1/8)	15.4% (2/13)	1.000
Hepatic artery	0 (/3)	22.2% (4/18)	1.000	0 (/5)	25% (4/16)	0.532	37.5% (3/8)	7.7% (1/13)	0.253
Portal stroma	0 (/3)	22.2% (4/18)	1.000	0 (/5)	25% (4/16)	0.532	37.5% (3/8)	7.7% (1/13)	0.253
Central vein	0 (/3)	11.1% (2/18)	1.000	0 (/5)	12.5% (2/16)	1.000	0 (/8)	15.4% (2/13)	0.505
Sinusoids	33.3% (1/3)	5.6% (1/18)	0.271	0 (/5)	6.3% (1/16)	0.429	0 (/8)	15.4% (2/13)	0.505
Any compartment	66.7% (2/3)	55.6%(10/18)	1.000	20% (1/5)	62.5%(10/16)	0.611	87.5% (7/8)	38.5% (5/13)	0.067

Table 80 (below). **DSA II + C4d+ and fibrosis in sinusoids, central veins and portal tracts**

DSA **II** + C4d+ in	**Sinusoidal fibrosis**			**Centrilobular fibrosis**			**Portal fibrosis**		
	≥2	**0/1**	p value	**≥2**	**0/1**	p value	**≥2**	**0/1**	p value
Portal microvascular endothelium	0 (/3)	27.8% (5/18)	0.549	0 (/5)	31.3% (5/16)	0.278	37.5% (3/8)	15.4% (2/13)	0.325
Portal vein	33.3% (1/3)	44.4% (8/18)	1.000	20% (1/5)	50% (8/16)	0.338	75% (6/8)	23.1% (3/13)	**0.032**
Portal capillaries	0 (/3)	16.7% (3/18)	1.000	0 (/5)	18.8% (3/16)	0.549	12.5% (1/8)	15.4% (2/13)	1.000
Hepatic artery	0 (/3)	22.2% (4/18)	1.000	0 (/5)	25% (4/16)	0.532	37.5% (3/8)	7.7% (1/13)	0.253
Portal stroma	0 (/3)	22.2% (4/18)	1.000	0 (/5)	25% (4/16)	0.532	37.5% (3/8)	7.7% (1/13)	0.253
Central vein	0 (/3)	11.1% (2/18)	1.000	0 (/5)	12.5% (2/16)	1.000	0 (/8)	15.4% (2/13)	0.505
Sinusoids	0 (/3)	5.6% (1/18)	1.000	0 (/5)	6.3% (1/16)	1.000	0 (/8)	7.7% (1/13)	1.000
Any compartment	33.3% (1/3)	55.6% (10/18)	0.586	20% (1/5)	62.5% (10/16)	0.149	87.5% (7/8)	30.8% (4/13)	**0.024**

The following parameters did not show significant association with DSA/DSA II+C4d positivity in any compartment: RAI, portal vein endotheliitis, bile duct lesion, bile duct loss, cholestasis and ductular reaction. Despite not statistically significant, patients with bile duct loss had more than double the proportion of DSA/DSA II+C4d+ in portal microvascular endothelium than those without bile duct loss (83% versus 40%, p=0.220). The lack of statistical significance of this last association could be due to the small number of patients with bile duct loss who had C4d staining performed (only 6 patients).

4.3.12 Criteria for acute AMR

The Banff study group on allograft pathology[53] considers a series of criteria to establish the diagnosis of acute AMR in liver allografts (Chapter 1). These consist of: compatible histology, circulating DSA, diffuse C4d in portal microvascular endothelium and reasonable exclusion of other possible aetiologies that might produce a similar pattern of liver injury.

In the current cohort of rejection biopsies, 21 patients could be assessed using the Banff criteria to diagnose acute AMR (these were the patients who had C4d immunostaining performed). Thirteen out of these 21 had circulating DSA, and 5 (24%) fulfilled all the criteria for definite acute/active AMR, including presence of DSA, diffuse portal microvascular C4d deposition and compatible histology. The Banff criteria for the diagnosis of acute AMR are specified in

Table 81 and the C4d-scored and h-score which are part of the criteria are detailed in

Table 82, both tables extracted from the 2016 Update of the Banff Working Group Report[53].

Table 81. **Banff criteria for diagnosing acute AMR in liver grafts**

Definite for acute/active1 AMR (all four criteria required): (1) Histopathological pattern of injury consistent with acute AMR, usually including the following: portal microvascular endothelial cell hypertrophy, portal capillary and inlet venule dilatation, monocytic, eosinophilic, and neutrophilic portal microvasculitis, portal edema, ductular reaction; cholestasis is usually present, but variable; edema and periportal hepatocyte necrosis are more common/prominent in ABO-incompatible grafts; variable active lymphocytic and/or necrotizing arteritis (2) Positive serum DSA (3) Diffuse (C4d score = 3) microvascular C4d deposition[1] on frozen or formalin-fixed, paraffin-embedded tissue in ABO-compatible tissues or portal stromal C4d deposition in ABO-incompatible grafts. (4) Reasonable exclusion of other insults[2] that might cause a similar pattern of injury (see text). Most cases will score (C4d-score: 3+ h-score = 5 or 6; see below).
Suspicious for AMR (both criteria required): (1) DSA is positive (see definitions). (2) Non-zero h-score with: C4d-score + h-score of 3 or 4.
Indeterminate for AMR (requires 1+2 and 3 or 4): (1) C4d-score + h-score is 2. (2) DSA not available, equivocal, or negative. (3) C4d staining not available, equivocal, or negative. (4) Co-existing insult might be contributing to the injury.

AMR, antibody-mediated rejection; DSA, donor-specific antibody.
[1]Optimized C4d staining including positive control is critical for proper evaluation.
[2]Thrombocytopenia, low serum complement levels, persistence of DSA early after transplantation, and elevated liver injury tests are usually present, but might not be prominent in mild cases.

Table 82. **C4d-score and h-(histopathology)-scoring for acute AMR**

C4d-(immune)-score (formalin-fixed, paraffin-embedded[1,2]):
(0) No C4d deposition in portal microvasculature
(1) Minimal (<10% portal tracts) C4d deposition in >50% of the circumference of portal microvascular endothelia (portal veins and capillaries)
(2) Focal (10–50% portal tracts) C4d deposition in >50% of the circumference of portal microvascular endothelia (portal veins and capillaries) - usually without extension into periportal sinusoids
(3) Diffuse (>50% portal tracts) C4d deposition in >50% of the circumference of portal microvascular endothelia (portal veins and capillaries)—often with extension into inlet venules or periportal sinusoids
h-(histopathology)-score[3,4,5]
(1) Portal microvascular endothelial cell enlargement (portal veins, capillaries, and inlet venules) involving a majority of portal tracts with sparse microvasculitis defined as three to four marginated and/or intraluminal monocytes, neutrophils, or eosinophils in the maximally involved capillary with generally mild dilation (Figure 1).
(2) Monocytic, eosinophilic, or neutrophilic microvasculitis/capillaritis, defined as at least 5–10 leukocytes marginated and/or intraluminal in the maximally involved capillary prominent portal and/or sinusoidal microvascular endothelial cell enlargement involving a majority of portal tracts or sinusoids, with variable but noticeable portal capillary and inlet venule dilatation and variable portal edema (Figure 2).
(3) As above, with marked capillary dilatation, marked microvascular inflammation (10 or more marginated and/or intraluminal leukocytes in the most severely affected vessels), at least focal microvascular disruption with fibrin deposition, and extravasation of red blood cells into the portal stroma and/or space of Disse (subsinusoidal space) (Figure 3).

AMR, antibody-mediated rejection; PAS, periodic acid-Schiff; RBC, red blood cells.
[1]Formalin-fixed, paraffin-embedded tissues are known to show weaker staining than fresh-frozen tissues, but interpretation of frozen tissues can be more difficult because of background/nonspecific staining and poor preservation of morphology. Sinusoidal staining should be localized to sinusoidal endothelial cells; false positive staining of connective tissue fibers can occur in livers with subsinusoidal fibrosis.
[2]Ideally the C4d positive control should be a liver graft, but peritubular capillary staining of a kidney graft is an acceptable alternative.
[3]Special stains that help identify capillaries, such as CD31, CD34, and/or PAS are often needed to help identify involved portal-based capillaries.
[4]Other features commonly seen, but not necessarily associated with severity include ductular reaction and cholestasis.
[5]Fibrin deposition and RBC sludging occurs earlier and is more common and prominent in ABO-incompatible grafts.

All five liver recipients with definite AMR had class II DSA (three also had class I) and all had DQ (three also had DR). The total sum of MFI in each of these patients was above 10,000, ranging from 13,441 to 54,626. The sum of MFI of class II DSA varied from 7,081 to 45,583.

Table 83 details clinical parameters of the 5 patients with definite AMR. The following figures show biopsy sections of one of the patients who had diagnosis of definite acute AMR.

Table 83. Clinical data of patients with definite AMR

	Patient 1	Patient 2	Patient 3	Patient 4	Patient 5
Age (years)	52	13	27	30	22
Indication for LT	Autoimmune hepatitis	Biliary atresia	Acute liver failure (drug induced)	Acute liver failure (drug induced)	Acute liver failure (drug induced)
Time post-transplant	12 days	5 years	3 years	10 days	5 years
Baseline immunosuppression	Tacrolimus	Cyclosporine + Mycophenolate	Tacrolimus	Tacrolimus	Tacrolimus + sirolimus
AST (IU/L, reference 10-50)	108	104	236	44	173
Bilirubin (μmol/L, reference 3-20)	247	13	311	241	18
AP (IU/L, reference 30-130)	377	417	263	488	169

GGT (IU/L, reference 1-55)	638	34	351	651	183
INR (ratio, reference 0.9-1.2)	2.21	1.05	1.33	1.28	0.97
DSA class	I and II	II	I and II	I and II	II
DSA type	A, DR, DQ	DQ	A, DQ	A, B, Cw, DQ, DR	DQ, DR
DSA I MFI	18854	-	6360	9043	-
DSA II MFI	18359	27328	7081	45583	24267
DSA total MFI	37213	27328	13441	54626	24267
Outcome	Good	Good	Poor - Graft failure for chronic rejection, and death	Good	Good

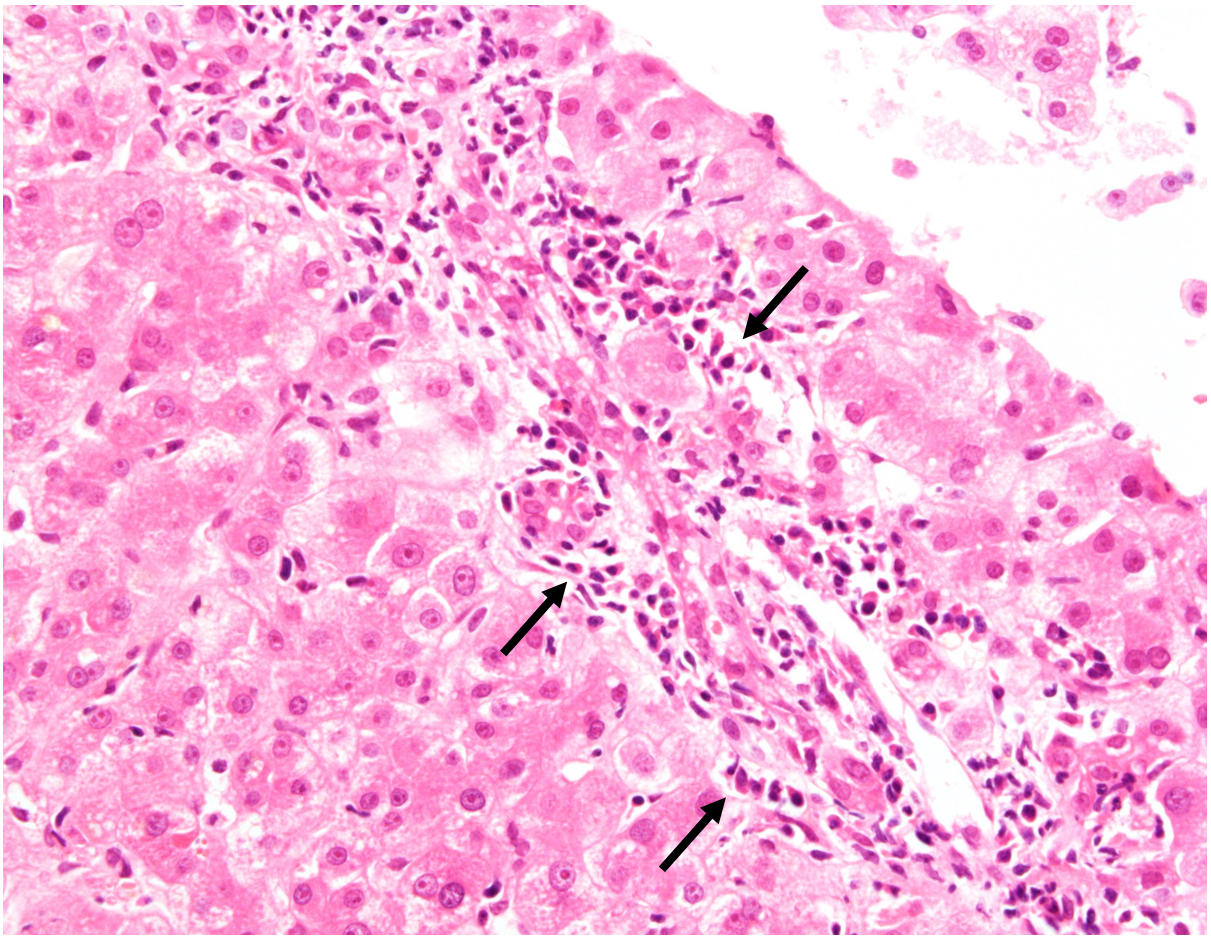

Figure 46. **Patient with diagnosis of acute AMR. Portal tract with mild/moderate inflammation and capillary dilatation with microvasculitis (intraluminal leukocytes, arrows)(HE, 400x)**

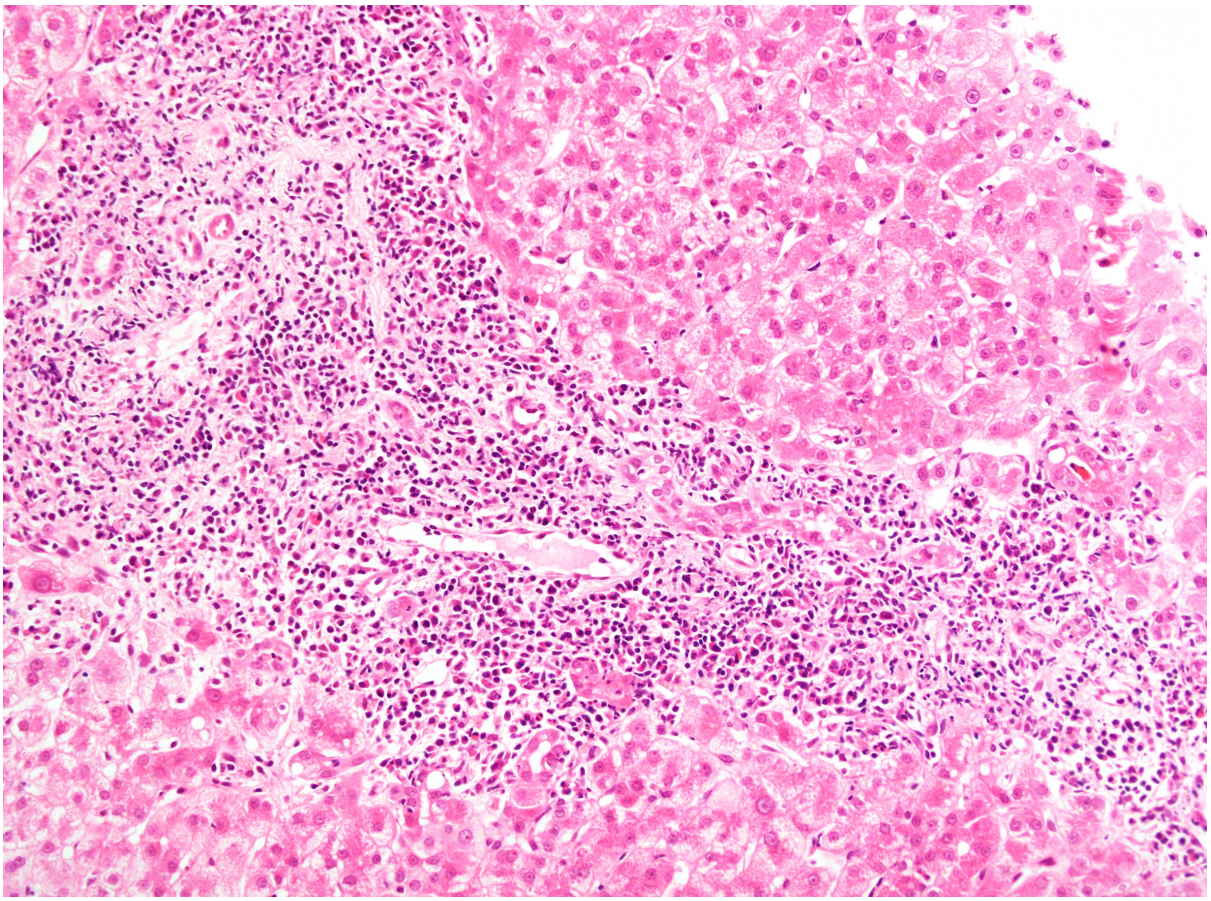

Figure 47. **Same biopsy as above, different area. Portal tract with oedema and severe inflammation (HE, 200x)**

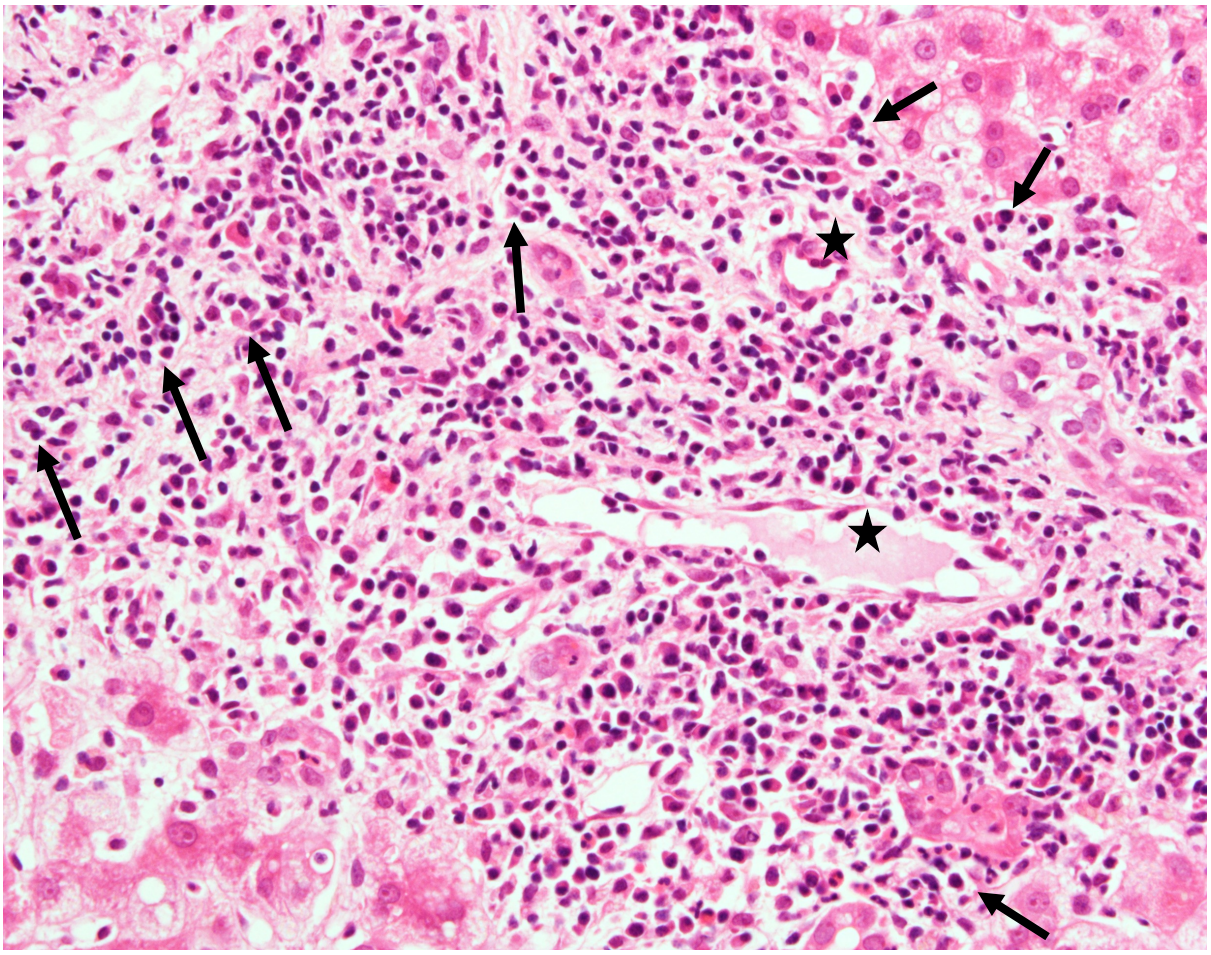

Figure 48. **Same portal tract as Figure 47, higher magnification. Dilated portal capillaries with numerous intraluminal leukocytes (arrows). Endothelial cell enlargement is also noticed (stars) (HE, 400x).**

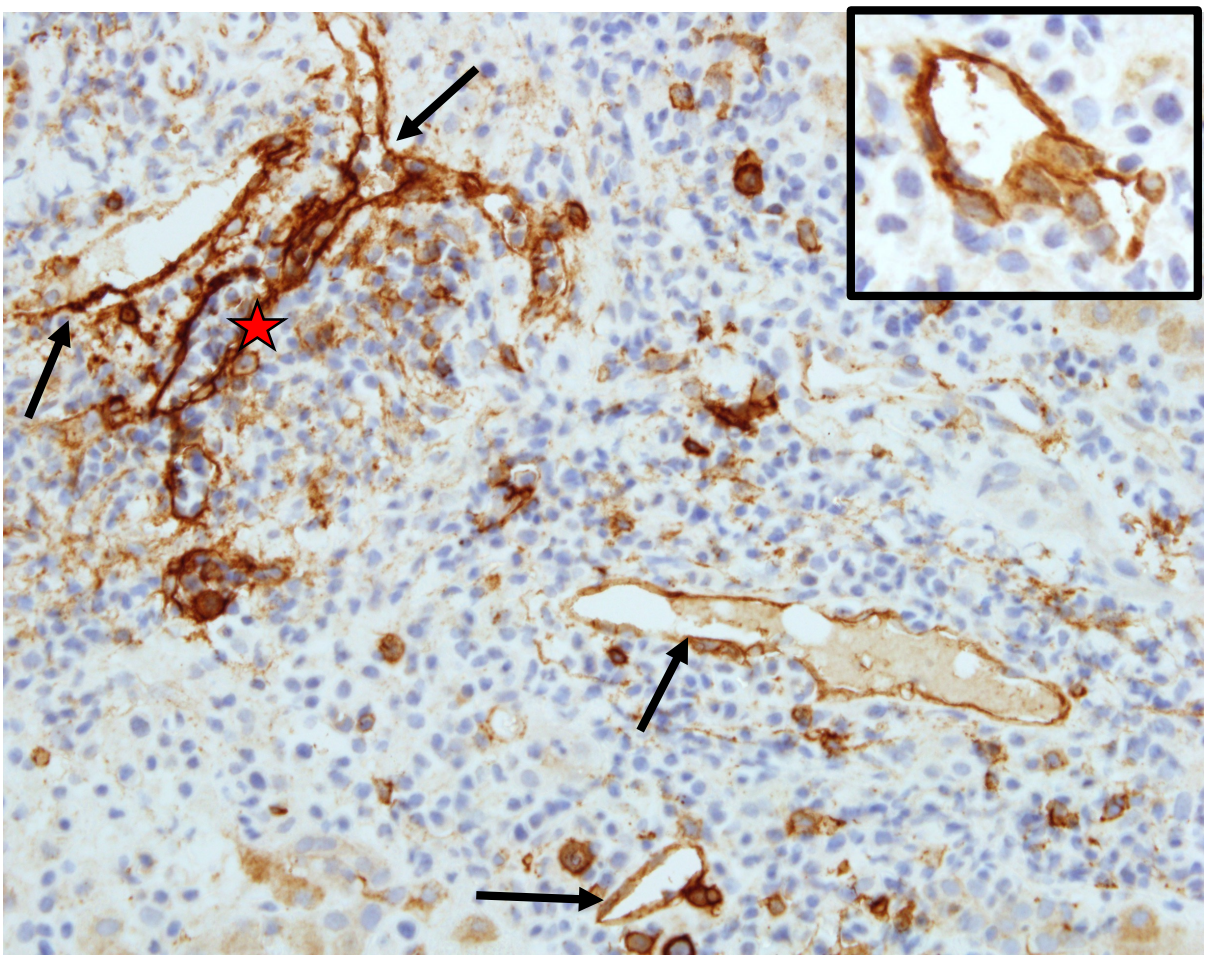

Figure 49. **Same portal tract as Figure 48, C4d immunostaining. Diffuse C4d positivity in portal microvascular endothelium (portal vein branches and portal capillaries, arrows). Intraluminal inflammatory cells can be visualised (star) (400x). The inset (top right) shows endothelial cell hypertrophy in a capillary in the same portal tract.**

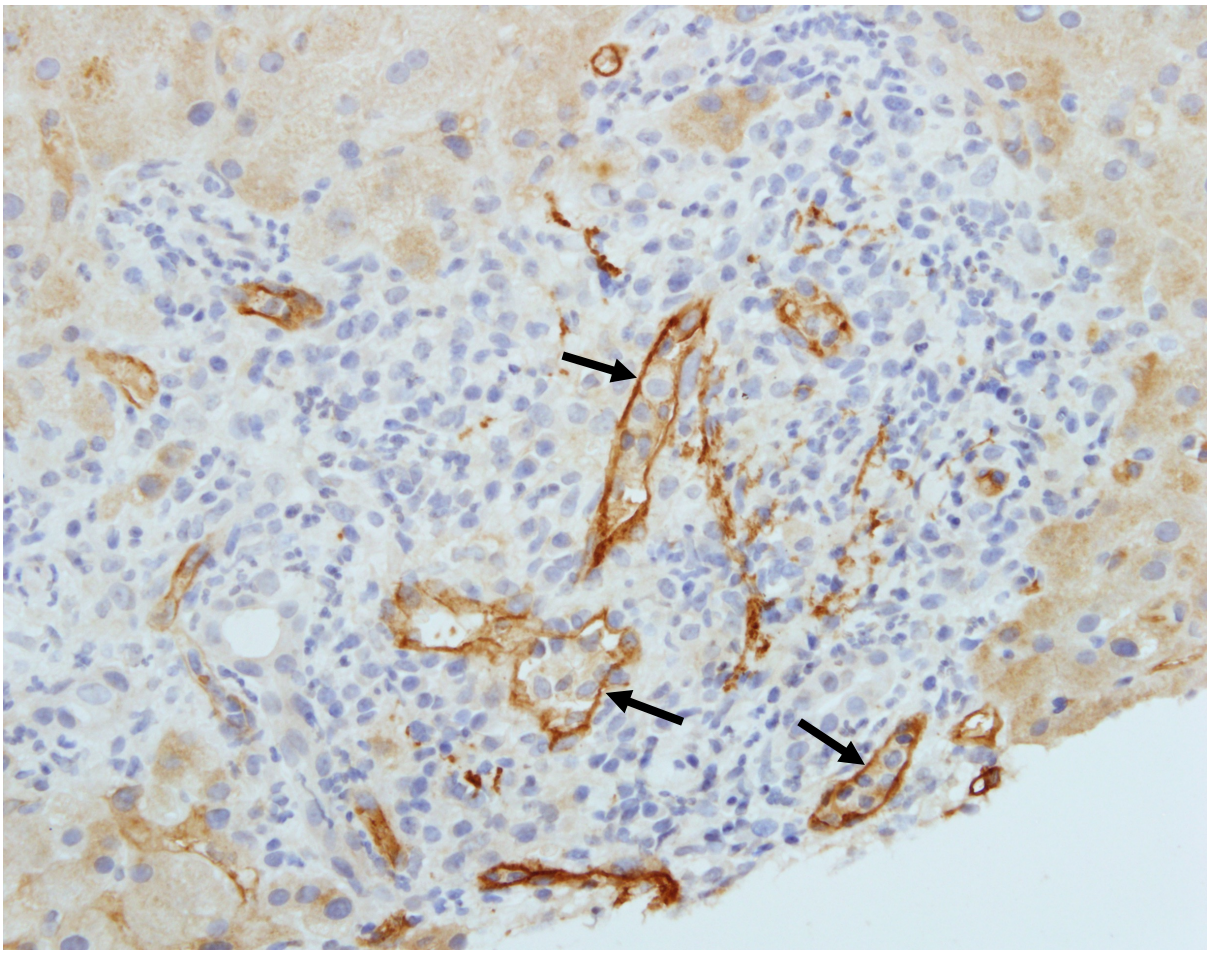

Figure 50. **Same biopsy section as Figure 49, different biopsy field. Diffuse microvascular C4d+. Vascular dilatation and intraluminal inflammatory cells are conspicuous (arrows) (C4d immunohistochemistry, 400x).**

4.3.13 Gene expression

Forty-two patients had enough tissue in their respective biopsy specimens for RNA analysis. Following the RNA sequencing and analysis of the gene expression patterns using the gene libraries (section 4.2.5, page 192), a comparison was made between patients with and without DSA as well as with or without DSA II. Analysis of gene expression and of inflammatory pathways known to be upregulated/activated in specific liver conditions, including TCMR and recurrent HCV, and in AMR in kidney allografts was conducted. Since gene expression patterns of AMR are still not

established for the liver allograft, as the diagnosis of AMR in liver itself has only recently been recognised, there are no libraries including gene signatures of AMR in the liver. In fact, recognising gene signatures linked to AMR in liver was the reason why the RNASeq was conducted in the present study. No significant difference was observed between the groups analysed (DSA+ versus DSA- and DSA II+ versus DSA II-) in terms of expression of genes or pathways.

It was not possible to compare patients with and without C4d+ or DSA+C4d+ since the number of liver recipients with C4d staining available was too small to generate significant results for the molecular analysis.

4.4 DISCUSSION

4.4.1 Overview

This chapter presented the study of 44 liver allograft biopsies with TCMR and DSA testing who had no evidence of recurrent disease. In the Results section above, the histological assessment, including HE and reticulin staining and C4d immunohistochemistry, and the correlation between histology, circulating DSA and gene expression were presented. In the current section, the findings are discussed in view of relevant up-to-date literature.

In terms of the histological assessment of HE and reticulin staining, a third (32%) of biopsies had fibrosis scoring ≥2 in one or more compartments analysed. A fourth had portal fibrosis (≥2), 16% showed centrilobular fibrosis (≥2) and 6.8%, sinusoidal fibrosis (≥2) (see

Table 65 and Figure 40 - Figure 42, page 203). This rate of fibrosis was almost half of that found in long-term paediatric protocol biopsies (Chapter 3), despite the greatly

shorter time post-transplant of the biopsies of the present cohort (median 5.5 months). Fibrosis was observed to be linked to a longer time from transplantation to biopsy, as expected, and it reflects some degree of ongoing graft injury or previous flares of acute injury, such as episodes of rejection.

It is important to consider that the histological analysis of portal fibrosis, especially when no bridging/fibrous septa is present (Ishak stages 1 and 2), is more difficult in biopsies with portal oedema, which is typical of acute rejection. Therefore, the diagnosis of portal fibrosis in this group is potentially less reliable than in the long-term protocol biopsies. Whereas liver fibrosis is well documented in post-transplant graft protocol biopsies, studies on acute rejection do not normally involve evaluation of fibrosis.

Another interesting finding in the present study cohort was the presence of bile duct loss in over a fourth of the biopsies. Bile duct loss was considered significant when more than 10% of portal tracts lacked bile ducts, and the residual interlobular ducts displayed obvious damage. This not unusual finding of bile duct loss denotes a severe nature to the rejection episode, which is progressing towards CR. Since the bile duct loss in all but one patient involved <50% of bile ducts, it could be potentially reversible through appropriate changes in immunosuppression. In fact, most patients (55%) who showed bile duct loss on histology did have good outcome (allograft preservation) during follow-up. Musat *et al*.[90] found a comparable rate of bile duct loss in for cause biopsies of patients with TCMR, 21%.

Compared to the protocol biopsy study group, the for-cause biopsies with rejection showed less fibrosis and more inflammation in all compartments assessed, as shown in Table 84. The biopsies with rejection also had higher proportion of bile duct lesion, canalicular cholestasis and bile duct loss. This higher degree of

inflammation and bile duct injury was expected, since these biopsies were diagnosed as rejection (which requires inflammation and bile duct injury). In contrast, the protocol biopsies belonged to asymptomatic recipients with normal or nearly normal LFTs.

Table 84**. Overall biopsy assessment (HE and reticulin staining) of two study groups: protocol biopsies and for cause biopsies with rejection**

Histological parameters	Paediatric protocol biopsies	For cause biopsies with rejection
Portal Inflammation		
Absent	46.2%	2.3%
Mild (grade 1)	42.3%	23%
Moderate (grade 2)	11.5%	55%
Severe (grade 3)	0	21%
Interface activity		
Absent	82.7%	30%
Mild (grade 1)	15.4%	39%
Moderate (grade 2)	1.9%	23%
Severe (grade 3)	0	9.1%
Lobular inflammation		
Absent	55.8%	0
Minimal (grade 1)	36.5%	46%
Moderate (grade 2)	7.7%	43%
Severe (grade 3)	0	11%
CP		
Absent	73.1%	21%

Mild (grade 1)	19.2%	21%
Moderate (grade 2)	7.7%	36%
Severe (grade 3)	0	23%
Bile duct lesion		
Absent	88.5%	0
Minimal (grade 1)	11.5%	18%
Moderate (grade 2)	0	43%
Marked (grade 3)	0	39%
Bile duct loss		
Absent	100%	73%
Present <50%	0	25%
Present >50%	0	2.3%
Portal vein endotheliitis		
Absent	100%	14%
Mild (grade 1)	0	43%
Moderate (grade 2)	0	39%
Marked (grade 3)	0	4.5%
Ductular reaction		
Absent	78.9%	73%
Present	21.1%	27%
Hepatocanalicular cholestasis		
Absent	98.1%	55%
Focal	1.9%	30%
Diffuse centrilobular	0	6.8%
Diffuse centrilobular and midzonal	0	9.1%
Steatosis		
< 5% of hepatocytes	94.2%	100%

5-33% of hepatocytes (grade 1) 33-66% of hepatocytes (grade 2) > 66% of hepatocytes (grade 3)	5.8% 0 0	0 0 0
Portal fibrosis (Ishak) Stage 0/1 Stage 2 Stage 3 Stage 4 Stage 5	 44.2% 15.4% 25% 11.5% 3.8%	 75% 18% 2.3% 2.3% 2.3%
Centrilobular fibrosis (Venturi): Stage 0 Stage 1 Stage 2 Stage 3	 32.7% 28.8% 26.9% 11.5%	 68% 16% 9.1% 6.8%
Sinusoidal fibrosis (Venturi): Stage 0 Stage 1 Stage 2 Stage 3	 40.4% 44.2% 9.6% 5.8%	 80% 14% 2.3% 4.5%

On C4d immunohistochemistry, over half of the patients showed positivity in portal microvascular endothelium (portal veins and/or portal capillaries). Overall, incidence of positive C4d staining in the present for-cause cohort was substantially higher than in the previous protocol biopsy group, in which only 28% of patients had

C4d staining in portal microvascular endothelium. Table 85 shows a comparison of the frequency of C4d positivity per compartment in each of the two study groups.

Table 85. **C4d staining per compartment in two study groups: protocol biopsies and for cause biopsies with rejection**

C4d+ in	Paediatric protocol biopsies	For cause biopsies with rejection
Portal endothelium	28%	52.4%
Portal vein	16%	38.1%
Portal capillaries	16%	14.3%
Hepatic artery	10%	28.6%
Portal stroma	18%	52.4%
Central vein	4%	9.6%
Sinusoids	2%	14.4%
Any compartment	34%	85.7%

The higher frequency of C4d positivity observed in biopsies with acute rejection in comparison to long-term protocol biopsies is consistent with previous research reporting lower sensitivity of C4d staining in the context of chronic graft injury/chronic AMR[53,97-98]. The shorter storage time of the paraffin blocks in the current study group biopsies can also have influenced the frequency of C4d positivity[98]. Finally, acute AMR frequently occurs in combination with TCMR, which will be further discussed.

4.4.2 DSA

DSA were present in almost two-thirds of patients in this cohort, and 93.1% of these had class II DSA. High prevalence of DSA was expected in this group, in

which DSA test was clinically indicated, thus AMR was suspected (prior to or after the biopsy result). Compared to the previous study group (protocol biopsies), the patients with rejection had a slightly lower prevalence of circulating DSA: 66% versus 71%. The higher proportion of DSA in children undergoing protocol biopsy might be related to the longer time between transplantation and biopsy in that group. Another reason for the higher prevalence of DSA in the protocol biopsy group could be the patients' age: all patients in that cohort were children at transplantation, whereas in the rejection group, both children and adults were included. As to DSA class, the frequency of class II DSA was similar in both cohorts: 64.7% and 62.1% in the protocol and rejection groups, respectively. In both cohorts, class II was the most prevalent type of DSA, as shown in Table 86.

Table 86. **DSA in two study groups: protocol biopsies and for cause biopsies with rejection**

DSA in	Paediatric protocol biopsies	For cause biopsies with rejection
Class II only	52.9%	43.9%
Class I and II	11.8%	18.2%
Class I only	5.9%	4.5%
No DSA	29.4%	34.1%

Previous studies showed an association between both pretransplant and *de novo* DSA and higher risk of developing acute rejection[90,207]. Conversely, previous episodes of acute rejection seem to be the main predictor for the development of *de novo* DSA post-liver transplant[57,218]. A likely explanation is that continued or recurrent

tissue injury secondary to rejection leads to alloantigen exposure, causing upregulation of expression of HLA molecules and resulting in the production of DSA[57].

More class II than class I DSA were present, and in particular anti-DQ, in both protocol and for cause cohorts. This is consistent with previous publications showing that anti-HLA II of DQ subtype is the most frequent *de novo* DSA in the liver allograft[83,95]. The high rate of DSA against DQ might be due to the higher polymorphism of the genes encoding DQ antigens, which happens for α chain as well as for the β[85] (Chapter 1). Del Bello *et al*.[202] found that class II DSA accounted for 92% of post-transplant DSA in adult liver recipients, and 73% of them were against DQ. In another series, 95% of liver recipients developed class II DSA, with 85% against DQ isotype[84]. In yet another series, 92% of DSA were towards class II HLA and over two-thirds of these (70%) were directed to DQ[207].

As to DSA and clinical parameters, a strong association was found between DSA II >10,000 MFI and younger recipient age (p=0.007, Figure 38 on page 201). Most patients (56%) with DSA II above that threshold were children, in comparison to only 16% of those with lower or no DSA II (Table 64 on page 201). In the protocol biopsy group, patients with circulating DSA II were younger at transplantation and this was close to statistical significance (p=0.052). In both cohorts, DSA were not associated with the time from transplantation to biopsy. Other authors have also found younger liver recipient age to be related to post-transplant DSA II[52,199-204] (Chapter 3). Despite the frequency of this association, the physiological mechanisms that make younger patients more prone to develop *de novo* DSA is not understood.

There was a relationship between circulating antibodies and histology: DSA II were associated with each portal fibrosis, bile duct loss and C4d deposition, particularly in portal microvascular endothelium. Patients with DSA II had higher

proportion of portal fibrosis (≥2) than those without (p=0.031, Table 68 on page 210) and vice-versa (Figure 43). Higher prevalence of fibrosis in recipients with circulating DSA, particularly class II DSA, has been repeatedly reported[28,50,95,198,200,205-207].

This association between fibrosis and DSA has been mostly observed in protocol or long-term post-transplant biopsies, and suggests that antibody-mediated mechanisms play a role in the process of unexplained graft fibrosis. In recent study of adult liver recipients by Vandevoorde *et al.*[207], DSA were associated with portal fibrosis (and with TCMR) at 1-year after LT.

Another interesting finding in the present study was the strong statistical association between circulating DSA II and bile duct loss (p=0.001). In fact, bile duct loss was exclusively found in patients with circulating class II DSA (Table 68 on page 210). In the 80's and 90's, studies reported an association between preformed antibodies against donor HLA and the development of CR in the liver allograft[219-221]. These studies did not consider *de novo* DSA, and the method used for antibody detection (cell-based cytotoxic assays) was limited compared to current solid-phase immunoassays. However, the mechanism of bile duct destruction proposed then is still valid in the present context. More recently, other authors have corroborated the association between DSA and ductopenia/chronic rejection[75,79,90,222-223].

The liver graft has classically been considered to be greatly spared from the pathogenic effects of preformed HLA antibodies, for reasons previously stated (Chapter 1 and Figure 1 on page 171). Currently, it is known that whereas the hepatic parenchyma is notably protected from humoral damage, the biliary tree works in a similar way to kidney and heart allografts, due to its purely arterial circulation and its arteriolar and capillary network. As a consequence, sustained antibody-mediated injury to the arterioles and peribiliary plexus can potentially lead to bile duct loss[221].

The pathogenic cascade of antibody-mediated injury starts with the binding of DSA to endothelial cells in the portal microvasculature. This triggers complement activation, leading to destruction of the portal microvascular endothelium, including the arteries from which the periductal vascular plexus arises. The consequence is bile duct ischemia and subsequent loss[90,221]. Morphometric studies in human liver allografts have confirmed that the destruction of the portal microvasculature (including peribiliary small vessels) precedes bile duct destruction in CR. These findings support the role of antibody-mediated damage and of ischemia in chronic rejection[224-225].

On the other hand, in a retrospective study of 268 successive liver transplants, Muro *et al.*[226] did not find difference in the frequency of CR between liver recipients with positive and negative crossmatch. However, the authors only considered preformed antibodies, not *de novo* DSA. As mentioned in Chapter 1, most preformed anti-HLA antibodies disappear from the recipient's circulation after liver transplantation[57,222]. Grabhorn *et al.*[227] observed that all DSA present in liver recipients with CR were in fact *de novo* DSA. O'Leary *et al.*[67] found an association between high MFI DSA and CR, and suggested that AMR can manifest as CR. For DSA subtype, all 12 liver recipients with bile duct loss in the current series had anti-DQ DSA (Table 70). Wosniak *et al.*[52] found DQ DSA specifically to be strongly associated with late TCMR and with CR.

Interestingly, in the failed allografts cohort (Chapter 2), despite its decrease over the years as a cause of retransplantation, CR still accounted for over 10% of allograft losses in both adult and paediatric liver recipients in the most recent era. Considering the link between bile duct loss and antibody-mediated injury, it is possible that tacrolimus prevents the development of CR resulting from pure TCMR or from TCMR associated with mild forms of AMR, but it might not be able to treat more severe

cases of AMR. Therefore, the allograft failures due to CR at present might be a consequence of active AMR rather than an evolution of pure TCMR.

Strong statistical association was also found between the presence of DSA II and C4d staining in each vascular compartment, the strongest being portal microvascular endothelium and portal veins ($p<0.001$). The proportion of patients with and without portal vascular C4d+ who had DSA II was 100% versus 10%, respectively (Figure 44 on page 215). Thus, C4d was a highly specific (exclusively present in patients with DSA II) and reasonably sensitive indicator of the presence of circulating DSA in the present cohort. The consistency of the results means that the protocol for C4d immunohistochemistry employed in this research has potential to be applied to clinical practice.

Although in the protocol biopsy cohort (Chapter 3) C4d was not significantly associated with DSA, C4d+ in portal veins was only present in patients with these circulating antibodies (Table 37 on page 141). The lack of statistical association is likely due to a combination of limited sample size (only 34 patients with DSA data) and the low occurrence of C4d positivity in that population, due to the lower sensitivity of this staining in the chronic setting and to longer tissue storage times.

4.4.3 C4d and DSA combined with C4d

Regarding the link between C4d and other histological parameters, I observed that patients with C4d positivity in portal microvascular endothelium had a significantly higher proportion of portal fibrosis. They also had higher frequency of interface and lobular inflammation, but these were not significant.

Portal fibrosis was not only linked to DSA II, but also to C4d+ in portal microvasculature ($p=0.024$, Table 75 on page 219) and to the combination of

DSA+C4d+. Considering the latter, patients with portal fibrosis (≥2) showed significantly higher proportion of DSA+C4d+ in portal microvascular endothelium (88% versus 23%, p=0.024, Table 79, page 226). Considering its association with DSA and C4d individually and in combination, the presence of portal fibrosis in biopsies with rejection should be viewed as a warning sign of ongoing antibody-mediated damage. Thus, unexplained fibrosis in both long-term post-transplant and acute rejection settings might be a sign of AMR[96,183].

Although not significant, patients with interface and lobular inflammation ≥2 showed higher proportion of C4d+ in portal microvascular endothelium and of DSA+C4d+ in this compartment. Recipients with central perivenulitis also displayed higher frequency of C4d+ in portal veins and of DSA+C4d+ in the same location (Table 77 on page 223). A link between DSA+C4d+ in portal microvascular endothelium and each interface and central perivenulitis was also observed in the protocol biopsy cohort (Table 43 on page 149).

Currently, interface is included in the histological criteria of chronic AMR but not of acute AMR in the liver allograft[53]. Since acute AMR often occurs in combination with TCMR, some of the criteria traditionally considered to be features of TCMR might be in fact related to the antibody-mediated component[58,59,228]. Therefore, the presence of moderate/severe interface in biopsies with rejection should be regarded with particular attention as a possible marker of concomitant AMR. In Musat's series, 54% of patients with TCMR also showed signs of simultaneous humoral rejection (characterised as DSA with diffuse C4d staining).

Interestingly, whilst in the protocol biopsies central perivenulitis was associated with DSA+C4d+ (and with C4d+) in portal microvascular endothelium, in the current group of rejection biopsies, central perivenulitis was not significantly associated with

any parameter of humoral activation: DSA, C4d or their combination. Nevertheless, patients with central perivenulitis ≥2 showed considerably higher proportion of C4d+ in portal veins and of DSA+C4d+ in the same site (Table 73 and Table 77 on pages 216 and 223, respectively). Based on the current results and considering the limited size of the present cohort (21 patients with C4d data), it is not possible to confirm or refute an association between central perivenulitis and AMR in the context of rejection.

Furthermore, patients with lobular inflammation ≥2 had more than double the proportion of C4d+ and of DSA+C4d+ in portal veins than those with no/grade 1 lobular inflammation (53.9% versus 25%), although this difference was not significant (Table 73 and Table 77 on pages 216 and 223, respectively). Even though not significant, this higher proportion of C4d+/DSA+C4d+ in patients with more prominent lobular inflammatory activity is consistent with the findings of the protocol biopsy group, in which lobular inflammation was significantly linked to DSA and C4d+ individually.

In regard to bile duct loss, the frequency of DSA+C4d+ in portal microvascular endothelium in patients with bile duct loss was more than double that of patients with preserved number of bile ducts (83.3% versus 40%), although not statistically significant (p=0.220). This lack of significance is probably due to the tiny number of patients with bile duct loss who had C4d immunohistochemistry performed (6 patients only). Five (83.3%) of these 6 recipients had both circulating DSA (class II in all) and C4d+ (at least focal) in portal vascular endothelium. The other patient had circulating class II DSA but no C4d deposition in any compartment. Combined to the strong association I found between bile duct loss and DSA, these findings support the hypothesis that bile duct loss in the context of rejection is likely consequence of AMR.

Other authors have found C4d deposition in 8-57.9% and 17-100% of liver allograft biopsies with acute and CR, respectively[141,229-231]. This wide range is

consistent with the diversity of C4d immunostaining methods. In a study by Musat *et al.*[90] of for cause liver allograft biopsies with rejection, all patients with bile duct loss had both DSA and diffuse tissue C4d staining. In the current study, overall only 3 patients showed diffuse C4d staining: thus, the current C4d staining seems to be less sensitive than that of the mentioned study. Nevertheless, considering focal (as opposed to only diffuse) C4d deposition as positive, the C4d immunohistochemistry in the current study showed good statistical links with several relevant histological parameters, as aforementioned.

Considering the current Banff diagnostic criteria for acute AMR[53], five of the 21 patients for which C4d was available (24%) fulfilled all conditions for definite acute AMR: circulating DSA, diffuse endothelial C4d deposition, compatible histology and no other injury that could justify the histological findings. This is a significant proportion of patients previously diagnosed with purely TCMR. Of note, 3 out of the 5 patients with definite AMR had their biopsies performed years after transplantation. This contrasts with the classical reports of acute AMR, which typically occur in the early post-transplant period (within weeks).

4.4.4 Summary

In the current analysis of post-transplant biopsies with rejection, C4d positivity in portal microvascular endothelium was a highly specific and sensitive indicator of the presence of DSA II (present in 92% of patients with DSA II and in none of the patients without, $p<0.001$). Portal fibrosis (≥) was associated with antibody-mediated injury, as it was significantly linked to C4d+ and circulating DSA, both separately and in

combination. Bile duct loss was also strongly linked with DSA, and was present exclusively in patients with circulating class II DSA.

Furthermore, patients with more severe interface and lobular activity also showed higher rates of C4d+ and DSA+C4d+ in portal microvascular endothelium, which could indicate a potential link with AMR, but due to the lack of statistical significance of these associations, this is simply a speculation. Similarly, an association between central perivenulitis and humoral activation in the present context could not be confirmed (as it was in the protocol biopsy cohort). A fourth of patients with TCMR also fulfilled the Banff criteria for definite acute AMR.

These findings showed that, in the context of TCMR, C4d is a good marker of AMR and a specific indicator of circulating DSA and that portal fibrosis and bile duct loss should be regarded as potentially linked to AMR. This is consistent with the hypothesis that some findings classically considered to be part of the T cell-mediated rejection spectrum might be the consequence of an overlapping antibody-mediated component.

In comparison, in paediatric long-term protocol biopsies, the sensitivity of C4d staining was very low. Although not significant, in that context, C4d+ in portal veins was exclusively found in patients with DSA. Additionally, C4d+ was associated with higher numbers of B cells and plasma cells. In the same group, sinusoidal fibrosis, interface, central perivenulitis and lobular inflammation were related to AMR (the first 3 parameters were linked to DSA+C4d+, and lobular inflammation was associated with DSA and C4d separately).

In for cause biopsies with rejection, essentially the portal features (and perhaps lobular inflammation) were associated with AMR. In contrast, in the protocol biopsies, injury of the central/lobular region also showed significant links with potential chronic

AMR, including sinusoidal and centrilobular fibrosis, central perivenulitis and lobular inflammation.

In the RNA sequencing analysis, no difference in the expression of genes related to known pathological conditions of the liver was observed between patients with and without DSA or class II DSA. Due to the relatively small number of patients who had C4d staining performed, it was not possible to compare gene signatures in patients with and without C4d+ or DSA+C4d+. It is important to stress that gene expression patterns were evaluated by comparing the patterns from samples with recognized pathologies of the liver graft, such as recurrent HCV, AIH and TCMR. Since TCMR often occurs intertwined with AMR, it is possible that some of the gene signatures which are currently considered to be markers of the former could actually also include the latter. This could explain the lack of differentiation of patients with and without DSA in the molecular level.

The results highlight the role of histological analysis, since a detailed microscopic assessment of biopsies with basic staining to evaluate liver structures, inflammation and fibrosis, combined to C4d immunohistochemistry, could greatly help in recognising cases of AMR. In this assessment, the technical aspects of C4d staining should be considered. Particular attention should be given to the recognition of histological findings considered in the Banff diagnostic criteria of acute AMR, some of which are not routinely scored by liver pathologists (such as microvasculitis). Biopsies with TCMR should also be assessed for the presence of concomitant AMR. In particular, the presence of bile duct loss in the context of rejection should always raise the possibility of antibody-mediated injury and prompt to tissue C4d staining and possibly blood DSA testing.

5 CONCLUSION

The current work consisted of a histopathological study of liver allografts, with particular emphasis on idiopathic post-transplant chronic hepatitis (IPTH) and antibody-mediated injury. Three groups corresponding to three distinct post-transplantation settings were analysed: failed allografts removed at retransplantation; long-term protocol biopsies of asymptomatic paediatric liver recipients, and for cause biopsies with a diagnosis of TCMR.

In Chapter 2 (Failed Liver Allografts), a histological review of 460 explanted liver allografts through almost three decades showed a steady increase in the proportion of allograft loss for IPTH associated with fibrosis. In the last era, IPTH with fibrosis represented the main cause for late retransplantation in children and the second cause in adults (following recurrent disease). The results of Chapter 3, the protocol biopsy cohort, suggest that this pattern of idiopathic chronic hepatitis and fibrosis is a slowly-progressing form of rejection with an antibody-mediated component.

The findings from the explanted allografts motivated analysis of protocol biopsies in the search of similar histological injury at an earlier stage after transplantation, asymptomatic liver recipients with normal/nearly normal liver function tests and with the advantage of being able to perform DSA test. In this series of protocol biopsies, evidence was found to support the hypothesis that unexplained inflammation (especially interface activity, central perivenulitis and lobular inflammation) and fibrosis in sinusoids and/or centrilobular areas probably result from chronic AMR. Of note, the presence of AMR does not exclude a concomitant component of (late) TCMR.

Interestingly, in the context of allograft failure leading to retransplantation, three fourths of paediatric recipients who lost their graft because of IPTH associated with fibrosis had former biopsies showing central perivenulitis. Centrilobular fibrosis was also previously detected in over half of them (58%). As no obvious reason had been found to justify the inflammation, it is possible that such central-based injuries resulted from AMR.

In the protocol biopsy paediatric cohort, fibrosis in each location was significantly associated with higher numbers of plasma cells (and portal fibrosis also with more B cells), but not T cells. This provides an additional indication of the involvement of antibody-mediated mechanisms in the development of fibrosis.

Specific association between B cells (and plasma cells) and fibrosis was confirmed. This association had been previously described in mouse models and in other human organs, but not in the liver. Furthermore, B lymphocytes in the liver allograft were found to express granzyme B. To the best of current knowledge, this finding has not been reported in human liver, and could represent a potential local role of B cells involved in the development and progression of fibrosis. This would mean that the functions of B cells extend beyond antibody-mediated immunity.

The digital measurement of fibrosis through CPA did not add useful information compared to the conventional assessment of fibrosis in three compartments (portal, centrilobular and sinusoidal) in the context of protocol biopsies. Nonetheless, previous studies support the role of CPA measurement in other settings, such as predicting decompensation in patients with post-transplant recurrent HCV[44-45,233-234].

In the protocol biopsy group, C4d+ in portal microvascular endothelium (portal veins and portal capillaries) was associated with a humoral inflammatory profile (B cells and plasma cells). Although the tissue injury in this setting is not enough to cause

significant abnormality in liver enzymes and liver function tests, it might cause irreversible allograft changes such as advanced-stage fibrosis, and eventually allograft failure. Routine protocol biopsy is currently the only reliable way to diagnosis significant allograft injury in paediatric liver recipients.

In the third study cohort, a possible role for humoral-mediated injury was investigated in the context of clinically evident allograft dysfunction, in biopsies with cellular rejection. C4d positivity in portal microvascular endothelium and specifically in portal veins was a reliable and specific indicator of the presence of DSA II. Moreover, bile duct loss was strongly associated with DSA (only present in patients with these antibodies). Portal fibrosis was strongly linked to C4d+ and to DSA+C4d+ in portal microvascular endothelium.

These observations demonstrate that the portal tract is a target of AMR in the setting of acute TCMR. It also shows that histological parameters frequently interpreted as consequence of ongoing TCMR, such as bile duct loss and portal fibrosis, might be also linked to AMR. Thus, the pathologist should always have in mind the possibility of AMR when establishing a diagnosis of TCMR, especially in severe episodes of rejection or those that do not respond to steroid treatment; otherwise, the diagnosis of concurrent AMR will likely be overlooked.

Interface and lobular inflammation were also potentially but not significantly associated with C4d+ and DSA+C4d+ in the rejection cohort. In the protocol biopsy group, interface and lobular inflammation were respectively linked to DSA+C4d+ and to DSA and C4d+ separately. Thus, these two compartments should be carefully assessed for inflammation, since they might indicate antibody-mediated injury in both acute rejection and long-term protocol biopsy settings. Other aetiologies for the liver insult should be excluded before the diagnosis of AMR is established. Because portal

fibrosis results of long-standing or repeated/successive injuries, the link between portal fibrosis and DSA+C4d+ in the context of acute allograft dysfunction could reflect an ongoing injury with a humoral component prior to the rejection episode.

In both biopsy cohorts, C4d+ in portal veins was exclusively present in patients with circulating DSA (100% specificity). In the for cause biopsy group, C4d+ in portal microvascular endothelium was also a specific indicator of the presence of DSA II (92% of patients with DSA II had C4d+ in this location versus none of the patients without these antibodies, $p<0.001$).

In view of the low sensitivity of C4d staining in chronic post-transplant FFPE biopsies, the possibility of AMR should not be discarded in cases with minimal or absent C4d staining, even though a definite diagnosis cannot be made. Considering the current Banff criteria for chronic active AMR, over a fourth (26%) of paediatric protocol biopsies in the present research were diagnosed as either probable or possible AMR. Over the next years, as the histological parameters for the diagnosis of chronic AMR are refined and more extensively validated, it might be possible to confirm cases of chronic AMR despite negative C4d staining. AMR with negative C4d staining has been recognised in other allografts, such as kidney[72].

Considering the Banff criteria for acute AMR, a definite diagnosis of AMR could be made retrospectively in almost a fourth of patients formerly diagnosed with cellular rejection. This emphasizes the importance of looking for signs of AMR after a diagnosis of TCMR is established.

In the acute rejection cohort, all patients who showed bile duct loss had circulating class II DSA ($p=0.001$). Patients with bile duct loss also showed more than double the proportion of C4d+ and of DSA+C4d+ in the portal microvascular endothelium, but this was not statistically significant, probably due to the very small

number of the sample (only 6 patients with bile duct loss had C4d staining performed). In the failed allografts cohort, for both adults and children, chronic rejection (CR) accounted for over 10% of allograft loss in the most recent era, despite its decrease through the years, particularly after the introduction of tacrolimus. Considering the link between bile duct loss and DSA (and possibly DSA+C4d+), and the recognised role of microvascular endothelial damage in the destruction of bile ducts in CR, it is possible that the use of tacrolimus efficiently prevents the development of CR resulting from pure TCMR or from TCMR associated with mild AMR. Tacrolimus however, might not be capable of treating more severe forms of AMR. This is consistent with previous evidence that therapeutic agents targeting the cellular component of immunity might efficiently treat less severe cases of AMR.

The close link between both TCMR and AMR is progressively becoming more evident. The fact that T cell-mediated injury might indirectly increase antibody-production through upregulation of antigen expression in the liver allograft further corroborates this association. Therefore, at present, the finding of bile duct loss/CR in liver allografts might indicate AMR or combined T-cell and antibody-mediated rejection, rather than an evolution of pure TCMR.

Liver pathologists should consider the diagnosis of AMR when bile duct loss becomes evident in liver allograft biopsy. Interestingly, this parameter is not included in the Banff diagnostic criteria of AMR. C4d staining should be recommended in all cases of bile duct loss as it is a simple and relatively inexpensive test that might add valuable information. DSA testing should be considered, since results might lead to a change in therapeutic strategy if a diagnosis of AMR is confirmed.

The RNASeq found no association between the presence of circulating DSA/DSA II and particular patterns of gene expression. However, the genes analysed

in the samples were evaluated in comparison to previously recognized pathologies of the liver allograft, such as recurrent HCV and TCMR, and to AMR in kidney allografts (since specific gene expression patterns of AMR are still not known in the liver allograft). Because AMR often occurs intertwined with TCMR, it is possible that some of the gene signatures which are currently considered to be markers of TCMR could also include an antibody-mediated component of rejection. In Londoño *et al.* recent study on adult liver 10-year protocol biopsies[138], subclinical inflammation (particularly in portal tracts and interface) and portal fibrosis were associated with gene expression profiles of TCMR. In fact, the patients who had the highest expression levels of these genes developed progressive graft fibrosis. Thus, it is possible that these gene signatures considered as TCMR include AMR.

Considering the present research limitations, the impossibility of having DSA data for the failed allografts group, together with the retrospective nature of the study, restricted further interpretation of the histology. Additionally, because many of the allograft losses happened before the use of electronic patient records, it was not possible to retrieve clinical information to correlate with histology, such as the specific immunosuppression regime for each patient. Another limitation in this first cohort was that only the allografts that were removed at retransplantation were studied, when some recipients whose allografts failed died without undergoing retransplantation.

The study of paediatric protocol biopsies was limited by several factors, such as its retrospective nature, the small number of patients who had a protocol biopsy performed compared to the size of King's transplantation programme, the impossibility of testing for DSA in over a third of the patients, the absence of adult recipients in the cohort and the lack of clinical data for some patients, especially at the time of transplantation (such as initial immunosuppression regime).

In terms of the histology, many of the liver recipients in the protocol biopsy group did not have previous biopsies for comparison, which could enable a temporal correlation of histological findings. Numerous patients only had a previous biopsy in the first-year post-transplant and no other histological assessment until the “10-year” protocol biopsy. The time at which the long-term protocol biopsy was performed also showed considerable variation (from 8.6 to 15.6 years), which made the cohort less homogeneous. Furthermore, multiplex staining revealed itself to be technically challenging, both with Qdots and immunofluorescence. It is not easily performed and reproducible and might not be applicable to diagnostic clinical practice. However, considerable experience was gained and some success was achieved, which can certainly help in the development of useful research protocols.

Similarly, in the rejection cohort, the retrospective nature of the analysis was a limiting factor. Another important limitation is that only patients who had been previously tested for DSA were selected. This means that AMR was considered at some point in these patients, either before or after the biopsy findings or after poor response to treatment, so the proportion of AMR was certainly higher in the study series when compared to all liver recipients with an episode of TCMR.

Technical issues resulting in unavailability of a continued supply of C4d antibody limited the number of biopsies that were stained for C4d. This narrowed the number of significant associations that could be established between C4d+ and/or DSA+C4d+ and other clinical and histological parameters. For instance, patients with bile duct loss were noted to have double the frequency of C4d+ compared to those without, but there were only 6 patients with bile duct loss who had C4d staining performed, and this link was not statistically significant. The lack of C4d data for many patients also limited the diagnosis of definite AMR, since C4d+ is one of the mandatory

diagnostic criteria for this condition. The choice of C4d antibody was made based on a multicentre study of C4d performance on FFPE liver allograft tissue.

In summary, IPTH has been an increasingly significant cause of allograft loss in recent years. Supporting evidence was found for the role of chronic AMR in the development of active graft injury, including inflammation and fibrosis in different compartments, frequently present in protocol biopsies of asymptomatic children with normal/mildly abnormal liver biochemistry. Concurrent AMR was also present in episodes of TCMR, and the finding of bile duct loss was associated with DSA. Despite not being included in the criteria for acute or chronic AMR, this histological finding should be considered as a potential sign of humoral injury.

C4d positivity in immunohistochemistry of FFPE biopsies was a good marker of antibody-mediated tissue injury and strongly associated with DSA in rejection setting. Although sensitivity in the (long-term) protocol biopsies (older samples) was low, when positive, C4d was specifically associated with plasma cells and B cells. C4d positivity in portal veins was restricted to patients with DSA in both biopsy series.

The histological criteria for chronic AMR are in need of further consideration. In order to better understand and characterise AMR in the liver graft, prospective multicentre studies that correlate detailed histological findings, tissue C4d, circulating DSA and outcome of the graft are necessary. This correlation might help overcome the limitations of C4d staining in this context.

Future research is also needed to better comprehend the relationship between B cells and fibrosis. The expression of granzyme B by B cells (and perhaps plasma cells) also needs to be better characterized in liver grafts, and the significance of such expression clarified. In particular, studies with live B cells obtained by liver recipients could provide useful information in this direction.

Further progress in multiplex staining with protocols optimization could also enable a more detailed characterization of coexisting cell populations and the analysis of the relationships among different cells and between such cells and the liver compartments. This could add a considerable and relevant amount of information to the diagnosis of liver injuries. Besides quantification, more complex data analysis can be performed, such as studying the locations and relationships between cells. This complex examination, however, brings a new challenge, how to analyse vast amounts of data. This requires knowledge about the physiology of the cells studied and of experience with image analysis software, and is greatly time consuming.

The analysis of specific inflammatory cell populations could be useful in a variety of settings. In immunosuppression withdrawal studies, for instance, it could help to identify patients who are likely to be tolerant or to develop rejection at an earlier stage, before liver biochemistry or conventional histological analysis can detect abnormalities. Further studies correlating gene expression through RNA sequencing and histology could also help to find gene signatures of conditions such as AMR and tolerance.

6 REFERENCES

1. Starzl TE, Marchioro TL, Vonkaulla KN, Hermann G, Brittain RS, Waddell WR. Homotransplantation of the liver in humans. Surg Gynecol Obstet. 1963;117:659-76. Available from: https://www.ncbi.nlm.nih.gov/pmc/articles/PMC2634660/
2. Hübscher SG, Clouston AD. Transplantation pathology. In: Burt AD, Portmann BC, Ferrell LD, editors. MacSween's pathology of the liver. 6th ed. London:Churchill Livingstone Elsevier; 2012.
3. Marroni CA, Fleck AM, Jr., Fernandes SA, Galant LH, Mucenic M, de Mattos Meine MH, et al. Liver transplantation and alcoholic liver disease: history, controversies, and considerations. World J Gastroenterol. 2018;24(26):2785-805.
4. Lai JC. Defining the threshold for too sick for transplant. Curr Opin Organ Transplant. 2016:127-32. Available from: doi: 10.1097/MOT.0000000000000286
5. Otto G. Liver transplantation: an appraisal of the present situation. Dig Dis. 2013:164-9. Available from: doi: 10.1159/000347213
6. Fox AN, Brown RS, Jr. Is the patient a candidate for liver transplantation? Clin Liver Dis. 2012:435-48. Available from: doi: 10.1016/j.cld.2012.03.014
7. Statistics and Clinical Studies, NHS Blood and Transplant. Organ donation and transplantation. Activity report 2017/18. [Internet]. 2018. Available from: https://nhsbtdbe.blob.core.windows.net/umbraco-assets/1848/transplant-activity-report-2017-2018.pdf
8. Dawwas MF, Gimson AE, Lewsey JD, Copley LP, van der Meulen JH. Survival after liver transplantation in the United Kingdom and Ireland compared with the United States. Gut. 2007:1606-13. Available from: doi: 10.1136/gut.2006.111369
9. Barber K, Blackwell J, Collett D, Neuberger J, UK Transplant Liver Advisory Group. Life expectancy of adult liver allograft recipients in the UK. Gut. 2007;56:279-82. Available from: doi: 10.1136/gut.2006.093195
10. Durand F. How to improve long-term outcome after liver transplantation? Liver Int. 2018;38 Suppl 1:134-8. Available from: doi: 10.1111/liv.13651
11. McCaughan GW, Shackel NA, Strasser SI, Dilworth P, Tang P, Australian and New Zealand Liver Transplant Study Group. Minimal but significant improvement in survival for non-hepatitis C-related adult liver transplant patients beyond the one-year posttransplant mark. Liver Transpl. 2010;16:130-7. Available from: doi: 10.1002/lt.21978
12. Demetris AJ, Bellamy CO, Gandhi CR, Prost S, Nakanuma Y, Stolz DB. Functional immune anatomy of the liver-as an allograft. Am J Transplant. 2016;16:1653-80. Available from: doi: 10.1111/ajt.137y9
13. Mells G, Mann C, Hübscher S, Neuberger J. Late protocol liver biopsies in the liver allograft: a neglected investigation? Liver Transpl. 2009;15:931-8. Available from: doi: 10.1002/lt.21781
14. Ekong UD, Melin-Aldana H, Seshadri R, Lokar J, Harris D, Whitington PF, et al. Graft histology characteristics in long-term survivors of pediatric liver transplantation. Liver Transpl. 2008;14:1582-7. Available from: doi: 10.1002/lt.21549

15. Duclos-Vallee JC, Sebagh M, Rifai K, Johanet C, Ballot E, Guettier C, et al. A 10 year follow up study of patients transplanted for autoimmune hepatitis: histological recurrence precedes clinical and biochemical recurrence. Gut. 2003;52(6):893-7.
16. Isse K, Grama K, Abbott IM, Lesniak A, Lunz JG, Lee WM, et al. Adding value to liver (and allograft) biopsy evaluation using a combination of multiplex quantum dot immunostaining, high-resolution whole-slide digital imaging, and automated image analysis. Clin Liver Dis. 2010;14:669-85. Available from: doi: 10.1016/j.cld.2010.07.004
17. Shetty S, Adams DH, Hübscher SG. Post-transplant liver biopsy and the immune response: lessons for the clinician. Expert Rev Clin Immunol. 2012;8:645-61. Available from: doi: 10.1586/eci.12.65
18. Syn WK, Nightingale P, Gunson B, Hübscher SG, Neuberger JM. Natural history of unexplained chronic hepatitis after liver transplantation. Liver Transpl. 2007;13:984-9. Available from: doi: 10.1002/lt.21108
19. Hübscher S. What does the long-term liver allograft look like for the pediatric recipient? Liver Transpl. 2009;15 Suppl 2:S19-24. Available from: doi: 10.1002/lt.21902
20. Shaikh OS, Demetris AJ. Idiopathic posttransplantation hepatitis? Liver Transpl. 2007;13:943-6. Available from: doi: 10.1002/lt.21202
21. Neil DA, Hübscher SG. Current views on rejection pathology in liver transplantation. Transpl Int. 2010;23:971-83. Available from: doi: 10.1111/j.1432-2277.2010.01143.x
22. Dattani N, Baker A, Quaglia A, Melendez HV, Rela M, Heaton N. Clinical and histological outcomes following living-related liver transplantation in children. Clin Res Hepatol Gastroenterol. 2014;38:164-71. Available from: doi: 10.1016/j.clinre.2013.10.009
23. Evans HM, Kelly DA, McKiernan PJ, Hübscher S. Progressive histological damage in liver allografts following pediatric liver transplantation. Hepatology. 2006;43:1109-17. Available from: doi: 10.1002/hep.21152
24. Banff Working Group, Demetris AJ, Adeyi O, Bellamy CO, Clouston A, Charlotte F, et al. Liver biopsy interpretation for causes of late liver allograft dysfunction. Hepatology. 2006;44:489-501. Available from: doi: 10.1002/hep.21280
25. Suriawinata AA, Thung SN. Transplant liver disorders. In: Suriawinata AA, Thung SN, editors. Liver pathology: an atlas and concise guide. 1st ed. New York: Demos Medical; 2011. p. 125-56.
26. Seyam M, Neuberger JM, Gunson BK, Hübscher SG. Cirrhosis after orthotopic liver transplantation in the absence of primary disease recurrence. Liver Transpl. 2007;13:966-74. Available from: doi: 10.1002/lt.21060
27. Sundaram SS, Melin-Aldana H, Neighbors K, Alonso EM. Histologic characteristics of late cellular rejection, significance of centrilobular injury, and long-term outcome in pediatric liver transplant recipients. Liver Transpl. 2006;12:58-64. Available from: doi: 10.1002/lt.20661
28. Miyagawa-Hayashino A, Yoshizawa A, Uchida Y, Egawa H, Yurugi K, Masuda S, et al. Progressive graft fibrosis and donor-specific human leukocyte antigen antibodies in pediatric late liver allografts. Liver Transpl. 2012;18:1333-42. Available from: doi: 10.1002/lt.23534
29. Scheenstra R, Peeters PM, Verkade HJ, Gouw AS. Graft fibrosis after pediatric liver transplantation: ten years of follow-up. Hepatology. 2009;49:880-6. Available from: doi: 10.1002/hep.22686
30. Tomita H, Hoshino K, Fuchimoto Y, Ebinuma H, Ohkuma K, Tanami Y, et al. Acoustic radiation force impulse imaging for assessing graft fibrosis after pediatric living donor liver

transplantation: a pilot study. Liver Transpl. 2013;19:1202-13. Available from: doi: 10.1002/lt.23708
31. Briem-Richter A, Ganschow R, Sornsakrin M, Brinkert F, Schirmer J, Schaefer H, et al. Liver allograft pathology in healthy pediatric liver transplant recipients. Pediatr Transpl. 2013;17:543-9. Available from: doi: 10.1111/petr.12119
32. Bataller R, Brenner DA. Liver fibrosis. J Clin Invest. 2005;115:209-18. Available from: doi: 10.1172/JCI200524282
33. Crawford JM, Burt AD. Anatomy, pathophysiology and basic mechanisms of disease. In: Burt AF, L.; Portmann, B. , editors. MacSween's Pathology of the Liver. 6th ed. London: Churchill Livingstone Elsevier; 2012. p. 49-51.
34. Wallace K, Burt AD, Wright MC. Liver fibrosis. Biochem J. 2008;411:1-18. Available from: doi: 10.1042/BJ20071570
35. Brenner DA. Molecular pathogenesis of liver fibrosis. Trans Am Clin Climatol Assoc. 2009;120:361-8.
36. Bedossa P, Poynard T. An algorithm for the grading of activity in chronic hepatitis C. The METAVIR Cooperative Study Group. Hepatology. 1996;24:289-93. Available from: doi: 10.1002/hep.510240201
37. Ishak K, Baptista A, Bianchi L, Callea F, De Groote J, Gudat F, et al. Histological grading and staging of chronic hepatitis. J Hepatol. 1995;22(6):696-9.
38. Poynard T, Bedossa P, Opolon P. Natural history of liver fibrosis progression in patients with chronic hepatitis C. The OBSVIRC, METAVIR, CLINIVIR, and DOSVIRC groups. Lancet. 1997;349(9055):825-32.
39. Venturi C, Reding R. Long-term liver allograft fibrosis in children: more questions than answers. Pediatr Transplant. 2011;15:449-50. Available from: doi: 10.1111/j.1399-3046.2011.01511.x
40. Fouquet V, Alves A, Branchereau S, Grabar S, Debray D, Jacquemin E, et al. Long-term outcome of pediatric liver transplantation for biliary atresia: a 10-year follow-up in a single center. Liver Transpl. 2005;11:152-60. Available from: doi: 10.1002/lt.20358
41. Yamada H, Kondou H, Kimura T, Ikeda K, Tachibana M, Hasegawa Y, et al. Humoral immunity is involved in the development of pericentral fibrosis after pediatric live donor liver transplantation. Pediatr Transplant. 2012;16:858-65. Available from: doi: 10.1111/j.1399-3046.2012.01781.x
42. Venturi C, Sempoux C, Bueno J, Ferreres Pinas JC, Bourdeaux C, Abarca-Quinones J, et al. Novel histologic scoring system for long-term allograft fibrosis after liver transplantation in children. Am J Transplant. 2012;12:2986-96. Available from: doi: 10.1111/j.1600-6143.2012.04210.x
43. Pavlides M, Birks J, Fryer E, Delaney D, Sarania N, Banerjee R, et al. Interobserver variability in histologic evaluation of liver fibrosis using categorical and quantitative scores. Am J Clin Pathol. 2017;147:364-9. Available from: doi: 10.1093/ajcp/aqx011
44. Calvaruso V, Di Marco V, Bavetta MG, Cabibi D, Conte E, Bronte F, et al. Quantification of fibrosis by CPA predicts hepatic decompensation in hepatitis C cirrhosis. Aliment Pharmacol Ther. 2015;41:477-86. Available from: doi: 10.1111/apt.13051
45. Manousou P, Burroughs AK, Tsochatzis E, Isgro G, Hall A, Green A, et al. Digital image analysis of collagen assessment of progression of fibrosis in recurrent HCV after liver transplantation. J Hepatol. 2013;58:962-8. Available from: doi: 10.1016/j.jhep.2012.12.016

46. Manousou P, Dhillon AP, Isgro G, Calvaruso V, Luong TV, Tsochatzis E, et al. Digital image analysis of liver collagen predicts clinical outcome of recurrent hepatitis C virus 1 year after liver transplantation. Liver Transpl. 2011;17:178-88. Available from: doi: 10.1002/lt.22209
47. Calvaruso V, Burroughs AK, Standish R, Manousou P, Grillo F, Leandro G, et al. Computer-assisted image analysis of liver collagen: relationship to Ishak scoring and hepatic venous pressure gradient. Hepatol. 2009;49:1236-44. Available from: doi: 10.1002/hep.22745
48. Restellini S, Goossens N, Clement S, Lanthier N, Negro F, Rubbia-Brandt L, et al. CPA correlates to hepatic venous pressure gradient in non-abstinent cirrhotic patients with alcoholic liver disease. World J Hepatol. 2018;10:73-81. Available from: doi: 10.4254/wjh.v10.i1.73
49. Germani G, Burroughs AK, Dhillon AP. The relationship between liver disease stage and liver fibrosis: a tangled web. Histopathology. 2010;57:773-84. Available from: doi: 10.1111/j.1365-2559.2010.03609.x
50. Markiewicz-Kijewska M, Kalicinski P, Kluge P, Piatosa B, Jankowska I, Rekawek A, et al. Immunological factors and liver fibrosis in pediatric liver transplant recipients. Ann Transplant. 2015;20:279-84. Available from: doi: 10.12659/AOT.892544
51. Ohe H, Uchida Y, Yoshizawa A, Hirao H, Taniguchi M, Maruya E, et al. Association of anti-human leukocyte antigen and anti-angiotensin II type 1 receptor antibodies with liver allograft fibrosis after immunosuppression withdrawal. Transplantation. 2014;98:1105-11. Available from: doi: 10.1097/TP.0000000000000185
52. Wozniak LJ, Hickey MJ, Venick RS, Vargas JH, Farmer DG, Busuttil RW, et al. Donor-specific HLA antibodies are associated with late allograft dysfunction after pediatric liver transplantation. Transplantation. 2015;99:1416-22. Available from: doi: 10.1097/TP.0000000000000796
53. Demetris AJ, Bellamy C, Hübscher SG, O'Leary J, Randhawa PS, Feng S, et al. 2016 Comprehensive Update of the Banff Working Group on Liver Allograft Pathology: Introduction of Antibody-Mediated Rejection. Am J Transplant. 2016.
54. Taner T, Gandhi MJ, Sanderson SO, Poterucha CR, De Goey SR, Stegall MD, et al. Prevalence, course and impact of HLA donor-specific antibodies in liver transplantation in the first year. Am J Transplant. 2012;12:1504-10. Available from: doi: 10.1111/j.1600-6143.2012.03995.x
55. Hübscher SG. AMRin the liver allograft. Curr Opin Organ Transplant. 2012;17:280-6. Available from: doi: 10.1097/MOT.0b013e328353584c
56. Adsay NV, Hasteh F, Cheng JD, Bejarano PA, Lauwers GY, Batts KP, et al. Lymphoepithelial cysts of the pancreas: a report of 12 cases and a review of the literature. Mod Pathol. 2002;15:492-501. Available from: doi: 10.1038/modpathol.3880553
57. Taner T, Stegall MD, Heimbach JK. AMRin liver transplantation: current controversies and future directions. Liver Transpl. 2014;20:514-27. Available from: doi: 10.1002/lt.23826
58. Demetris AJ, Zeevi A, O'Leary JG. ABO-compatible liver allograft antibody-mediated rejection: an update. Curr Opin Organ Transplant. 2015;20:314-24. Available from: doi: 10.1097/MOT.0000000000000194
59. O'Leary JG, Shiller SM, Bellamy C, Nalesnik MA, Kaneku H, Jennings LW, et al. Acute liver allograft antibody-mediated rejection: an inter-institutional study of significant histopathological features. Liver Transpl. 2014;20:1244-55. Available from: doi: 10.1002/lt.23948

60. Smith JD, Banner NR, Hamour IM, Ozawa M, Goh A, Robinson D, et al. De novo donor HLA-specific antibodies after heart transplantation are an independent predictor of poor patient survival. Am J Transplant. 2011;11:312-9. Available from: doi: 10.1111/j.1600-6143.2010.03383.x
61. Colvin RB, Smith RN. Antibody-mediated organ-allograft rejection. Nat Rev Immunol. 2005;5:807-17. Available from: doi: 10.1038/nri1702
62. Hogen R, DiNorcia J, Dhanireddy K. Antibody-mediated rejection: what is the clinical relevance? Curr Opin Organ Transplant. 2017;22:97-104. Available from: doi: 10.1097/MOT.0000000000000391
63. Ius F, Sommer W, Tudorache I, Kuhn C, Avsar M, Siemeni T, et al. Early donor-specific antibodies in lung transplantation: risk factors and impact on survival. J Heart Lung Transplant. 2014;33:1255-63. Available from: doi: 10.1016/j.healun.2014.06.015
64. Zhang Q, Hickey M, Drogalis-Kim D, Zheng Y, Gjertson D, Cadeiras M, et al. Understanding the correlation between DSA, complement activation and antibody mediated rejection in heart transplant recipients. Transplantation. 2018;102:e431-8. Available from: doi: 10.1097/TP.0000000000002333
65. Barten MJ, Schulz U, Beiras-Fernandez A, Berchtold-Herz M, Boeken U, Garbade J, et al. The clinical impact of donor-specific antibodies in heart transplantation. Transplant Rev (Orlando). 2018 May;pii:S0955-470X(17)30114-3. Available from: doi: 10.1016/j.trre.2018.05.002
66. Hulbert AL, Pavlisko EN, Palmer SM. Current challenges and opportunities in the management of AMRin lung transplantation. Curr Opin Organ Transplant. 2018;23:308-15. Available from: doi: 10.1097/MOT.0000000000000537
67. O'Leary JG, Kaneku H, Susskind BM, Jennings LW, Neri MA, Davis GL, et al. High mean fluorescence intensity donor-specific anti-HLA antibodies associated with chronic rejection postliver transplant. Am J Transplant. 2011;11:1868-76. Available from: doi: 10.1111/j.1600-6143.2011.03593.x
68. Iacob S, Cicinnati VR, Dechene A, Lindemann M, Heinemann FM, Rebmann V, et al. Genetic, immunological and clinical risk factors for biliary strictures following liver transplantation. Liver int. 2012;32:1253-61. Available from: doi: 10.1111/j.1478-3231.2012.02810.x
69. O'Leary JG, Kaneku H, Demetris AJ, Marr JD, Shiller SM, Susskind BM, et al. AMRas a contributor to previously unexplained early liver allograft loss. Liver transpl. 2014;20:218-27. Available from: doi: 10.1002/lt.23788
70. Fontana M, Moradpour D, Aubert V, Pantaleo G, Pascual M. Prevalence of anti-HLA antibodies after liver transplantation. Transpl Int. 2010;23:858-9. Available from: doi: 10.1111/j.1432-2277.2009.01022.x
71. Waki K, Sugawara Y, Mizuta K, Taniguchi M, Ozawa M, Hirata M, et al. Predicting operational tolerance in pediatric living-donor liver transplantation by absence of HLA antibodies. Transplantation. 2013;95:177-83. Available from: doi: 10.1097/TP.0b013e3182782fef
72. Haas M, Sis B, Racusen LC, Solez K, Glotz D, Colvin RB, et al. Banff 2013 meeting report: inclusion of c4d-negative AMRand antibody-associated arterial lesions. Am J Transplant. 2014;14:272-83. Available from: doi: 10.1111/ajt.12590
73. Castillo-Rama M, Castro MJ, Bernardo I, Meneu-Diaz JC, Elola-Olaso AM, Calleja-Antolin SM, et al. Preformed antibodies detected by cytotoxic assay or multibead array decrease

liver allograft survival: role of human leukocyte antigen compatibility. Liver transpl. 2008;14:554-62. Available from: doi: 10.1002/lt.21408
74. Goh A, Scalamogna M, De Feo T, Poli F, Terasaki PI. Human leukocyte antigen crossmatch testing is important for liver retransplantation. Liver transpl. 2010;16:308-13. Available from: doi: 10.1002/lt.21981
75. Kaneku H, O'Leary JG, Taniguchi M, Susskind BM, Terasaki PI, Klintmalm GB. Donor-specific human leukocyte antigen antibodies of the immunoglobulin G3 subclass are associated with chronic rejection and graft loss after liver transplantation. Liver Transpl. 2012;18:984-92. Available from: doi: 10.1002/lt.23451
76. Gatault P, Jollet I, Rabot N, Boulanger MD, Taupin JL, Barbet C, et al. Mothers without HLA antibodies before transplantation have a low risk of alloimmunization post-transplantation. Tissue Antigens. 2011;78:241-8. Available from: doi: 10.1111/j.1399-0039.2011.01757.x
77. Vella JP, O'Neill D, Atkins N, Donohoe JF, Walshe JJ. Sensitization to human leukocyte antigen before and after the introduction of erythropoietin. Nephrol Dial Transplant. 1998;13(8):2027-32.
78. Mehra NK, Siddiqui J, Baranwal A, Goswami S, Kaur G. Clinical relevance of antibody development in renal transplantation. Ann N Y Acad Sci. 2013;1283:30-42. Available from: doi: 10.1111/nyas.12034
79. Baranwal AK, Bhat DK, Goswami S, Agarwal SK, Kaur G, Kaur J, et al. Comparative analysis of Luminex-based donor-specific antibody mean fluorescence intensity values with complement-dependent cytotoxicity & flow crossmatch results in live donor renal transplantation. Indian J Med Res. 2017;145:222-8. Available from: doi: 10.4103/ijmr.IJMR_222_16
80. O'Leary JG, Kaneku H, Jennings LW, Banuelos N, Susskind BM, Terasaki PI, et al. Preformed class II donor-specific antibodies are associated with an increased risk of early rejection after liver transplantation. Liver Transpl. 2013;19:973-80. Available from: doi: 10.1002/lt.23687
81. O'Leary JG, Demetris AJ, Friedman LS, Gebel HM, Halloran PF, Kirk AD, et al. The role of donor-specific HLA alloantibodies in liver transplantation. Am J Transplant 2014;14:779-87. Available from: doi: 10.1111/ajt.12667
82. Daar AS, Fuggle SV, Fabre JW, Ting A, Morris PJ. The detailed distribution of HLA-A, B, C antigens in normal human organs. Transplantation. 1984;38(3):287-92.
83. Lautenschlager I, Taskinen E, Inkinen K, Lehto VP, Virtanen I, Hayry P. Distribution of the major histocompatibility complex antigens on different cellular components of human liver. Cell Immunol. 1984;85(1):191-200.
84. Daar AS, Fuggle SV, Fabre JW, Ting A, Morris PJ. The detailed distribution of MHC Class II antigens in normal human organs. Transplantation. 1984;38(3):293-8.
85. Tambur AR, Leventhal JR, Zitzner JR, Walsh RC, Friedewald JJ. The DQ barrier: improving organ allocation equity using HLA-DQ information. Transplantation. 2013;95:635-40. Available from: doi: 10.1097/TP.0b013e318277b30b
86. Kaneku H, O'Leary JG, Banuelos N, Jennings LW, Susskind BM, Klintmalm GB, et al. De novo donor-specific HLA antibodies decrease patient and graft survival in liver transplant recipients. Am J Transplant. 2013;13:1541-8. Available from: doi: 10.1111/ajt.12212
87. Deng CT, El-Awar N, Ozawa M, Cai J, Lachmann N, Terasaki PI. Human leukocyte antigen class II DQ alpha and beta epitopes identified from sera of kidney allograft recipients. Transplantation. 2008;86:452-9. Available from: doi: 10.1097/TP.0b013e3181804cd2

88. Lee M. Antibody-mediated rejection after liver transplant. Gastroenterol Clin North Am. 2017;46:297-309. Available from: doi: 10.1016/j.gtc.2017.01.005
89. Demetris AJ, Bellamy C, Hübscher SG, O'Leary J, Randhawa PS, Feng S, et al. Comprehensive update of the Banff Working Group on liver allograft pathology: introduction of antibody-mediated rejection. Am J Transplant. 2016;16:2816-35. Available from: doi: 10.1111/ajt.13909
90. Musat AI, Agni RM, Wai PY, Pirsch JD, Lorentzen DF, Powell A, et al. The significance of donor-specific HLA antibodies in rejection and ductopenia development in ABO compatible liver transplantation. Am J Transplant. 2011;11:500-10. Available from: doi: 10.1111/j.1600-6143.2010.03414.x
91. Bellamy CO, Herriot MM, Harrison DJ, Bathgate AJ. C4d immunopositivity is uncommon in ABO-compatible liver allografts, but correlates partially with lymphocytotoxic antibody status. Histopathology. 2007;50:739-49. Available from: doi: 10.1111/j.1365-2559.2007.02677.x
92. Steinhoff G, Wonigeit K, Pichlmayr R. Analysis of sequential changes in major histocompatibility complex expression in human liver grafts after transplantation. Transplantation. 1988;45(2):394-401.
93. Hübscher SG, Adams DH, Elias E. Changes in the expression of major histocompatibility complex class II antigens in liver allograft rejection. J Pathol. 1990;162:165-71. Available from: doi: 10.1002/path.1711620210
94. O'Leary JG, Kaneku H, Jennings L, Susskind BM, Terasaki PI, Klintmalm GB. Donor-specific alloantibodies are associated with fibrosis progression after liver transplantation in hepatitis C virus-infected patients. Liver Transpl. 2014;20:655-63. Available from: doi: 10.1002/lt.23854
95. Aday AW, O'Leary JG. Donor specific antibodies' meaningful impact on liver transplantation. Liver Transpl. 2018;24:999-1000. Available from: doi: 10.1002/lt.25299
96. Koo J, Wang HL. Acute, chronic, and humoral rejection: pathologic features under current immunosuppressive regimes. Surg Pathol Clin. 2018;11:431-52. Available from: doi: 10.1016/j.path.2018.02.011
97. Bellamy CO. Complement C4d immunohistochemistry in the assessment of liver allograft biopsy samples: applications and pitfalls. Liver Transpl. 2011;17:747-50. Available from: doi: 10.1002/lt.22323
98. Neil DAH, Bellamy CO, Smith M, Haga H, Zen Y, Sebagh M, et al. Global quality assessment of liver allograft C4d staining during acute AMRin formalin-fixed, paraffin-embedded tissue. Hum Pathol. 2018;73:144-55. Available from: doi: 10.1016/j.humpath.2017.12.007
99. Murata K, Baldwin WM, 3rd. Mechanisms of complement activation, C4d deposition, and their contribution to the pathogenesis of antibody-mediated rejection. Transplant Rev (Orlando). 2009;23:139-50. Available from: doi: 10.1016/j.trre.2009.02.005
100. Cohen D, Colvin RB, Daha MR, Drachenberg CB, Haas M, Nickeleit V, et al. Pros and cons for C4d as a biomarker. Kidney Int. 2012;81:628-39. Available from: doi: 10.1038/ki.2011.497
101. Neuman UP, Neuhaus P. C4d immunostaining in acute humoral rejection after ABO blood group-incompatible liver transplantation. Liver Transpl. 2006;12:356-7. Available from: doi: 10.1002/lt.20658
102. .Kozlowski T, Andreoni K, Schmidz J, Hayashi PH, Nickeleit V. Sinusoidal C4d deposits in liver allografts indicate an antibody-mediated response: diagnostic considerations in the

evaluation of liver allografts. Liver Transpl. 2012; 18:641-58. Available from: doi: 10.1002/lt.23403
103. Sakashita H, Haga H, Ashihara E, Wen MC, Tsuji H, Miyagawa-Hayashino A, et al. Significance of C4d staining in ABO-identical/compatible liver transplantation. Mod Pathol. 2007;20:676-84. Available from: doi: 10.1038/modpathol.3800784.
104. O'Leary JG, Cai J, Freeman R, Banuelos N, Hart B, Johnson M, et al. Proposed diagnostic criteria for chronic antibody-mediated rejection in liver allografts. Am J Transplant. 2016;16:603-14. Available from: doi: 10.1111/ajt.13476
105. Lionaki S, Panagiotellis K, Iniotaki A, Boletis JN. Incidence and clinical significance of de novo donor specific antibodies after kidney transplantation. Clin Dev Immunol. 2013;849835. 9 p. Available from: doi: 10.1155/2013/849835
106. Racanelli V, Rehermann B. The liver as an immunological organ. Hepatology (Baltimore, Md). 2006;43(2 Suppl 1):S54-62. Available from: doi: 10.1002/hep.21060
107. Burrows PD, Cooper MD. B cell development and differentiation. Curr Opin Immunol. 1997;9:239-44. Available from: doi: 10.1016/S0952-7915(97)80142-2
108. Radbruch A, Muehlinghaus G, Luger EO, Inamine A, Smith KG, Dorner T, et al. Competence and competition: the challenge of becoming a long-lived plasma cell. Nat Rev Immunol. 2006;6:741-50. Available from: doi: 10.1038/nri1886
109. Zarkhin V, Chalasani G, Sarwal MM. The yin and yang of B cells in graft rejection and tolerance. Transplant Rev (Orlando). 2010;24:67-78. Available from: doi: 10.1016/j.trre.2010.01.004
110. Novobrantseva TI, Majeau GR, Amatucci A, Kogan S, Brenner I, Casola S, et al. Attenuated liver fibrosis in the absence of B cells. J Clin Invest. 2005;115(11):3072-82. Available from: doi: 10.1172/JCI24798
111. Abraham SC, Freese DK, Ishitani MB, Krasinskas AM, Wu TT. Significance of CP in pediatric liver transplantation. Am J Surg Pathol. 2008;32:1479-88. Available from: doi: 10.1097/PAS.0b013e31817a8e96
112. Whitfield ML, Finlay DR, Murray JI, Troyanskaya OG, Chi JT, Pergamenschikov A, et al. Systemic and cell type-specific gene expression patterns in scleroderma skin. PNAS. 2003;100:12319-24. Available from: doi: 10.1073/pnas.1635114100
113. Kondo K, Okada T, Matsui T, Kato S, Date K, Yoshihara M, et al. Establishment and characterization of a human B cell line from the lung tissue of a patient with scleroderma; extraordinary high level of IL-6 secretion by stimulated fibroblasts. Cytokine. 2001;13:220-6. Available from: doi: 10.1006/cyto.2000.0822
114. Hagn M, Schwesinger E, Ebel V, Sontheimer K, Maier J, Beyer T, et al. Human B cells secrete GrB when recognizing viral antigens in the context of the acute phase cytokine IL-21. J Immunol. 2009;183:1838-45. Available from: doi: 10.4049/jimmunol.0901066
115. Buzza MS, Bird PI. Extracellular granzymes: current perspectives. Biological chemistry. 2006;387:827-37. Available from: doi: 10.1515/BC.2006.106
116. Romero V, Andrade F. Non-apoptotic functions of granzymes. Tissue Antigens. 2008;71:409-16. Available from: doi: 10.1111/j.1399-0039.2008.01013.x
117. Feier F, da Fonseca EA, Candido HL, Pugliese R, Benavides MR, Neiva R, et al. Outcomes and technical aspects of liver retransplantation with living donors in children. Pediatr Transplant. 2016;20:813-8. Available from: doi: 10.1111/petr.12735
118. Xu W, Narayanan P, Kang N, Clayton S, Ohne Y, Shi P, et al. Human plasma cells express GrB. Eur J Immunol. 2014;44:275-84. Available from: doi: 10.1002/eji.201343711

119. Feng S, Demetris AJ, Spain KM, Kanaparthi S, Burrell BE, Ekong UD, et al. Five-year histological and serological follow-up of operationally tolerant pediatric liver transplant recipients enrolled in WISP-R. Hepatology. 2017;65:647-60. Available from: doi: 10.1002/hep.28681
120. Mells G, Neuberger J. Protocol liver allograft biopsies. Transplantation. 2008;85:1686-92. Available from: doi: 10.1097/TP.0b013e318176b1fd
121. Ekong UD. The long-term liver graft and protocol biopsy: do we want to look? What will we find? Curr Opin Organ Transplant. 2011;16:505-8. Available from: doi: 10.1097/MOT.0b013e32834a8caf
122. Mengel M, Sis B, Haas M, Colvin RB, Halloran PF, Racusen LC, et al. Banff 2011 meeting report: new concepts in antibody-mediated rejection. Am J Transplant. 2012;12:563-70. Available from: doi: 10.1111/j.1600-6143.2011.03926.x
123. Sweeney E, Ward TH, Gray N, Womack C, Jayson G, Hughes A, et al. Quantitative multiplexed quantum dot immunohistochemistry. Biochem Biophys Res Commun. 2008;374:181-6. Available from: doi: 10.1016/j.bbrc.2008.06.127
124. Tholouli E, Sweeney E, Barrow E, Clay V, Hoyland JA, Byers RJ. Quantum dots light up pathology. J Pathol. 2008;216:275-85. Available from: doi: 10.1002/path.2421
125. Prost S, Kishen RE, Kluth DC, Bellamy CO. Choice of illumination system & fluorophore for multiplex immunofluorescence on FFPE tissue sections. PloS One. 2016;11:e0162419. Available from: doi: 10.1371/journal.pone.0162419
126. Naesens M, Sarwal MM. Molecular diagnostics in transplantation. Nat Rev Nephrol. 2010;6:614-28. Available from: doi: 10.1038/nrneph.2010.113
127. Dong X, You Y, Wu JQ. Building an RNA sequencing transcriptome of the central nervous system. Neuroscientist. 2016;22:579-92. Available from: doi: 10.1177/1073858415610541
128. Mastoridis S, Martinez-Llordella M, Sanchez-Fueyo A. Emergent transcriptomic technologies and their role in the discovery of biomarkers of liver transplant tolerance. Front Immunol. 2015;6:304. Available from: doi: 10.3389/fimmu.2015.00304
129. Wang Z, Gerstein M, Snyder M. RNA-Seq: a revolutionary tool for transcriptomics. Nat Rev Genet. 2009;10:57-63. Available from: doi: 10.1038/nrg2484
130. Zhang Y, Chen K, Sloan SA, Bennett ML, Scholze AR, O'Keeffe S, et al. An RNA-sequencing transcriptome and splicing database of glia, neurons, and vascular cells of the cerebral cortex. J Neurosci. 2014;34:11929-47. Available from: doi: 10.1523/JNEUROSCI.1860-14.2014
131. Hall N. Advanced sequencing technologies and their wider impact in microbiology. J Exp Biol. 2007;210(Pt 9):1518-25. Available from: doi: 10.1242/jeb.001370
132. FitzGerald LM, Jung CH, Wong EM, Joo JE, Gould JA, Vasic V, et al. Obtaining high quality transcriptome data from formalin-fixed, paraffin-embedded diagnostic prostate tumor specimens. Lab Invest. 2018;98:537-50. Available from: doi: 10.1038/s41374-017-0001-8
133. Knudsen BS, Kim HL, Erho N, Shin H, Alshalalfa M, Lam LLC, et al. Application of a clinical whole-transcriptome assay for staging and prognosis of prostate cancer diagnosed in needle core biopsy specimens. J Mol Diagn. 2016;18:395-406. Available from: doi: 10.1016/j.jmoldx.2015.12.006
134. Lee A, Lee SH, Jung CK, Park G, Lee KY, Choi HJ, et al. Use of the Ion AmpliSeq Cancer Hotspot panel in clinical molecular pathology laboratories for analysis of solid tumours: With emphasis on validation with relevant single molecular pathology tests and the

Oncomine Focus Assay. Pathol Res Pract. 2018;214:713-9. Available from: doi: 10.1016/j.prp.2018.03.009
135. Paradiso V, Garofoli A, Tosti N, Lanzafame M, Perrina V, Quagliata L, et al. Diagnostic targeted sequencing panel for hepatocellular carcinoma genomic screening. J Mol Diagn. 2018;S1525-1578(18)30025-4. Available from: doi: 10.1016/j.jmoldx.2018.07.003
136. Neyaz A, Husain N, Gupta S, Kumari S, Arora A, Awasthi NP, et al. Investigation of targetable predictive and prognostic markers in gallbladder carcinoma. J Gastrointest Oncol. 2018;9:111-25. Available from: doi: 10.21037/jgo.2017.10.02
137. Li J, Fu C, Speed TP, Wang W, Symmans WF. Accurate RNA sequencing from formalin-fixed cancer tissue to represent high-quality transcriptome from frozen tissue. JCO Precis Oncol. 2018;2018. Available from: doi: 10.1200/PO.17.00091
138. Londoño MC, Souza LN, Lozano JJ, Miquel R, Abraldes JG, Llovet LP, et al. Molecular profiling of subclinical inflammatory lesions in long-term surviving adult liver transplant recipients. J Hepatol. 2018;69:626-34. Available from: doi: 10.1016/j.jhep.2018.04.012
139. Neves Souza L, de Martino RB, Sanchez-Fueyo A, Rela M, Dhawan A, O'Grady J, et al. Histopathology of 460 liver allografts removed at retransplantation: a shift in disease patterns over 27 years. Clin Transplant. 2018;32:e13227. Available from: doi: 10.1111/ctr.13227
140. Fayek SA. The value of C4d deposit in post liver transplant liver biopsies. Transpl Immunol. 2012;27:166-70. Available from: doi: 10.1016/j.trim.2012.08.004
141. Ali S, Ormsby A, Shah V, Segovia MC, Kantz KL, Skorupski S, et al. Significance of complement split product C4d in ABO-compatible liver allograft: diagnosing utility in acute antibody mediated rejection. Transpl Immunol. 2012;26:62-9. Available from: doi: 10.1016/j.trim.2011.08.005
142. Kozlowski T, Rubinas T, Nickeleit V, Woosley J, Schmitz J, Collins D, et al. Liver allograft AMRwith demonstration of sinusoidal C4d staining and circulating donor-specific antibodies. Liver Transpl. 2011;17:357-68. Available from: doi: 10.1002/lt.22233.
143. Robertson D, Isacke CM. Multiple immunofluorescence labeling of formalin-fixed paraffin-embedded tissue. Methods Mol Biol. 2011;724:69-77. Available from: doi: 10.1007/978-1-61779-055-3_4
144. Kajimura J, Ito R, Manley NR, Hale LP. Optimization of single- and dual-color Immunofluorescence protocols for formalin-fixed, paraffin-embedded archival tissues. J Histochem Cytochem. 2016;64:112-24. Available from: doi: 10.1369/0022155415610792
145. Robertson D, Savage K, Reis-Filho JS, Isacke CM. Multiple immunofluorescence labelling of formalin-fixed paraffin-embedded (FFPE) tissue. BMC Cell Biol. 2008;9:13. Available from: doi: 10.1186/1471-2121-9-13
146. Pan J, Thoeni C, Muise A, Yeger H, Cutz E. Multilabel immunofluorescence and antigen reprobing on formalin-fixed paraffin-embedded sections: novel applications for precision pathology diagnosis. Mod Pathol. 2016;29(6):557-69.
147. Lei PP, Shuai Q, Wang SW, Tao SM, Qu YQ, Wang DH. The comparison of methods to identify the presence of fibrocytes in formalin-fixed, paraffin-embedded archival cardiac tissue with coronary heart disease. Pathol Res Pract. 2014;210:929-33. Available from: doi: 10.1016/j.prp.2014.07.004
148. Viana LM, O'Malley JT, Burgess BJ, Jones DD, Oliveira CA, Santos F, et al. Cochlear neuropathy in human presbycusis: confocal analysis of hidden hearing loss in post-mortem tissue. Hear Res. 2015;327:78-88. Available from: doi: 10.1016/j.heares.2015.04.014

149. AbCam plc. Pre-adsorbed secondary antibodies. [Internet]. [cited 2018 Sep 28]. Available from: https://www.abcam.com/secondary-antibodies/pre-adsorbed-secondary-antibodies
150. Yamaguchi U, Hasegawa T, Sakurai S, Sakuma Y, Takazawa Y, Hishima T, et al. Interobserver variability in histologic recognition, interpretation of KIT immunostaining, and determining MIB-1 labeling indices in gastrointestinal stromal tumors and other spindle cell tumors of the gastrointestinal tract. Appl Immunohistochem Mol Morphol. 2006;14:46-51. Available from: doi: 10.1097/01.pai.0000151023.88969.d7
151. Wang XP, Zhang Y, Konig M, Papadopoulou E, Walkenfort B, Kasimir-Bauer S, et al. iSERS microscopy guided by wide field immunofluorescence: analysis of HER2 expression on normal and breast cancer FFPE tissue sections. Analyst. 2016;141:5113-9. Available from: doi: 10.1039/C6AN00927A
152. Petersen M, Davids LM, Kidson SH. Simultaneous immunofluorescent labeling using anti-BrdU monoclonal antibody and a melanocyte-specific marker in formalin-fixed paraffin-embedded human skin samples. Appl Immunohistochem Mol Morphol. 2012;20:614-7. Available from: doi: 10.1097/PAI.0b013e31824f70d8
153. ThermoFisher Scientific. Fluorescence SpectraViewer. [Internet]. 2018 [The Spectra Viewer is a tool to assist scientists in planning their experiments and analyses]. Available from: https://www.thermofisher.com/us/en/home/life-science/cell-analysis/labeling-chemistry/fluorescence-spectraviewer.html.
154. Chazotte B. Labeling nuclear DNA using DAPI. Cold Spring Harb Protoc. 2011;2011(1):pdb prot5556. Available from: doi: 10.1101/pdb.prot5556
155. Chazotte B. Labeling the nucleus with fluorescent dyes for imaging. CSH Protoc. 2008;2008:pdb prot4950. Available from: doi: 10.1101/pdb.prot4950
156. Gorris MAJ, Halilovic A, Rabold K, van Duffelen A, Wickramasinghe IN, Verweij D, et al. Eight-color multiplex immunohistochemistry for simultaneous detection of multiple immune checkpoint molecules within the tumor microenvironment. J Immunol. 2018;200:347-54. Available from: doi: 10.4049/jimmunol.1701262
157. Parra ER, Uraoka N, Jiang M, Cook P, Gibbons D, Forget MA, et al. Validation of multiplex immunofluorescence panels using multispectral microscopy for immune-profiling of formalin-fixed and paraffin-embedded human tumor tissues. Sci Rep. 2017;7:13380. Available from: doi: 10.1038/s41598-017-13942-8
158. The Human Protein Atlas - The Tissue Atlas [Internet]. Available from: https://www.proteinatlas.org/tissue.
159. Uhlén M, Fagerberg L, Hallström BM, Lindskog C, Oksvold P, Mardinoglu A, et al. Tissue-based map of the human proteome. Science. 2015: 347(6220):1260419. Available from: doi: 10.1126/science.1260419
160. Abcam plc. Double and triple immunostaining using secondary antibodies. [Internet]. [cited 2018 Sep 28]. Available from: http://www.abcam.com/secondary-antibodies/double-and-triple-immunostaining-using-secondary-antibodies.
161. Davis AS, Richter A, Becker S, Moyer JE, Sandouk A, Skinner J, et al. Characterizing and diminishing autofluorescence in formalin-fixed paraffin-embedded human respiratory tissue. J Histochem Cytochem. 2014;62:405-23. Available from: doi: 10.1369/0022155414531549
162. Viegas MS, Martins TC, Seco F, do Carmo A. An improved and cost-effective methodology for the reduction of autofluorescence in direct immunofluorescence studies on formalin-

fixed paraffin-embedded tissues. Eur J Histochem. 2007;51:59-66. Available from: doi: 10.4081/1013
163. Sun Y, Yu H, Zheng D, Cao Q, Wang Y, Harris D, et al. Sudan black B reduces autofluorescence in murine renal tissue. Arch Pathol Lab Med. 2011;135:1335-42. Available from: doi: 10.5858/arpa.2010-0549-OA
164. Planz V, Seif S, Atchison JS, Vukosavljevic B, Sparenberg L, Kroner E, et al. Three-dimensional hierarchical cultivation of human skin cells on bio-adaptive hybrid fibers. Integr Biol (Camb). 2016;8:775-84. Available from: doi: 10.1039/c6ib00080k
165. Benbadis SR, Perry M, Wolgamuth BR, Turnbull J, Mendelson WB. Mean versus median for the multiple sleep latency test. Sleep. 1995;342-5. Avaiable from: https://www.ncbi.nlm.nih.gov/pubmed/7676167
166. Demetris A, Adams D, Bellamy C, Blakolmer K, Clouston A, Dhillon AP, et al. Update of the International Banff Schema for liver allograft rejection: working recommendations for the histopathologic staging and reporting of chronic rejection. An international panel. Hepatology. 2000;31:792-9. Available from: doi: 10.1002/hep.510310337
167. Aday AW, MacRae CA. Genomic medicine in cardiovascular fellowship training. Circulation. 2017;136:345-6. Available from: doi: 10.1161/CIRCULATIONAHA.117.027568
168. Banff schema for grading liver allograft rejection: an international consensus document. Hepatology. 1997;25:658-63. Available from: doi: 10.1002/hep.510250328
169. Hytiroglou P, Snover DC, Alves V, Balabaud C, Bhathal PS, Bioulac-Sage P, et al. Beyond "cirrhosis": a proposal from the International Liver Pathology Study Group. Am J Clin Pathol. 2012;137:5-9. Available from: doi: 10.1309/AJCP2T2OHTAPBTMP
170. Madalosso C, de Souza NF, Jr., Ilstrup DM, Wiesner RH, Krom RA. Cytomegalovirus and its association with hepatic artery thrombosis after liver transplantation. Transplantation. 1998;66(3):294-7162/183. Murphy MS, Harrison R, Davies P, Buckels JA, Mayer AD, Hübscher S, et al. Risk factors for liver rejection: evidence to suggest enhanced allograft tolerance in infancy. Arch Dis Child. 1996;75(6):502-6. Available from: doi: 10.1136/adc.75.6.502
171. Hübscher SG. What is the long-term outcome of the liver allograft? J Hepatol. 2011;55:702-17. Available from: doi: 10.1016/j.jhep.2011.03.005
172. Marudanayagam R, Shanmugam V, Sandhu B, Gunson BK, Mirza DF, Mayer D, et al. Liver retransplantation in adults: a single-centre, 25-year experience. HPB (Oxford). 2010;12:217-24. Available from: doi: 10.1111/j.1477-2574.2010.00162.x
173. Jain A, Reyes J, Kashyap R, Dodson SF, Demetris AJ, Ruppert K, et al. Long-term survival after liver transplantation in 4,000 consecutive patients at a single center. Ann Surg. 2000;232(4):490-500. Available from: https://www.ncbi.nlm.nih.gov/pubmed/10998647
174. Jain A, Demetris AJ, Kashyap R, Blakomer K, Ruppert K, Khan A, et al. Does tacrolimus offer virtual freedom from chronic rejection after primary liver transplantation? Risk and prognostic factors in 1,048 liver transplantations with a mean follow-up of 6 years. Liver Transpl. 2001;7(7):623-30. Available from: doi: 01.1053/jlts.2001.25364
175. Deshpande RR, Rela M, Girlanda R, Bowles MJ, Muiesan P, Dhawan A, et al. Long-term outcome of liver retransplantation in children. Transplantation. 2002;74:1124-30. Available from: doi: 10.1097/01.TP.0000030640.11006.CE
176. Morel P, Rilo HL, Tzakis AG, Todo S, Gordon RD, Starzl TE. Liver retransplantation in adults: overall results and determinant factors affecting the outcome. Transplant Proc. 1991;23(6):3029-31. Available from: https://www.ncbi.nlm.nih.gov/pmc/articles/PMC3005254/

177. Kashyap R, Jain A, Reyes J, Demetris AJ, Elmagd KA, Dodson SF, et al. Causes of retransplantation after primary liver transplantation in 4000 consecutive patients: 2 to 19 years follow-up. Transplant Proc. 2001;33(1-2):1486-7. Available from: https://www.ncbi.nlm.nih.gov/pmc/articles/PMC2987633/
178. Unzueta A, Rakela J. Hepatitis E infection in liver transplant recipients. Liver Transpl. 2014;20:15-24. Available from: doi: 10.1002/lt.23764
179. Haagsma EB, van den Berg AP, Porte RJ, Benne CA, Vennema H, Reimerink JH, et al. Chronic hepatitis E virus infection in liver transplant recipients. Liver Transpl. 2008;14:547-53. Available from: doi: 10.1002/lt.21480
180. Adams DH, Sanchez-Fueyo A, Samuel D. From immunosuppression to tolerance. J Hepatol. 2015;62(1 Suppl):S170-85. Available from: doi: 10.1016/j.jhep.2015.02.042
181. Zhang CX, Wen PH, Sun YL. Withdrawal of immunosuppression in liver transplantation and the mechanism of tolerance. Hepatobiliary Pancreat Dis Int. 2015;14(5):470-6. Available from: https://www.ncbi.nlm.nih.gov/pubmed/26459722
182. Benítez C, Londoño MC, Miquel R, Manzia TM, Abraldes JG, Lozano JJ, et al. Prospective multicenter clinical trial of immunosuppressive drug withdrawal in stable adult liver transplant recipients. Hepatology. 2013;58:1824-35. Available from: doi: 10.1002/hep.26426
183. Grinda JM, Bricourt MO, Amrein C, Salvi S, Guillemain R, Francois A, et al. Human leukocyte antigen sensitization in ventricular assist device recipients: a lesser risk with the DeBakey axial pump. Ann Thorac Surg. 2005;80:945-8. Available from: doi: 10.1016/j.athoracsur.2005.03.096
184. O'Leary JG, Cai J, Freeman R, Banuelos N, Hart B, Johnson M, et al. Proposed Diagnostic Criteria for Chronic AMRin Liver Allografts. Am J Transplant. 2015;16:603-14. Available from: doi: 10.1111/ajt.13476
185. Murphy MS, Harrison R, Davies P, Buckels JA, Mayer AD, Hübscher S, et al. Risk factors for liver rejection: evidence to suggest enhanced allograft tolerance in infancy. Arch Dis Child. 1996;75(6):502-6. Available from: doi: 10.1136/adc.75.6.502
186. Kim JS, Grotelüschen R, Mueller T, Ganschow R, Bicak T, Wilms C, et al. Pediatr Transplant: the Hamburg experience. Transplantation. 2005;79:1206-9. Available from: doi: 10.1097%2F01.TP.0000160758.13505.D2
187. Rosenthal P, Emond JC, Heyman MB, Snyder J, Roberts J, Ascher N, et al. Pathological changes in yearly protocol liver biopsy specimens from healthy pediatric liver recipients. Liver Transpl. 1997;3:559-62. Available from: doi: 10.1002/lt.500030601
188. Kelly D, Verkade HJ, Rajanayagam J, McKiernan P, Mazariegos G, Hübscher S. Late graft hepatitis and fibrosis in pediatric liver allograft recipients: current concepts and future developments. Liver Transpl. 2016;22:1593-602. Available from: doi: 10.1002/lt.24616
189. Kosola S, Lampela H, Jalanko H, Makisalo H, Lohi J, Arola J, et al. Low-dose steroids associated with milder histological changes after pediatric liver transplantation. Liver Transpl. 2013;19:145-54. Available from: doi: doi: 10.1002/lt.23565
190. Miyagawa-Hayashino A, Haga H, Egawa H, Hayashino Y, Uemoto S, Manabe T. Idiopathic post-transplantation hepatitis following living donor liver transplantation, and significance of autoantibody titre for outcome. Transpl Int. 2009;22(3):303-12. Available from: doi: 10.1111/j.1432-2277.2008.00803.x
191. Venturi C, Sempoux C, Quinones JA, Bourdeaux C, Hoyos SP, Sokal E, et al. Dynamics of allograft fibrosis in pediatric liver transplantation. Am J Transplant. 2014;14:1648-56. Available from: doi: 10.1111/ajt.12740

192. Krasinskas AM, Demetris AJ, Poterucha JJ, Abraham SC. The prevalence and natural history of untreated isolated CP in adult allograft livers. Liver Transpl. 2008;14:625-32. Available from: doi: 10.1002/lt.21404
193. Turlin B, Slapak GI, Hayllar KM, Heaton N, Williams R, Portmann B. Centrilobular necrosis after orthotopic liver transplantation: a longitudinal clinicopathologic study in 71 patients. Liver Transpl Surg. 1995;1:285-9. Available from: doi: 10.1002/lt.500010503
194. Simon AK, Hollander GA, McMichael A. Evolution of the immune system in humans from infancy to old age. Proc Biol Sci. 2015;282:20143085. Available from: doi: 10.1098/rspb.2014.3085
195. Egawa H, Miyagawa-Hayashino A, Haga H, Teramukai S, Yoshizawa A, Ogawa K, et al. Non-inflammatory centrilobular sinusoidal fibrosis in pediatric liver transplant recipients under tacrolimus withdrawal. Hepatol Res. 2012;42:895-903. Available from: 10.1111/j.1872-034X.2012.01003.x
196. Sanada Y, Matsumoto K, Urahashi T, Ihara Y, Wakiya T, Okada N, et al. Protocol liver biopsy is the only examination that can detect mid-term graft fibrosis after pediatric liver transplantation. World J Gastroenterol. 2014;20:6638-50. Available from: doi: 10.3748/wjg.v20.i21.6638
197. Venkat VL, Nick TG, Wang Y, Bucuvalas JC. An objective measure to identify pediatric liver transplant recipients at risk for late allograft rejection related to non-adherence. Pediatr Transplant. 2008;12:67-72. Available from: doi: 10.1111/j.1399-3046.2007.00794.x
198. Herzog D, Soglio DB, Fournet JC, Martin S, Marleau D, Alvarez F. Interface hepatitis is associated with a high incidence of late graft fibrosis in a group of tightly monitored pediatric orthotopic liver transplantation patients. Liver Transpl. 2008;14:946-55. Available from: doi: 10.1002/lt.21444
199. Tokodai K, Miyagi S, Nakanishi C, Hara Y, Nakanishi W, Goto M, et al. Impact of the trough level of calcineurin inhibitor on the prevalence of donor-specific human leukocyte antigen antibodies during long-term follow-up after pediatric liver transplantation: antibody strength and complement-binding ability. Transplant Direct. 2017;3(8):e196. Available from: doi: 10.1097/TXD.0000000000000713
200. Tokodai K, Kawagishi N, Miyagi S, Nakanishi C, Hara Y, Fujio A, et al. The Significance of Screening for HLA Antibodies in the Long-Term Follow-up of Pediatric Liver Transplant Recipients. Transplantation proceedings. 2016;48(4):1139-41.
201. Kivela JM, Kosola S, Perasaari J, Makisalo H, Jalanko H, Holmberg C, et al. Donor-specific antibodies after pediatric liver transplantation: a cross-sectional study of 50 patients. Transpl Int. 2016;29:494-505. Available from: doi: 10.1111/tri.12747
202. Del Bello A, Congy-Jolivet N, Danjoux M, Muscari F, Lavayssiere L, Esposito L, et al. De novo donor-specific anti-HLA antibodies mediated rejection in liver-transplant patients. Transpl Int. 2015;28:1371-82. Available from: doi: 10.1111/tri.12654
203. Del Bello A, Congy-Jolivet N, Muscari F, Lavayssiere L, Esposito L, Cardeau-Desangles I, et al. Prevalence, incidence and risk factors for donor-specific anti-HLA antibodies in maintenance liver transplant patients. Am J Transplant. 2014;14:867-75. Available from: doi: 10.1111/ajt.12651
204. Abu-Elmagd KM, Wu G, Costa G, Lunz J, Martin L, Koritsky DA, et al. Preformed and de novo donor specific antibodies in visceral transplantation: long-term outcome with special reference to the liver. Am J Transplant. 2012;12:3047-60. Available from: doi: 10.1111/j.1600-6143.2012.04237.x

205. Tokodai K, Miyagi S, Nakanishi C, Hara Y, Nakanishi W, Unno M, et al. Effect of recipient age at liver transplantation on prevalence of post-transplant donor-specific HLA antibody. Ann Transplant. 2017;22:333-7. Available from: doi: 10.12659/AOT.903926
206. Ruiz R, Tomiyama K, Campsen J, Goldstein RM, Levy MF, McKenna GJ, et al. Implications of a positive crossmatch in liver transplantation: a 20-year review. Liver Transpl. 2012;18:455-60. Available from: doi: 10.1002/lt.22474
207. Salah A, Fujimoto M, Yoshizawa A, Yurugi K, Miyagawa-Hayashino A, Sumiyoshi S, et al. Application of complement component 4d immunohistochemistry to ABO-compatible and ABO-incompatible liver transplantation. Liver Transpl. 2014;20(2):200-9. Available from: doi: 10.1002/lt.23789
208. Vandevoorde K, Ducreux S, Bosch A, Guillaud O, Hervieu V, Chambon-Augoyard C, et al. Prevalence, risk factors, and impact of donor-specific alloantibodies after adult liver transplantation. Liver Transpl. 2018. Available from: doi: 10.1002/lt.25177
209. Alvarez-Marquez A, Aguilera I, Gentil MA, Caro JL, Bernal G, Fernandez Alonso J, et al. Donor-specific antibodies against HLA, MICA, and GSTT1 in patients with allograft rejection and C4d deposition in renal biopsies. Transplantation. 2009;87:94-9. Available from: doi: 10.1097/TP.0b013e31818bd790
210. Dao M, Habes D, Taupin JL, Mussini C, Redon MJ, Suberbielle C, et al. Morphological characterization of chronic antibody mediated rejection in ABO-identical or compatible pediatric liver graft recipients. Liver Transpl. 2018;24:897-907. Available from: doi: 10.1002/lt.25187
211. Gaston RS, Cecka JM, Kasiske BL, Fieberg AM, Leduc R, Cosio FC, et al. Evidence for antibody-mediated injury as a major determinant of late kidney allograft failure. Transplantation. 2010;90:68-74. Available from: doi: 10.1097/TP.0b013e3181e065de
212. O'Leary JG, Smith C, Cai J, Hart B, Jennings LW, Everly M, et al. Chronic AMR in liver transplant: validation of the 1-Year cAMR score's ability to determine long-term outcome. Transplantation. 2017;101:2062-70. Available from: doi: 10.1097/TP.0000000000001802
213. Hübscher SG. CP: a common and potentially important finding in late posttransplant liver biopsies. Liver Transpl. 2008;14(5):596-600.
214. Quaglia AF, Del Vecchio Blanco G, Greaves R, Burroughs AK, Dhillon AP. Development of ductopaenic liver allograft rejection includes a "hepatitic" phase prior to duct loss. J Hepatol. 2000;33:773-80. Available from: doi: 10.1016/S0168-8278(00)80309-8
215. Demetris AJ, Qian S, Sun H, Fung JJ, Yagihashi A, Murase N, et al. Early events in liver allograft rejection. Delineation of sites of simultaneous intragraft and recipient lymphoid tissue sensitization. Amer J Pathol. 1991;138(3):609-18. Available from: http://europepmc.org/backend/ptpmcrender.fcgi?accid=PMC1886268&blobtype=pdf
216. Gouw AS, van den Heuvel MC, van den Berg AP, Slooff MJ, de Jong KP, Poppema S. The significance of parenchymal changes of acute cellular rejection in predicting chronic liver graft rejection. Transplantation. 2002;73:243-7. Available from: doi: 10.1097/00007890-200201270-00016
217. Neil DA, Hübscher SG. Histologic and biochemical changes during the evolution of chronic rejection of liver allografts. Hepatology. 2002;35:639-51. Available from: doi: 10.1053/jhep.2002.31726
218. Nakazawa Y, Walker NI, Kerlin P, Steadman C, Lynch SV, Strong RW, et al. Clinicopathological analysis of liver allograft biopsies with late centrilobular necrosis: a comparative study in 54 patients. Transplantation. 2000;69(8):1599-608. Available from: https://www.ncbi.nlm.nih.gov/pubmed/10836369

219. Crawford AR, Lin XZ, Crawford JM. The normal adult human liver biopsy: a quantitative reference standard. Hepatology. 1998;28:323-31. Available from: doi: 10.1002/hep.510280206
220. Wiebe C, Gibson IW, Blydt-Hansen TD, Karpinski M, Ho J, Storsley LJ, et al. Evolution and clinical pathologic correlations of de novo donor-specific HLA antibody post kidney transplant. Am J Transplant. 2012;12(5):1157-67. Available from: doi: 10.1111/j.1600-6143.2012.04013.x
221. Batts KP, Moore SB, Perkins JD, Wiesner RH, Grambsch PM, Krom RA. Influence of positive lymphocyte crossmatch and HLA mismatching on vanishing bile duct syndrome in human liver allografts. Transplantation. 1988;45(2):376-9. Available from: https://www.ncbi.nlm.nih.gov/pubmed/3278430
222. Donaldson PT, Alexander GJ, O'Grady J, Neuberger J, Portmann B, Thick M, et al. Evidence for an immune response to HLA class I antigens in the vanishing-bileduct syndrome after liver transplantation. Lancet. 1987;1(8539):945-51. Available from: https://www.ncbi.nlm.nih.gov/pubmed/2882341
223. Demetris AJ, Nakamura K, Yagihashi A, Iwaki Y, Takaya S, Hartman GG, et al. A clinicopathological study of human liver allograft recipients harboring preformed IgG lymphocytotoxic antibodies. Hepatology. 1992;16(3):671-81. Available from: https://www.ncbi.nlm.nih.gov/pubmed/1505910
224. O'Leary JG, Klintmalm GB. Impact of donor-specific antibodies on results of liver transplantation. Curr Opin Organ Transplant. 2013;18:279-84. Available from: doi: 10.1097/MOT.0b013e3283614a10
225. Del Bello A, Congy-Jolivet N, Danjoux M, Muscari F, Kamar N. Donor-specific antibodies and liver transplantation. Hum Immunol. 2016;77:1063-70. Available from: doi: 10.1016/j.humimm.2016.02.006
226. Takemura M, Oguma S, Mori S, Ishii M, Starzl TE, Demetris AJ, et al. Peribiliary vascular diseases in rejected livers; computer-aided three-dimensional reconstruction and morphometry. Transplantation proceedings. 1991;23(1 Pt 2):1409-12. Available from: https://www.ncbi.nlm.nih.gov/pmc/articles/PMC2976044/
227. Matsumoto Y, McCaughan GW, Painter DM, Bishop GA. Evidence that portal tract microvascular destruction precedes bile duct loss in human liver allograft rejection. Transplantation. 1993;56(1):69-75. Available from: https://www.ncbi.nlm.nih.gov/pubmed/8333070
228. Muro M, Marin L, Miras M, Moya-Quiles R, Minguela A, Sanchez-Bueno F, et al. Liver recipients harbouring anti-donor preformed lymphocytotoxic antibodies exhibit a poor allograft survival at the first year after transplantation: experience of one centre. Transpl Immunol. 2005;14:91-7. Available from: 10.1016/j.trim.2005.03.013
229. Grabhorn E, Binder TM, Obrecht D, Brinkert F, Lehnhardt A, Herden U, et al. Long-term clinical relevance of de novo donor-specific antibodies after pediatric liver transplantation. Transplantation. 2015;99:1876-81. Available from: doi: 10.1097/TP.0000000000000638
230. Kim PT, Demetris AJ, O'Leary JG. Prevention and treatment of liver allograft AMRand the role of the 'two-hit hypothesis'. Curr Opin Organ Transplant. 2016;21:209-18. Available from: doi: 10.1097/MOT.0000000000000275
231. Troxell ML, Higgins JP, Kambham N. Evaluation of C4d staining in liver and small intestine allografts. Arch Pathol Lab Med. 2006;130:1489-96. Available from: doi: 10.1043/1543-2165(2006)130[1489:EOCSIL]2.0.CO;2

232. Gierej B, Kobryn K, Gierej P, Gornicka B. C4d in acute rejection after liver transplantation and its usefulness in differential diagnosis between acute liver rejection and hepatitis C recurrence. Ann Transplant. 2014;19:373-81. Available from: doi: 10.12659/AOT.890234
233. Lorho R, Turlin B, Aqodad N, Triki N, de Lajarte-Thirouard AS, Camus C, et al. C4d: a marker for hepatic transplant rejection. Transplant Proc. 2006;38:2333-4. Available from: doi: 10.1016/j.transproceed.2006.06.120
234. Lauwers GY, Terris B, Balis UJ, Batts KP, Regimbeau JM, Chang Y, et al. Prognostic histologic indicators of curatively resected hepatocellular carcinomas: a multi-institutional analysis of 425 patients with definition of a histologic prognostic index. Am J Surg Pathol. 2002;26:25-34. Available from: doi: 10.1097/00000478-200201000-00003
235. Calvaruso V, Dhillon AP, Tsochatzis E, Manousou P, Grillo F, Germani G, et al. Liver CPA predicts decompensation in patients with recurrent hepatitis C virus cirrhosis after liver transplantation. J Gastroenterol Hepatol. 2012;27(7):1227-32. Available from: doi: 10.1111/j.1440-1746.2012.07136.x

7 PERSONAL BIBLIOGRAPHY

138. Londoño MC, **Souza LN**, Lozano JJ, Miquel R, Abraldes JG, Llovet LP, et al. Molecular profiling of subclinical inflammatory lesions in long-term surviving adult liver transplant recipients. J Hepatol. 2018;69:626-34. Available from: doi: 10.1016/j.jhep.2018.04.012
139. **Neves Souza L**, de Martino RB, Sanchez-Fueyo A, Rela M, Dhawan A, O'Grady J, et al. Histopathology of 460 liver allografts removed at retransplantation: a shift in disease patterns over 27 years. Clin Transplant. 2018;32:e13227. Available from: doi: 10.1111/ctr.13227
98. Neil DAH, Bellamy CO, Smith M, Haga H, Zen Y, Sebagh M, et al. Global quality assessment of liver allograft C4d staining during acute AMRin formalin-fixed, paraffin-embedded tissue. Hum Pathol. 2018;73:144-55. Available from: doi: 10.1016/j.humpath.2017.12.007 (acknowledged)